



UNIVERSITÀ DI PARMA

UNIVERSITA' DEGLI STUDI DI PARMA

DOTTORATO DI RICERCA IN
"Scienze Chimiche"

CICLO XXXVII

Macrocycles in catalysis: New applications and methodologies

Coordinatore:
Chiar.mo Prof. Alessia Bacchi

Tutore:
Chiar.mo Prof. Gianpiero Cera

Dottorando: Gabriele Giovanardi

Anni Accademici 2021/2022 – 2023/2024

Table of Contents

Abstract	5
Chapter 1. General introduction	6
1.1 Macrocycles in catalysis	6
1.2 Calix[n]arenes and their applications	14
1.3 Macrocycle-based gold(I)-complexes in catalysis	17
1.4 Bibliography	25
Chapter 2. Synthesis and Catalytic studies of novel Calix[6]arene-based gold(I) dimeric complexes A, B and C(AuCl)₂	28
2.1 Introduction	28
2.2 Results and discussion	34
2.3 Conclusions	46
2.4 Experimental Section	47
2.5 Bibliography	72
Chapter 3. Gold(I)-catalyzed hydroarylation reaction for the preparation of inherently chiral calix[4]arenes (ICCs)	75
3.1 Introduction	75
3.2 Results and discussion	81
3.3 Conclusions	95
3.4 Experimental section	96
3.5 Bibliography	138
Chapter 4. Regioselective functionalization of calix[4]arenes via Iridium-catalyzed C-H Borylations	140
4.1 Introduction	140
4.2 Results and discussion	143

4.3 Conclusions	153
4.4 Experimental section	154
4.5 Bibliography	190
Chapter 5. New enantioselective approach for the total synthesis of Indidene natural products empowered by gold-catalysis	193
5.1 Introduction	193
5.2 Results and discussion	199
5.3 Conclusions	208
5.4 Experimental section	209
5.5 Bibliography	216
Publications	218

Abstract

Macrocycles are a versatile class of compounds with extensive applications across various fields of chemistry, particularly in sensor development, molecular machines, and catalysis. This work explores novel applications of macrocycles in transition metal-catalyzed reactions. The findings can be summarized as follows:

Chapter 2 details the synthesis and characterization of three new dimeric calix[6]arene-based gold(I) complexes. The influence of the macrocyclic cavity on these complexes' catalytic activity is investigated, specifically in the gold(I)-catalyzed cycloisomerization of 1,6-dienynes.

In Chapter 3, the focus shifts to the use of gold(I)-catalyzed hydroarylation for synthesizing inherently chiral calix[4]arene derivatives. Preliminary studies toward developing enantioselective methodologies are also included.

Chapter 4 describes a regioselective distal functionalization of the upper rim of calix[4]arene derivatives via iridium-catalyzed C-H borylation. The versatility of these valuable intermediates is also discussed.

Finally, Chapter 5 presents a new synthetic approach for preparing indene-based natural products using an enantioselective gold(I)-catalyzed alkoxy-cycloisomerization reaction facilitated by resorcin[4]arene-based gold(I) complexes.

Chapter 1. General introduction

1.1 Macrocycles in catalysis

A key objective in the rapidly advancing field of supramolecular chemistry is the design and synthesis of novel organometallic catalysts that can modulate reaction selectivity through external stimuli.^[1] Inspired by natural enzymes, extensive research has been directed towards the development of multivalent ligands featuring a macrocyclic scaffold with a well-defined cavity.^[2] This cavity plays a pivotal role in influencing both the activity and selectivity of the catalyst. It can do so in multiple ways: i) by confining or encapsulating the metal center within the cavity itself,^[3,4] or ii) by imposing steric restrictions or facilitating weak interactions between the inner walls of the macrocyclic host and the substrate bound to the metal.^[5,6] Numerous studies have documented the synthesis of such macrocyclic ligands and explored how their cavities affect catalytic performance.

A notable example provided by Lejune and collaborators involves the synthesis of a calix[4]arene-based mono-phosphine ligand, **MBr4** (Figure 1). Experimental studies have demonstrated that, in its reaction with $[\text{RuCl}_2(p\text{-cymene})]$, an organometallic complex is formed, where the $\{\text{Ru-Arene}\}$ unit is confined within the macrocyclic cavity of the calix[4]arene scaffold, which was also confirmed by X-ray crystallography and NMR spectroscopy.^[7,8] The confinement is attributed to π - π interactions between the p -cymene ligand and the calixarene cavity (Figure 1.1).

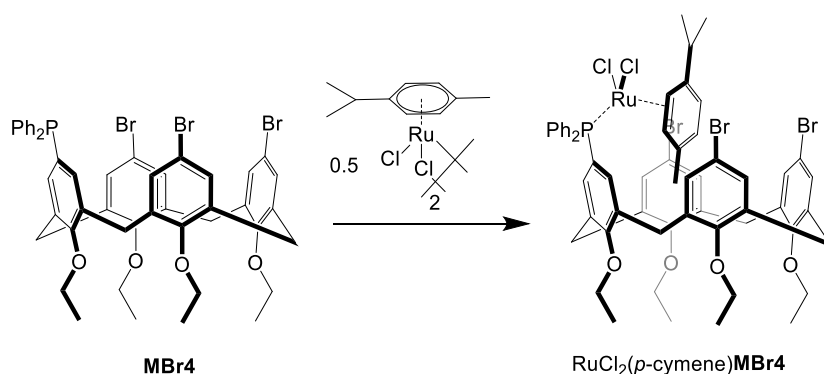


Figure 1.1: Structure of the **MBr4** ligand and representation of the confinement of the p -cymene unit within the calix[4]arene cavity upon reaction of the ligand with $[\text{RuCl}_2(p\text{-cymene})]$.

Chapter 1

Subsequently, the effect of using this type of diphenylphosphine calix[4]arene ligands (Figure 1.2, a) was tested in the model Suzuki-Miyaura coupling reaction, described in Figure 1.2, b.

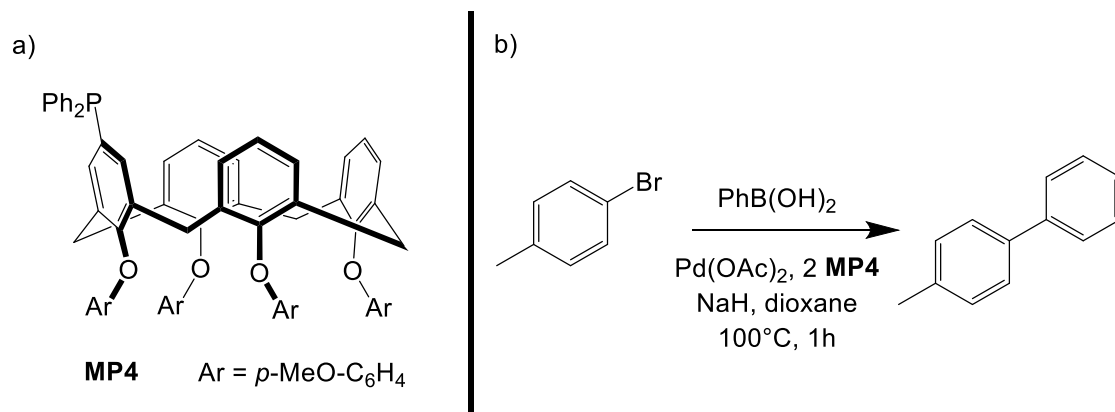


Figure 1.2: a) Structure of the calix[4]arene-based monophosphine ligand **MP4**; b) Schematic representation of the model Suzuki-Miyaura coupling reaction.

The catalytic activity observed, especially with the **MP4** derivative, is comparable to that of Buchwald-type biarylphosphines,^[9] notably the phosphine **PB** (Figure 1.3, a), which are recognized as some of the most efficient ligands for these catalytic reactions (Figure 1.3, a). The enhanced activity is thought to arise from **MP4**'s ability to form a mono-phosphine catalytic complex, $[\text{Pd}^0(\text{ArBr})\text{L}]$, similar to **PB**. Having only one ligand bound to the metal center significantly simplifies the subsequent oxidative step. **MP4**'s ability to form this mono-phosphine complex is due to its role as a supramolecular receptor, functioning as a mixed chelator (P, π -arene) towards the $\{\text{Pd}^0(\eta^2\text{-ArBr})\}$ unit, much like **MBr4** (Figure 1.3, b). This behavior is driven by π - π interactions between the aryl halide and the aromatic units of the calixarene scaffold.

Chapter 1

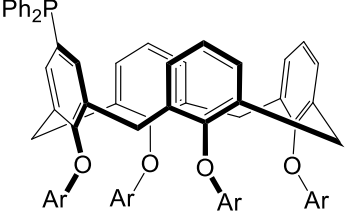
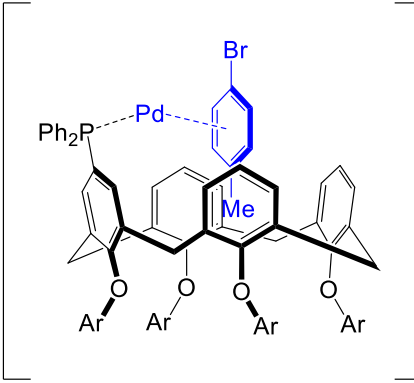
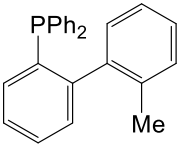
a)	Ligand employed for the catalysis	TOF (s ⁻¹)	b)
	 MP4 Ar = <i>p</i> -MeO-C ₆ H ₄	321 000	
	 PB	214 000	
	P(<i>o</i> -tolyl) ₃	103 000	
	PPh ₃	65 000	

Figure 1.3: a) Comparison of TOF values determined for the **MP4** ligand with those obtained using other arylphosphines; b) Representation of the role played by the calix[4]arene scaffold in forming π - π interactions with the organometallic fragment $\{Pd^0(ArBr)\}$.

This conformation significantly increases the bulk around the metal center, promoting the formation of a more activated mono-phosphine catalytic complex.^[10]

Another example illustrating how the macrocyclic cavity of the ligand can modify the selectivity of the final catalyst came from the work of Gibson and Rebek Jr.^[11] Here, they described a resorcin[4]arene-based ligand functionalized with a phosphito-isoxazoline P,N-chelating unit, **RC** (Figure 4), which facilitates the formation of the corresponding palladium catalytic complex. Their study investigates its activity in the catalytic alkylation of allyls with carbon nucleophiles (Table 1).

Chapter 1

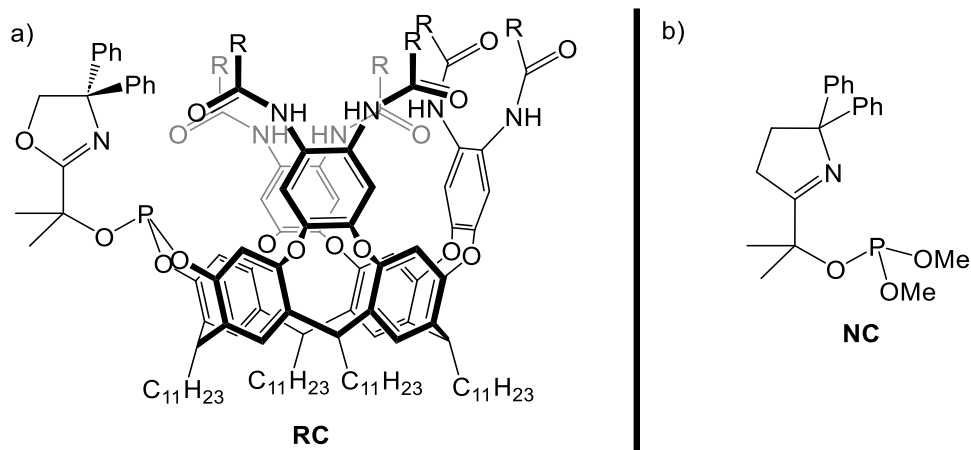
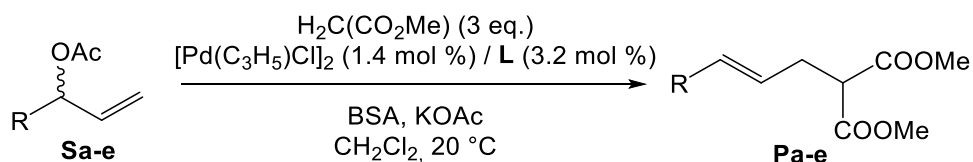


Figure 1.4: a) Structure of the resorcin[4]arene-based macrocyclic ligand **RC**; b) Structure of the non-macrocyclic ligand **NC**.

In this study, catalytic alkylation experiments were performed on substrates **Sa-e**, using dimethyl malonate as the nucleophile. The results obtained with the Pd/**RC** catalyst were compared to those from its non-macrocyclic analog, Pd/**NC** (Figure 1.4). The findings revealed the exclusive formation of linear products (Table 1.1). This behavior can be attributed to the tendency of the complexes with the general formula $[\text{Pd}(\eta^3\text{-HC=CH-CHR})\text{RC}]^+$ to adopt an A-type conformation, where the R group is positioned within the macrocyclic cavity (Figure 1.5).



Entry	R	L = RC		L = NC	
		t (d)	Yield (%)	t (h)	Yield (%)
1	-CH-CH(CH ₃) ₂ (Sa)	6	38	2	85
2	-CH(CH ₃) ₂ (Sb)	2	76	2	91
3	-C(CH ₃) ₃ (Sc)	2	96	2	81
4	-C ₆ H ₁₁ (Sd)	6	74	2	78
5	-CH(CH ₂ CH ₃)(<i>n</i> -C ₄ H ₉) (Se)	6	60	2	82

Table 1.1: Catalytic experiments for alkylation reactions of substrates **Sa-e** with dimethyl malonate.

Chapter 1

In contrast, the type B conformation is disfavoured due to the formation of steric repulsive interactions between the R group and the phenyl substituents of the isoxazoline unit (Figure 1.5). This prevents the nucleophile from reacting at the more hindered carbon, leading to the exclusive formation of linear products **Pa-e**.

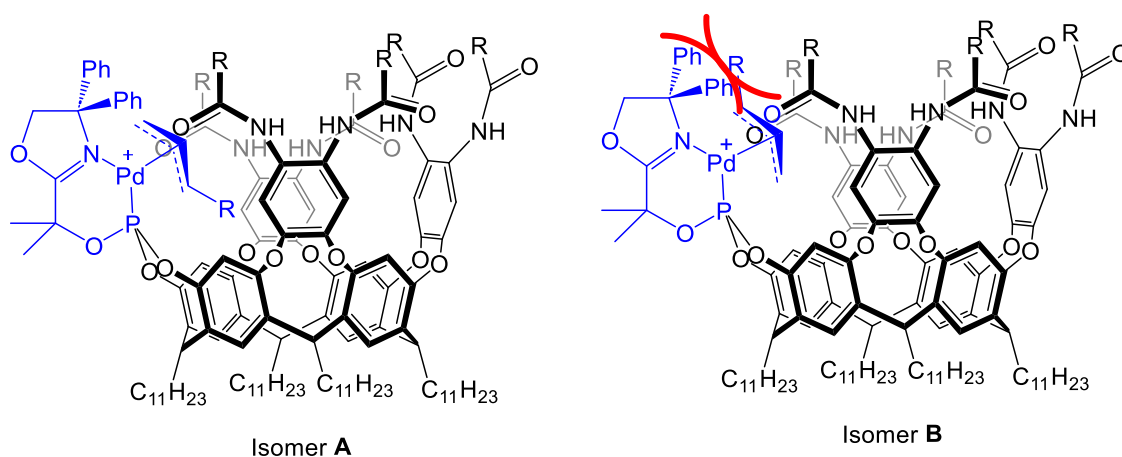


Figure 1.5: Structure of intermediate complexes with the general formula $[Pd(\eta^3\text{-HC=CHR})\text{RC}]^+$, highlighting the steric repulsion between the R group and the phenyl substituents in isomer **B**.

Additionally, it is important to note that, unlike the **NC** ligand, the reaction rate using the **RC** ligand varies significantly depending on the substrate. While the conversion of substrates **Sb** and **Sc** was complete after 2 days (Table 1.1, entries 2-3), the reactions involving **Sd** and **Se** were approximately four times slower, taking 6 days to reach completion (Table 1.1, entries 4-5). The slowest reactivity was observed with substrate **Sa**. Further analysis revealed that the η^3 -allyl complex formed between **Sa** and [Pd] developed more rapidly than the corresponding complex with **Sb**; however, the latter was nearly inert to nucleophilic attack. Overall, the rate of the initial oxidative addition step is influenced by the number of carbon atoms attached to the homoallylic carbon of the substrate, following the trend **Sa** (C 2°) > **Sb** (C 3°) > **Sc** (C 4°).

Following this, experiments were conducted in which substrates **Sb**, **Sd**, and **Se**, all substituted with a 3° carbon at the homoallylic position, competed to react with the Pd/**RC** and Pd/**NC** catalysts. These experiments were performed using binary mixtures (1:1) of the aforementioned substrates (Table 1.2).

Chapter 1

L = RC				
Entry	Substrates (1:1)	Ratio of complexes η^3	Yield (%)	Products distribution
1	Sb + Sd	Sb/Sd 32:68	20	Pb/Pd 29:71
2	Sb + Se	Sb/Se 70:30	35	Pb/Pe 67:33
3	Sd + Se	Sd/Se 87:13	29	Pd/Pe 86:14

L = NC				
Entry	Substrates (1:1)	Ratio of complexes η^3	Yield (%)	Products distribution
4	Sb + Sd	Sb/Sd 48:52	46	Pb/Pd 42:58
5	Sb + Se	Sb/Se 59:51	58	Pb/Pe 52:48
6	Sd + Se	Sd/Se 50:50	64	Pd/Pe 47:53

Table 1.2: Catalysis experiments conducted with binary mixtures of substrates **Sb**, **Sd**, and **Se**.

Conditions: 1.4 mol% $[Pd(\eta^3-C_3H_5)Cl]_2$, 3.2 mol% L, 3 eq. of $CH_2(COOMe)_2$, and BSA.

The results indicate that when using Pd/**RC**, the distribution of the two possible reaction products consistently favors one over the other in each experiment (Table 1.2, entries 1-3). This suggests that the Pd/**RC** catalyst selectively influences the reaction outcome, likely through steric interactions within the macrocyclic cavity.

The studies thus far illustrate how the macrocyclic cavity of the ligand can affect catalytic activity and selectivity by forming non-covalent interactions with organometallic fragments generated through substrate coordination to the metal center. Another possible strategy involves encapsulating the metal core within the ligand's macrocyclic cavity to potentially enhance catalytic activity.

One example of this approach was presented by Matt and collaborators, where they show the use of the diphosphine ligand **DPC**, which consists of two covalently linked calix[4]arene units, to form a Ni(I)-based complex (Figure 1.6, a). This catalyst has been tested for the polymerization of butadiene.^[12]

Chapter 1

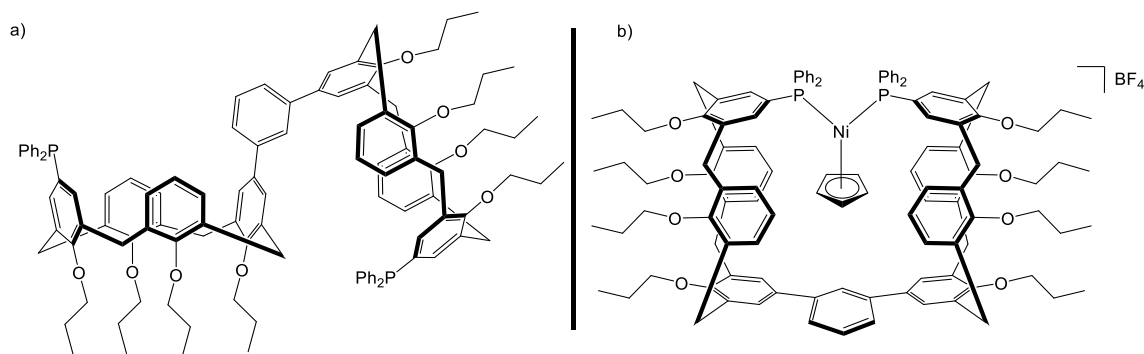


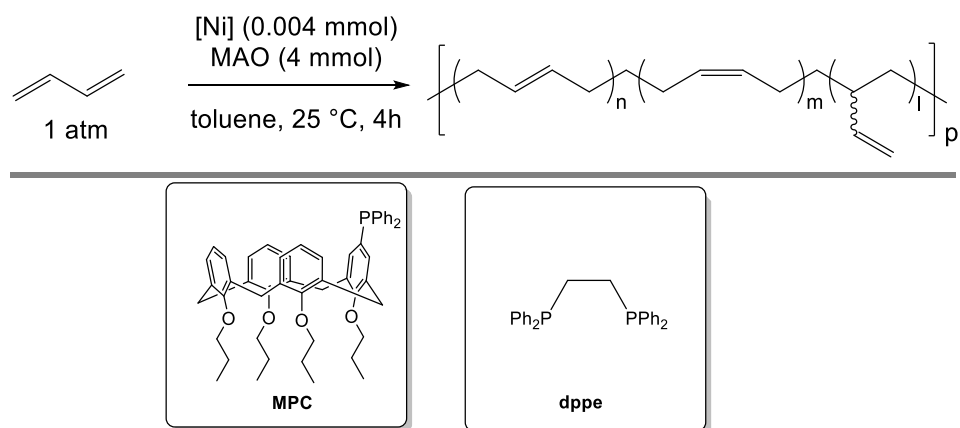
Figure 1.6: a) Structure of the diposphine ligand **DPC**; b) structure of the catalytic complex $\text{Ni}(\eta^5\text{-C}_5\text{H}_5)(\text{DPC})$.

This ligand can adopt a rigid structure by coordinating with a metal core with two available coordination sites in a cis configuration, chelating with the two phosphine units (Figure 1.6, b). Moreover, the resulting structure will encapsulate the metal core within the ligand, positioning it close to the calix[4]arene cavities.

The authors investigated the activity of the Ni(I) catalyst formed by the reaction of the ligand with $\text{Ni}(\eta^5\text{-C}_5\text{H}_5)(\text{cod})$ in the polymerization of butadiene. They found it to be significantly more active, up to 40 times, than non-confined catalytic complexes (Table 1.3, entries 2-3). Additionally, they compared the activity of $\text{Ni}(\eta^5\text{-C}_5\text{H}_5)(\text{DPC})$ with that of the catalyst $\text{Ni}(\eta^5\text{-C}_5\text{H}_5)(\text{MPC})_2$ (Table 1.3), which was synthesized by complexing Ni with the two monophosphine calix[4]arene ligands, **MPC** (Table 13, entry 4). This comparison underscored the important role of **DPC**-induced inclusion in enhancing catalytic activity.

It is proposed that the enhanced activity is attributable to the formation of a complex of the type $[\text{Ni}(\eta^1\text{-CH}_2\text{-CH=CH}\cdot\text{P})(\text{DPC})]$, where *P* denotes the growing polymer chain, just before the addition of a new butadiene unit. The steric bulk surrounding the metal is thought to induce this complex, facilitating the insertion of the subsequent butadiene unit and thereby increasing the catalyst's activity.

Chapter 1



Entry	Catalyst	Yield (g)	Activity (g/(mol Ni · h))	M_n	M_w/M_n	1,4- <i>cis</i> (%)	1,4- <i>trans</i> (%)	1,2 (%)
1	$[\text{Ni}(\eta^5\text{-C}_5\text{H}_5)(\text{DPC})](\text{BF}_4)$	2.841	178000	37300	2.21	89.4	6.5	4.1
2	$[\text{Ni}(\eta^5\text{-C}_5\text{H}_5)(\text{dppe})](\text{BF}_4)$	0.075	4670	31800	1.63	89.1	6.5	4.4
3	$[\text{Ni}(\eta^5\text{-C}_5\text{H}_5)(\text{PPh}_3)_2](\text{BF}_4)$	0.096	6010	33900	1.77	88.0	7.0	5.0
4	$[\text{Ni}(\eta^5\text{-C}_5\text{H}_5)(\text{MPC})_2](\text{BF}_4)$	0.199	12500	59200	1.66	88.5	6.3	5.2

Table 1.3: Catalytic experiments for the polymerization of butadiene to evaluate the effect induced using **DPC**.

Chapter 1

1.2 Calix[n]arenes and their applications

Calix[n]arenes are macrocyclic oligomers composed of phenolic units synthesized via the condensation of *p*-tert-butylphenol and formaldehyde under basic conditions.^[13] By fine-tuning the reaction parameters, macrocycles of different sizes can be selectively obtained in high yields by varying the number of phenolic units in the calix[n]arene scaffold.^[13] The most widely used calix[n]arene derivatives are calix[4]arene, calix[6]arene, and calix[8]arene (Figure 7).

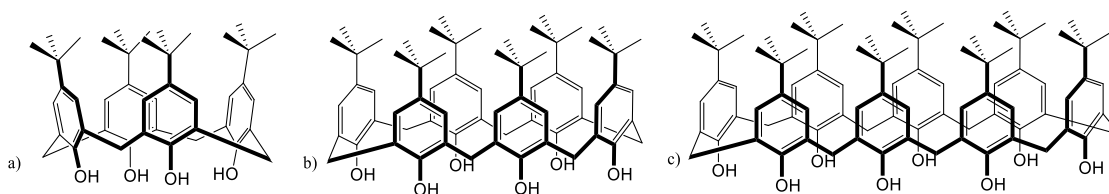


Figure 1.7: Structure of calixarene derivatives: calix[4]arene (a), calix[6]arene (b), and calix[8]arene (c).

Calix[n]arenes find extensive applications in the preparation of molecular sensors and host-guest supramolecular chemistry, offering an electron-rich, hydrophobic cavity that can encapsulate neutral or charged species through non-covalent interactions.^[14-16]

A key feature of calix[n]arenes is their synthetic versatility, enabling regioselective functionalization of the macrocycle. By adjusting reaction conditions, calix[6]arene receptors can be tailored to adopt specific conformations in nonpolar solvents. For instance, our research group has developed various receptors capable of forming interlocked (pseudo)rotaxane structures, serving as prototypes for molecular machines or nanodevices.^[17] Notably, triphenylurea calix[6]arenes (**TPU**)^[18] and triarylsulfonamide **TST** adopt a cone conformation, while the diphenylurea derivative **DPU**^[19] exhibits a *1,2,3-alternate* conformation (Figure 1.9).

Chapter 1

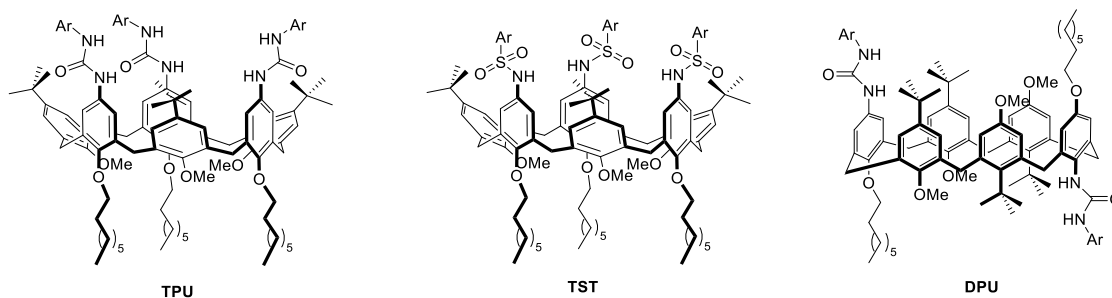


Figure 1.8: Examples of heterodytropic calix[6]arene derivatives.

The hydrogen bond (HB) donor groups on the upper rim of the calixarene scaffold, such as the urea and sulfonamide groups shown in Figure 1.8, play a crucial role in facilitating the complexation of the macrocyclic cavity by mono- or bi-charged organic cations. These groups enable non-covalent interactions with the organic cation-anion ion pair, effectively separating the ionic species and encouraging the positively charged axis to enter the electron-rich macrocyclic cavity (Figure 1.9).

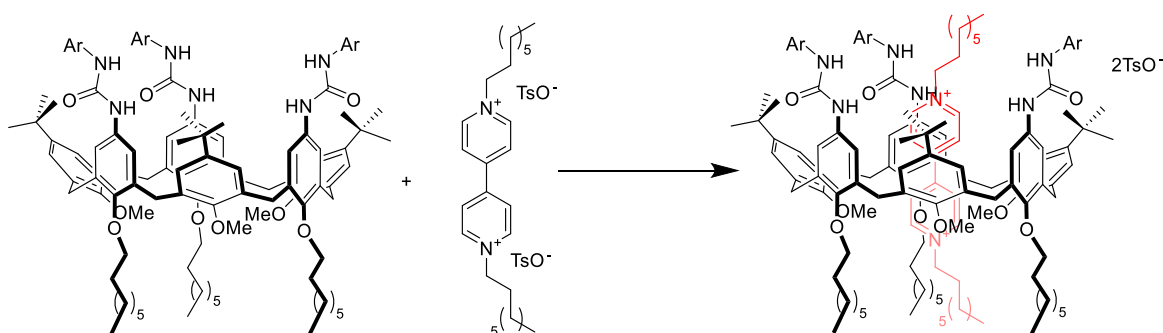


Figure 1.9: Example of complexation of di-n-octylviologen disulfonate (DOV·2TsO) by a calix[6]arene receptor functionalized with three ureido groups as hydrogen bond donors.

A notable property of calix[6]arene derivatives with sulfonamide groups on the upper rim is their ability to function as receptors for specific ion pairs in low-polarity solvents, thereby demonstrating molecular recognition. In the presence of coordinating counterions such as tosylate, a pseudorotaxane complex, P[**TSA**(pC)⊃DOV]2OTs, is formed, where the calixarene adopts a partial cone (pC) conformation. In contrast, with non-coordinating counterions like halides, a complex of the form P[**TSA**(C)⊃DOV]2I is generated, where the macrocycle assumes the more typical cone (C) conformation (Figure 1.10).^[20]

Chapter 1

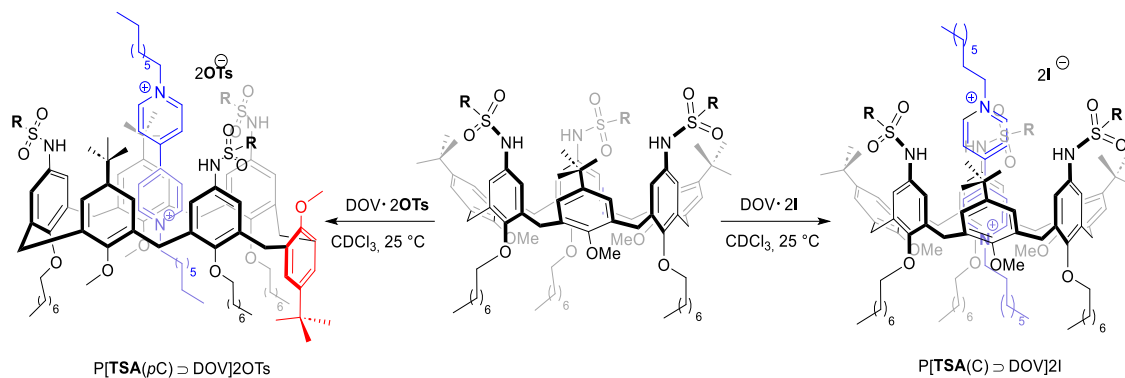


Figure 1.10: Reactivity of sulfonamide calix[6]arenes in the presence of coordinating and non-coordinating counterions.

Notably, the sulfonamide groups confer Brønsted acid properties to these macrocycles, enabling their use in polar solvents to catalyze Friedel-Crafts-type alkylation reactions.^[21,22] Specifically, these derivatives have proven effective in promoting the Michael addition of indoles to conjugated olefins under conditions close to physiological (Figure 1.11).

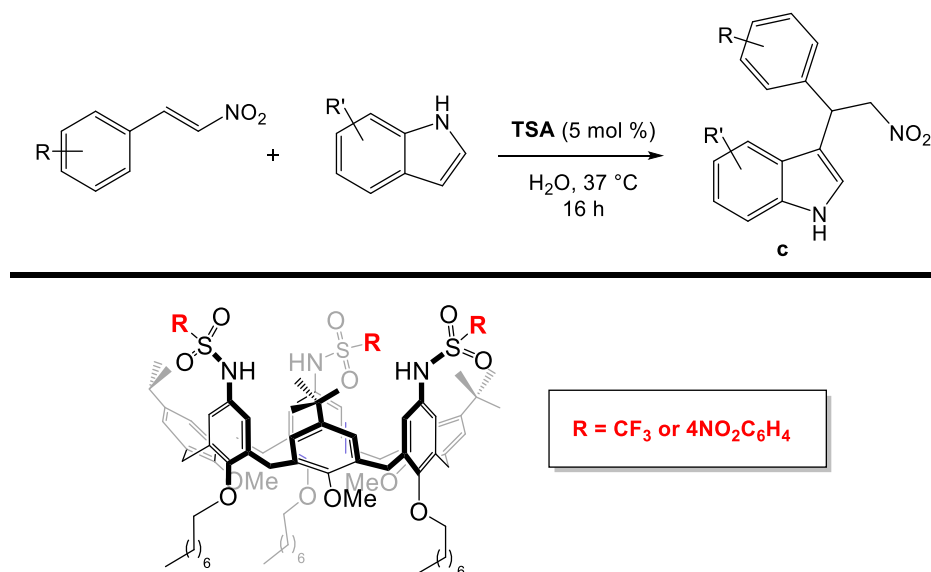


Figure 1.11: Michael reaction catalyzed by TSA.

Chapter 1

1.3 Macrocycle-based gold(I)-complexes in catalysis

Gold(I) complexes typically form bicoordinated, linear structures.^[23,24] This geometry allows for catalytic activation by simply displacing one of the two coordinated ligands to produce a cationic complex. Additionally, organometallic gold(I) complexes exhibit low nucleophilicity; the electrons in the 5d orbital are strongly retained by the metal nucleus, with decreased electron-electron repulsion due to the extended size of these orbitals. This results in low nucleophilicity, disfavoring oxidative addition processes,^[25] which in turn makes gold(I) complexes notably stable under oxidative conditions, with resilience against moisture and oxygen.

Research on gold complex catalysis has underscored the ability of gold(I) and gold(III) species to activate alkynes toward nucleophilic addition reactions,^[26] occurring both intra- and intermolecularly.^[27-29] Alkynes act as Lewis bases, donating bonding electrons to the vacant d orbitals of the metal cation and serving as π -ligands, while the metal back-donates electron density from its filled d orbitals to the alkyne's π^* orbitals. This interaction enhances the electrophilicity of the alkyne, promoting nucleophilic attack.

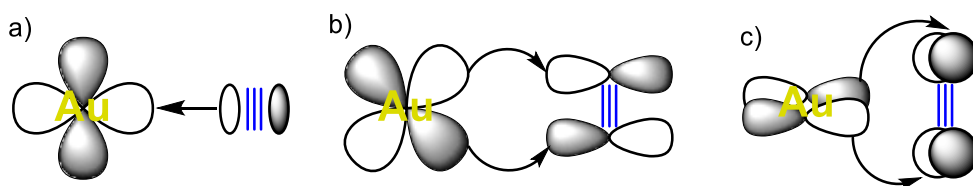


Figure 1.12: a) σ -donation $L \rightarrow M$; b) π -backdonation $M \rightarrow L$; c) perpendicular π -backdonation $M \rightarrow L$.

Comparative studies on alkyne-Au(I) versus alkene-Au(I) complexes have shown that alkynes exhibit a lower LUMO, which favors nucleophilic addition.^[30,31] This lower LUMO is likely one of the factors behind the observed "alkynophilicity" in gold(I)-catalyzed reactions. Among the widely studied reactions in this area is the cycloisomerization of 1,6-enynes (Figure 1.13).^[32]

Chapter 1

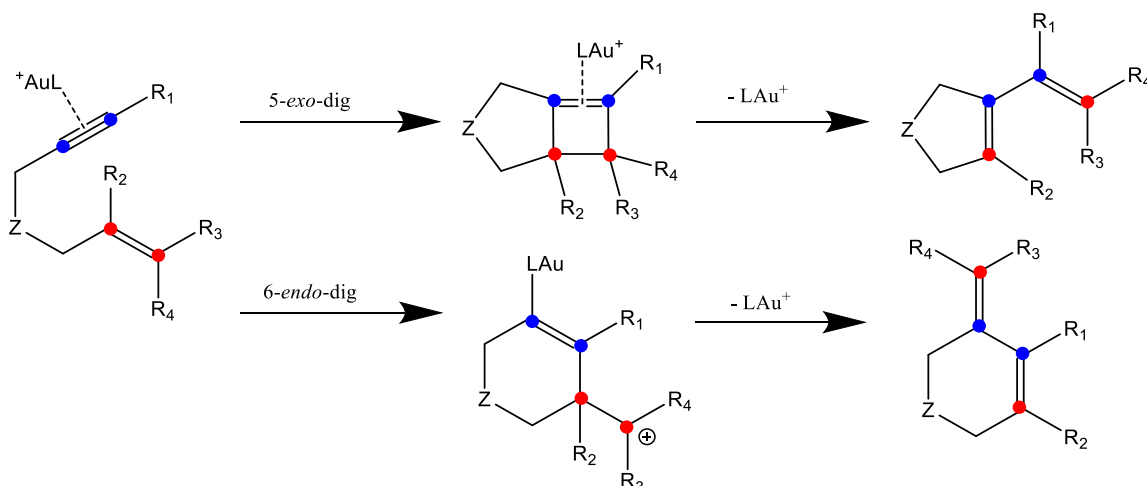


Figure 1.13: Proposed mechanism for gold(I)-catalyzed cycloisomerization reaction of 1,6-enynes.

The cycloisomerization process begins with the chemoselective coordination of the Au center to the alkyne, as shown in Figure 1.13, followed by the subsequent attack of the alkene on the resulting electrophilic adduct. The reaction can proceed along two possible pathways, *5-exo-dig* or *6-endo-dig*, leading to organometallic intermediates that can further evolve into the cyclic products described above.

Recent studies on gold(I)-catalyzed alkyne activation suggest that using macrocyclic ligands can significantly enhance the selectivity and/or activity of the catalytic metal center by promoting supramolecular non-covalent interactions. A compelling example is presented by Iwasawa, Schramm, and colleagues, who describe the synthesis of a mixed phosphite-phosphate Au(I) catalyst based on a resorcin[4]arene scaffold (Figure 1.14, a), which effectively catalyzes the selective hydration of variously substituted alkynes (Figure 1.14, b).^[33]

Chapter 1

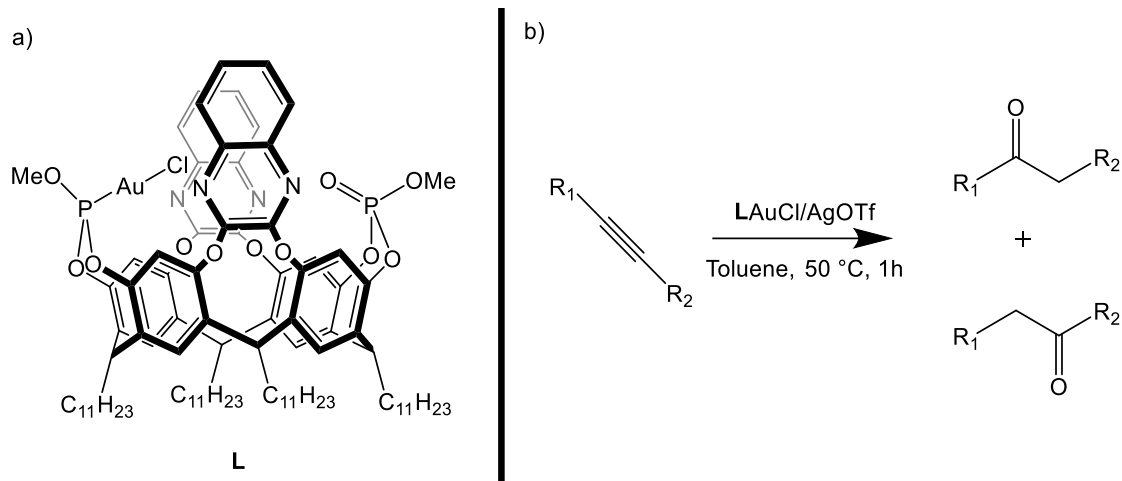


Figure 1.14: a) Structure of the Au(I) catalyst formed from the mixed phosphite-phosphate ligand based on resorcin[4]arene; b) General scheme of the hydration reaction of differently substituted alkynes catalyzed by Au(I), with R_1 being the bulkier substituent compared to R_2 .

A distinct feature of this derivative is that both the lone pair on phosphorus and the P=O group are oriented toward the macrocyclic cavity, flanked by two quinoxaline barriers that enclose the center of the macromolecule.

Studies with the cationic complex, generated by removing the Cl atom from L by adding AgOTf, revealed that the cavity can accommodate the less bulky end of the gold-alkyne adduct (Figure 1.15, a). This orientation, along with the phosphate P=O group's ability to bind a water molecule, introduces specific selectivity in the catalytic alkyne hydration reaction, favouring the formation of the product $R_1CH_2(C=O)R_2$ (Figure 1.15, b).

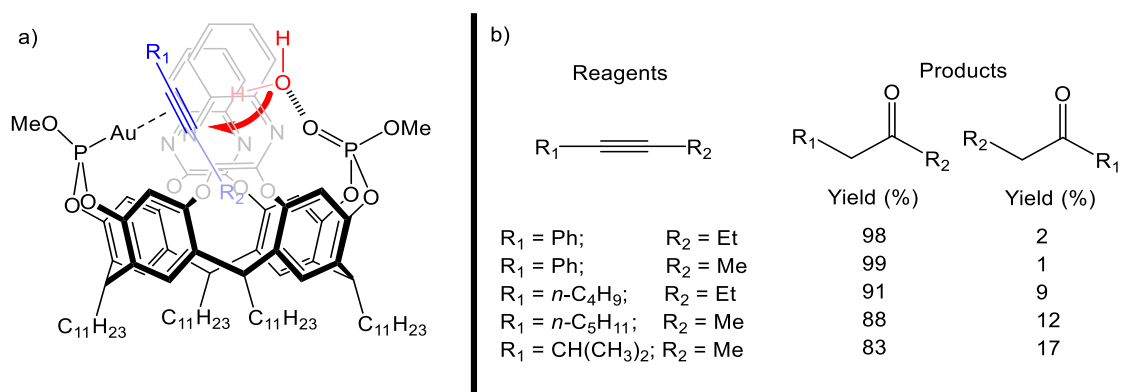


Figure 1.15: a) Proposed mechanism for the hydration of substrates; b) Yields determined for the two possible products obtained through the selective hydration of various alkyne substrates.

Chapter 1

A second example comes from the work of Schramm and collaborators, who synthesized a phosphine ligand on a resorcin[4]arene scaffold to form the corresponding Au(I) complex (**CM**, Figure 1.16, a).^[34] In their study, they investigated whether the presence of the macrocyclic cavity would influence the catalytic activity of **CM** by comparing it to a non-macrocyclic catalyst (**CP**, Figure 1.16, a) in the cycloisomerization of alkynyl-functionalized biphenyls (Figure 1.16, b).

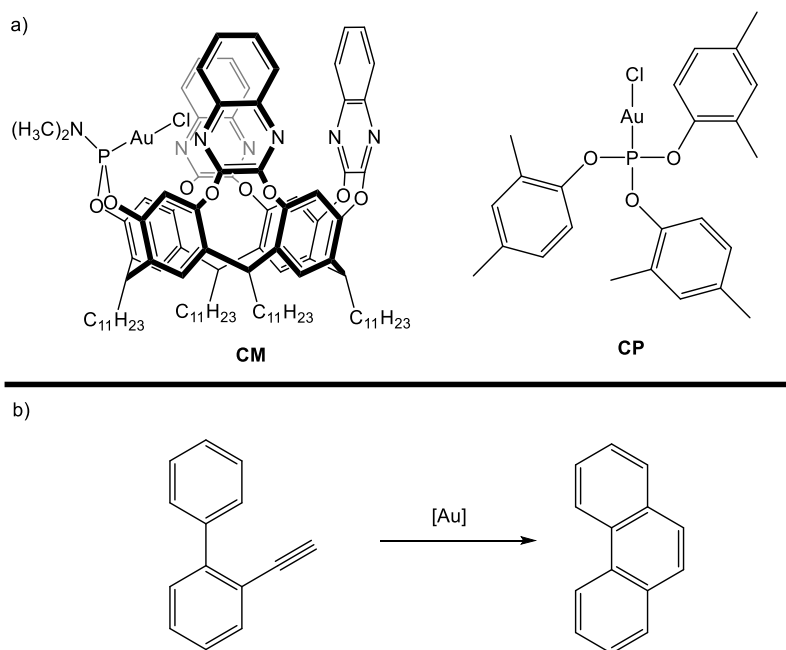


Figure 1.16: a) Structures of the **CM** (left) and **CP** (right) catalysts; b) General scheme of the cycloisomerization reaction of alkynyl-functionalized biphenyls.

Three different substrates, **Sf-Sh**, were prepared (Figure 1.17).

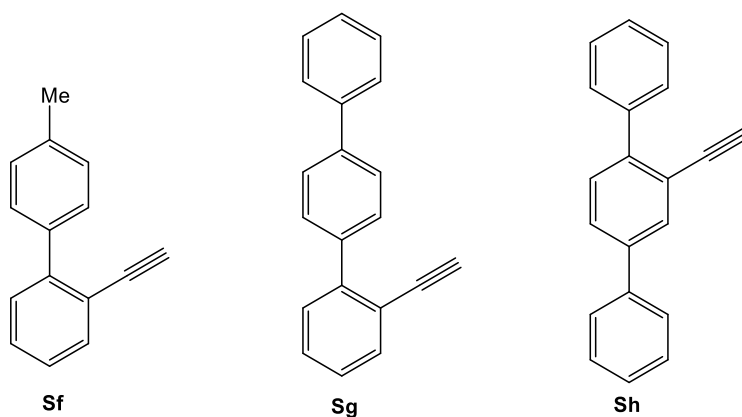
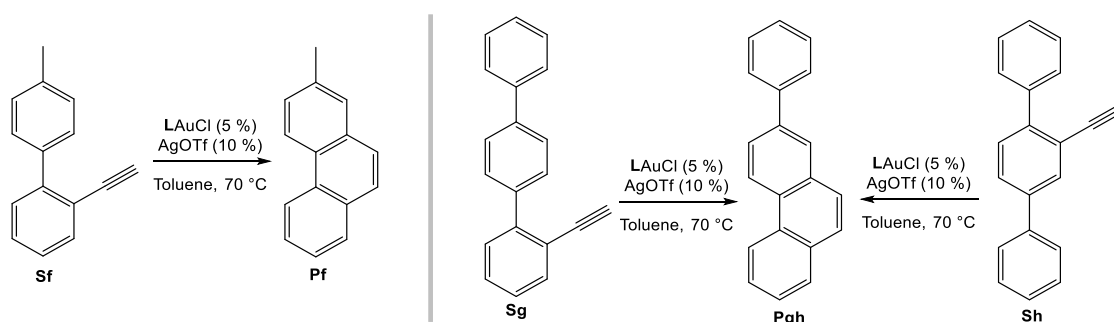


Figure 1.17: Structure of substrates **Sf-Sh**.

Chapter 1

The catalytic experiments on these substrates were evaluated using both catalysts (Table 1.4). In the reaction with substrate **Sf**, the **CM** catalyst proved ineffective in yielding the corresponding product **Pf** (Table 1.4, entry 1), whereas **CP** displayed significantly higher activity (Table 1.4, entry 2). For substrate **Sg**, **CM** also showed reduced conversion to product **Pgh** (Table 1.4, entry 3), contrasting with the smaller reduction observed for **CP** (Table 1.4, entry 4). Lastly, with substrate **Sh** (Table 1.4, entry 5), **CM** was nearly inactive, producing only trace amounts of product **Pgh**, while **CP** achieved a yield comparable to that obtained with substrate **Sf** (Table 1.4, entry 6).



Entry	Substrate	Catalyst	Time (h)	Conversion (%)
1	Sf	CM	1	0
		CM	16	0
2	Sf	CP	1	0
		CP	16	76
3	Sg	CM	1	1
		CM	16	19
4	Sg	CP	1	13
		CP	16	53
5	Sh	CM	1	0
		CM	16	5
6	Sh	CP	1	20
		CP	16	75

Table 1.4: Catalytic tests conducted using **CM** and **CP** as catalysts on substrates **Sf**, **Sg**, and **Sh**.

Chapter 1

The variations in catalytic activity can be explained by the incompatibility of the substituents on the substrates in the **Sf-h** group with the resorcin[4]arene cavity, which inhibits catalytic performance. The reduced activity observed with substrate **Sg** is likely due to the biphenyl substituent's partial affinity for the macrocyclic cavity. In contrast, the complexation of substrates **Sf** and **Sh** results in the inactivation of the **CM** complex during the reaction.

The last example was taken from the Sollogoub group, where they recently presented a cyclodextrin-based NHC gold(I)-complex characterized by the inclusion of the gold nuclei inside the macrocyclic cavity (Figure 1.18).^[35] This property allowed to control the selectivity of the reaction catalyzed by the complex on three different levels: substrate selection, product selection and enantioselection.

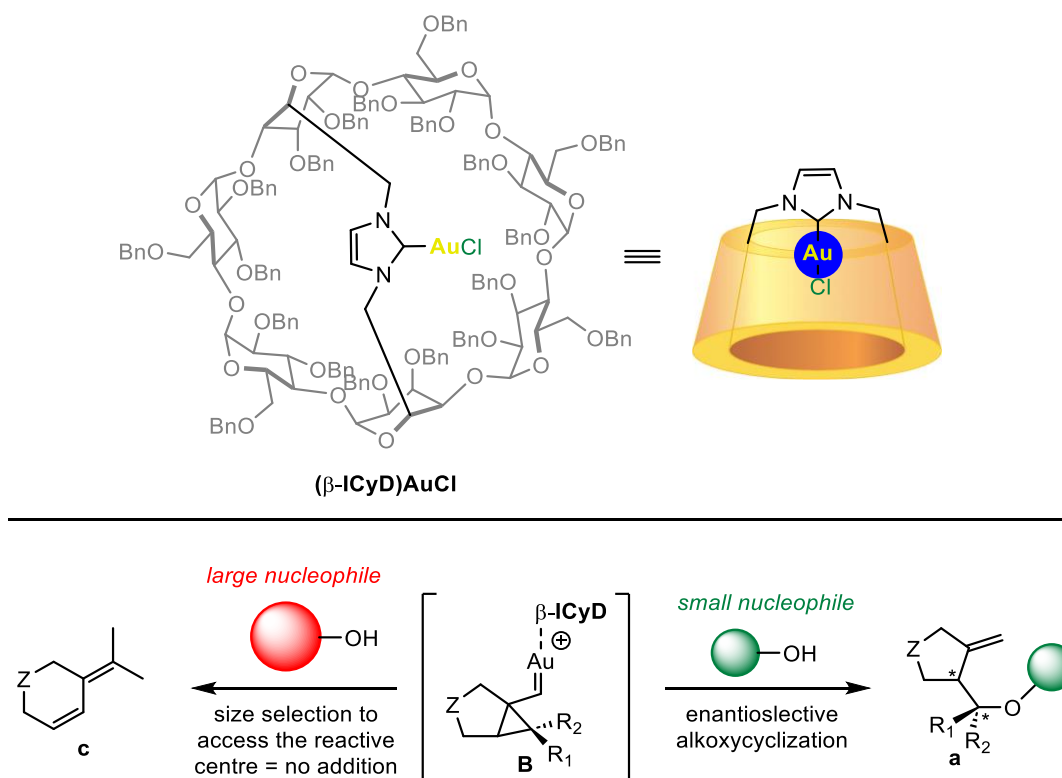
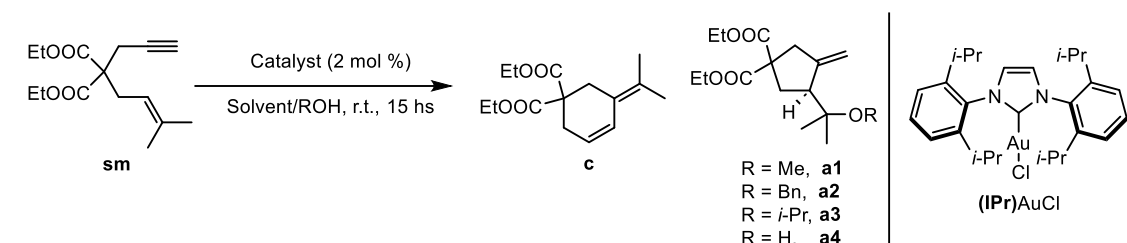


Figure 1.18: Structure of $(\beta\text{-ICyD})\text{AuCl}$ complex and scheme presenting the enantioselection, size-exclusion selection and product selection applied to the alkoxymercuration reaction of 1,6-enynes.

The hypothesis proposed was that nucleophilic addition on the α -cyclopropylcarbene intermediate **B** would depend on the nucleophile's accessibility to the intermediate and that the $\beta\text{-ICyD}$ cavity could influence this accessibility. By varying the size of the

Chapter 1

nucleophile, it might be possible to control the formation of either product **c** or **a**, with potential stereoselective control for **a**. To test this, the alkoxycyclization reaction catalyzed by (β -**ICyD**)AuCl was investigated with different external nucleophiles to assess if modulation of the reaction outcome could be achieved (Table 1.5).



Entry	Catalyst	R	Yield (%) ^f (e.r.) ^g	
			c	a
1 ^b	(IPr)AuCl	Me	--	a1 : 98
2 ^b	(β - ICyD)AuCl	Me	--	a1 : 95 (97:3) (-)
3 ^c	(β - ICyD)AuNTf ₂	Me	--	a1 : 77 (95:5) (-)
4 ^b	(IPr)AuCl	Bn	--	a2 : 90
5 ^b	(β - ICyD)AuCl	Bn	--	a2 : 90 (92:8) (-)
6 ^c	(β - ICyD)AuNTf ₂	Bn	12	a2 : 69 (88:12) (-)
7 ^b	(IPr)AuCl	<i>i</i> -Pr	--	a3 : 86
8 ^b	(β - ICyD)AuCl	<i>i</i> -Pr	30	a3 : 53 (73:27) (-)
9 ^c	(β - ICyD)AuNTf ₂	<i>i</i> -Pr	12	a3 : 51 (93:7) (-)
10 ^d	(IPr)AuCl	H	--	a4 : >99
11 ^d	(β - ICyD)AuCl	H	10	a4 : 51 (93:7) (-)
12 ^e	(β - ICyD)AuNTf ₂	H	10	a4 : 61 (94:6) (-)

a) All experiments were performed at 0.05 mol/L. b) Substrate **sm** in DCM was added to a mixture of **LAuCl** (2 mol %) and AgSbF₆ (2 mol %) in ROH (ROH/DCM 7/3 v/v). c) ROH/CH₂Cl₂ (7/3 v/v). d) Substrate **sm** was added to a mixture of **LAuCl** (2 mol %) and AgSbF₆ (2 mol %) in dioxane/H₂O (7/1 v/v). e) Dioxane/H₂O (7/1 v/v). f) Isolated yields. g) e.r. values were determined using chiral HPLC.

Table 1.5: Studies of the selectivity of (β -**ICyD**)AuCl for the alkoxycyclization reaction of **sm**.

The alkoxycyclization reaction for substrate **sm** was tested employing different alcohols (Table 1.5). The results suggested that nucleophile size played a crucial role, with *i*-PrOH, being the largest alcohol, also acting as the least effective nucleophile. However, water's behavior in this series was unexpected, as its smaller size should theoretically favor the hydroxycyclization pathway. Further tests led to the conclusion that water was overall a

Chapter 1

"worst" nucleophile compared to MeOH due to the hydrophobic nature of the macrocyclic cavity. In summary, the cavity in the β -**ICyD**-based catalytic system played a significant role in alkoxy cyclization reactions. The asymmetric shape of these chiral nanoreactors induced highly stereoselective transformations, in some cases achieving the highest enantiomeric ratio (e.r.) values reported for this reaction. While the formation of a six-membered ring occurred in the absence of alcohols as external nucleophiles, a result also governed by the cavity's shape, the confined environment of the metal within β -**ICyD** further enabled selectivity in the alcohol addition process through size exclusion or hydrophobic effects.

Chapter 1

1.4 Bibliography

- [1] a) S. Kubik, *Supramolecular Chemistry: From Concepts to Applications*. Walter De Gruyter GmbH, Berlin (Germany), **2020**, ISBN: 978-3-11-059560-4; b) P. D. Beer, T. A. Barendt, J. Y. C. Lim, *Supramolecular Chemistry: Fundamentals and Applications*. Oxford University Press, Oxford (UK), **2022**; ISBN: 978-0-19-883284-3; c) M. Morimoto, S. M. Bierschenk, K. T. Xia, R. G. Bergman, K. N. Raymond, F. D. Toste, *Nat. Catal.*, **2020**, 3, 969-984.
- [2] L. J. Jongkind, X. Caumes, A. P. T. Hartendorp, J. N. H. Reek, *Acc. Chem. Res.*, **2018**, 51, 2115-2128.
- [3] a) D. H. Leung, R. G. Bergman, K. N. Raymond, *J. Am. Chem. Soc.*, **2006**, 128, 9781-9797; b) Z. J. Wang, C. J. Brown, R. G. Bergman, K. N. Raymond, F. D. Toste, *J. Am. Chem. Soc.*, **2011**, 133, 7358-7360; c) H. Amouri, C. Desmarets, J. Moussa, *Chem. Rev.*, **2012**, 112, 2015-2041.
- [4] D. Armspach, D. Matt, *C. R. Chim.*, **2011**, 14, 135-148.
- [5] C. Jeunesse, D. Armspach, D. Matt, *Chem. Commun.*, **2005**, 5603-5614.
- [6] D. Sémeril, C. Jeunesse, D. Matt, L. Toupet, *C. R. Chim.*, **2008**, 11, 583-594.
- [7] M. Lejeune, C. Jeunesse, D. Matt, N. Kyritsakas, R. Welter, J. P. Kintzinger, *J. Chem. Soc. Dalton Trans.*, **2002**, 1642-1650.
- [8] S. Sameni, M. Lejeune, C. Jeunesse, D. Matt, R. Welter, *Dalton Trans.*, **2009**, 7912-7923.
- [9] L. Monnereau, D. Sémeril, D. Matt, L. Toupet, *Chem. Eur. J.*, **2010**, 16, 9237-9247.
- [10] L. Monnereau, D. Sémeril, D. Matt, *Actual. Chim.*, **2012**, 8-12.
- [11] C. Gibson, J. Rebek Jr., *Org. Lett.*, **2002**, 4, 1887-1890.
- [12] D. Matt, J. Harrowfield, *ChemCatChem*, **2021**, 13, 153-168.
- [13] C. D. Gutsche, *Calixarenes Revisited*; Springer; **1998**
- [14] A. Arduini, A. Pochini, A. Secchi, *Eur. J. Org. Chem.*, **2000**, 12, 2325-2334.

Chapter 1

- [15] S. Le Gac, I. Jabin, *Chem. Eur. J.*, **2008**, 14, 548-557.
- [16] M. Cametti, M. Nissinen, A. Dalla Cort, L. Mandolini, K. Riassanen, *J. Am. Chem. Soc.*, **2007**, 129, 3641-3648.
- [17] G. Cera, A. Arduini, A. Secchi, A. Credi, S. Silvi, *Chem. Rec.*, **2021**, 21, 1161-1181.
- [18] a) A. Arduini, F. Ciesa, M. Fragassi, A. Pochini, A. Secchi, *Angew. Chem. Int. Ed.*, **2005**, 44, 278-281; b) A. Arduini, R. Ferdani, A. Pochini, A. Secchi, F. Ugozzoli, *Angew. Chem. Int. Ed.*, **2000**, 39, 3453-3456.
- [19] M. Bazzoni, V. Zanichelli, L. Casimiro, C. Massera, A. Credi, A. Secchi, S. Silvi, A. Arduini, *Eur. J. Org. Chem.*, **2019**, 3513-3524.
- [20] G. Cera, M. Bazzoni, A. Arduini, A. Secchi, *Org. Lett.*, **2020**, 22, 3702-3705.
- [21] G. Cera, D. Balestri, M. Bazzoni, L. Marchiò, A. Secchi and A. Arduini, *Org. Biomol. Chem.*, **2020**, 18, 6241-6246.
- [22] G. Cera, F. Cester Bonati, M. Bazzoni, A. Secchi, A. Arduini, *Org. Biomol. Chem.*, **2021**, 19, 1546-1554.
- [23] Carvajal, M. A., Novoa, J. J. & Alvarez, S. *J. Am. Chem. Soc.*, **2004**, 126, 1465-1477.
- [24] Schwerdtfeger, P., Hermann, H. L. & Schmidbaur, H. *Inorg. Chem.*, **2003**, 42, 1334-1343.
- [25] Nakanishi, W., Yamanaka, M. & Nakamura, E., *J. Am. Chem. Soc.*, **2005**, 127, 1446-1453.
- [26] Hashmi, A. S. K. *Gold Bull.*, **2004**, 37, 51-65.
- [27] Fukuda, Y., Utimoto, K. & Nozaki, M. *Heterocycles*, **1987**, 25, 297-300.
- [28] Hashmi, A. S. K., Schwarz, L., Choi, J.-H. & Frost, T. M. *Angew. Chem. Int. Ed.*, **2000**, 39, 2285-2288.
- [29] Fukuda, Y. & Utimoto, K., *J. Org. Chem.*, **1991**, 56, 3729-3731.
- [30] Hartwig, R., *J. Phys. Chem.*, **1996**, 100, 12253-12260.
- [31] Nechaev, M., Rayon, V., Frenking, G., *J. Phys. Chem. A*, **2004**, 108, 3134-3142.
- [32] R. Dorel, A. Echavarren, *Chem. Rev.*, **2015**, 115, 9028-9072.

Chapter 1

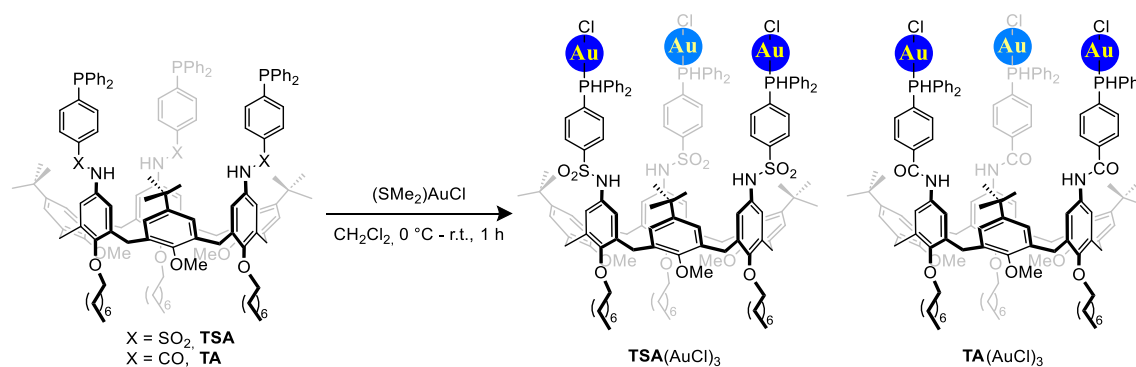
- [33] M. Inoue, K. Ugawa, T. Maruyama, T. Iwasawa, *Eur. J. Org. Chem.* **2018**, 5304-5311.
- [34] L. E. Rusali, M. P. Schramm, *Tetrahedron Lett.*, **2020**, 61, 152333.
- [35] C. Tugny, N. del Rio, M. Koohgard, N. Vanthuyne, D. Lesage, K. Bijouard, P. Zhang, J. M. Suárez, S. Roland, E. Derat, O. Bistri-Aslanoff, M. Sollogoub, L. Fensterbank, V. Mouriès-Mansuy, *ACS Catal.*, **2020**, 10, 5964-5972.

Chapter 2. Synthesis and Catalytic studies of novel Calix[6]arene-based gold(I) dimeric complexes **A**, **B** and **C**(AuCl)₂

2.1 Introduction

The use of macromolecule-based phosphine ligands in catalysis has gained a lot of interest in recent years,^[1] due to the possibility to exploit the macrocyclic cavity to control both regio- and enantioselectivity of the catalytic reaction.^[2] Among the literature, there are many examples using cavitands like resorcin[4]arenes^[3] and calix[4]arenes.^[4] Employing calix[6]arene as potential macrocyclic ligand presents a much more difficult challenge due to the flexibility of the cavity, a feature that makes them a much more desirable candidate for the formation of rotaxane and pseudo-rotaxane complexes or molecular machines.^[5] In a recent paper, published from our research group, this challenge was tackled and a new calix[6]arene-based multi-functional gold(I)-complexes, **TA**(AuCl)₃ and **TSA**(AuCl)₃, were synthesized and studied.^[6]

In this paper, we describe the synthesis of the calix[6]arene-based ligands **TA** and **TSA** starting from the known calix[6]arene intermediate **TN**^[7] and the formation of the corresponding gold(I)-complexes **TA**(AuCl)₃ and **TSA**(AuCl)₃ by mixing the desired triphosphine derivative with 3 equivalents of (SMe₂)AuCl (Scheme 2.1).



Scheme 2.1: Structure of the triphosphine ligands **TSA** and **TA** and the formation of the corresponding gold(I)-complexes **TSA**(AuCl)₃ and **TA**(AuCl)₃.

Chapter 2

Afterward, solutions of **TA** and **TSA** derivative were equilibrated with a dialkylviologen salt to test if they were suitable to form pseudo-rotaxane type of complexes with said *host* (Figure 2.1). From this experiment, it was possible to identify **TSA** and the corresponding gold(I)-complex **TSA(AuCl)₃** as the ones able to host **DOV·2OTs** in their cavities, since **TA** couldn't generate hydrogen bonds strong enough to separate the ionic couple of the viologen salt and to promote its trading into the cavity.^[8]

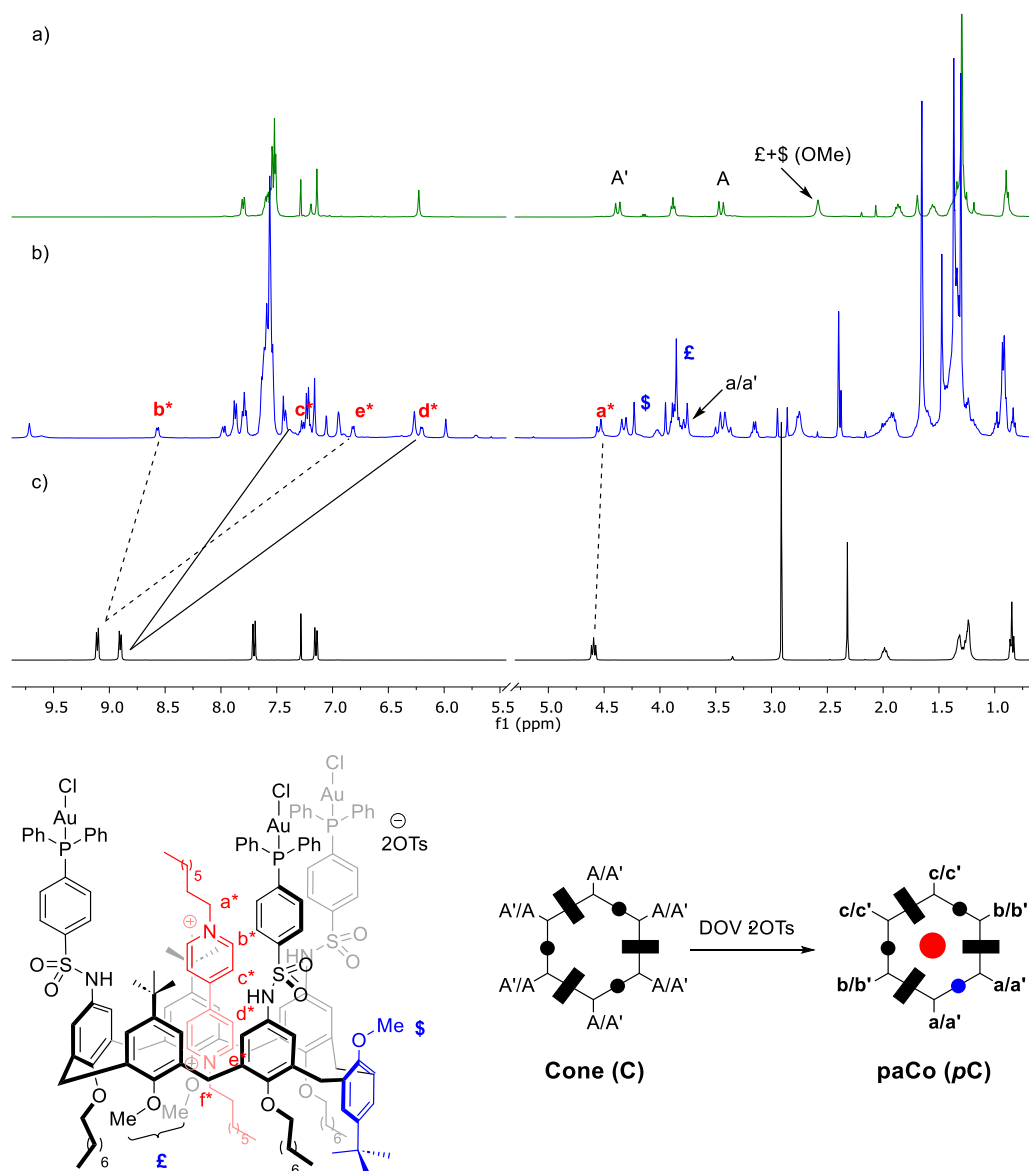
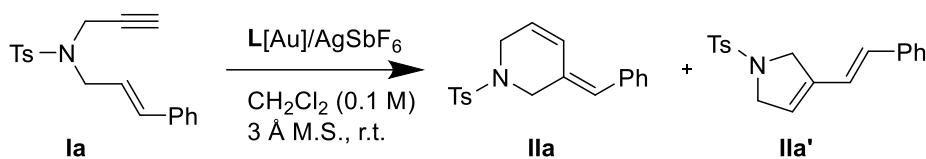


Figure 2.1: (Top) Stack plot of the ¹H NMR spectra of: a) free Host **TSA(AuCl)₃**, c) free Guest **DOV·2OTs**, and b) complex **P[TSA(AuCl)₃(pC)·DOV]2OTs**. (Bottom) Structure of complex **P[TSA(AuCl)₃(pC)·DOV]2OTs** and schematic representation of the complexation reaction.

Chapter 2

Secondly, the catalytic activity of these catalysts was evaluated for a well-known gold(I)-catalyzed cycloisomerization reaction of 1,6-enynes (Table 2.1).^[9]



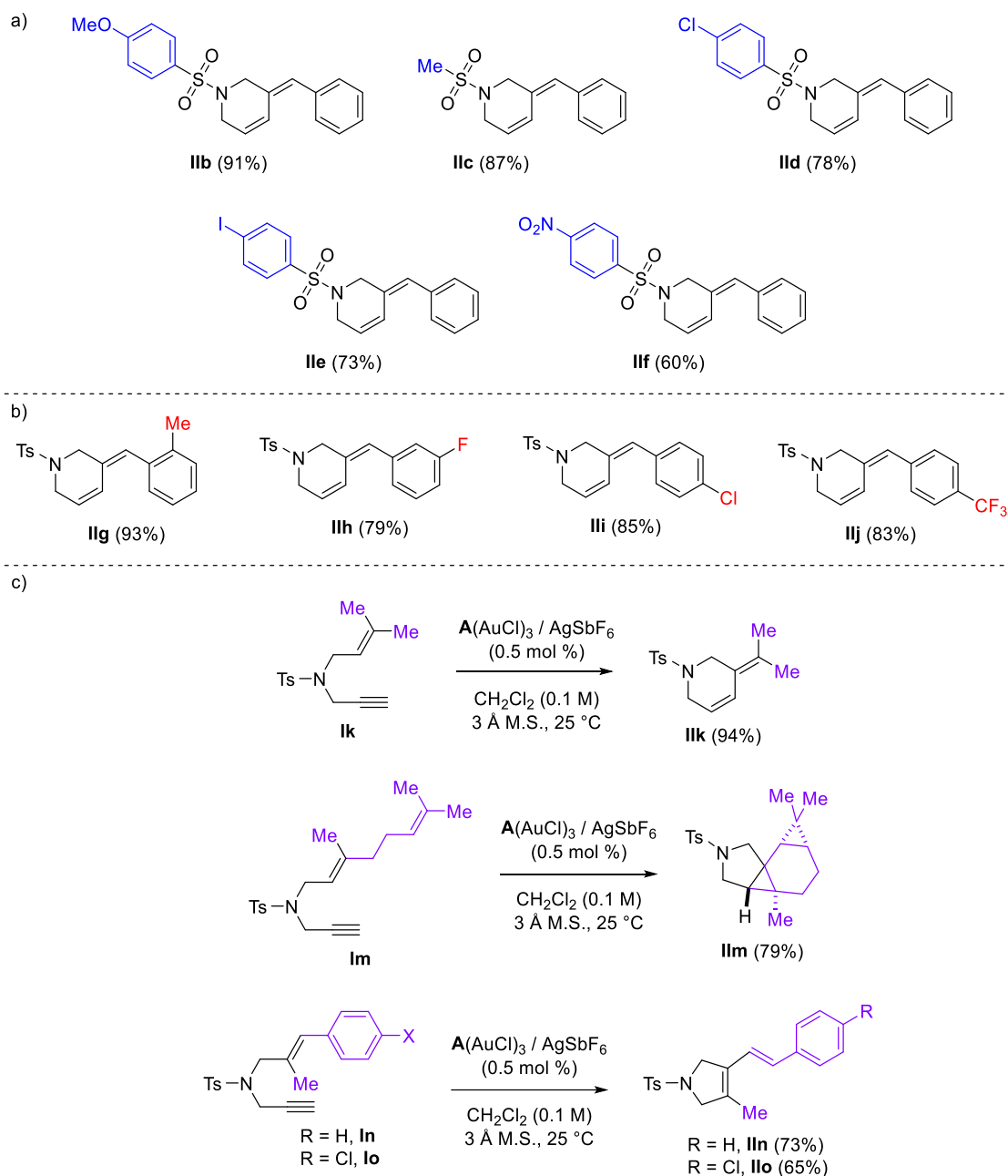
Entry	L[Au] _n	t (min.)	11a/11a'	11a [%]
1 ^[a]	TSA(AuCl) ₃ (0.50 mol %)	30	14:1	91
2 ^[b]	TSA(AuCl) ₃ (0.25 mol %)	60	-	85
3 ^[c]	TA(AuCl) ₃ (0.50 mol %)	30	13:1	87
4 ^[d]	PPh ₃ AuCl (2.0 mol %)	5	1:0	100
5 ^[d]	JohnPhosAuCl (2.0 mol %)	120	7:1	87

[a] Reaction conditions: **1a** (0.2 mmol), AgSbF₆ (1.5 mol%), isolated yields. [b] **1a** (0.2 mmol), AgSbF₆ (0.75 mol%). [c] **1a** (0.2 mmol), B (0.5 mol%), (SMe₂)AuCl (1.5 mol%), AgSbF₆ (1.5 mol%). [d] Reported data.^[10] Ts=4-toluensulfonyl.

Table 2.1: Table of optimization for the cycloisomerization reaction of model substrate **1a**.

From these experiments it was determined that both catalysts generate selectively the 6-endo-dig rearranged product **11a**. Then, the scope of the catalytic reaction was explored using TSA(AuCl)₃ testing alteration in both the sulfonamide and alkene moieties. It was possible to achieve good conversion inserting both electron-withdrawing and electron-donating groups on the sulfonamide moieties (Scheme 2.2, a). Substitution on the ortho position of the phenyl group didn't affect the reactivity leading (Scheme 2.2, b product **11g**), but by inserting electron-withdrawing groups in both the meta and para positions, the catalyst required additional time to achieve full conversion, isolating the corresponding products **11h-j** in good yields (Scheme 2.2, b). The introduction of different substituents in the alkene moiety could influence the outcome of the reaction, like in the case of the tetracyclic product **11m** and the 5-exo-dig product **11n-o** (Scheme 2.2, c).

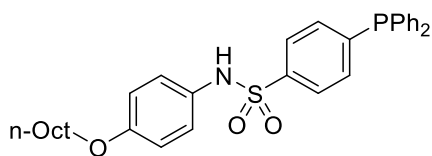
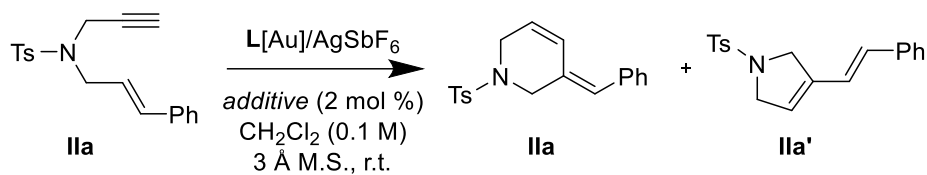
Chapter 2



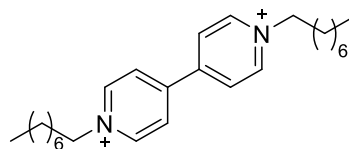
Scheme 2.2: Scope of the cycloisomerization reaction testing for different: a) sulfonamide moieties, b) substituents on the aryl unit and c) alkene substituents.

Finally, the role of the cavity was tested by comparing the reactivity of **TSA**(AuCl)₃ with the corresponding monomeric catalysts **SA**(AuCl) and performing the catalytic reaction in the presence of the *host* complexing agent DOV·2OTs (Table 2.2).

Chapter 2



SA



DOV·2OTs

Entry	$L[Au]_n$	additive	IIa/IIa'	IIa [%]
1	SA (AuCl)	-	11:1	93
2	TSA (AuCl) ₃	DOV · 2OTs	14:1	89

[a] Yield determined via NMR (1,3,5-trimethoxybenzene as I.S.)

Table 2.2: Cycloisomerization reaction experiment on model substrate **IIa** to evaluate the role of the macrocyclic cavity of **TSA**(AuCl)₃.

Even if the regioselectivity for the 6-endo-dig product dropped using the monomeric catalyst, indicating an important cooperative role between the three phosphine implanted on **TSA**(AuCl)₃, the experiment with the complexating agent didn't shown any substantial variation from the control reaction. This led to the conclusion that the catalytic event take place outside the cavity, probably due to the steric hindrance that the three phosphine units exert to each other.

Chapter 2

Taking inspiration from this work, this chapter will focus on the synthesis and characterization of novel dimeric calix[6]arene-based phosphine ligands **A**, **B** and **C** and the corresponding Au(I) complexes **A**, **B** and **C**(AuCl)₂ (Figure 2.2).^[11] These derivatives are characterized by the segregation of the two metal binding sites at the opposite sides of the macrocyclic cavity, to try to maximize the possible interaction between the cavity and the gold(I) nuclei.

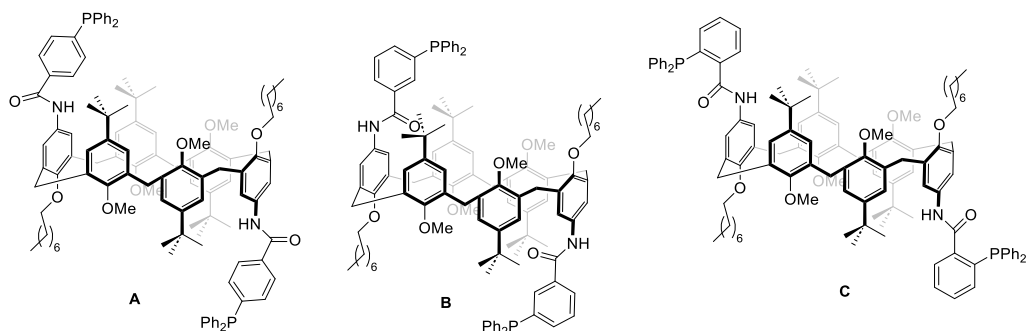
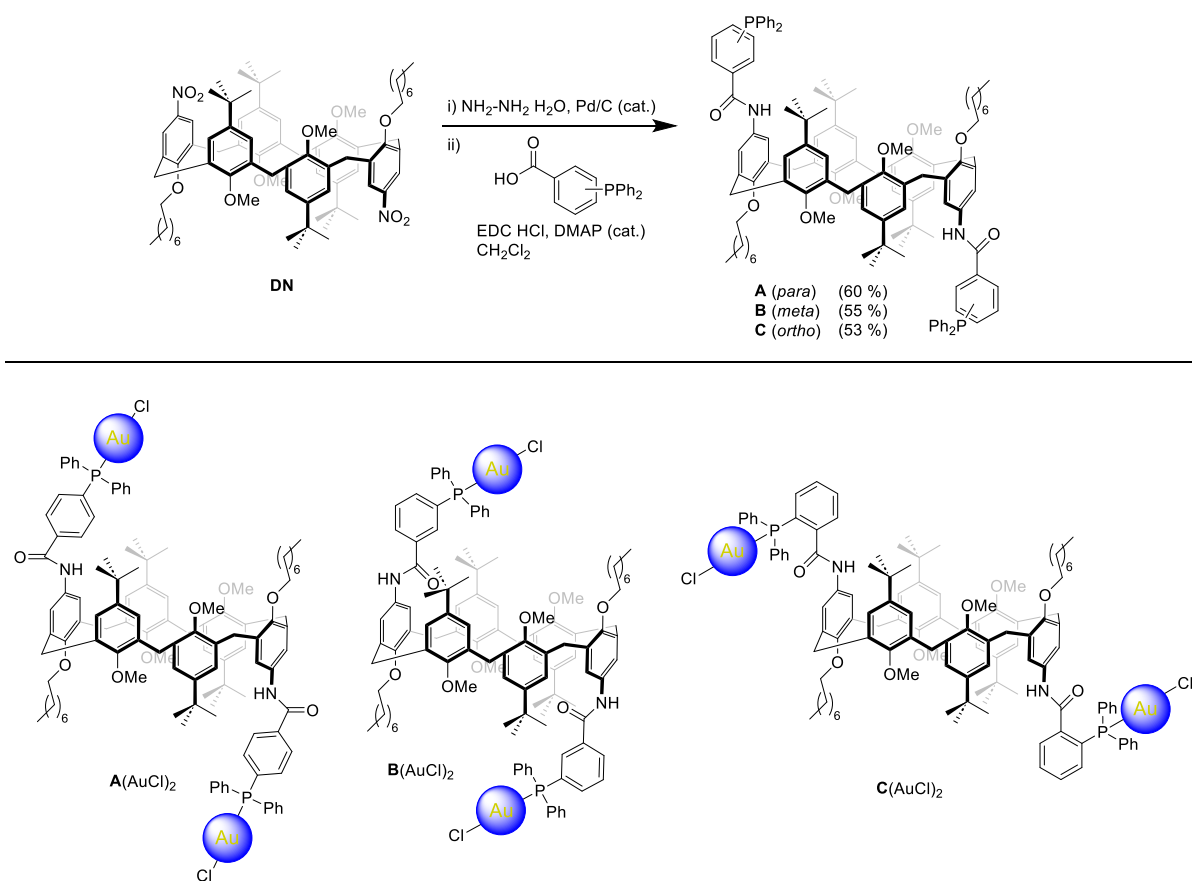


Figure 2.2: Structures of the three novel calix[6]arene-based diphosphine ligands **A**, **B** and **C**.

Chapter 2

2.2 Results and discussion

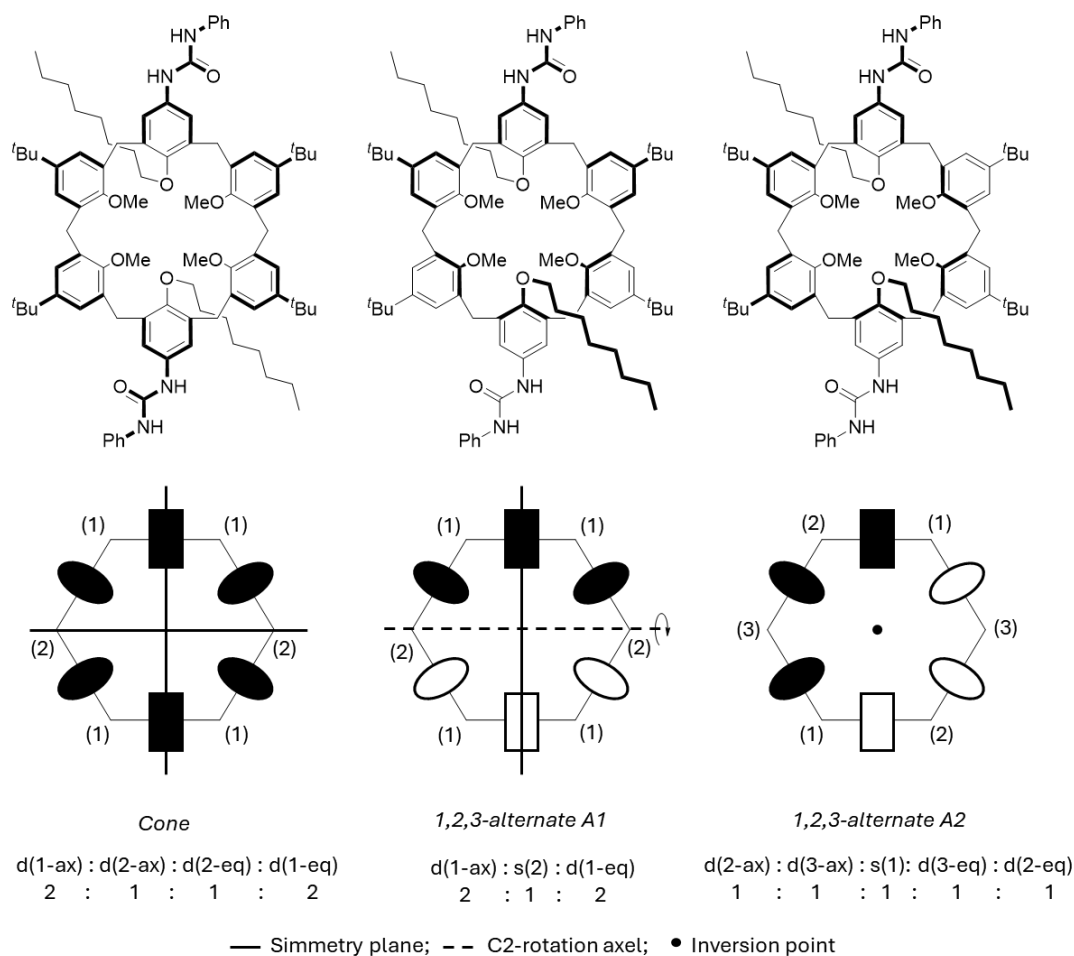
The synthesis of novel macrocyclic calix[6]arene ligands was first attempted starting from the known dioctyloxydinitro derivative **DN** (Scheme 2.3, top). Reduction of the nitro groups with hydrazine, in the presence of catalytic amounts of Pd/C (10 mol %) led to the corresponding diamino intermediate. This latter could be subsequently reacted with the desired phosphino benzoic acid derivative through a user-friendly amide coupling in the presence of EDC·HCl and catalytic amounts of DMAP in CH₂Cl₂. Under these conditions, the corresponding diphosphine intermediates **A** (*para*), **B** (*meta*), and **C** (*ortho*) were isolated in moderate yields (60 %, 55 % and 53 % respectively). Finally, gold(I) catalysts could be obtained via conventional protocols using (Me₂S)AuCl. Notably, the organometallic macrocycles **A**, **B**, **C**(AuCl)₂ could be isolated via column chromatography separation (Scheme 2.3, bottom).



Scheme 2.3: (Top) Synthetic pathway followed for the preparation of macrocyclic ligands **A** (*para*), **B** (*meta*), and **C** (*ortho*); (Bottom) structure of the corresponding gold(I)-complexes **A**, **B**, **C**(AuCl)₂.

Chapter 2

Gold(I) catalysts were subsequently fully characterized by NMR analysis and high-resolution mass spectrometry. The conformations, in low polarity solvents, is dominated by the *1,2,3-alternate* conformation assumed by the **DN** intermediate, as previously demonstrated in our recent contributions.^[12] In these papers, it's reported that this type of difunctionalized calix[6]arene derivatives can assume, in low polarity solvents, different conformations. Notably, these conformations generate different symmetries, leading to a unique signal pattern in the ¹H NMR spectrum, in particular for the bridging methylenes of the macrocyclic's scaffold (Scheme 2.4).



Scheme 2.4: Schematic representation of the different conformation of **DPU** derivative identified in low polarity solvent and the corresponding distribution of the signals in the ¹H NMR spectrum for the bridging methylenes.

The three conformations described are: *cone*, *1,2,3-alternate A1* and *1,2,3-alternate A2*. The first is characterized by the presence of two symmetry planes “cutting” the molecule in

Chapter 2

two halves, one plane passing through the substituted aromatic rings of the calix[6]arene scaffold, and the other passing through the bridging methylenes (2) (Scheme 2.4, bottom left). This symmetry generates two sets of doublets in the NMR spectrum, two doublets (one for the equatorials and one for the axials hydrogens) for the methylenes (1), integrating for a total of 4 protons, and another two doublets for the methylenes (2), integrating for two protons. The second conformation is characterized by the presence of a C₂ rotation axis passing through the two bridging methylenes (2) and by a symmetry plane passing again through the two functionalized aryl rings of the macrocyclic scaffold (scheme 2.4, bottom middle). This symmetry element generates in NMR spectrum one pair of doublets for the methylenes (1) integrating for 4 protons each, and one singlet, also integrating for 4 protons, for the methylenes (2), whose hydrogens are now symmetrical. Finally, the third conformation present an inversion point that generate two pairs of doublets for the methylenes (1) and (2), integrating for 2 protons each, and a singlet for the methylenes (3), also integrating for 2 protons (Scheme 2.4, bottom right).

Hence, the most notable features of ¹H NMR for **A**(AuCl)₂ are represented by a pattern for the methylene bridging protons in a 1:1:1 integration ratio (Figure 2.3). These include: i) two doublets at 4.2 and 3.6 ppm with a geminal coupling of $2J = 14.2$ Hz for the *a/a'* couple and ii) a singlet at 3.92 ppm for the *b* protons, typical of an *anti*-orientation.^[13] This situation suggests a single inversion point which confers to the macrocycle a high symmetrical geometry, like discussed before. Finally, a single broad peak for the four methoxy groups (\$) appears at 2.96 ppm. In analogy with parental diureido and dithioureido calix[6]arenes, we were able to observe the presence of a second minor *cone* conformer, in a $\approx 4:1$ ratio, highlighted by the presence of a second, single resonance for the methoxy groups (\$*) at 3.11 ppm. An analogous situation was observed for **B**(AuCl)₂ and **C**(AuCl)₂ as well. However, here the singlets for the *b/b'* couple overlap with the signals of the octyloxy chains (£) at 3.91 and 3.87 ppm, respectively.

Chapter 2

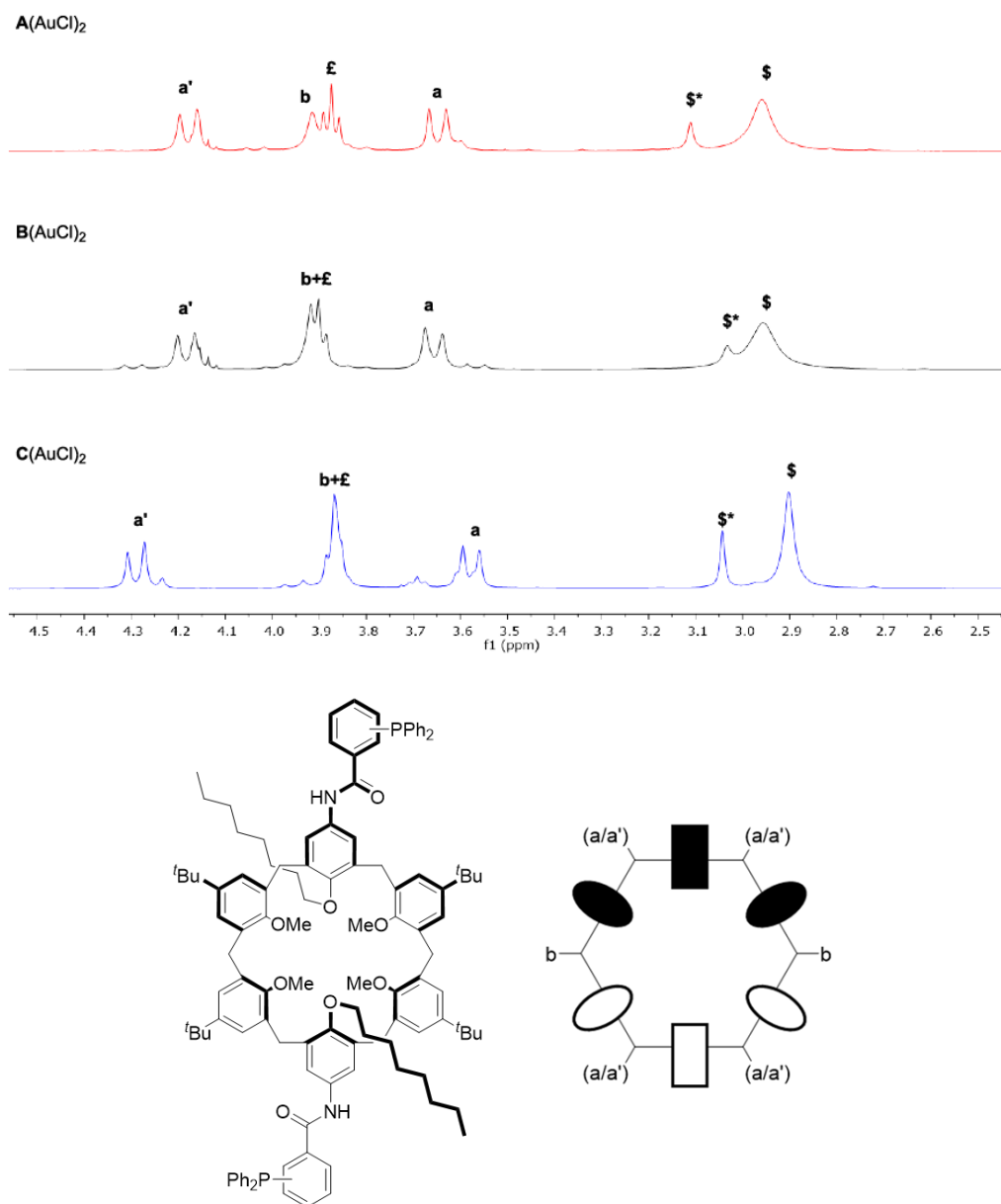


Figure 2.3: Stack plot of the region between 2.5 and 4.5 ppm of the ^1H NMR spectre of pre-catalysts **A**, **B** and **C**(AuCl)₂.

The presence of these two major conformers, in slow exchange on the NMR timescale, was finally confirmed by variable temperature NMR analysis performed for **A**(AuCl)₂ using tetrachloroethane- *d*₂ as the solvent (Figure 2.4).

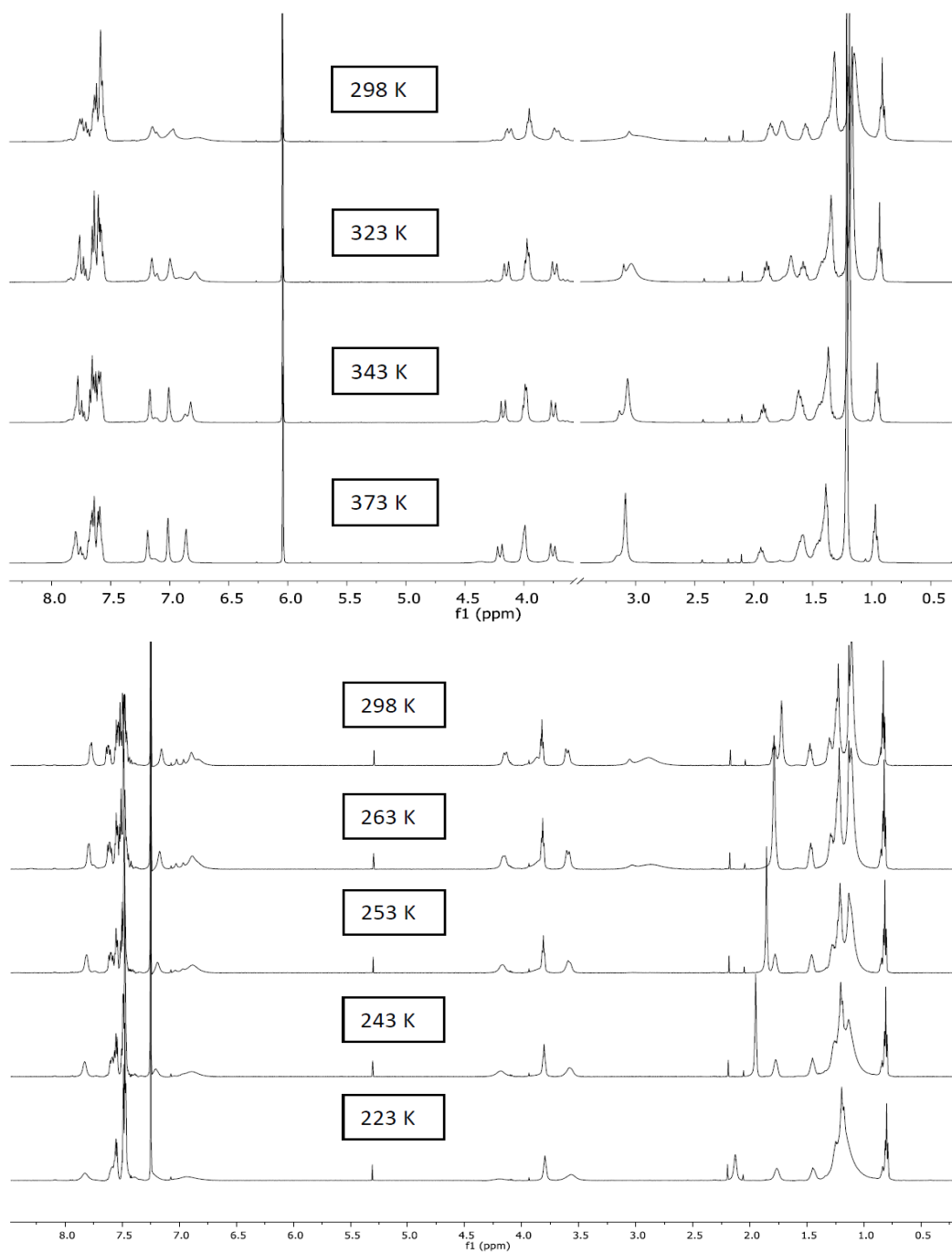


Figure 2.4: Stack plot of ^1H NMR spectra of $\mathbf{A}(\text{AuCl})_2$ taken at increasing (top) and decreasing (bottom) temperatures.

To get more insights, we attempted to obtain the solid-state structures of all the three compounds. Good quality crystals of **A**, **B**, and **C**(AuCl) $_2$, suitable for structural determination, were obtained from slow evaporation of different solvent/anti-solvent

Chapter 2

mixtures (chloroform/acetonitrile, chloroform/n-hexane, and toluene/diethyl ether, respectively). These structures, which are parallel to the ones observed on other heteroditopic, disubstituted calix[6]arenes, confirmed our hypothesis since the gold(I) nuclei point outside the macrocyclic cavity (Figure 2.5).

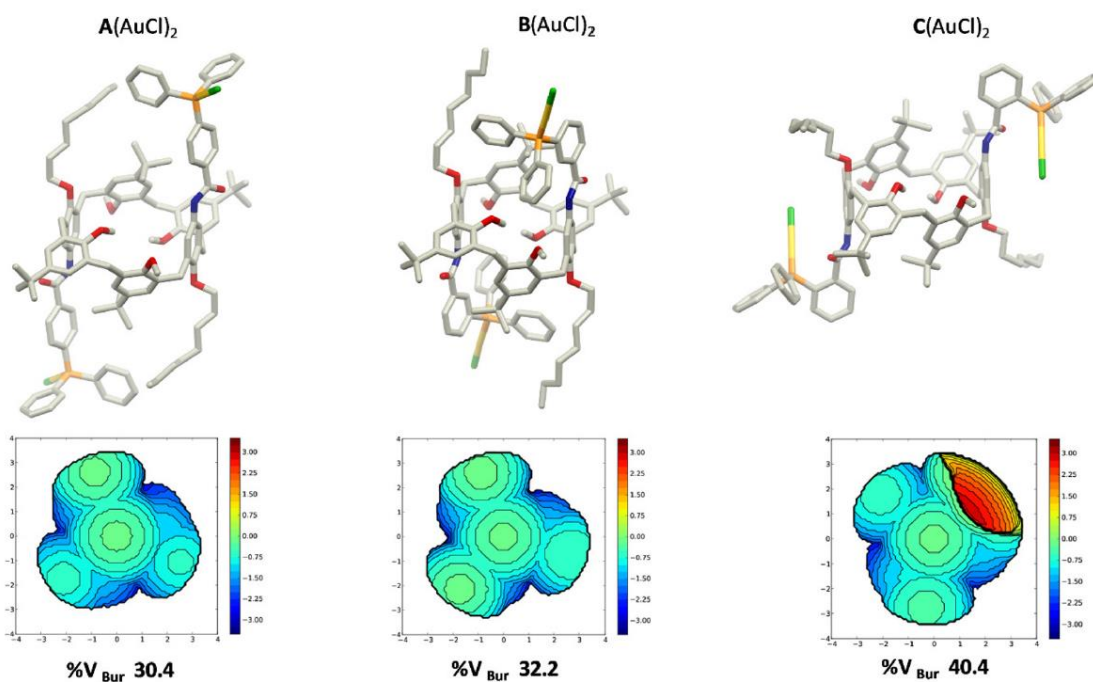


Figure 2.5: Single crystal X-ray structure of **A**, **B**, and **C**(AuCl)₂ in stick representation. Steric maps and calculated percentage of buried volume by SambVca 2.1^[14] for the corresponding complexes (bottom).

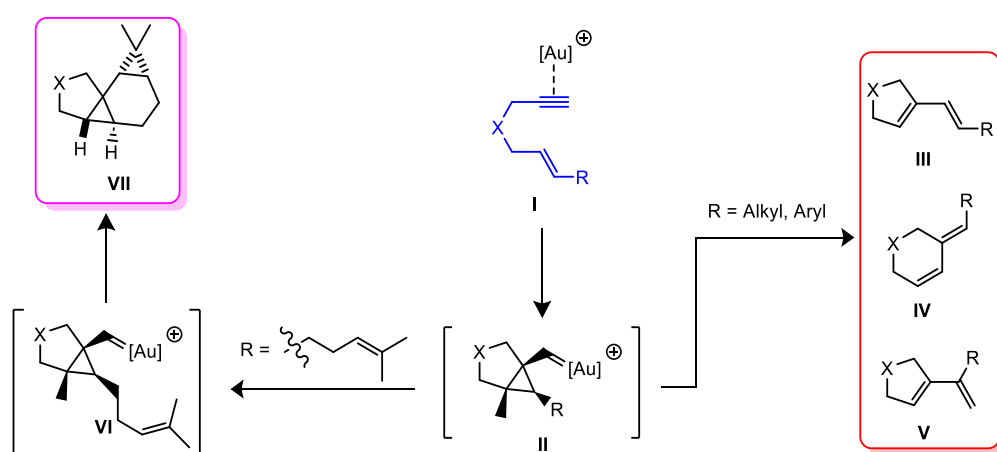
It is noteworthy that the conformation adopted by the three diametric calix[6]arene complexes is a highly symmetric *1,2,3- alternate* conformation **A2**, which differs from the one adopted in low-polar solution **A1**, for the position of the ring bearing the amide groups with respect to the inversion points of the macrocyclic ring. The different orientations of the phosphine moiety proved to be almost ineffective on the bond lengths and angles: P–Au distances range between 2.22 and 2.34 Å, while Au–Cl distances are within 2.27–2.29 Å. The P–Au–Cl angle is almost linear for the three compounds with values ranging from 175.2 to 175.5°. Differently, the steric hindrance showed an increasing trend moving from the para to the ortho-substituted complex, as highlighted by the topographic steric maps (Figure 2.5, bottom). The calculated buried volume (%V_{Bur}, Figure 2.5), defined as the proportion of the

Chapter 2

metal center's first coordination sphere occupied by the organic ligand,^[14] ranges from 30.4% for **A**(AuCl)₂ to 40.4% for **C**(AuCl)₂ (30.8% for PPh₃AuCl).^[15]

It is noteworthy that any effort to observe this conformation in solution by variable temperature NMR analysis failed, thus confirming the unique conformational features shown by these compounds in the solid state.

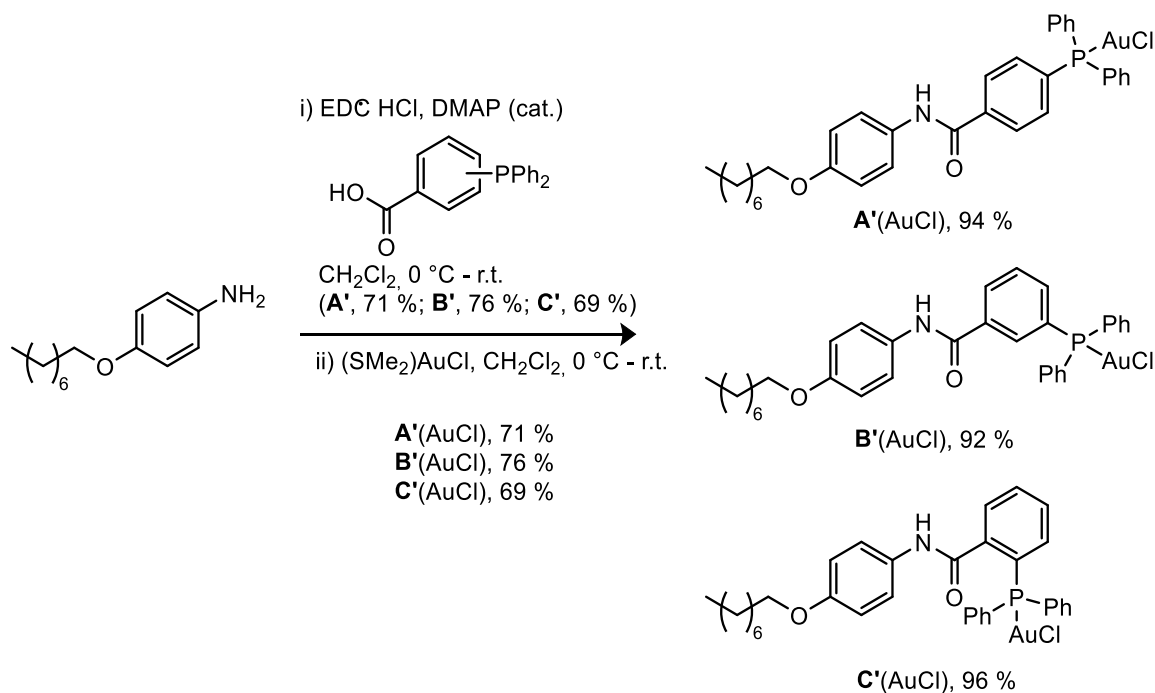
With more information on the conformation of the newly devised complexes in low-polarity solvents and their solid-state structures, the next logical step was to investigate their catalytic reactivity. To this end, the cycloisomerization of 1,6-enynes, catalyzed by gold(I), was chosen to evaluate the catalytic activity and selectivity of **A**, **B**, and **C**(AuCl)₂. These substrates exhibit intriguing reactivity, proceeding through the electrophilic activation of **I**, which generates a cyclopropyl gold carbene intermediate (**II**) via 5-*exo-dig* cyclization. This intermediate can undergo skeletal rearrangements to form complex polycyclic structures. The chemoselectivity of the reaction is influenced by both the tethering unit and the R group. For example, when the alkene fragment (R) is substituted with simple alkyl or aryl groups, single or double cleavage of C–C bonds lead to stereoisomers **III–V** (Scheme 2, red box). Interestingly, the presence of a functionalized alkene, such as in 1,6-dienynes, enhances the carbene-like reactivity of gold catalysts, promoting intramolecular cyclopropanation to form polycycles **VII** (Scheme 2, purple box). The high stereoselectivity of this process is attributed to the kinetically controlled trapping of the anti-cyclopropyl gold(I) carbene intermediate **VI** (Scheme 2.5).^[16]



Scheme 2.5. Proposed mechanism for the intramolecular cyclization reaction of 1,6-enynes.

Chapter 2

To investigate the role of the calix[6]arene cavity and the influence of the positioning of the gold(I) centers within the scaffold, we synthesized three monomeric gold catalyst analogues: **A'**, **B'**, and **C'**(AuCl). These compounds were prepared using a previously optimized protocol, starting from a 4-(octyloxy)aniline intermediate (Scheme 2.6).

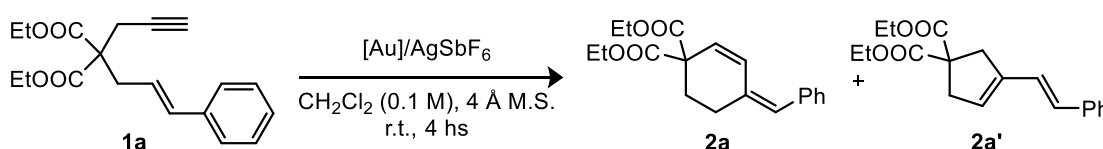


Scheme 2.6: Synthesis of the monomeric gold(I)-complexes **A'**, **B'** and **C'**(AuCl).

Substrate **1a** was reacted with the monomeric gold(I) catalyst **A'**(AuCl) (2 mol%) in the presence of AgSbF₆ as a chloride scavenger. After 4 hours, NMR analysis of the crude reaction mixture revealed high conversion of the starting material, yielding a 1:1 ratio of the 6-*endo-dig* rearranged diene **2a** and the regioisomer **2a'**, the latter formed through an initial 5-*exo-dig* cyclization (Table 2.3, entry 1). This result was compared with that obtained using the macrocyclic analogue **A**(AuCl)₂ (1 mol%), where no significant variation in product distribution was observed (Table 2.3, entry 2). Similarly, the reactivity of meta-substituted catalysts **B'**(AuCl) and **B**(AuCl)₂ was examined, with both showing comparable reactivity and selectivity (Table 2.3, entries 3-4). These findings suggest that the macrocycle in catalysts **A** and **B**(AuCl)₂ does not significantly influence product distribution, likely due to the distance between the catalytically active gold(I) centres and the macrocyclic cavity.

Chapter 2

The catalytic reaction was also conducted using **C'**(AuCl), which showed a selectivity towards product **2a** with a ratio of 1.5:1. This selectivity may be attributed to the different orientation of the phosphine ligand on the aromatic ring (Table 2.3, entry 5). Notably, this effect was significantly enhanced when using the calix[6]arene-based complex **C**(AuCl)₂ (Table 2.3, entry 6). Overall, the ortho-substituted macrocycle **C**(AuCl)₂ demonstrated improved selectivity compared to the parental macrocycles **A** and **B**(AuCl)₂, likely due to the closer proximity of the two gold(I) centers to the calix[6]arene scaffold. While preliminary, these results suggest that the conformational properties of this macrocyclic class can indeed influence selectivity in gold(I)-catalyzed cycloisomerization of 1,6-enynes.



Entry ^a	[Au]	Conv. [%]	2a/2a'
1	A' (AuCl) (2 mol %)	89	1.0:1.0
2	A (AuCl) ₂ (1 mol %)	88	1.1:1.0
3	B' (AuCl) (2 mol %)	86	1.2:1.0
4	B (AuCl) ₂ (1 mol %)	91	1.1:1.0
5	C' (AuCl) (2 mol %)	86	1.5:1.0
6	C (AuCl) ₂ (1 mol %)	89	1.8:1.0

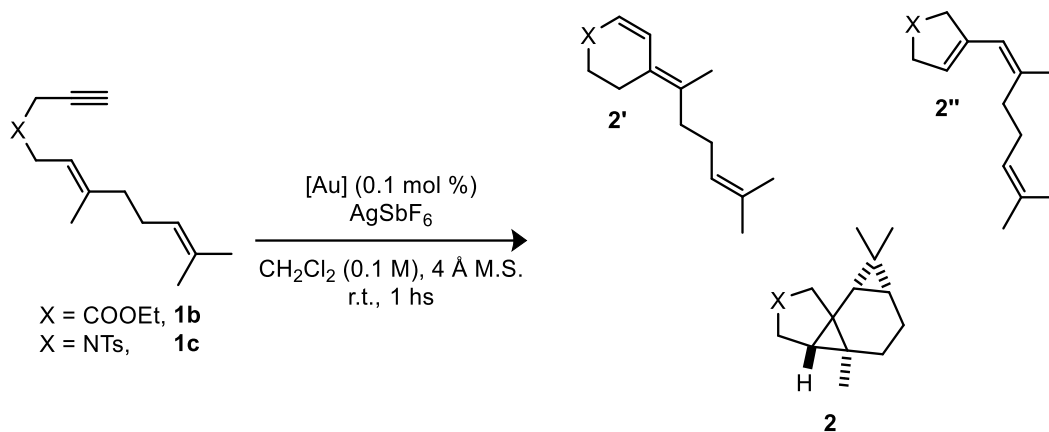
[a] Reaction conditions: **1a** (0.2 mmol), AgSbF₆ (2 mol %)

Table 2.3: Comparison of the chemoselectivity for the cyclization reaction products **2a** and **2a'** between the monomeric gold(I)-complexes **A'**, **B'**, and **C'**(AuCl) and the corresponding macrocyclic complexes **A**, **B**, and **C**(AuCl)₂.

To further investigate the influence of the relative positioning of the gold(I) centres within the calix[6]arene macrocycle in the regioselectivity of the catalytic reaction, substrates **1b** and **1c** were synthesized, featuring different tethering units and an alkyl chain with two alkene groups. The model catalytic reaction was performed under the same conditions as for **1a**: 1 mol% of the gold(I) catalyst with 2 mol% of AgSbF₆ as a chloride scavenger in CH₂Cl₂ (Table 2.4). After 1 hour, all three dinuclear gold(I) catalysts resulted in complete consumption of starting material **1b**. However, NMR analysis of the crude mixture revealed slight differences in product distribution. Catalyst **A**(AuCl)₂ gave the highest yield of tetracycle **2b** (Table 2.4, entry 1), along with monocycle **2b'**, formed via the initial 5-*exo-dig* cyclization, as the major

Chapter 2

byproduct. Catalysts **B**(AuCl)₂ and **C**(AuCl)₂ were less selective, with the latter producing increased amounts of stereoisomer **2b''** (Table 2.4, entries 2-3), likely due to the greater steric hindrance from the phosphine group at the ortho position of the amide moiety.



Entry ^a	1	[Au]	Conv. [%]	2' : 2'' : 2
1	1b	A (AuCl) ₂	100	1.0 : 0.1 : 7.2
2	1b	B (AuCl) ₂	100	1.0 : 0.1 : 5.4
3	1b	C (AuCl) ₂	100	1.0 : 0.16 : 4.7
4	1c	A (AuCl) ₂	100	0.0 : 1.0 : 7.1
5	1c	B (AuCl) ₂	100	0.0 : 1.0 : 5.0
6	1c	C (AuCl) ₂	100	0.0 : 1.0 : 4.7

[a] Reaction conditions: **1** (0.15 mmol), AgSbF₆ (2 mol %)

Table 2.4: Comparison of the chemoselectivity of the macrocyclic gold(I)-complexes **A**, **B**, and **C**(AuCl)₂ for the cyclopropanation reaction products **2**, **2'** and **2''**.

A similar trend was observed when the N-tethered diene **1c** was subjected to the gold(I) catalysts (Table 2.4, entries 4–6), with a higher formation of compound **2c''**, likely due to the increased rigidity of the N-tethering unit. These findings, in contrast to previous results with bulkier styryl-substituted 1,6-enynes, suggest that the proximity of the gold(I) centers to the calix[6]arene scaffold has little influence on the reactivity of unbiased 1,6-enynes like **1b-c**. Mechanistically, an interesting observation was made when comparing the selectivity for tetracycles **2b** and **2c** with the buried volumes of the catalysts. A strong linear correlation indicated that the selectivity of the transformation is governed entirely by the steric hindrance of the catalysts, ruling out any significant effect from complexation of substrates **1b** and **1c** within the calix[6]arene cavity (Figure 2.6).

Chapter 2

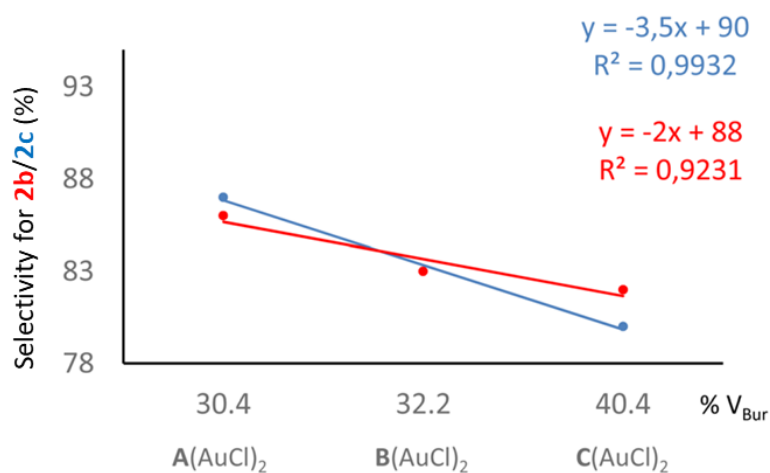
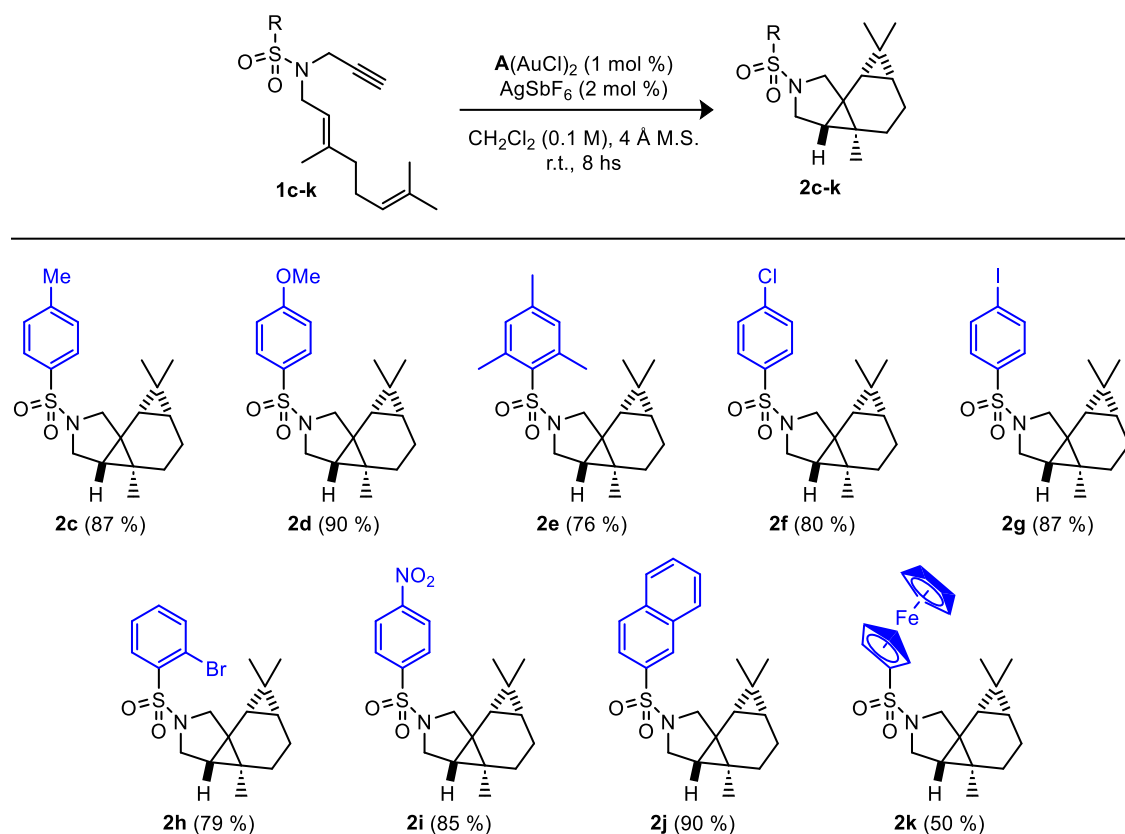


Figure 2.6: Plot of the selectivity of the catalysts **A**, **B** and **C**(AuCl)₂ for cyclization products **2b** and **2c** versus the buried volumes of said catalysts.

To further explore the applicability and activity of these new promising calix[6]arene-based catalysts, a small family of 1,6-dienynes (**1**) with variously substituted sulfonamide-based N-tethering moieties was synthesized and subjected to the unbiased complex **A**(AuCl)₂ (Scheme 2.7). Tetracycle **2c** was obtained in excellent yield (87%) as a single diastereomer after stirring the catalytic reaction for 8 hours. The presence of strong electron-donating groups at the para position of the sulfonamide, such as in the methoxy derivative **1d**, did not alter the outcome, yielding **2d** in 90%. Conversely, a reaction with the bulkier mesitylene-2-sulfonamide derivative **1e** produced an inseparable mixture of **2e'** and **2e** (76% overall yield), despite high conversion of the starting material.

Chapter 2



Scheme 2.7: Scope of the cyclopropanation reaction with substrates **1c-k** using $\mathbf{A}(\text{AuCl})_2$.

The catalyst also showed good tolerance to electron-withdrawing groups (EWGs), with halogens being particularly well tolerated. Chlorine and iodine at the para position led to full conversion of the corresponding 1,6-dienynes to tetracycles **2f** and **2g** in very good yields (80–87%), while bromine at the more hindered ortho position also provided a high yield of **2h** (79%). Among the EWGs, the nitro group was especially reactive, yielding **2i** in 85% when the catalyst loading was increased to 1.5 mol%. The reaction also proceeded smoothly with extended π -systems, such as the 2-naphthyl unit in **1j**, delivering **2j** in excellent yield (90%). Finally, we successfully introduced a ferrocene unit by synthesizing diene **1k**, which was converted into tetracycle **2k** in a synthetically useful yield (50%).

Chapter 2

2.3 Conclusions

In conclusion, the synthesis and characterization of a novel family of diametric diphosphine gold(I) complexes **A**, **B** and **C**(AuCl)₂ is presented. Their geometry in low-polarity solvents is controlled by the *1,2,3-alternate* conformation of the calix[6]arene precursor. The solid-state structure of these catalysts is reported, and the three-dimensional arrangement of these compounds is characterised in the solid state by a *1,2,3-alternate* conformation, different from the one assumed in solution, which causes the extrusion from the cavity of the catalytically active gold(I) species. Despite this discovery, the catalysts show to affect the selectivity towards the gold(I)-catalyzed cycloisomerization reaction of 1,6-enyne **1a** based on the relative position of the phosphine towards the macrocyclic scaffold. In parallel, the role of the cavity is investigated by comparing the product distribution obtained employing the macrocyclic catalysts and the monomeric counterparts **A'**, **B'** and **C'**(AuCl). The results show that only **C**(AuCl)₂ demonstrate improve selectivity, likely due to the closer proximity of the gold(I)-nuclei to the cavity. Changing the substrates to dienynes **1b-c** show a strong linear correlation between the selectivity for the tetracyclo rearrangement products **2b-c** and the buried volume of the cavity. This suggest that the selectivity of the transformation is guided mainly by the steric hindrance of the ligand, ruling out any effect due to the complexation of the substrate inside the cavity. Finally, the still promising catalytic activity of these new catalysts is tested on a family of dienynes substrate, showing good tolerance for different substituents on the sulfonamide moiety. This work show that in principle calix[6]arene scaffold can be used for the design of macrocyclic-phosphine ligands that are able to control the selectivity of gold(I)-catalyzed reaction.

Chapter 2

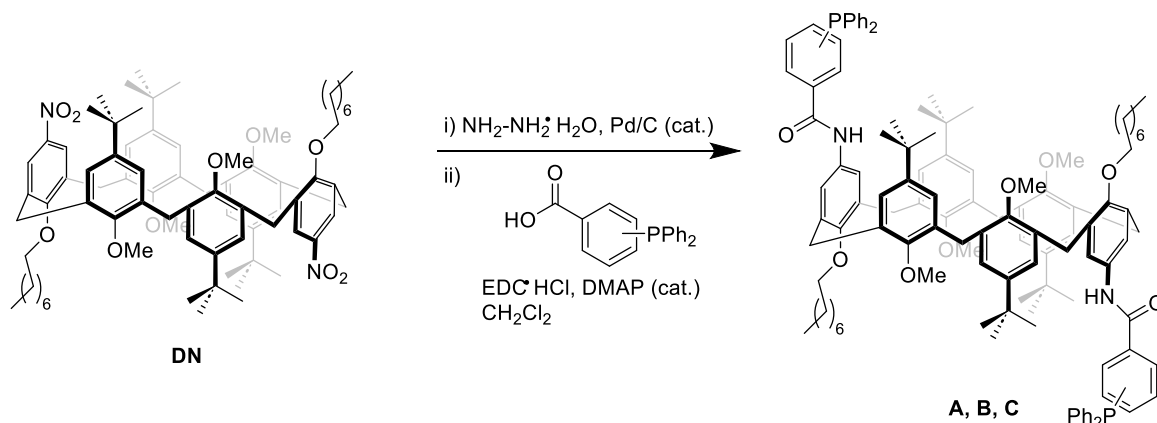
2.4 Experimental Section

- **General remarks**

All chemicals those syntheses are not reported hereafter were purchased from commercial sources and used as received. Solvents were dried and stored over molecular sieves previously activated in an oven (450 °C over-night). Anhydrous CH₂Cl₂ for catalytic reactions was supplied by Fluka in Sureseal® bottles and used without any further purification. Column chromatography was performed on silica gel 60 (70– 230 mesh). Melting points were measured with an electrothermal apparatus and are uncorrected. NMR spectra were recorded on a Bruker 400 MHz using solvents as internal standards (7.26 ppm for ¹H NMR and 77.00 ppm for ¹³C NMR for CDCl₃). The terms m, s, d, t, q, and quint represent multiplet, singlet, doublet, triplet, quadruplet, and quintuplet respectively, and the term br means a broad signal. ¹³C APT NMR spectra are reported for compounds. Exact masses were recorded on a LTQ ORBITRAP XL Thermo Mass Spectrometer (ESI source). Materials: **DN** derivative,^[17] (diphenylphosphino)benzoic acids,^[18] and enyne **1a**^[19] and **1b-c**^[20] were synthesized according to known procedures. Targeted *N*-propargyl sulfonamides **1d-k** were synthesized in variable yields (70-88%) from commercial sulfonyl chlorides following typical protocols. Propargylamine/RSO₂Cl/TEA (1.0/1.2/2 eq.), CH₂Cl₂ (0.2 M), r.t., 4 hours.^[21]

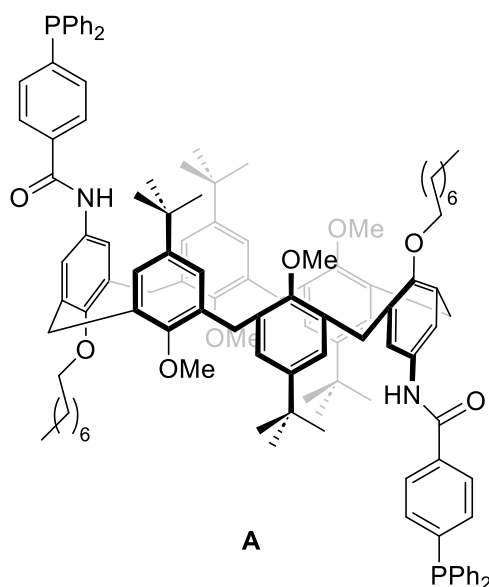
Chapter 2

- General procedure for the synthesis of ligands A, B and C



To a two-necked round-bottomed flask, under N_2 atmosphere, Pd/C (10 mol %) was added to a suspension of **DN** (234 mg, 0.27 mmol) in EtOH (100 mL). Subsequently, $\text{NH}_2\text{NH}_2\cdot\text{H}_2\text{O}$ (5 mmol, 20 equiv) was added dropwise, and after the addition was completed, the reaction mixture was refluxed at 80 °C for 24 h (oil bath). After completion of the reaction as determined by TLC analysis, the reaction mixture was cooled to room temperature, and then filtered through a Celite pad to remove the solids. The mixture was concentrated at reduced pressure and water (30 mL) was added. After extraction with CH_2Cl_2 (3 × 30 mL), organic phases were dried over Na_2SO_4 and concentrated at reduced pressure to afford a pale yellow solid. The crude was dissolved in dry CH_2Cl_2 (15 mL) under N_2 atmosphere and DMAP (10 mol %) and EDC·HCl (0.8 mmol, 3.0 equiv) were added. Subsequently, the mixture was cooled to 0 °C and the corresponding (diphenylphosphino)benzoic acid (0.7 mmol, 2.5 equiv) was added and the reaction mixture was stirred for 16 h. After completion, H_2O (20 mL) was added, and the mixture extracted with CH_2Cl_2 (3 × 30 mL). The organic layers were dried over Na_2SO_4 , concentrated at reduced pressure, and the crude purified by column chromatography on silica gel (*n*-Hex/AcOEt 80:20).

Chapter 2



General procedure was followed using 4-(diphenylphosphino)benzoic acid. Purification by column chromatography on silica gel (*n*-Hex/EtOAc 80:20) yielded **A** (285 mg, 60%) as a white solid. **M. p.** = 130-133 °C.

¹H NMR *1,2,3-alternate conformer* (400 MHz, CDCl₃) δ = 7.79 – 7.64 (m, 4H), 7.45 – 7.23 (m, 28H), 7.23 (d, *J* = 2.5 Hz, 4H), 6.94 (br s, 4H), 6.89 (br s, 2H), 4.21 (d, *J* = 14.2 Hz, 4H), 3.93 (s, 4H), 3.88 (t, *J* = 6.6 Hz, 4H), 3.66 (d, *J* = 14.2 Hz, 4H), 2.94 (br s, 12H), 1.90 – 1.79 (m, 4H), 1.61 – 1.51 (m, 4H), 1.44 – 1.27 (m, 16H), 1.17 (s, 36H), 0.91 (s,

6H).

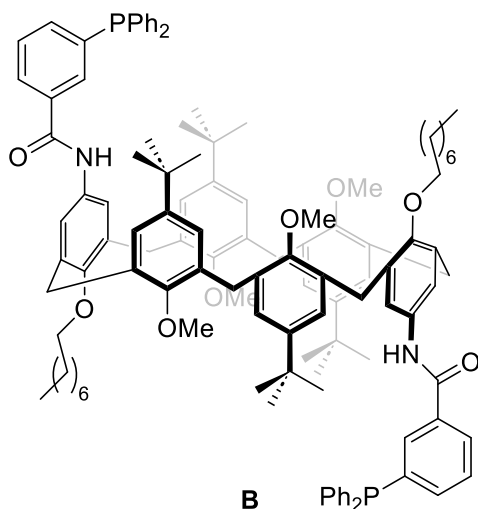
¹³C NMR *1,2,3-alternate conformer* (101 MHz, CDCl₃) δ = 165.0 (C_q), 154.0 (C_q), 151.6 (C_q), 146.3 (2 x C_q), 142.0 (d, *J*_{C-P} = 13.8 Hz, C_q), 136.5 (d, *J*_{C-P} = 10.8 Hz, C_q), 135.3 (C_q), 135.1 (C_q), 132.9 (C_q), 133.8 (d, *J*_{C-P} = 19.8 Hz, CH), 133.7 (d, *J*_{C-P} = 17.2 Hz, CH), 132.8 (C_q), 129.1 (CH), 128.7 (d, *J*_{C-P} = 7.3 Hz, CH), 127.1 (d, *J*_{C-P} = 6.6 Hz, CH), 126.8 (CH), 126.6 (CH), 121.2 (CH), 73.3 (CH₂), 60.0 (CH₃), 34.1 (C_q), 31.9 (CH₂), 31.4 (CH₃), 30.8 (2 x CH₂), 30.5 (CH₂), 29.6 (CH₂), 29.3 (CH₂), 26.3 (CH₂), 22.7 (CH₂), 14.2 (CH₃).

³¹P NMR *1,2,3-alternated conformer* (162 MHz, CDCl₃) δ = -5.36.

ESI-MS: *m/z* [M+Na]⁺ calcd. For C₁₁₆H₁₃₆N₂NaO₈P₂: 1769.97; found: 1769.52.

HR-MS (ESI) *m/z*: [M+H]⁺ calcd. for C₁₁₆H₁₃₇N₂O₈P₂: 1747.9884; found 1747.9886.

Chapter 2



General procedure was followed using 3-(diphenylphosphino)benzoic acid. Purification by column chromatography on silica gel (*n*-Hex/EtOAc 80:20) yielded **B** (261 mg, 55%) as a white solid. **M. p.** = 171-173 °C.

¹H NMR *1,2,3-alternated conformer* (400 MHz, CDCl₃) δ = 7.80 – 7.73 (m, 2H), 7.72 – 7.75 (m, 6H), 7.54 – 7.41 (m, 6H), 7.40 – 7.19 (m, 20H), 6.98 (br s, 4H), 6.86 (br s, 4H), 4.23 (d, *J* = 14.2 Hz, 4H), 3.92 (bs, 4H), 3.88 (t, *J* = 7.9 Hz, 4H), 3.62 (d, *J* = 14.2 Hz,

4H), 2.86 (br s, 12H), 1.97 – 1.83 (m, 4H), 1.65 – 1.53 (m, 4H), 1.45 – 1.29 (m, 16H), 1.15 (s, 36H), 0.94 – 0.82 (m, 6H).

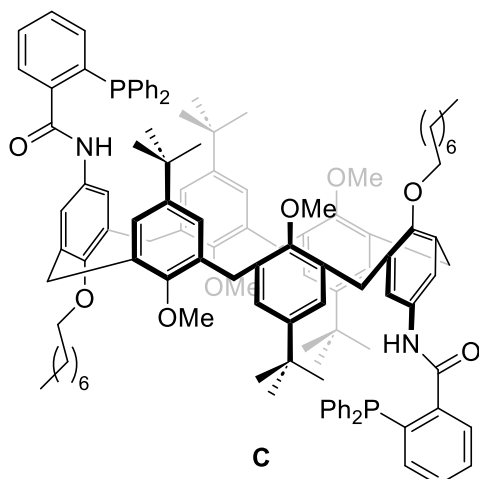
¹³C NMR *1,2,3-alternated conformer* (101 MHz, CDCl₃) δ = 164.8 (C_q), 156.3 (C_q), 151.7 (C_q), 146.2 (C_q), 138.4 (d, *J*_{C-P} = 12.1 Hz, C_q), 136.4 (d, *J*_{C-P} = 15.8 Hz, CH), 136.3 (d, *J*_{C-P} = 9.6 Hz, C_q), 135.5 (C_q), 135.3 (d, *J*_{C-P} = 7.2 Hz, C_q), 133.8 (C_q), 133.7 (d, *J*_{C-P} = 19.2 Hz, CH), 133.0 (C_q), 132.9 (C_q), 132.1 (d, *J*_{C-P} = 9.4 Hz, CH), 129.1 (CH), 128.8 (d, *J*_{C-P} = 7.0 Hz, CH), 128.7 (d, *J*_{C-P} = 7.0 Hz, CH), 127.4 (CH), 126.8 (CH), 126.4 (CH), 120.7 (CH), 73.2 (CH₂), 59.9 (CH₃), 34.1 (C_q), 31.9 (CH₂), 31.3 (CH₃), 30.7 (CH₂), 30.6 (2 x CH₂), 29.6 (CH₂), 29.3 (CH₂), 26.4 (CH₂), 22.7 (CH₂), 14.1 (CH₃).

³¹P NMR *1,2,3-alternate conformer* (162 MHz, CDCl₃) δ = -3.22.

ESI-MS: *m/z* [M+Na]⁺ calcd. for C₁₁₆H₁₃₆N₂NaO₈P₂: 1769.97; found: 1769.13.

HR-MS (ESI) *m/z*: [M+H]⁺ calcd. for C₁₁₆H₁₃₇N₂O₈P₂: 1747.9884; found 1747.9894.

Chapter 2



General procedure was followed using 2-(diphenylphosphino)benzoic acid. Purification by column chromatography on silica gel (*n*-Hex/EtOAc 80:20) yielded **C** (250 mg, 53%) as a white solid. **M. p.** = 175-172 °C.

¹H NMR 1,2,3-alternate conformer (400 MHz, CDCl₃) δ = 7.63–7.58 (m, 2H), 7.47 – 7.42 (m, 2H), 7.39 – 7.16 (m, 26H), 7.09 – 7.25 (m, 6H), 6.91 – 6.87 (m, 6H), 4.27 (d, *J* = 14.3 Hz, 4H), 3.90 (s, 4H),

3.88 (t, *J* = 7.9 Hz, 4H), 3.57 (d, *J* = 14.3 Hz, 4H), 2.85 (br s, 12H), 1.95 – 1.84 (m, 4H), 1.64 – 1.52 (m, 4H), 1.47 – 1.28 (m, 16H), 1.18 (s, 36H), 0.94 – 0.88 (m, 6H).

¹³C NMR 1,2,3-alternate conformer (101 MHz, CDCl₃) δ = 166.5 (C_q), 154.2 (C_q), 151.8 (C_q), 146.0 (C_q), 142.0 (d, *J*_{C-P} = 25.0 Hz, C_q), 136.9 (d, *J*_{C-P} = 6.4 Hz, C_q), 135.1 (C_q), 135.0 (d, *J*_{C-P} = 15.0 Hz, C_q), 134.2 (CH), 133.9 (d, *J*_{C-P} = 18.8 Hz, CH), 133.7 (C_q), 133.2 (C_q), 132.7 (C_q), 130.2 (CH), 128.9 (CH), 128.8 (CH), 128.5 (d, *J*_{C-P} = 7.8 Hz, CH), 128.0 (d, *J*_{C-P} = 5.3 Hz, CH), 126.9 (CH), 126.3 (CH), 120.7 (CH), 73.5 (CH₂), 59.9 (CH₃), 34.1 (C_q), 31.9 (CH₂), 31.4 (CH₃), 30.9 (CH₂), 30.6 (2 x CH₂), 29.6 (CH₂), 29.3 (CH₂), 26.3 (CH₂), 22.7 (CH₂), 14.1 (CH₃).

³¹P NMR 1,2,3-alternate conformer (162 MHz, CDCl₃) δ = -8.67.

ESI-MS: *m/z* [M+Na]⁺ calcd. for C₁₁₆H₁₃₆N₂NaO₈P₂: 1769.97; found: 1769.32.

HR-MS (ESI) *m/z*: [M+H]⁺ calcd. for C₁₁₆H₁₃₇N₂O₈P₂: 1747.9884; found 1747.9896.

Chapter 2

- **X-ray crystallographic analysis of A(AuCl)₂, B(AuCl)₂ and C (AuCl)₂**

Single crystal data were collected at 200K with a Bruker D8 diffractometer equipped with a Photon II area detector, using a MoK α microfocus radiation source ($\lambda = 0.71073$). The data collection strategy covered the sphere of the reciprocal space. Data were indexed, integrated, and scaled using the CrysAlisPRO software.^[22] The structures were solved by the dual space algorithm implemented in the SHELXT code^[23] in Olex2.^[24] Fourier analysis and refinement were performed by the full-matrix least-squares methods based on F2 implemented in SHELXL-2014.^[25] For all the structures, anisotropic displacement parameters were refined except for hydrogen atoms. Crystallographic data have been deposited at the Cambridge Crystallographic Data Centre with the deposition numbers 2174929–2174931.

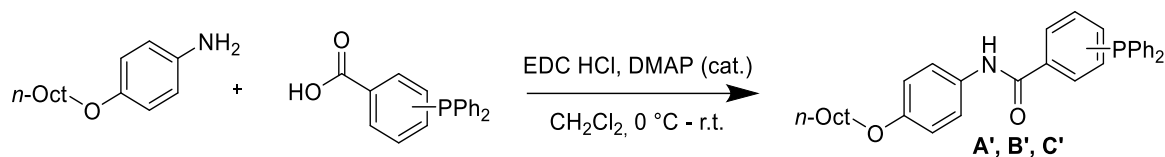
Crystal data for **A(AuCl)₂**. C₁₁₆H₁₃₆N₂O₈P₂Au₂Cl₂, 3(C₂H₃N), (M: 2336.19): triclinic, space group $P\bar{1}$, $a = 12.0018(3)$ Å, $b = 15.5165(4)$ Å, $c = 17.7252(4)$ Å, $\alpha = 68.278(2)^\circ$, $\beta = 84.913(2)^\circ$, $\gamma = 85.553(2)^\circ$, $V = 3050.85(14)$ Å³, $Z = 1$, 75 557 reflections collected ($4.084 < 2\theta < 51.362$), 11 536 unique ($R_{\text{int}} = 0.0918$, $R_{\text{sigma}} = 0.0454$) which were used in all calculations. The final R_1 was 0.0486 ($I \geq 2\sigma(I)$) and $wR_2 = 0.1360$ (all data).

Crystal data for **B(AuCl)₂**. C₁₁₆H₁₃₆N₂O₈P₂Au₂Cl₂, 1.5(CHCl₃), (M: 2392.08): monoclinic, space group C2/c, $a = 30.4353(6)$ Å, $b = 15.4148(2)$ Å, $c = 25.1048(4)$ Å, $\alpha = 90^\circ$, $\beta = 90.541(2)^\circ$, $\gamma = 90^\circ$, $V = 11777.5(3)$ Å³, $Z = 4$, 115 349 reflections collected ($3.384 < 2\theta < 51.362$), 11 167 unique ($R_{\text{int}} = 0.0631$, $R_{\text{sigma}} = 0.0272$). The final R_1 was 0.0358 ($I \geq 2\sigma(I)$) and wR_2 was 0.0999 (all data).

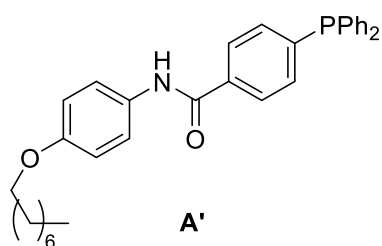
Crystal data for **C(AuCl)₂**. C₁₁₆H₁₃₆ N₂O₈P₂Au₂Cl₂, 6(C₇H₈), 2(C₄H₁₀O), (M: 2914.07): triclinic, space group $P\bar{1}$, $a = 14.1201(3)$ Å, $b = 14.4758(3)$ Å, $c = 18.9307(3)$ Å, $\alpha = 88.005(2)^\circ$, $\beta = 85.593(2)^\circ$, $\gamma = 86.527(2)^\circ$, $V = 3849.14(13)$ Å³, $Z = 1$, 103 242 reflections collected ($3.604 < 2\theta < 51.364$), 14 588 unique ($R_{\text{int}} = 0.0559$, $R_{\text{sigma}} = 0.0352$). The final R_1 was 0.0374 ($I \geq 2\sigma(I)$) and wR_2 was 0.0871 (all data).

Chapter 2

- **General procedure for monomeric ligands A', B' and C'**



4-(Octyloxy)aniline (0.7 mmol, 1.0 equiv) was dissolved in dry CH₂Cl₂ (15 mL) under N₂ atmosphere and DMAP (10 mol %) and EDC•HCl (0.8 mmol, 1.1 equiv) were added. Subsequently, the mixture was cooled to 0 °C and the desired (diphenylphosphino)benzoic acid (0.8 mmol, 1.1 equiv) was added. The reaction mixture was stirred for 16 h. After completion, H₂O (20 mL) was added, and the mixture extracted with CH₂Cl₂ (3 × 30 mL). The organic layers were dried over Na₂SO₄, concentrated at reduced pressure, and the crude purified by column chromatography on silica gel (*n*-Hex/AcOEt 80:20).



General procedure was followed using 4-(diphenylphosphino)benzoic acid. Purification by column chromatography on silica gel (*n*-Hex/EtOAc 80:20) yielded **A'** (255 mg, 71%) as a white solid. **M. p.** = 138-140 °C.

¹H NMR (400 MHz, CDCl₃) δ = 7.85 (s, 1H), 7.84 – 7.78 (d, *J* = 8.2 Hz, 2H), 7.56 – 7.50 (d, *J* = 8.2 Hz, 2H), 7.41 – 7.32 (m, 12H), 6.91 (d, *J* = 9.0 Hz, 2H), 3.97 (t, *J* = 6.6 Hz, 2H), 1.85 – 1.73 (m, 2H), 1.54 – 1.43 (m, 2H), 1.38 – 1.27 (m, 8H), 0.96 – 0.83 (m, 3H).

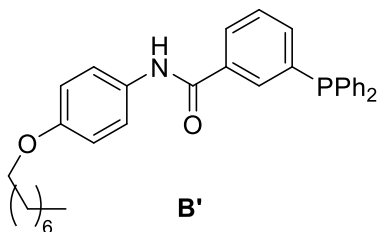
¹³C NMR (101 MHz, CDCl₃) δ = 165.3 (C_q), 156.3 (C_q), 142.1 (d, *J*_{C-P} = 12.9 Hz, C_q), 136.0 (d, *J*_{C-P} = 9.3 Hz, C_q), 135.1 (C_q), 133.9 (d, *J*_{C-P} = 19.6 Hz, CH), 133.7 (d, *J*_{C-P} = 19.0 Hz, CH), 130.7 (C_q), 129.2 (CH), 128.7 (d, *J*_{C-P} = 7.3 Hz, CH), 126.9 (d, *J*_{C-P} = 6.6 Hz, CH), 122.1 (CH), 114.9 (CH), 68.3 (CH₂), 31.9 (CH₂), 29.4 (CH₂), 29.3 (CH₂), 29.3 (CH₂), 26.1 (CH₂), 22.7 (CH₂), 14.1 (CH₃).

³¹P NMR (162 MHz, CDCl₃) δ = -3.18.

ESI-MS: *m/z* [M+Na]⁺ calcd. for C₃₃H₃₆NNaO₂P: 532.24; found: 532.27.

HR-MS (ESI) *m/z*: [M+H]⁺ calcd. for C₃₃H₃₇NO₂P: 510.2562; found 510.2556.

Chapter 2



General procedure was followed using 3-(diphenylphosphino)benzoic acid. Purification by column chromatography on silica gel (*n*-Hex/EtOAc 80:20) yielded **B'** (271 mg, 76%) as a white solid. **M. p.** = 137-138 °C.

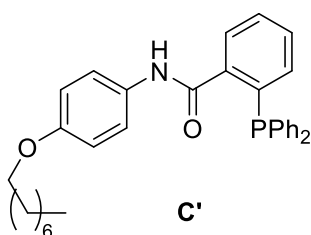
¹H NMR (400 MHz, CDCl₃) δ = 7.92 – 7.82 (m, 2H), 7.78 (s, 1H), 7.49 (d, *J* = 8.6 Hz, 2H), 7.45 (dd, *J* = 6.1, 2.6 Hz, 2H), 7.40 – 7.32 (m, 10H), 6.99 – 6.78 (m, 2H), 3.96 (t, *J* = 6.6 Hz, 2H), 1.85 – 1.73 (m, 2H), 1.47 (q, *J* = 7.0 Hz, 2H), 1.39 – 1.26 (m, 8H), 0.96 – 0.85 (m, 3H).

¹³C NMR (101 MHz, CDCl₃) δ = 165.2 (C_q), 156.2 (C_q), 138.4 (d, *J*_{C-P} = 12.1 Hz, C_q), 136.6 (d *J*_{C-P} = 15.8 Hz, CH), 136.1 (d, *J*_{C-P} = 9.6 Hz, C_q), 135.3 (d, *J*_{C-P} = 7.2 Hz, C_q), 133.8 (d, *J*_{C-P} = 19.9 Hz, CH), 131.9 (d, *J*_{C-P} = 23.6 Hz, CH), 130.7 (C_q), 129.2 (CH), 129.0 (d *J*_{C-P} = 5.6 Hz, CH), 128.7 (d, *J*_{C-P} = 7.0 Hz, CH), 127.8 (CH), 122.0 (CH), 114.9 (CH), 68.3 (CH₂), 31.8 (CH₂), 29.4 (CH₂), 29.3 (CH₂), 29.3 (CH₂), 26.1 (CH₂), 22.7 (CH₂), 14.1 (CH₃).

³¹P NMR (162 MHz, CDCl₃) δ = - 2.99.

ESI-MS: *m/z* [M+Na]⁺ calcd. for C₃₃H₃₆NNaO₂P: 532.24; found: 532.26.

HR-MS (ESI) *m/z*: [M+H]⁺ calcd. for C₃₃H₃₇NO₂P: 510.2562; found 510.2568.



General procedure was followed using 2-(diphenylphosphino)benzoic acid. Purification by column chromatography on silica gel (*n*-Hex/EtOAc 80:20) yielded **C'** (247 mg, 69%) as a white solid. **M. p.** = 117-118 °C.

¹H NMR (400 MHz, CDCl₃) δ = 7.82 (dd, *J* = 8.0, 3.8 Hz, 1H), 7.75 (s, 1H), 7.46 (td, *J* = 7.5, 1.3 Hz, 1H), 7.42 – 7.31 (m, 11H), 7.24 – 7.19 (m, 2H), 7.05 (ddd, *J* = 7.7, 4.5, 1.3 Hz, 1H), 6.87 – 6.74 (m, 2H), 3.94 (t, *J* = 6.6 Hz, 2H), 1.88 – 1.70 (m, 2H), 1.52 – 1.41 (m, 2H), 1.40 – 1.25 (m, 8H), 0.97 – 0.82 (m, 3H).

¹³C NMR (101 MHz, CDCl₃) δ = 166.8 (C_q), 156.1 (C_q), 141.6 (d, *J*_{C-P} = 24.7 Hz, C_q), 135.9 (d, *J*_{C-P} = 6.4 Hz, C_q), 135.1 (d, *J*_{C-P} = 15.4 Hz, C_q), 134.1 (d, *J*_{C-P} = 5.3 Hz, CH), 134.0 (d, *J*_{C-P} = 20.0 Hz, CH), 130.5 (C_q), 130.4 (CH), 129.3 (2x CH), 128.8 (d, *J*_{C-P} = 7.3 Hz, CH), 128.6 (d, *J*_{C-P} = 5.1

Chapter 2

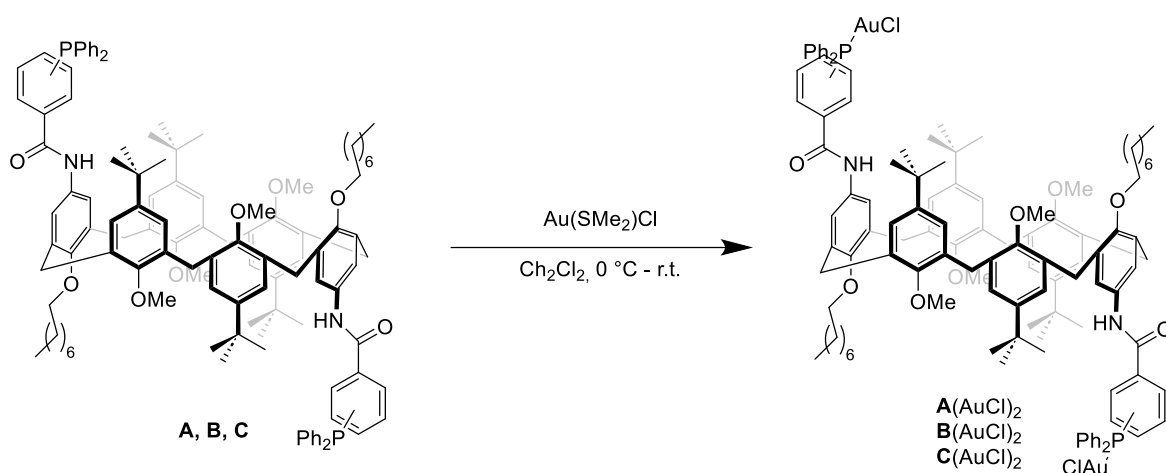
Hz, CH), 121.7 (CH), 114.6 (CH), 68.3 (CH₂), 31.8 (CH₂), 29.4 (CH₂), 29.3 (CH₂), 29.3 (CH₂), 26.1 (CH₂), 22.7 (CH₂), 14.1 (CH₃).

³¹P NMR (162 MHz, CDCl₃) δ = - 7.70.

ESI-MS: *m/z* [M+Na]⁺ calcd. for C₃₃H₃₆NNaO₂P: 532.24; found: 532.22.

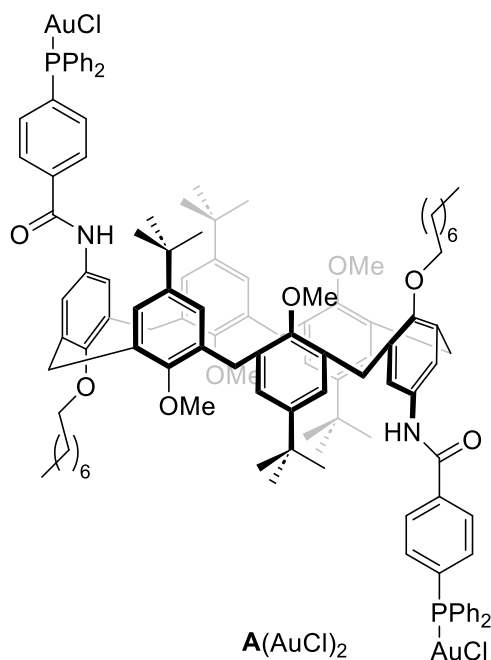
HR-MS (ESI) *m/z*: [M+H]⁺ calcd. for C₃₃H₃₇NO₂P: 510.2562; found 510.2572.

- General procedure for synthesis of complexes A, B and C(AuCl)₂



In a two-necked Schlenk flask, under N₂ atmosphere, Au(DMS)Cl (26.5 mg, 0.09 mmol, 2.0 equiv) was added to a solution of the corresponding phosphine (80 mg, 0.045 mmol, 1.0 equiv) in CH₂Cl₂ (4.0 mL) at 0 °C. The reaction mixture was stirred at the same temperature for 30 min and then allowed to reach room temperature. After 1 h, the mixture was filtered through celite, washed with CH₂Cl₂ (20 mL), and the volatiles were removed under vacuum. The crude was purified by column chromatography on silica gel (*n*-Hex/AcOEt 80:20→70:30).

Chapter 2



General procedure was followed using phosphine **A**. Purification by column chromatography on silica gel (*n*-Hex/EtOAc 80:20→70:30) yielded **A(AuCl)₂** (92.1 mg, 93%) as a white solid. **M. p.** = 187-188 °C.

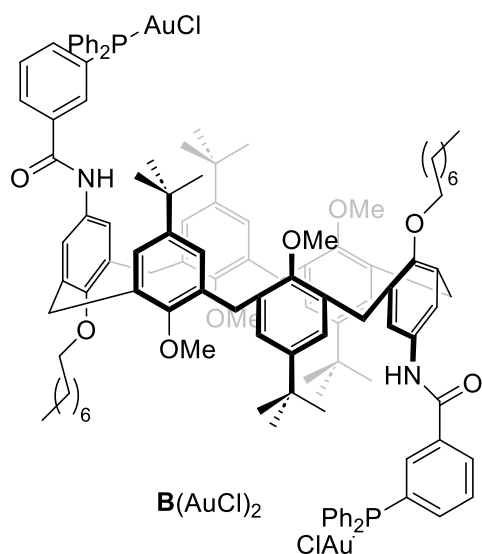
¹H NMR *1,2,3-alternate conformer* (400 MHz, CDCl₃) δ = 7.83–7.76 (m, 4H), 7.71–7.62 (m, 4H), 7.61–7.47 (m, 22H), 7.18 (br s, 4H), 6.94 (br s, 4H), 6.86 (br s, 4H), 4.18 (d, *J* = 14.2 Hz, 4H), 3.91 (s, 4H), 3.88 (t, *J* = 6.7 Hz, 4H), 3.65 (d, *J* = 14.2 Hz, 4H), 2.96 (br s, 12H), 1.90–1.79 (m, 4H), 1.58–1.47 (m, 4H), 1.37–1.23 (m, 16H), 1.15 (s, 36H), 0.93–0.80 (m, 6H).

¹³C NMR *1,2,3-alternate conformer* (101 MHz, CDCl₃) δ = 163.9 (C_q), 154.0 (C_q), 151.8 (C_q), 146.3 (2 x C_q), 138.4 (d, *J*_{C-P} = 2.5 Hz, C_q), 135.3 (C_q), 134.4 (d, *J*_{C-P} = 13.8 Hz, CH), 134.2 (d, *J*_{C-P} = 13.8 Hz, CH); 134.0 (C_q), 133.4 (C_q), 132.6 (C_q), 132.3 (d, *J*_{C-P} = 2.2 Hz, CH), 129.4 (d, *J*_{C-P} = 12.2 Hz, CH), 128.1 (d, *J*_{C-P} = 61.9 Hz, C_q), 127.8 (d, *J*_{C-P} = 9.8 Hz, CH), 126.7 (CH), 126.6 (CH), 121.3 (CH), 73.4 (CH₂), 60.1 (CH₃), 34.1 (C_q), 31.9 (CH₂), 31.4 (CH₃), 30.8 (CH₂), 30.4 (2 x CH₂), 29.5 (CH₂), 29.4 (CH₂), 26.3 (CH₂), 22.7 (CH₂), 14.2 (CH₃).

³¹P NMR *1,2,3-alternate conformer* (162 MHz, CDCl₃) δ = 32.9.

HRMS: *m/z* [M-(AuCl₂)]⁺ calcd. for C₁₁₆H₁₃₆AuN₂O₈P₂: 1944.9471; found: 1994.9465.

Chapter 2



General procedure was followed using phosphine **B**. Purification by column chromatography on silica gel (*n*-Hex/EtOAc 80:20→70:30) yielded **B(AuCl)₂** (73.5 mg, 74%) as a white solid. **M. p.** = 193-195 °C.

¹H NMR *1,2,3-alternate conformer* (400 MHz, CDCl₃) δ = 7.90 – 7.80 (m, 4H), 7.77 – 7.64 (m, 4H), 7.61 – 7.39 (m, 21H), 7.17 (br s, 4H), 6.93 (br s, 3H), 6.84 (br s, 6H), 4.18 (d, *J* = 14.2 Hz, 4H), 3.97 – 3.86 (m, 8H), 3.67 (d, *J* = 14.2 Hz, 4H), 2.96 (br s, 12H),

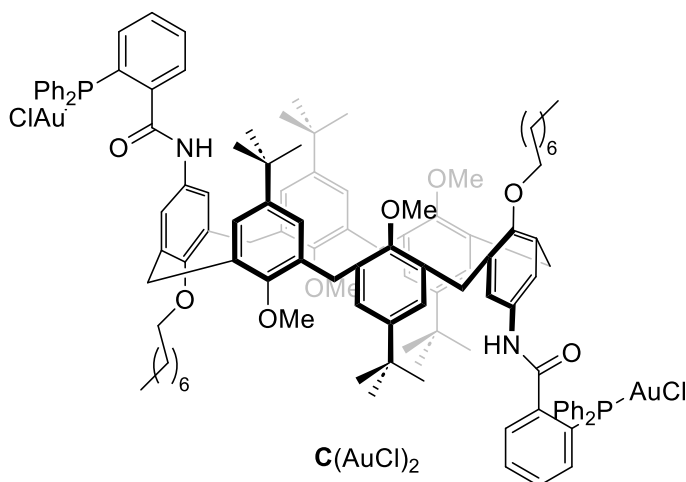
2.00 – 1.86 (m, 4H), 1.67 – 1.53 (m, 4H), 1.42 – 1.27 (m, 16H), 1.13 (s, 36H), 0.95 – 0.86 (m, 6H).

¹³C NMR *1,2,3-alternate conformer* (101 MHz, CDCl₃) δ = 163.6 (C_q), 154.0 (C_q), 151.8 (C_q), 146.2 (C_q), 137.3 (d, *J*_{C-P} = 13.8 Hz, CH), 136.1 (d, *J*_{C-P} = 10.2 Hz, C_q), 135.3 (C_q), 134.2 (d, *J*_{C-P} = 13.8 Hz, CH), 133.9 (C_q), 132.8 (d, *J*_{C-P} = 12.8 Hz, CH), 132.6 (C_q), 132.3 (d, *J*_{C-P} = 2.5 Hz, CH), 130.5 (C_q), 129.9 (C_q), 129.8 (CH), 129.6 (d, *J*_{C-P} = 12.2 Hz, CH), 129.4 (d, *J*_{C-P} = 12.2 Hz, CH), 128.1 (d, *J*_{C-P} = 62.5 Hz, C_q), 126.7 (CH), 126.3 (CH), 121.3 (CH), 73.3 (CH₂), 60.1 (CH₃), 34.1 (C_q), 31.9 (CH₂), 31.4 (CH₃), 30.8 (CH₂), 30.6 (2 x CH₂), 29.6 (CH₂), 29.3 (CH₂), 26.3 (CH₂), 22.7 (CH₂), 14.1 (CH₃).

³¹P NMR *1,2,3-alternate conformer* (162 MHz, CDCl₃) δ = 33.3.

HR-MS: *m/z* [M-Cl]⁺ calcd. for C₁₁₆H₁₃₆Au₂ClN₂O₈P₂: 2176.8825; found: 2176.8828.

Chapter 2



General procedure was followed using phosphine **C**. Purification by column chromatography on silica gel (*n*-Hex/EtOAc 80:20→70:30) yielded **C**(AuCl)₂ (68.7 mg, 69%) as a white solid. **M. p.** = 196-197 °C.

¹H NMR 1,2,3-alternate conformer (400 MHz, CDCl₃) δ =

7.62 – 7.58 (m, 4H), 7.58 – 7.50 (m, 9H), 7.48 – 7.41 (m, 6H), 7.40 – 7.34 (m, 9H), 7.33 – 7.30 (m, 4H), 7.25 – 7.27 (m, 2H), 7.15 (br s, 2H), 6.93 – 6.85 (m, 6H), 4.30 (d, *J* = 14.2 Hz, 4H), 3.92 – 3.84 (m, 8H), 3.58 (d, *J* = 14.2 Hz, 4H), 2.91 (br s, 12H), 1.97 – 1.84 (m, 4H), 1.64 – 1.52 (m, 4H), 1.44 – 1.28 (m, 16H), 1.21 (s, 36H), 0.95 – 0.87 (m, 6H).

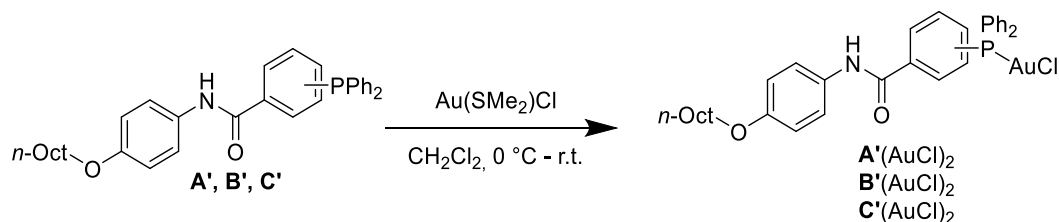
¹³C NMR 1,2,3-alternate conformer (101 MHz, CDCl₃) δ = 165.2 (C_q), 154.2 (C_q), 152.3 (C_q), 145.8 (C_q), 142.0 (d, *J*_{C-P} = 10.8 Hz, C_q), 135.3 (d, *J*_{C-P} = 9.2 Hz, CH), 135.1 (C_q), 134.2 (d, *J*_{C-P} = 13.9 Hz, CH), 133.6 (d, *J*_{C-P} = 5.1 Hz, C_q), 132.0 (C_q), 131.7 (CH), 131.6 (d, *J*_{C-P} = 2.6 Hz, CH), 130.3 (d, *J*_{C-P} = 10.4 Hz, CH), 129.7 (C_q), 129.0 (d, *J*_{C-P} = 13.0 Hz, CH), 128.4 (d, *J*_{C-P} = 8.9 Hz, C_q), 128.0 (d, *J*_{C-P} = 58.3 Hz, C_q), 127.1 (CH), 126.2 (CH), 122.5 (CH), 121.2 (CH), 73.7 (CH₂), 59.9 (CH₃), 34.1 (C_q), 31.9 (CH₂), 31.5 (CH₃), 30.9 (CH₂), 30.6 (2 x CH₂), 29.6 (CH₂), 29.3 (CH₂), 26.3 (CH₂), 22.7 (CH₂), 14.1 (CH₃).

³¹P NMR 1,2,3-alternate conformer (162 MHz, CDCl₃) δ = 34.6.

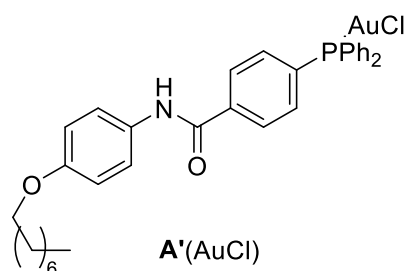
HRMS: *m/z* [M-Cl]⁺ calcd. for C₁₁₆H₁₃₆Au₂ClN₂O₈P₂: 2176.8825; found: 2176.8819.

Chapter 2

- **General procedure for synthesis of complexes **A'**, **B'** and **C'**(AuCl)₂**



In a two-necked Schlenk flask, under N₂ atmosphere, Au(DMS)Cl (29.4 mg, 0.1 mmol, 1.0 equiv) was added to a solution of the corresponding phosphine (50.9 mg, 0.1 mmol, 1.0 equiv) in CH₂Cl₂ (4.0 mL) at 0 °C. The reaction mixture was stirred at the same temperature for 30 min and then allowed to reach room temperature. After 1 h, the mixture was filtered through celite, washed with CH₂Cl₂ (20 mL), and the volatiles were removed under vacuum. The crude was purified by column chromatography on silica gel (*n*-Hex/AcOEt: 80:20→70:30).



General procedure was followed using **A'**. Purification by column chromatography on silica gel (*n*-Hex/EtOAc 80:20→70:30) yielded **A'**(AuCl) (69.8 mg, 94%) as a white solid. **M. p.** = 93-94 °C.

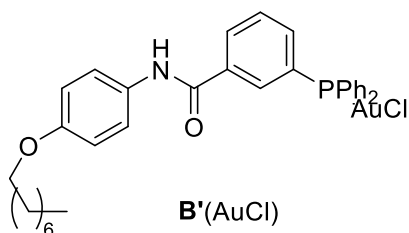
¹H NMR (400 MHz, CDCl₃) δ = 8.08 (s, 1H), 7.95 (dd, *J* = 8.3, 2.2 Hz, 2H), 7.66 – 7.44 (m, 14H), 6.97 – 6.84 (m, 2H), 3.96 (t, *J* = 6.6 Hz, 2H), 1.89 – 1.71 (m, 2H), 1.46 (q, *J* = 7.1 Hz, 2H), 1.42 – 1.24 (m, 8H), 1.00 – 0.84 (m, 3H).

¹³C NMR (101 MHz, CDCl₃) δ = 164.4 (C_q), 156.5 (C_q), 138.3 (C_q), 134.3 (d, *J*_{C-P} = 13.7 Hz, CH), 134.2 (d, *J*_{C-P} = 14.0 Hz, CH), 133.0 (C_q), 132.3 (d, *J*_{C-P} = 2.6 Hz, CH), 130.4 (C_q), 129.5 (d, *J*_{C-P} = 11.6 Hz, CH), 127.9 (d, *J*_{C-P} = 61.9 Hz, C_q), 127.7 (d, *J*_{C-P} = 12.2 Hz, CH), 122.2 (CH), 114.9 (CH), 68.4 (CH₂), 31.8 (CH₂), 29.4 (CH₂), 29.3 (CH₂), 29.3 (CH₂), 26.0 (CH₂), 22.7 (CH₂), 14.1 (CH₃).

³¹P NMR (162 MHz, CDCl₃) δ = 34.3.

ESI-MS: *m/z* [M-Cl]⁺ calcd. for C₃₃H₃₆AuNO₂P: 706.21; found: 706.18.

Chapter 2



General procedure was followed using **B'**. Purification by column chromatography on silica gel (*n*-Hex/EtOAc 80:20→70:30) yielded **B'**(AuCl) (68.5 mg, 92%) as a white solid. **M. p.** = 91-92 °C.

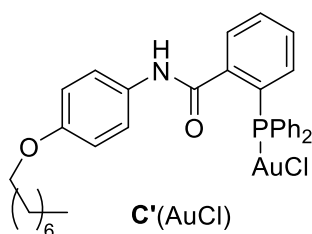
¹H NMR (400 MHz, CDCl₃) δ = 8.06 – 7.96 (m, 3H),

7.72 – 7.38 (m, 14H), 6.96 – 6.79 (m, 2H), 3.95 (t, *J* = 6.6 Hz, 2H), 1.89 – 1.72 (m, 2H), 1.46 (q, *J* = 7.3 Hz, 2H), 1.41 – 1.22 (m, 8H), 0.99 – 0.82 (m, 3H).

¹³C NMR (101 MHz, CDCl₃) δ = 164.3 (C_q), 156.5 (C_q), 136.7 (d, *J*_{C-P} = 13.7 Hz, CH), 136.3 (d, *J*_{C-P} = 10.9 Hz, C_q), 134.3 (d, *J*_{C-P} = 13.9 Hz, CH), 132.4 (d, *J*_{C-P} = 2.6 Hz, CH), 132.2 (d, *J*_{C-P} = 14.0 Hz, CH), 130.7 (CH), 130.3 (C_q), 129.9 (C_q), 129.7 (d, *J*_{C-P} = 11.8 Hz, CH), 129.5 (d, *J*_{C-P} = 12.0 Hz, CH), 128.0 (d, *J*_{C-P} = 62.0 Hz, C_q), 122.3 (CH), 114.9 (CH), 68.3 (CH₂), 31.8 (CH₂), 29.4 (CH₂), 29.3 (CH₂), 29.3 (CH₂), 26.1 (CH₂), 22.7 (CH₂), 14.1 (CH₃).

³¹P NMR (162 MHz, CDCl₃) δ = 43.2.

ESI-MS: *m/z* [M-Cl]⁺ calcd. for C₃₃H₃₆AuNO₂P: 706.21; found: 706.17.



General procedure was followed using **C'**. Purification by column chromatography on silica gel (*n*-Hex/EtOAc 80:20→70:30) yielded **C'**(AuCl) (71.0 mg, 96%) as a white solid. **M. p.** = 97-98 °C.

¹H NMR (400 MHz, CDCl₃) δ = 7.89 (s, 1H), 7.86 (dd, *J* = 7.7, 4.2 Hz, 1H), 7.65 (t, *J* = 7.6 Hz, 1H), 7.59 – 7.40 (m, 12H), 7.34 (d, *J* = 8.5 Hz, 2H), 7.08 (dd, *J* = 12.5, 7.8 Hz, 1H), 6.75 (d, *J* = 8.9 Hz, 2H), 3.88 (t, *J* = 6.6 Hz, 2H), 1.74 (q, *J* = 6.9 Hz, 2H), 1.48 – 1.40 (m, 2H), 1.39 – 1.24 (m, 8H), 1.02 – 0.84 (m, 3H).

¹³C NMR (101 MHz, CDCl₃) δ = 165.6 (C_q), 156.7 (C_q), 141.1 (d, *J*_{C-P} = 11.6 Hz, C_q), 134.7 (d, *J*_{C-P} = 8.0 Hz, CH), 134.3 (d, *J*_{C-P} = 14.2 Hz, CH), 131.9 (CH), 131.7 (d, *J*_{C-P} = 2.5 Hz, CH), 130.6 (d, *J*_{C-P} = 9.4 Hz, CH), 129.7 (C_q), 129.4 (C_q), 129.1 (d, *J*_{C-P} = 12.2 Hz, CH), 128.9 (d, *J*_{C-P} = 8.1 Hz, CH), 128.3 (d, *J*_{C-P} = 57.9 Hz, C_q) 123.5 (CH), 114.6 (CH), 68.2 (CH₂), 31.8 (CH₂), 29.4 (CH₂), 29.3 (CH₂), 29.3 (CH₂), 26.1 (CH₂), 22.7 (CH₂), 14.1 (CH₃).

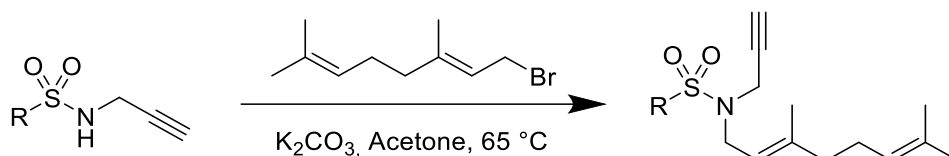
Chapter 2

^{31}P NMR (162 MHz, CDCl_3) $\delta = 34.5$.

ESI-MS: m/z $[\text{M}-\text{Cl}]^+$ calcd. for $\text{C}_{33}\text{H}_{36}\text{AuNO}_2\text{P}$: 706.21; found: 706.23.

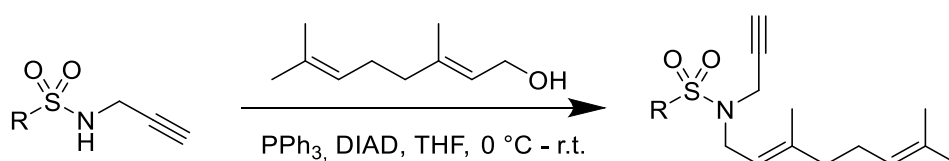
- **Synthesis and characterization of novel Enynes**

Method A



In a Schlenk flask, geranyl bromide (1.2 equiv.) was added dropwise to a solution of the corresponding *N*-substituted propargylsulfonamide derivative (1.0 equiv) and K_2CO_3 (1.5 equiv) in acetone (10 ml). Subsequently, the mixture was placed in a pre-heated oil bath at $50\text{ }^\circ\text{C}$ and stirred overnight. After completion, the reaction mixture was cooled down to room temperature and HCl 10 % (15 ml) was added. The mixture was extracted with EtOAc (3 x 15 ml), the organic layers separated and dried over Na_2SO_4 . The combined fractions were concentrated under reduced pressure and the crude purified by column chromatography on silica gel.

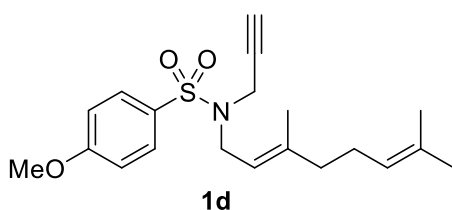
Method B



In an oven-dried two-necked round-bottomed flask, geraniol (1.2 equiv) was added to a 1.0 M solution in THF of the corresponding *N*-substituted-propargylsulfonamide derivative (1.0 equiv) and PPh_3 (1.2 equiv) under N_2 atmosphere. Subsequently, the mixture was placed at 0°C and DIAD (1.2 equiv) was carefully added dropwise over 10 min. The mixture was stirred until complete conversion (2-8 hs). Subsequently, a solution of HCl 10 % (10 ml) was added, the mixture extracted with EtOAc (3 x 15 ml), the organic layers separated and dried over

Chapter 2

Na₂SO₄. The combined fractions were concentrated under reduced pressure and the crude purified by column chromatography on silica gel.

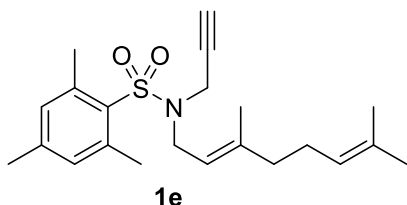


Representative procedure **A** was followed using 4-Methoxy-*N*-(prop-2-yn-1-yl)benzenesulfonamide (270 mg, 1.2 mmol). Purification by column chromatography on silica gel (*n*-hexanes/EtOAc 80:20) yielded **1d** (425 mg, 98 %) as a yellow oil.

¹H NMR (400 MHz, CDCl₃) δ = 7.80 (d, *J* = 8.9 Hz, 2H), 6.98 (d, *J* = 8.9 Hz, 2H), 5.11 (m, 1H), 5.05 (m, 1H), 4.08 (d, *J* = 2.4 Hz, 2H), 3.88 (s, 3H), 3.84 (d, *J* = 7.4 Hz, 2H), 2.13–2.02 (m, 4H), 2.01 (t, *J* = 2.6 Hz, 1H), 1.69 (s, 3H), 1.68 (s, 3H), 1.60 (s, 3H).

¹³C NMR (101 MHz, CDCl₃) δ = 162.9 (C_q), 142.5 (C_q), 131.9 (C_q), 130.8 (C_q), 129.9 (CH), 123.7 (CH), 117.83 (CH), 113.9 (CH), 76.8 (CH), 73.4 (C_q), 55.6 (CH₃), 43.8 (CH₂), 39.6 (CH₂), 35.2 (CH₂), 26.2 (CH₂), 25.7 (CH₃), 17.7 (CH₃), 16.2 (CH₃).

ESI-MS: *m/z* [M+Na]⁺ calcd for C₂₀H₂₇NNaO₃S: 384.16; found: 384.19.



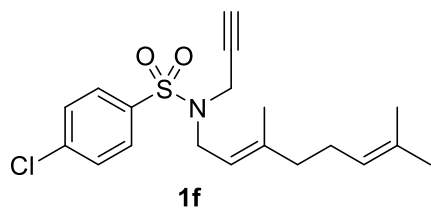
Representative procedure **B** was followed using 2,4,6-Trimethyl-*N*-(prop-2-yn-1-yl)benzenesulfonamide (319 mg, 1.3 mmol). Purification by column chromatography on silica gel (*n*-hexanes/EtOAc 80:20) yielded **1e** (473 mg, 94 %) as a pale-yellow oil.

¹H NMR (400 MHz, CDCl₃) δ = 6.97 (s, 2H), 5.12–5.00 (m, 2H), 3.99 (d, *J* = 2.4 Hz, 2H), 3.84 (d, *J* = 7.2 Hz, 2H), 2.63 (s, 6H), 2.32 (s, 3H), 2.25 (t, *J* = 2.4 Hz, 1H), 2.12–2.00 (m, 4H), 1.69 (s, 3H), 1.65 (s, 3H), 1.61 (s, 3H).

¹³C NMR (101 MHz, CDCl₃) δ = 142.6 (C_q), 142.4 (C_q), 140.5 (C_q), 131.9 (CH), 123.8 (CH), 117.9 (CH), 77.3 (CH), 72.7 (C_q), 43.0 (CH₂), 39.7 (CH₂), 33.9 (CH₂), 26.2 (CH₂), 25.7 (CH₃), 22.8 (CH₃), 20.7 (CH₃), 17.7 (CH₃), 16.0 (CH₃).

ESI-MS: *m/z* [M+Na]⁺ calcd for C₂₂H₃₁NNaO₂S: 396.20; found: 396.16.

Chapter 2



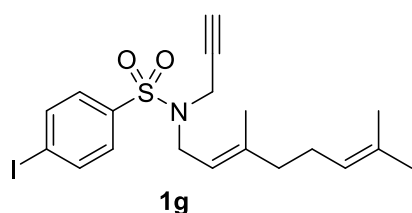
Representative procedure **B** was followed using 4-Chloro-*N*-(prop-2-yn-1-yl)benzenesulfonamide (200 mg, 1.3 mmol). Purification by column chromatography on silica gel (*n*-hexanes/EtOAc 80:20)

yielded **1f** (462 mg, 97 %) as a colourless oil.

¹H NMR (400 MHz, CDCl₃) δ = 7.82 (d, *J* = 8.6 Hz, 2H), 7.49 (d, *J* = 8.6 Hz, 2H), 5.16 – 5.09 (m, 1H), 5.09 – 5.01 (m, 1H), 4.10 (d, *J* = 2.6 Hz, 2H), 3.85 (d, *J* = 7.2 Hz, 2H), 2.14 – 2.04 (m, 4H), 2.01 (t, *J* = 2.3 Hz, 1H), 1.72 – 1.67 (m, 6H), 1.61 (s, 3H).

¹³C NMR (101 MHz, CDCl₃) δ = 143.0 (C_q), 139. (C_q), 137.7 (C_q), 132.0 (C_q), 129.3 (CH), 129.1 (CH), 123.7 (CH), 117.4 (CH), 77.3 (CH), 73.7 (C_q), 43.9 (CH₂), 39.6 (CH₂), 35.3 (CH₂), 26.1 (CH₂), 25.7 (CH₃), 17.7 (CH₃), 16.2 (CH₃).

ESI-MS: *m/z* [M+Na]⁺ calcd for C₁₉H₂₄ClNNaO₂S: 388.11; found: 388.11.



Representative procedure **A** was followed using 4-Iodo-*N*-(prop-2-yn-1-yl)benzenesulfonamide (320 mg, 1.0 mmol). Purification by column chromatography on silica gel (*n*-hexanes/EtOAc 80:20) yielded **1g** (375 mg, 82%)

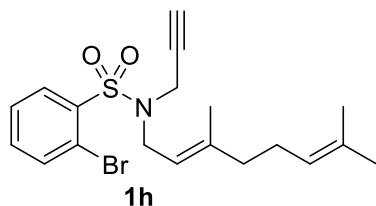
as a white solid. **M. p.** = 47 – 48 °C.

¹H NMR (400 MHz, CDCl₃) δ = 7.88 (d, *J* = 8.7 Hz, 2H), 7.69 (d, *J* = 8.7 Hz, 2H), 5.11 (m, 1H), 5.05 (m, 1H), 4.09 (d, *J* = 2.6 Hz, 2H), 3.85 (d, *J* = 7.3 Hz, 2H), 2.14 – 2.03 (m, 4H), 2.02 (t, *J* = 2.4 Hz, 1H), 1.69 (s, 3H), 1.68 (s, 3H), 1.61 (s, 3H).

¹³C NMR (101 MHz, CDCl₃) δ = 143.0 (C_q), 138.9 (C_q), 138.0 (CH), 132.0 (C_q), 129.2 (CH), 123.7 (CH), 117.4 (CH), 100.0 (C_q), 76.9 (CH), 73.7 (C_q), 43.9 (CH₂), 39.6 (CH₂), 35.2 (CH₂), 26.1 (CH₂), 25.7 (CH₃), 17.7 (CH₃), 16.2 (CH₃).

ESI-MS: *m/z* [M+Na]⁺ calcd for C₁₉H₂₄INNaO₂S: 480.05; found: 480.02.

Chapter 2



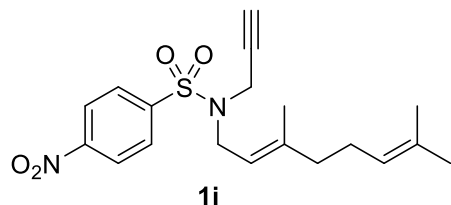
Representative procedure **B** was followed using 2-Bromo-*N*-(prop-2-yn-1-yl)benzenesulfonamide (271 mg, 1.0 mmol). Purification by column chromatography on silica gel (*n*-hexanes/EtOAc 80:20) yielded **1h** (350 mg, 86 %) as

a colourless oil.

¹H NMR (400 MHz, CDCl₃) δ = 8.17 (dd, *J* = 7.7, 1.9 Hz, 1H), 7.76 (dd, *J* = 7.7, 1.4 Hz, 1H), 7.46 (td, *J* = 7.5, 1.4 Hz, 1H), 7.40 (td, *J* = 7.7, 1.9 Hz, 1H), 5.13 – 5.00 (m, 2H), 4.15 (d, *J* = 2.6 Hz, 2H), 4.02 (d, *J* = 7.2 Hz, 2H), 2.19 (t, *J* = 2.4 Hz, 1H), 2.12 – 1.99 (m, 4H), 1.69 (s, 3H), 1.67 (s, 3H), 1.61 (s, 3H).

¹³C NMR (101 MHz, CDCl₃) δ = 142.6 (C_q), 139.2 (C_q), 135.6 (CH), 133.5 (CH), 132.2 (CH), 131.9 (C_q), 127.5 (CH), 123.7 (CH), 120.7 (C_q), 117.8 (CH), 77.4 (CH), 72.9 (C_q), 44.2 (CH₂), 39.6 (CH₂), 35.4 (CH₂), 26.2 (CH₂), 25.7 (CH₃), 17.7 (CH₃), 16.0 (CH₃).

ESI-MS: *m/z* [M+Na]⁺ calcd for C₁₉H₂₄BrNNaO₂S: 434.06; found: 434.06.



Representative procedure **B** was followed using 4-Nitro-*N*-(prop-2-yn-1-yl)benzenesulfonamide (277 mg, 1.2 mmol). Purification by column chromatography on silica gel (*n*-hexanes/EtOAc

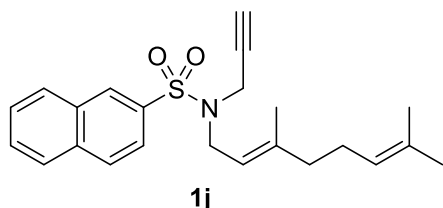
80:20) yielded **1i** (396 mg, 91 %) as a waxy pale-yellow solid.

¹H NMR (400 MHz, CDCl₃) δ = 8.37 (d, *J* = 8.8 Hz, 2H), 8.07 (d, *J* = 8.8 Hz, 2H), 5.18 – 5.09 (m, 1H), 5.09 – 5.00 (m, 1H), 4.14 (m, 2H), 3.89 (d, *J* = 7.4 Hz, 2H), 2.17 – 2.04 (m, 4H), 2.01 (t, *J* = 2.6 Hz, 1H), 1.69 (s, 6H), 1.61 (s, 3H).

¹³C NMR (101 MHz, CDCl₃) δ = 150.1 (C_q), 145.0 (C_q), 143.6 (C_q), 132.1 (C_q), 129.0 (CH), 124.0 (CH), 123.6 (CH), 117.0 (CH), 77.0 (CH), 74.0 (C_q), 44.1 (CH₂), 39.6 (CH₂), 35.3 (CH₂), 26.1 (CH₂), 25.7 (CH₃), 17.7 (CH₃), 16.4 (CH₃).

ESI-MS: *m/z* [M+Na]⁺ calcd for C₁₉H₂₄N₂NaO₄S: 399.14; found: 399.24.

Chapter 2



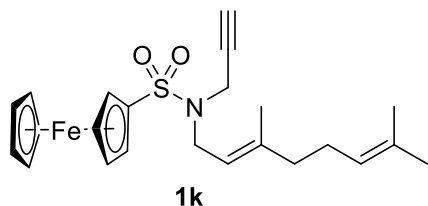
1j, 78 %) as a colourless oil.

Representative procedure **B** was followed using *N*-(prop-2-yn-1-yl)naphthalene-2-sulfonamide (383 mg, 1.6 mmol). Purification by column chromatography on silica gel (*n*-hexanes/EtOAc 80:20) yielded **1j** (465

¹H NMR (400 MHz, CDCl₃) δ = 8.46 (s, 1H), 8.02 – 7.91 (m, 3H), 7.87 (dd, *J* = 8.7, 2.0 Hz, 1H), 7.65 (m, 2H), 5.13 (m, 1H), 5.04 (m, 1H), 4.16 (d, *J* = 2.4 Hz, 2H), 3.92 (d, *J* = 7.2 Hz, 2H), 2.14 – 2.00 (m, 4H), 1.90 (t, *J* = 2.4 Hz, 1H), 1.69 (s, 3H), 1.67 (s, 3H), 1.59 (s, 3H).

¹³C NMR (101 MHz, CDCl₃) δ = 142.7 (C_q), 136.1 (C_q), 134.9 (C_q), 132.2 (C_q), 131.9 (C_q), 129.3 (CH), 129.2 (CH), 128.9 (CH), 128.7 (CH), 127.9 (CH), 127.4 (CH), 123.7 (CH), 123.2 (CH), 117.7 (CH), 76.7 (CH), 73.4 (C_q), 44.0 (CH₂), 39.6 (CH₂), 35.4 (CH₂), 26.2 (CH₂), 25.7 (CH₃), 17.7 (CH₃), 16.1 (CH₃).

ESI-MS: *m/z* for [M+K]⁺ calcd for C₂₃H₂₇KNO₂S: 420.14; found: 420.10.



1k, 87%) as a brown solid. **M. p.** = 83 – 84 °C.

Representative procedure **A** was followed using *N*-(prop-2-yn-1-yl)ferrocene-sulfonamide (303 mg, 1.0 mmol). Purification by column chromatography on silica gel (*n*-hexanes/EtOAc 80:20) yielded **1k** (381 mg,

¹H NMR (400 MHz, CDCl₃) δ = 5.13 – 5.02 (m, 2H), 4.69 (s, 2H), 4.43 (s, 5H), 4.39 (s, 2H), 3.96 (d, *J* = 2.5 Hz, 2H), 3.75 (d, *J* = 7.2 Hz, 2H), 2.12 – 2.00 (m, 5H), 1.69 (s, 3H), 1.67 (s, 3H), 1.60 (s, 3H).

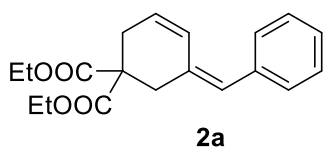
¹³C NMR (101 MHz, CDCl₃) δ = 142.1 (C_q), 131.8 (C_q), 123.8 (CH), 117.9 (CH), 86.0 (C_q), 77.2 (CH), 73.5 (C_q), 70.8 (CH), 70.4 (CH), 69.4 (CH), 43.7 (CH₂), 39.6 (CH₂), 35.3 (CH₂), 26.2 (CH₂), 25.7 (CH₃), 17.7 (CH₃), 16.2 (CH₃).

ESI-MS: *m/z* [M+Na]⁺ calcd for C₂₃H₂₉FeNNaO₂S: 462.12; found: 462.06.

Chapter 2

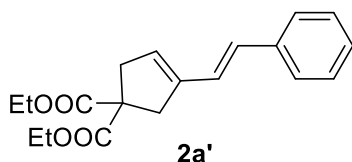
- **General procedure for catalysis with Enyne 1a**

In a 10 mL two-necked round-bottom flask containing the selected gold complex (1.0 mol % for calix[6]arene-based complexes and 2.0 mol % for monomeric complexes), dry CH₂Cl₂ (2.0 mL) was added under nitrogen atmosphere. Subsequently, a tip of spatula (micro spatula, Heyman type 16 cm) of AgSbF₆ (≈2.0 mol %, ≈2 mg) was added along with 20 mg of 4 Å molecular sieves. The flask was covered with an aluminum foil and the mixture stirred for 5 minutes. Subsequently, **1a** (0.2 mmol, 63.0 mg) was added and the reaction mixture was stirred for 4 hours. After completion, the mixture was diluted with 20 mL of CH₂Cl₂, filtered through a pad of celite, and transferred in a 100 mL flask where it was concentrated under reduced atmosphere. Conversions and selectivities for products **2a** and **2a'** were determined by ¹H NMR analysis (data confirmed by performing the reaction twice).



¹H NMR (400 MHz, CDCl₃) δ = 7.48–7.19 (m, 5H), 6.63 (dtd, *J* = 10.1, 2.1, 1.0 Hz, 1H), 6.37 (s, 1H), 5.90 (dtd, *J* = 10.1, 4.0, 1.6 Hz, 1H), 4.30–4.21 (m, 4H), 2.98 (d, *J* = 1.6 Hz, 2H), 2.78 (ddd, *J*

= 4.0, 2.1, 0.9 Hz, 2H), 1.32–1.24 (m, 6H). The analysis was coherent with the reported characterization.^[26]



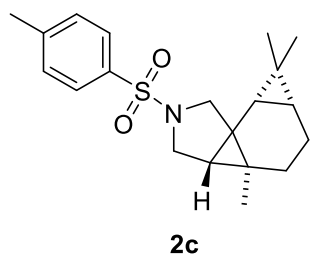
¹H NMR (400 MHz, CDCl₃) δ = 7.48–7.20 (m, 5H), 6.93 (d, *J* = 16.2 Hz, 1H), 6.48 (d, *J* = 16.2 Hz, 1H), 5.73 (ddd, *J* = 2.7, 1.9, 0.9 Hz, 1H), 4.23–4.14 (m, 4H), 3.28 (dd, *J* = 1.9, 0.9 Hz, 2H),

3.18 (dd, *J* = 1.9, 0.9 Hz, 2H), 1.32–1.21 (m, 6H). The analysis was coherent with the reported characterization.^[26]

Chapter 2

- **General procedure for catalysis with Enynes 1b-k**

In a 10 mL two-necked round-bottomed flask containing **A**(AuCl)₂ (1 mol %), dry CH₂Cl₂ (1.0 mL) was added under a N₂ atmosphere. Subsequently, AgSbF₆ (2.0 mol% ≈ 1 mg) was added along with 20 mg of 4 Å molecular sieves. The flask was covered with aluminium foil and the mixture was stirred for 5 minutes. Subsequently, the selected Enyne **1** (0.15 mmol) was added as a solution in CH₂Cl₂ and the reaction mixture was stirred for the desired time. After completion, the mixture was diluted with 20 mL of CH₂Cl₂, filtered through a pad of Celite, and transferred to a 100 mL flask where it was concentrated under a reduced atmosphere. Conversions and selectivities for **2** were determined by ¹H NMR analysis (data were confirmed by performing the reactions twice). New compounds were purified by column chromatography on silica gel.

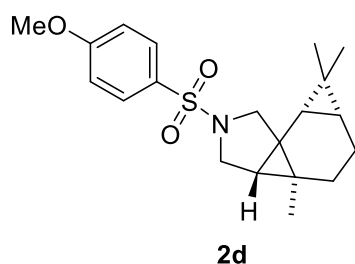


The general procedure was followed using **1c** (0.15 mmol, 69 mg) and stirring the reaction for 8 h. Purification by column chromatography on silica gel (*n*-Hex/ EtOAc 95:5) afforded **2c** (60 mg, 87%) as a colourless solid. **M. p.** = 110–111 °C.

¹H NMR (400 MHz, CDCl₃) δ = 7.73 (d, *J* = 8.3 Hz, 2H), 7.35 (d, *J* = 7.9 Hz, 2H), 3.44–3.31 (m, 4H), 2.46 (s, 3H), 1.69–1.65 (m, 1H), 1.65–1.60 (m, 1H), 1.08–1.04 (m, 1H), 1.01 (s, 1H), 0.93 (s, 3H), 0.91 (s, 3H), 0.89–0.81 (m, 4H), 0.74–0.66 (m, 1H), 0.61 (d, *J* = 8.8 Hz, 1H).

¹³C NMR (101 MHz, CDCl₃) δ = 143.2, 134.4, 129.6, 127.4, 51.8, 48.0, 35.1, 34.6, 29.8, 28.1, 24.5, 23.8, 22.3, 21.6, 20.4, 17.6, 16.4, 12.5.

ESI-MS: *m/z* [M+H]⁺ calcd. for C₂₀H₂₈NO₂S: 346.18; found: 346.22.



The general procedure was followed using **1d** (0.15 mmol, 54 mg) and stirring the reaction for 8 h. Purification by column chromatography on silica gel (*n*-Hex/ EtOAc 95:5) afforded **2d** (49 mg, 90%) as a colourless solid. **M. p.** = 74–75 °C.

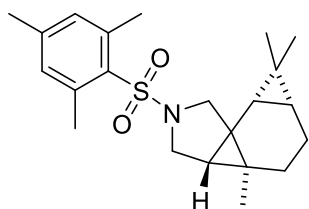
Chapter 2

¹H NMR (300 MHz, CDCl₃) δ = 7.79 (d, *J* = 9.0 Hz, 2H), 7.02 (d, *J* = 9.0 Hz, 2H), 3.9 (s, 3H), 3.43–3.34 (m, 3H), 3.32 (d, *J* = 9.8 Hz, 1H), 1.70–1.66 (m, 1H), 1.66–1.63 (m, 1H), 1.63–1.57 (m, 1H), 1.06 (d, *J* = 3.76 Hz, 1H), 1.01 (s, 3H), 0.93 (s, 3H), 0.91 (s, 3H), 0.89–0.84 (m, 1H), 0.74–0.70 (m, 1H), 0.63 (d, *J* = 8.8 Hz, 1H).

¹³C NMR (101 MHz, CDCl₃) δ = 162.8, 129.4, 129.2, 114.1, 55.6, 51.8, 48.0, 35.1, 34.6, 29.8, 28.1, 24.5, 23.8, 22.3, 20.4, 17.6, 16.4, 12.5.

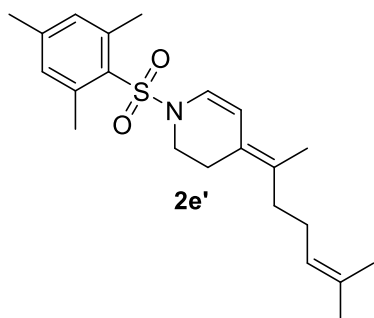
ESI-MS: *m/z* [M+H]⁺ calcd. for C₂₀H₂₈NO₃S: 362.18; found: 362.18.

HR-MS: *m/z* [M+H]⁺ calcd. for C₂₀H₂₈NO₃S: 362.1790; found: 362.1786.



2e

The general procedure was followed using **1e** (0.15 mmol, 56 mg) and stirring the reaction for 8 h. Purification by column chromatography on silica gel (*n*-Hex/ EtOAc 95:5) afforded a mixture of **2e** and **2e'** (3.6:1, 42.6 mg, 76%).



2e'

¹H NMR (400 MHz, CDCl₃, **2e**) δ = 6.96 (s, 2H), 3.57 (dd, *J* = 9.4, 5.6 Hz, 1H), 3.53 (d, *J* = 9.5 Hz, 1H), 3.29 (d, *J* = 9.5 Hz, 1H), 3.24 (d, *J* = 9.4 Hz, 1H), 2.63 (s, 6H), 2.31 (s, 3H), 1.69 (m, 3H), 1.16 (d, *J* = 5.1 Hz, 1H), 1.02 (s, 3H), 0.98 (s, 3H), 0.91 (s, 3H), 0.89–0.84 (m, 1H), 0.78–0.73 (m, 2H).

¹H NMR (400 MHz, CDCl₃, **2e'**) δ = 6.95 (s, 2H), 6.48 (dt, *J* = 10.2, 2.2 Hz, 1H), 5.66 (dt, *J* = 10.2, 3.6 Hz, 1H), 5.03 (m,

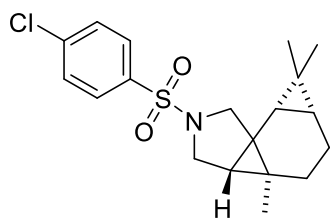
1H), 3.94 (m, 2H), 3.75 (m, 2H), 2.61 (s, 6H), 2.29 (s, 3H), 2.08–1.97 (m, 4H), 1.78 (s, 3H), 1.70 (s, 3H), 1.59 (s, 3H).

¹³C NMR (101 MHz, CDCl₃, **2ae**) δ = 142.2, 140.5, 139.9, 131.9, 50.9, 47.3, 35.3, 34.5, 30.1, 28.1, 24.4, 23.9, 23.1, 22.5, 20.9, 20.5, 17.6, 16.5, 12.6.

¹³C NMR (101 MHz, CDCl₃, **2ae'**) δ = 142.5, 140.5, 140.5, 133.6, 133.1, 131.6, 124.7, 123.6, 123.3, 121.8, 52.5, 48.0, 33.9, 27.0, 24.0, 22.8, 22.7, 22.6, 20.8.

ESI-MS: *m/z* [M+H]⁺ calcd. for C₂₂H₃₂NO₂S: 374.22; found: 374.22.

Chapter 2



2f

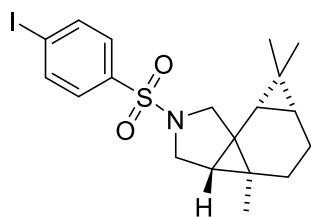
The general procedure was followed using **1f** (0.15 mmol, 55 mg) and stirring the reaction for 8 h. Purification by column chromatography on silica gel (*n*-Hex/ EtOAc 95:5) afforded **2f** (44 mg, 80%) as a colourless solid. **M. p.** = 118–119 °C.

¹H NMR (300 MHz, CDCl₃) δ = 7.79 (d, *J* = 8.7 Hz, 2H), 7.53 (d, *J* = 8.7 Hz, 2H), 3.39 (m, 3H), 3.71 (d, *J* = 9.8 Hz, 1H), 1.71–1.68 (m, 1H), 1.68–1.65 (m, 1H), 1.65–1.62 (m, 1H), 1.09 (dd, *J* = 4.4, 1.9 Hz, 1H), 1.02 (s, 3H), 0.93 (s, 3H), 0.91 (s, 3H), 0.88–0.84 (m, 1H), 0.76–0.66 (m, 1H), 0.63 (d, *J* = 8.8 Hz, 1H).

¹³C NMR (101 MHz, CDCl₃) δ = 139.0, 135.8, 129.3, 128.7, 51.8, 48.1, 35.0, 34.6, 29.8, 28.0, 24.5, 23.8, 22.2, 20.5, 17.6, 16.4, 12.4.

ESI-MS: *m/z* [M+Na]⁺ calcd. for C₁₉H₂₄ClNNaO₂S: 388.11; found: 388.11.

HR-MS: *m/z* [M+H]⁺ calcd. for C₁₉H₂₅ClNO₂S: 366.1295; found: 366.1298.



2g

The general procedure was followed using **1g** (0.15 mmol, 69 mg) and stirring the reaction for 8 h. Purification by column chromatography on silica gel (*n*-Hex/EtOAc 95:5) afforded **2g** (60 mg, 87%) as a colourless solid. **M. p.** = 144–145 °C.

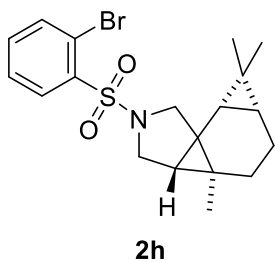
¹H NMR (400 MHz, CDCl₃) δ = 7.74 (d, *J* = 8.6 Hz, 2H), 7.35 (d, *J* = 8.6 Hz, 2H), 3.43–3.35 (m, 3H), 3.33 (d, *J* = 9.7 Hz, 1H), 1.71–1.67 (m, 1H), 1.67–1.63 (m, 1H), 1.63–1.57 (m, 1H), 1.05 (m, 1H), 1.01 (s, 3H), 0.93 (s, 3H), 0.91 (s, 3H), 0.89–0.83 (m, 1H), 0.75–0.71 (m, 1H), 0.62 (d, *J* = 8.8 Hz, 1H).

¹³C NMR (101 MHz, CDCl₃) δ = 138.3, 137.0, 128.7, 99.8, 51.8, 48.1, 35.0, 34.6, 29.8, 28.0, 24.5, 23.8, 22.2, 20.5, 17.6, 16.4, 12.4.

ESI-MS: *m/z* for [M+Na]⁺ calcd. for C₁₉H₂₄I NNaO₂S: 480.05; found: 480.02.

HR-MS: *m/z* for [M+H]⁺ calcd. for C₁₉H₂₅I NO₂S: 458.0651; found: 458.0647.

Chapter 2



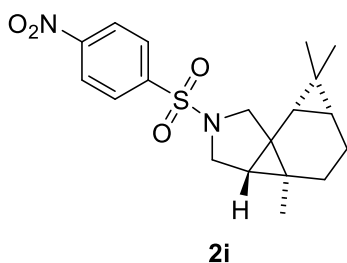
The general procedure was followed using **1h** (0.15 mmol, 62 mg) and stirring the reaction for 8 h. Purification by column chromatography on silica gel (*n*-Hex/ EtOAc 95:5) afforded **2h** (49 mg, 79%) as a colourless oil.

¹H NMR (400 MHz, CDCl₃) δ = 8.11 (dd, *J* = 7.8, 1.8 Hz, 1H), 7.77 (dd, *J* = 7.8, 1.3 Hz, 1H), 7.47 (td, *J* = 7.6, 1.3 Hz, 1H), 7.40 (td, *J* = 7.7, 1.8 Hz, 1H), 3.71 (dd, *J* = 9.7, 5.6 Hz, 1H), 3.61 (d, *J* = 9.7 Hz, 1H), 3.48 (d, *J* = 6.8 Hz, 1H), 3.46 (d, *J* = 7.0 Hz, 1H), 1.73–1.70 (m, 1H), 1.70–1.65 (m, 2H), 1.19 (d, *J* = 5.0 Hz, 1H), 1.03 (s, 3H), 1.00 (s, 3H), 0.96–0.92 (m, 4H), 0.79–0.71 (m, 2H).

¹³C NMR (101 MHz, CDCl₃) δ = 138.9, 135.6, 133.3, 132.0, 127.5, 120.3, 52.0, 48.4, 35.2, 34.4, 30.2, 28.1, 24.4, 23.9, 22.5, 20.5, 17.6, 16.5, 12.6.

ESI-MS: *m/z* for [M+Na]⁺ calcd. for C₁₉H₂₄BrNNaO₂S: 434.06; found: 434.06.

HR-MS: *m/z* for [M+H]⁺ calcd. for C₁₉H₂₅BrNO₂S: 410.0789; found: 410.0786.



The general procedure was followed using **1i** (0.15 mmol, 56 mg), 1.5 mol% of **A**(AuCl)₂ and stirring the reaction for 8 h. Purification by column chromatography on silica gel (*n*-Hex/EtOAc 95:5) afforded **2i** (47 mg, 85%) as a pale-yellow solid. **M. p.** = 170–171 °C.

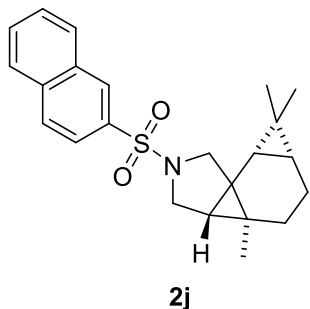
¹H NMR (400 MHz, CDCl₃) δ = 8.41 (d, *J* = 8.9 Hz, 2H), 8.01 (d, *J* = 8.9 Hz, 2H), 3.43 (m, 3H), 3.35 (d, *J* = 9.8 Hz, 1H), 1.71–1.68 (m, 1H), 1.68–1.65 (m, 1H), 1.65–1.61 (m, 1H), 1.11 (dd, *J* = 4.2, 2.1 Hz, 1H), 1.01 (s, 3H), 0.93 (s, 3H), 0.87–0.81 (m, 4H), 0.76–0.69 (m, 1H), 0.63 (d, *J* = 8.8 Hz, 1H).

¹³C NMR (101 MHz, CDCl₃) δ = 150.0, 143.2, 128.4, 124.4, 51.9, 48.3, 34.9, 34.5, 29.9, 28.0, 24.5, 23.8, 22.1, 20.6, 17.6, 16.4, 12.3.

ESI-MS: *m/z* for [M+Na]⁺ calcd. for C₁₉H₂₄N₂NaO₄S: 399.14; found: 399.15.

Chapter 2

HR-MS: m/z for $[M+H]^+$ calcd. for $C_{19}H_{25}N_2O_4S$: 377.1535; found: 377.1529.



The general procedure was followed using **1j** (0.15 mmol, 56 mg) and stirring the reaction for 8 h. Purification by column chromatography on silica gel (*n*-Hex/EtOAc 95:5) afforded **2j** (50 mg, 90%) as a colourless oil.

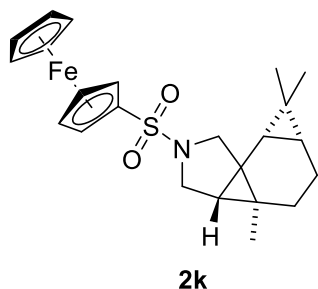
¹H NMR (400 MHz, CDCl₃) δ = 8.42 (s, 1H), 8.06–7.98 (m, 2H), 7.95 (d, J = 7.3 Hz, 1H), 7.86 (dd, J = 8.6, 1.8 Hz, 1H), 7.66 (m, 2H),

3.52–3.45 (m, 3H), 3.41 (d, J = 9.6 Hz, 1H), 1.72–1.66 (m, 1H), 1.66–1.61 (m, 1H), 1.61–1.56 (m, 1H), 1.06 (dd, J = 4.8, 1.7 Hz, 1H), 1.00 (s, 3H), 0.94 (s, 3H), 0.93 (s, 3H), 0.87–0.80 (m, 1H), 0.72–0.66 (m, 1H), 0.60 (d, J = 8.6 Hz, 1H).

¹³C NMR (101 MHz, CDCl₃) δ = 134.8, 134.6, 132.3, 129.3, 129.2, 128.6, 128.4, 127.9, 127.4, 123.0, 51.9, 48.2, 35.1, 34.6, 29.8, 28.0, 24.4, 23.8, 22.2, 20.5, 17.6, 16.4, 12.5.

ESI-MS: m/z for $[M+H]^+$ calcd. for $C_{23}H_{28}NO_2S$: 382.18; found: 382.20.

HR-MS: m/z for $[M+H]^+$ calcd. for $C_{23}H_{28}NO_2S$: 382.1841; found: 382.1836.



The general procedure was followed using **1k** (0.15 mmol, 66 mg) and stirring the reaction for 8 h. Purification by column chromatography on silica gel (*n*-Hex/EtOAc 95:5) afforded **2k** (33.2 mg, 50.3%) as a brown oil.

¹H NMR (400 MHz, CDCl₃) δ = 4.66 (d, J = 9.4 Hz, 2H), 4.41 (m, 7H), 3.48 (d, J = 4.8 Hz, 1H), 3.46 (d, J = 4.8 Hz, 1H), 1.73–1.66

(m, 3H), 1.62–1.56 (m, 2H), 1.19 (d, J = 4.2 Hz, 1H), 1.03 (s, 3H), 1.00 (s, 3H), 0.92 (s, 3H), 0.84–0.79 (m, 1H), 0.73–0.65 (m, 1H), 0.65–0.60 (d, J = 8.8 Hz, 1H).

¹³C NMR (101 MHz, CDCl₃) δ = 84.3, 70.7, 70.4, 70.3, 68.9, 68.8, 51.7, 47.9, 35.2, 34.6, 29.8, 28.1, 24.5, 23.8, 22.4, 20.4, 17.5, 16.5, 12.6.

ESI-MS: m/z for $[M+H]^+$ calcd. for $C_{23}H_{30}FeNO_2S$: 440.13; found: 440.12.

ESI-MS: m/z for $[M+H]^+$ calcd. for $C_{23}H_{30}FeNO_2S$: 440.1347; found: 440.1344.

Chapter 2

2.5 Bibliography

- [1] Kamer, P. C. J.; van Leeuwen, P. W. N. M., Eds. *Phosphorus(III) Ligands in Homogeneous Catalysis: Design and Synthesis*; John Wiley & Sons: Chichester, UK, 2012.
- [2] a) Z. Kaya, E. Bentouhami, K. Pelzer and D. Armspach, *Coord. Chem. Rev.*, **2021**, 445, 2140662; b) R. Gramage-Doria, D. Armspach and D. Matt, *Coord. Chem. Rev.*, **2013**, 257, 776-816.
- [3] a) Chavagnan, T.; Sémeril, D.; Matt, D.; Toupet, L. *Eur. J. Org. Chem.*, **2017**, 313–323; b) El Moll, H.; Sémeril, D.; Matt, D.; Toupet, L. *Adv. Synth. Catal.*, **2010**, 352, 901–908; c) El Moll, H.; Sémeril, D.; Matt, D.; Youinou, M.-T.; Toupet, L. *Org. Biomol. Chem.*, **2009**, 7, 495–501.
- [4] a) Schöttle, C.; Guan, E.; Okrut, A.; Grosso-Giordano, N. A.; Palermo, A.; Solovyov, A.; Gates, B. C.; Katz, A. *J. Am. Chem. Soc.* **2019**, 141, 4010–4015; b) Elaieb, F.; Hedhli, A.; Sémeril, D.; Matt, D. *Eur. J. Org. Chem.* **2016**, 1867–1873; c) Sémeril, D.; Matt, D.; Toupet, L. *Chem. – Eur. J.* **2008**, 14, 7144–7155.
- [5] a) L. Andreoni, G. M. Beneventi, G. Giovanardi, G. Cera, A. Credi, A. Arduini, A. Secchi, S. Silvi, *Chem. Eur. J.*, **2023**, 29, e202203472; b) G. Cera, A. Arduini, A. Secchi, A. Credi and S. Silvi, *Chem. Rec.*, **2021**, 21, 1161; c) F. Cester Bonati, L. Andreoni, S. Cattani, C. Baccini, S. Anzellotti, G. Cera, S. Silvi, A. Secchi, *Eur. J. Org. Chem.*, **2024**, 27, e202400237.
- [6] G. Cera, G. Giovanardi, A. Secchi, A. Arduini, *Chem. Eur. J.* **2021**, 27, 10261–10266.
- [7] A. Arduini, R. Ferdani, A. Pochini, A. Secchi, F. Ugozzoli, *Angew. Chem., Int. Ed.* **2000**, 39, 3453–3456.
- [8] A. Credi, S. Dumas, S. Silvi, M. Venturi, A. Arduini, A. Pochini, A. Secchi, *J. Org. Chem.*, **2004**, 69, 5881–5887.
- [9] Recent examples of gold(I)-catalyzed cycloisomerization of 1,6-enynes: a) C. Cecchini, G. Cera, M. Lanzi, L. Marchiò, D. Balestri and G. Maestri, *Org. Chem. Front.*, **2019**, 6, 3584; b) G. Zuccarello, J. G. Mayans, I. Escofet, D. Scharnagel, M. S. Kirillova, A. H. Pérez-Jimeno, P. Calleja, J. R. Boothe, A. M. Echavarren, *J.*

Chapter 2

- Am. Chem. Soc.*, **2019**, 141, 11858; c) R. Laher, C. Marin, V. Michelet, *Org. Lett.*, **2020**, 22, 4058.
- [10] C. Nieto-Oberhuber, M. Paz Muñoz, S. López, E. Jiménez-Núñez, C. Nevado, E. Herrero-Gómez, M. Raducan, A. M. Echavarren, *Chem. Eur. J.*, **2006**, 12, 1677–1693.
- [11] a) G. Giovanardi, A. Secchi, A. Arduini, G. Cera, *Beilstein J. Org. Chem.* **2022**, 18, 190–196; b) G. Giovanardi, D. Balestri, A. Secchi, G. Cera, *Org. Biomol. Chem.*, **2022**, 20, 6464–6472.
- [12] G. Cera, M. Bazzoni, L. Andreoni, F. Cester Bonati, C. Massera, S. Silvi, A. Credi, A. Secchi, A. Arduini, *Eur. J. Org. Chem.* **2021**, 5788–5798.
- [13] J. P. M. van Duynhoven, R. G. Janssen, W. Verboom, S. M. Franken, A. Casnati, A. Pochini, R. Ungaro, J. de Mendoza, P. M. Nieto, *J. Am. Chem. Soc.* **1994**, 116, 5814–5822.
- [14] L. Falivene, Z. Cao, A. Petta, L. Serra, A. Poater, R. Oliva, V. Scarano, L. Cavallo, *Nat. Chem.*, **2019**, 11, 872.
- [15] H. Clavier, S. P. Nolan, *Chem. Commun.*, **2010**, 46, 841.
- [16] a) E. Jiménez-Núñez, A. M. Echavarren, *Chem. Rev.* **2008**, 108, 3326–3350; b) N. Cabello, E. Jiménez-Núñez, E. Buñuel, D. J. Cárdenas, A. M. Echavarren, *Eur. J. Org. Chem.*, **2007**, 4217–4223; c) C. Nieto-Oberhuber, M. Paz Muñoz, S. López, E. Jiménez-Núñez, C. Nevado, E. Herrero-Gómez, M. Raducan and A. M. Echavarren, *Chem. – Eur. J.*, **2006**, 12, 1677.
- [17] M. Bazzoni, V. Zanichelli, L. Casimiro, C. Massera, A. Credi, A. Secchi, S. Silvi, A. Arduini, *Eur. J. Org. Chem.* **2019**, 3513–3524.
- [18] a) P. Dydio, R. J. Detz, B. de Bruin, J. N. H. Reek, *J. Am. Chem. Soc.*, **2014**, 136, 8418–8429; b) S. Tasan, O. Zava, B. Bertrand, C. Bernhard, C. Goze, M. Picquet, P. Le Gendre, P. Harvey, F. Denat, A. Casini, E. Bodio, *Dalton Trans.*, **2013**, 42, 6102–6109; c) Y. K. Kim, S. J. Lee, K. H. Ahn, *J. Org. Chem.*, **2000**, 65, 7807–7813.
- [19] M. E. Krafft, L. V. R. Bonaga, J. A. Wright, C. Hirosawa, *J. Org. Chem.*, **2002**, 67, 1233–1246.
- [20] C. Nieto-Oberhuber, S. López, M. Paz Muñoz, E. Jiménez-Núñez, E. Buñuel, D. J. Cárdenas, A. M. Echavarren, *Chem. – Eur. J.*, **2006**, 12, 1694.

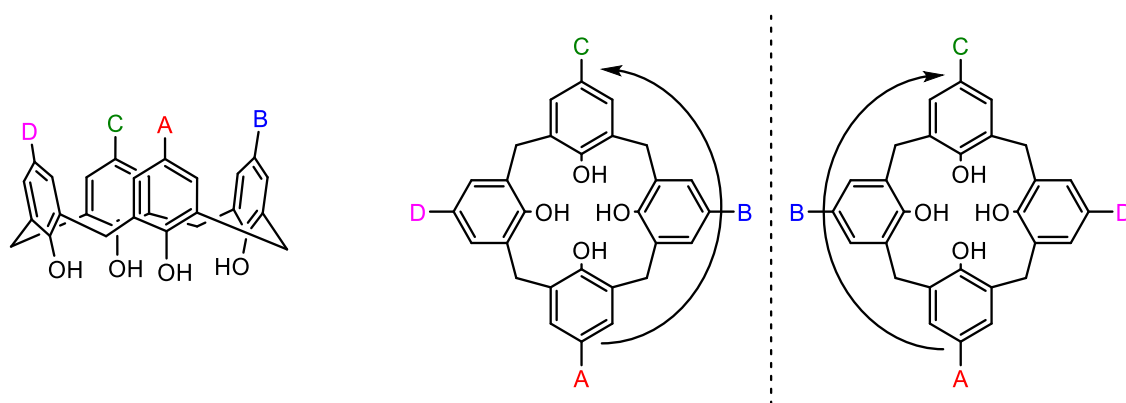
Chapter 2

- [21] a) X. Zhang, Q. Zhang, L. Li, S. Cao, Z. Liu, G. Zanoni, Y. Ning and Y. Wu, *Org. Lett.*, **2021**, 23, 3674; b) M. Gao, Q. Gao, X. Hao, Y. Wu, Q. Zhang, G. Liu and R. Liu, *Org. Lett.*, **2020**, 22, 3, 1139.
- [22] (a) D. Astruc, *Eur. J. Inorg. Chem.*, **2017**, 6; (b) M. Patra, G. Gasser, *Nat. Rev. Chem.*, **2017**, 1, 0066.
- [23] Agilent, CrysAlis PRO, Agilent Technologies Ltd, Yarnton, Oxfordshire, England, 2014.
- [24] G. M. Sheldrick, *Acta Cryst.*, **2015**, A71, 3.
- [25] O. V. Dolomanov, L. J. Bourhis, R. J. Gildea, J. A. K. Howard, H. Puschmann, *J. Appl. Crystallogr.*, **2009**, 42, 339.
- [26] C. Nieto-Oberhuber, M. Paz Muñoz, S. López, E. Jiménez-Núñez, C. Nevado, E. Herrero-Gómez, M. Raducan, A. M. Echavarren, *Chem. – Eur. J.*, **2006**, 12, 1677–1693.

Chapter 3. Gold(I)-catalyzed hydroarylation reaction for the preparation of inherently chiral calix[4]arenes (ICCs)

3.1 Introduction

Calix[n]arenes are a versatile family of macrocyclic molecules that have been exploited in supramolecular chemistry for a long time, mainly due to the possibility to easily and selectively functionalize the upper and lower rim of the macrocycle.^[1] Recently, there have been an overgrowing interest in a particular set of calix[4]arene derivatives, the inherently chiral calix[4]arenes (herein ICCs), that have attracted researcher for their potential application in many fields of chemistry. These types of derivatives, as the name suggests, have been functionalized in such a way that they become asymmetrical, generating two enantiomers. The peculiarity is that the chirality is not due to the presence of a stereogenic carbon but, as Schiaffino and Szumna describe, it “arise from the introduction of a curvature in an ideal planar structure that is devoid of perpendicular symmetry planes in its bidimensional representation” (Scheme 3.1).^[2]



Scheme 3.1: Tri-dimensional and bi-dimensional representation of ICCs and the corresponding curvature induced by the substituents in the upper rim (order of priority: $A > B > C > D$).

In the literature are described four main ways to functionalize the calix[4]arene scaffold in order to disrupt the symmetry of the macromolecule: asymmetric functionalization of

Chapter 3

upper- and lower-rim, the bridging methylene or the functionalization of the *meta*-position of the aromatic ring (Figure 3.1).

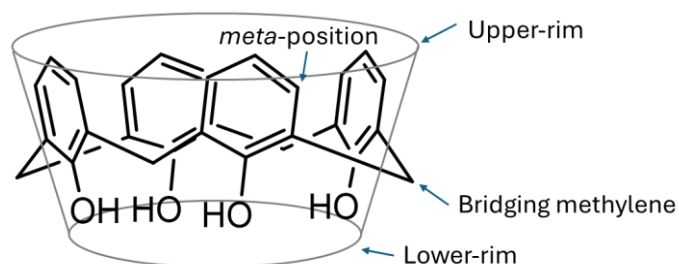


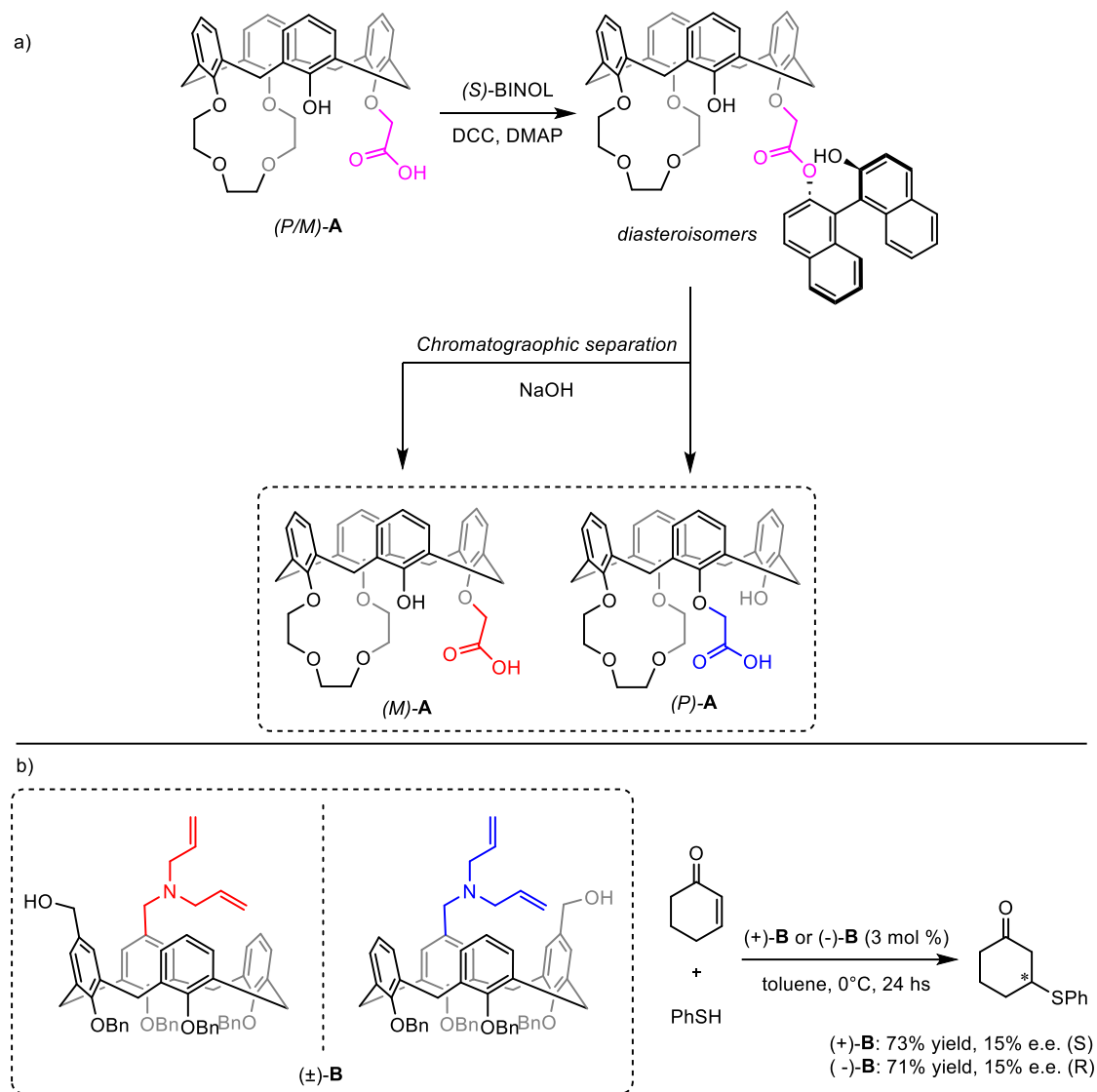
Figure 3.1: Highlight of the different sites of the calix[4]arene scaffold.

The first two strategies represent the earliest method for the generation of ICCs, for example Huang's group presented the synthesis of tri-*O*-alkylated ICCs by sequential alkylation of the lower-rim starting from 1,2-calix[4]crowns (Figure 4.2, a).^[3] Other examples regarding the functionalization of the upper-rim were presented by Shirakawa's group featuring the synthesis of amino alcohols by a multi-step synthetic sequence and the study of their application as organocatalysts (Figure 3.2, b).^[4]

The main disadvantage was that the separation of the enantiomers needed the use of a chiral derivatization agent to form the diastereomers, followed by chromatographic separation or crystallization.

A less used method consist in the direct functionalization of the bridging methylene of the calix[4]arene scaffold. An example was brought by Reinhoudt and Snieckus, were they presented the synthesis of ICCs by anionic *ortho*-Fries rearrangement for the lateral functionalization of calix[4]arenes (Figure 3.3).^[5] Later, the work of Li, Wang and Liu provided a method for the separation of these compounds by, again, the derivatization with a chiral agent.

Chapter 3



Scheme 3.2: a) Structure and separation technique for Huang's ICCs; b) Structure and catalytic applications for Shirakawa's ICCs.

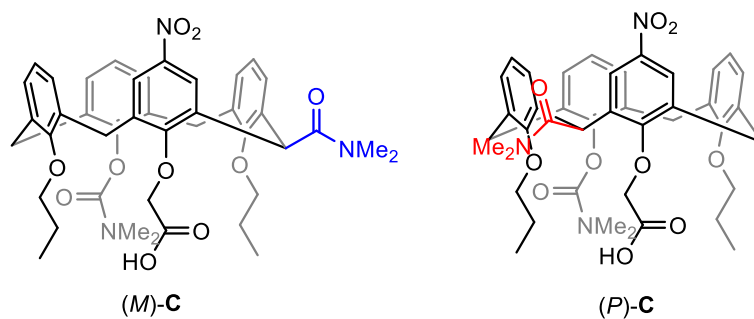
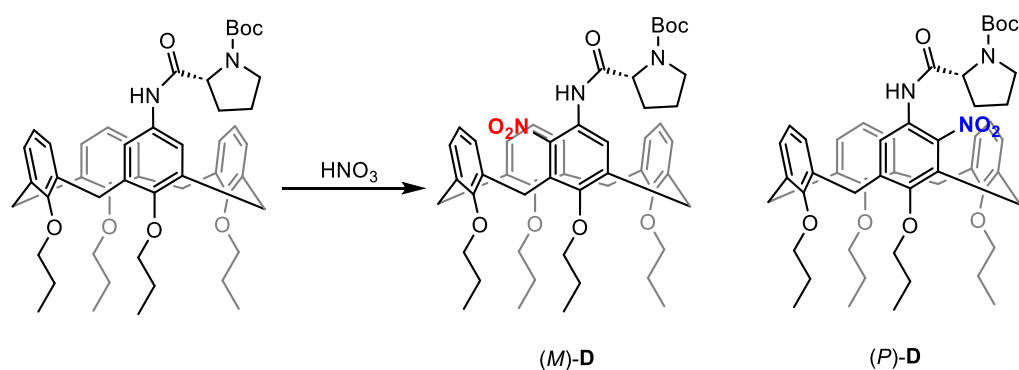


Figure 3.3: Structure of the enantiomers separated in Li, Wang and Liu's work.

Chapter 3

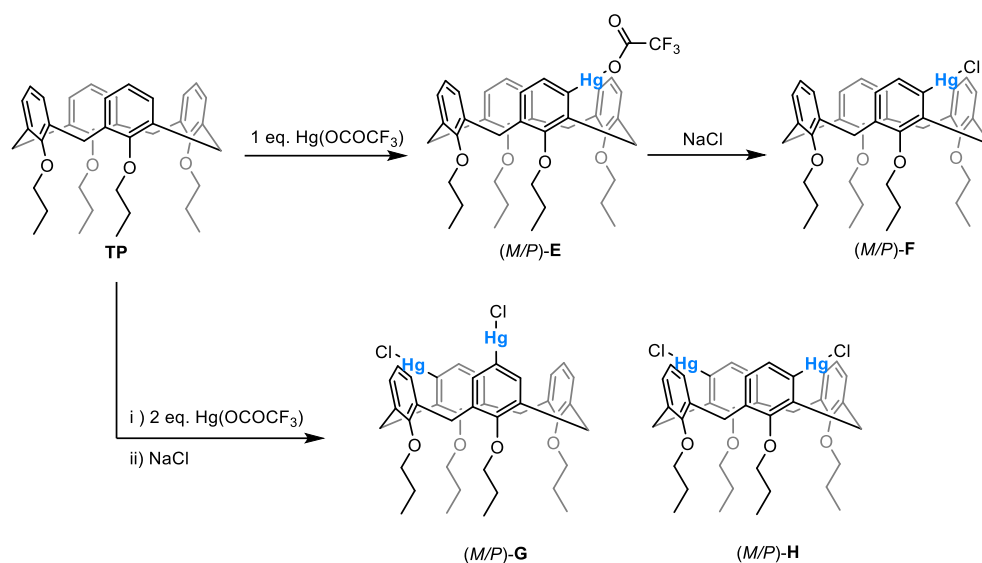
The last and more exploited methodology consist in the functionalization of the *meta*-position of the aryl moieties of the calix[4]arene scaffold.^[6] These strategies can be divided in three categories: *ortho*-oriented, direct substitution or ring-closure. One of the first attempt to *meta*-functionalise the calix[4]arene scaffold was made by Cheng and Huang and it fell into the first category. In this work, they show the direct nitration or bromination of the *meta*-position guided by a *N*-BOC-proline that have been successfully installed on the upper rim (Scheme 3.3).^[7] The main limitation was that the diastereoselectivity of this reaction was extremely low, which was unexpected seen the type of chiral auxiliary used.



Scheme 3.3: *ortho*-oriented direct nitration in the *meta*-position of the calix[4]arene scaffold.

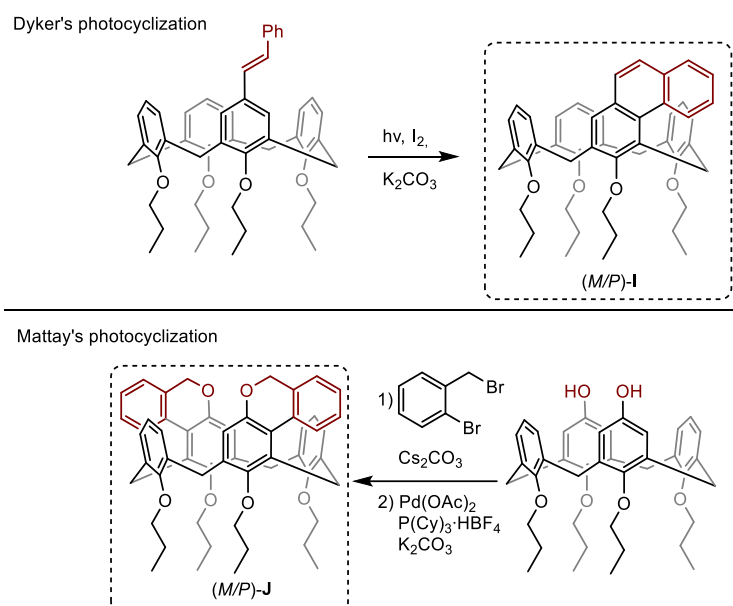
Lhotak reported, in a recent work, a novel methodology to regioselectivity functionalize the calix[4]arene scaffold on the *meta*-position by forming an organo-mercury intermediate, by reaction of derivative **TP** with Hg(II) trifluoroacetate (Scheme 3.4), that could then be further transformed to introduce the desired functionality.^[8]

Chapter 3



Scheme 3.4: Lhoták's direct mono- and di-mercuration on the meta-position of calix[4]arene derivative TP.

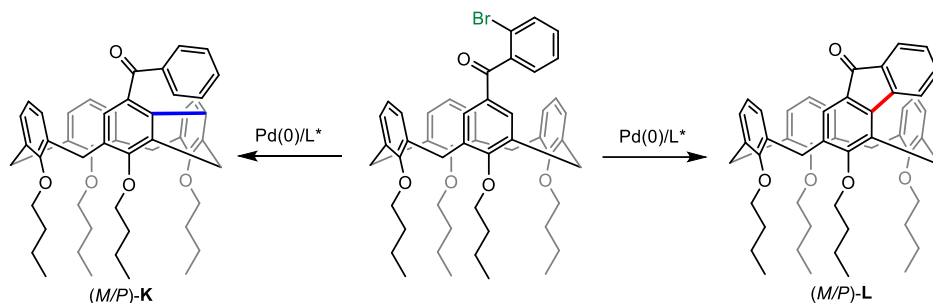
The main problematic associated with this strategy was the use of highly toxic metal in the synthesis of the intermediate and the co-production of mercury salts as wastes, that need to be properly managed. To overcome this limitation, new methodology that rely on ring-closure reactions have been developed, like Dyker's work on the use of a photocyclization reaction or Mattay's pd-catalyzed intramolecular cyclization (Scheme 3.5).^[9]



Scheme 3.5: Examples of meta-functionalization directed by catalyzed cyclization reactions.

Chapter 3

Very recently it has been reported from Zhang and collaborator a novel enantioselective approach via Pd-catalyzed C-H arylation reaction that could lead to the *meta*-functionalized derivative (M/P)-L or to the bridging *meta-meta* compound (M/P)-K.^[10]



Scheme 3.6: Zhang's Pd-catalyzed *meta*-functionalization.

It's from this results that our research group decided to develop a new methodology exploiting the well-known gold(I)-catalyzed intramolecular hydroarylation reaction,^[11] which this chapter will discuss. The advantages of using this type of reaction resides in its total atom economy and in the use of a fairly atoxic metal, compared to the previously reported methodologies.

Chapter 3

3.2 Results and discussion

A new calix[4]arene derivative was designed, characterized by the mono-functionalization of the upper rim with an alkyne moiety exploiting a sulfonamide as the tethering group to the macrocyclic scaffold.

The synthesis started with the well-known mono-ammine calix[4]arene intermediate **MN**, that was quantitatively reduced with $\text{NH}_2\text{-NH}_2 \cdot \text{H}_2\text{O}$ in the presence of Pd/C in MeOH. The mono-ammine intermediate was then immediately converted into the sulfonamide derivative **MS** by reacting with *p*-toluenesulfonyl chloride with triethylamine in CH_2Cl_2 at 0 °C. Finally, by simple alkylation of **MS** with propargyl bromide in the presence of K_2CO_3 in acetone, we achieved the desired model substrate **3a** (Figure 3.4).

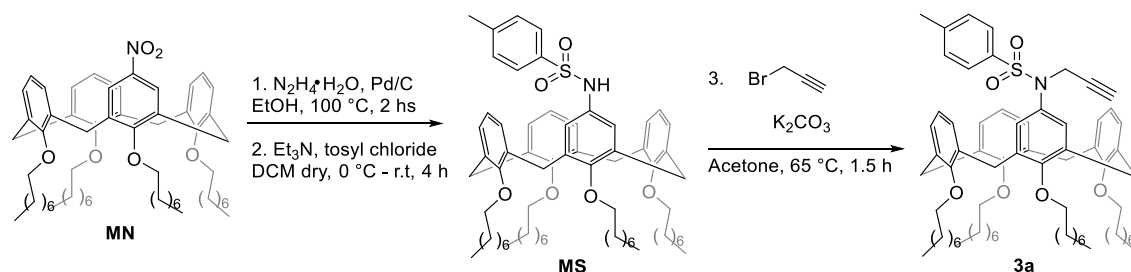


Figure 3.4: Synthetic strategy for the synthesis of **1a**.

Once established a protocol for the synthesis of the substrates, alkyne **3a** was subjected to standard gold(I) catalysis conditions using PPh_3AuCl (5 mol%) in combination with AgSbF_6 as a chloride scavenger, yielding calix[4]dihydroquinoline **4a** as the sole product in high yields, obtained as a racemic mixture (Table 3.1, entry 1).

The new racemic ICC **4a** was then analysed by NMR (Figure 3.5). The main feature that could be identified were the two signals located at 5.68 and 5.62 ppm, corresponding to the two olefinic protons ϵ and δ , that confirmed the successful hydroarylation of the *meta*-position. Other important signals were the ones at 4.71 and 4.14 ppm, generated from the methylene directly attached to the nitrogen atom (Figure 3.5, $\$$ and $\*); after the ring-closing reaction, one of them is oriented inside the cavity while the other is pointing outside, generating this important difference in ppm. Lastly, the two signals highlighted as # and #’ at 4.12 and 3.95 ppm, generated from the methylene of the octyloxy chain immediately under the functionalized ring, were a clear indicator of the generation of asymmetry,

Chapter 3

together with the splitting of the signals of the bridging methylenes into four pair of doublets (axial and equatorial protons).

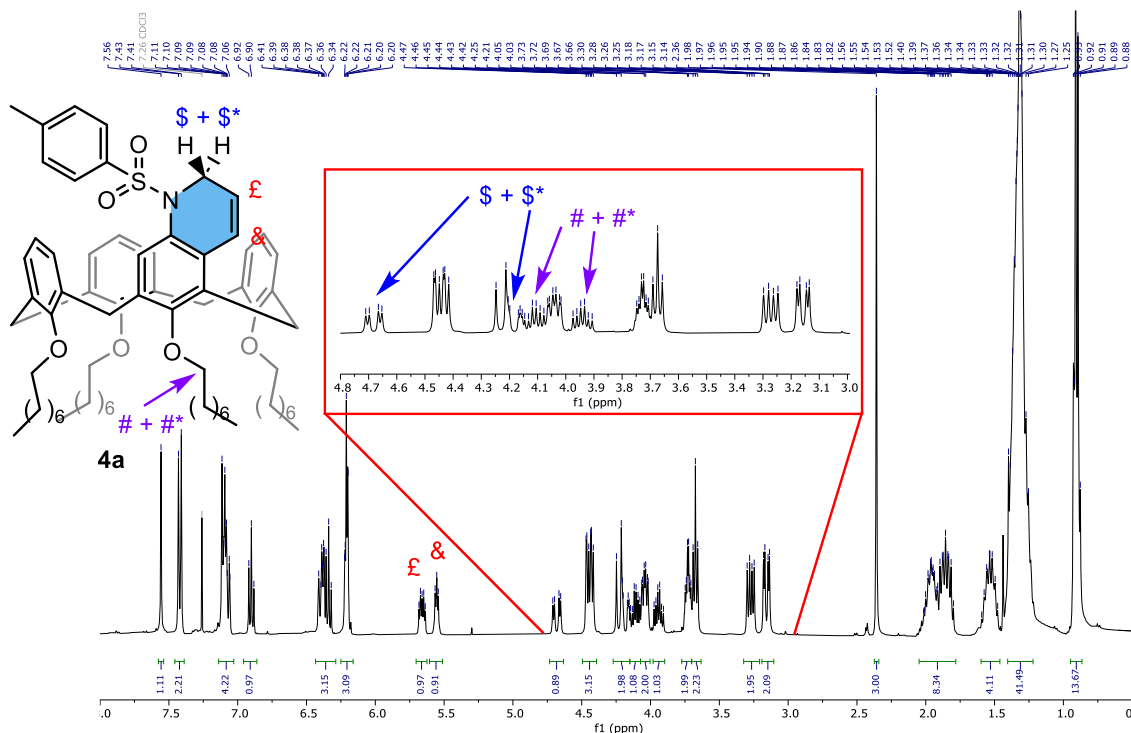


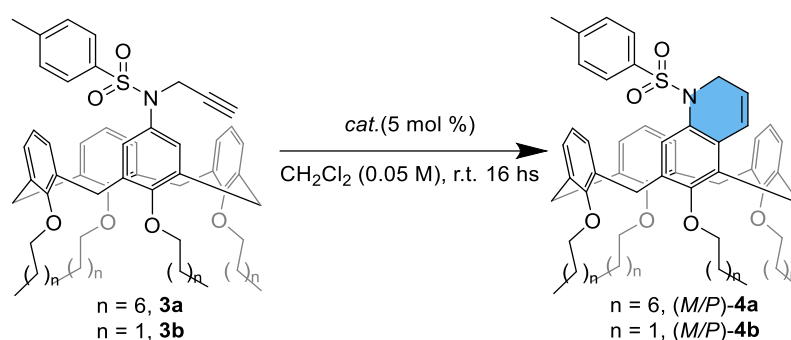
Figure 3.5: ¹H NMR spectra of **4a** and enlargement of the area between 4.8 – 3.0 ppm and relative structure.

Afterwards, the role of the silver salt was evaluated by performing the reaction in the absence of gold. Notably, no conversion of the starting material was observed (Table 3.1, entry 2), highlighting the essential role of silver salt as the chlorine scavenger to activate the gold(I) catalyst. The reaction was performed in the presence of different gold-catalysts; interestingly, when employing a dinuclear gold(I) catalyst, the transformation proceeded with low efficiency, affording **4a** in only 46% yield (Table 3.1, entry 3). Moreover, the use of a sterically bulky Buchwald-type ligand, XPhos, proved viable but with reduced efficiency compared to PPh₃AuCl (Table 3.1, entries 3 and 4).

Finally, when the silver-free catalyst JohnPhosAu(NCCH₃)SbF₆ was tested, the reaction afforded near-quantitative yields of **4a** (Table 3.1, entry 5), demonstrating superior performance.

Chapter 3

The impact of the alkyl chain length attached to the calix[4]arene scaffold was investigated by subjecting substrate **3b** to the best reaction conditions. As anticipated, a shorter alkyl chain did not significantly influence the catalysis, delivering product **4b** in similarly high yields (94%, Table 4.1 entry 6). Once established this, the reactivity of **3b** was tested with various common Lewis acid catalysts (Table 3.1, entries 7–10), which are known to promote intramolecular hydroarylations of alkynes.^[12] However, only trace amounts of **4b** were detected via NMR analysis of the crude mixtures in these cases, confirming gold as the best option.



Entry ^a	3	[M]	[Ag]	4 (%)
1	3a	PPh ₃ AuCl	AgSbF ₆	82
2	3a	--	AgSbF ₆	--
3	3a	(<i>rac</i>)-BINAP(AuCl) ₂	AgSbF ₆	46
4	3a	XPhosAuCl	AgSbF ₆	63
5	3a	JohnPhosAu(NCCH ₃)SbF ₆	--	95
6	3b	JohnPhosAu(NCCH ₃)SbF ₆	--	94
7	3b	In(OTf) ₃	--	--
8	3b	AgOTf	--	--
9	3b	CuI	--	--
10	3b	FeCl ₃	--	--

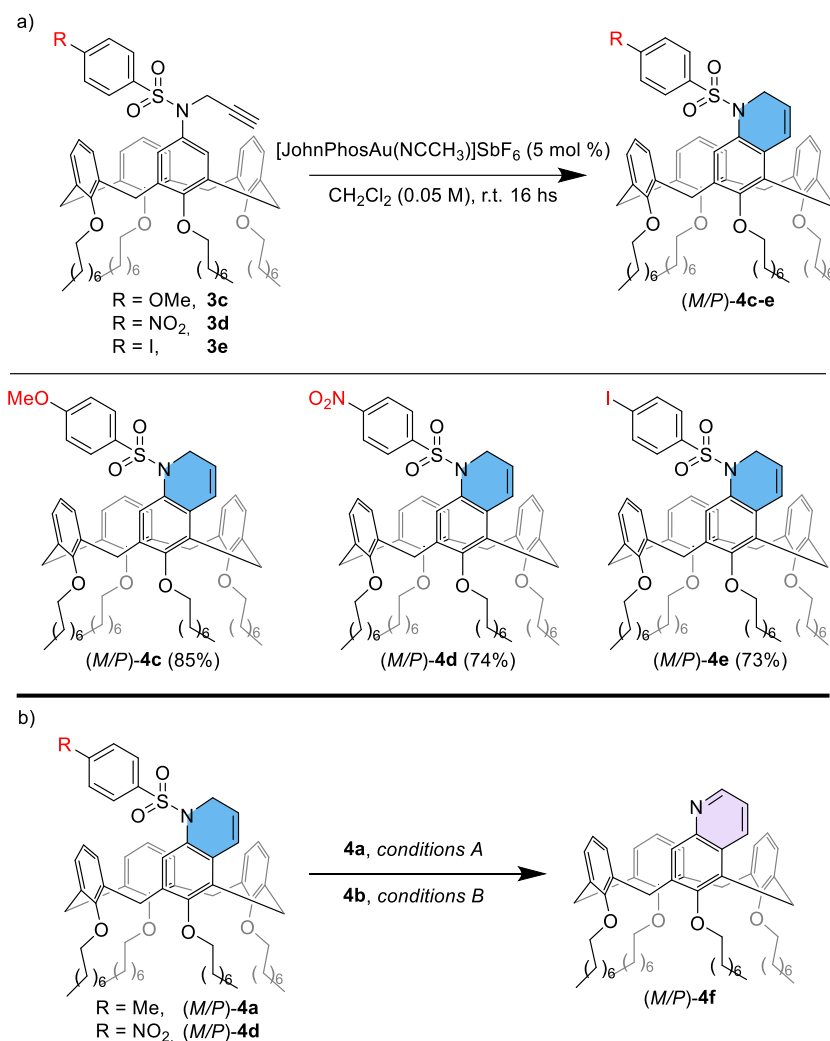
[a] Reaction conditions: **3** (0.05 mmol), r.t., 16 hs. Isolated yields.

Table 3.1: Table of optimization for the cycloarylation reaction of **3a** and **3b** testing different gold catalysts (entries 1-5) and different Lewis acids catalysts (entries 7-10).

Next, the tolerance for different sulfonamide-based tethering units was tested, submitting substrates **3c-e** to the optimized conditions. Unfortunately, it was noticed that the conversion for these modified substrates were lower compared to the model substrates **3a**

Chapter 3

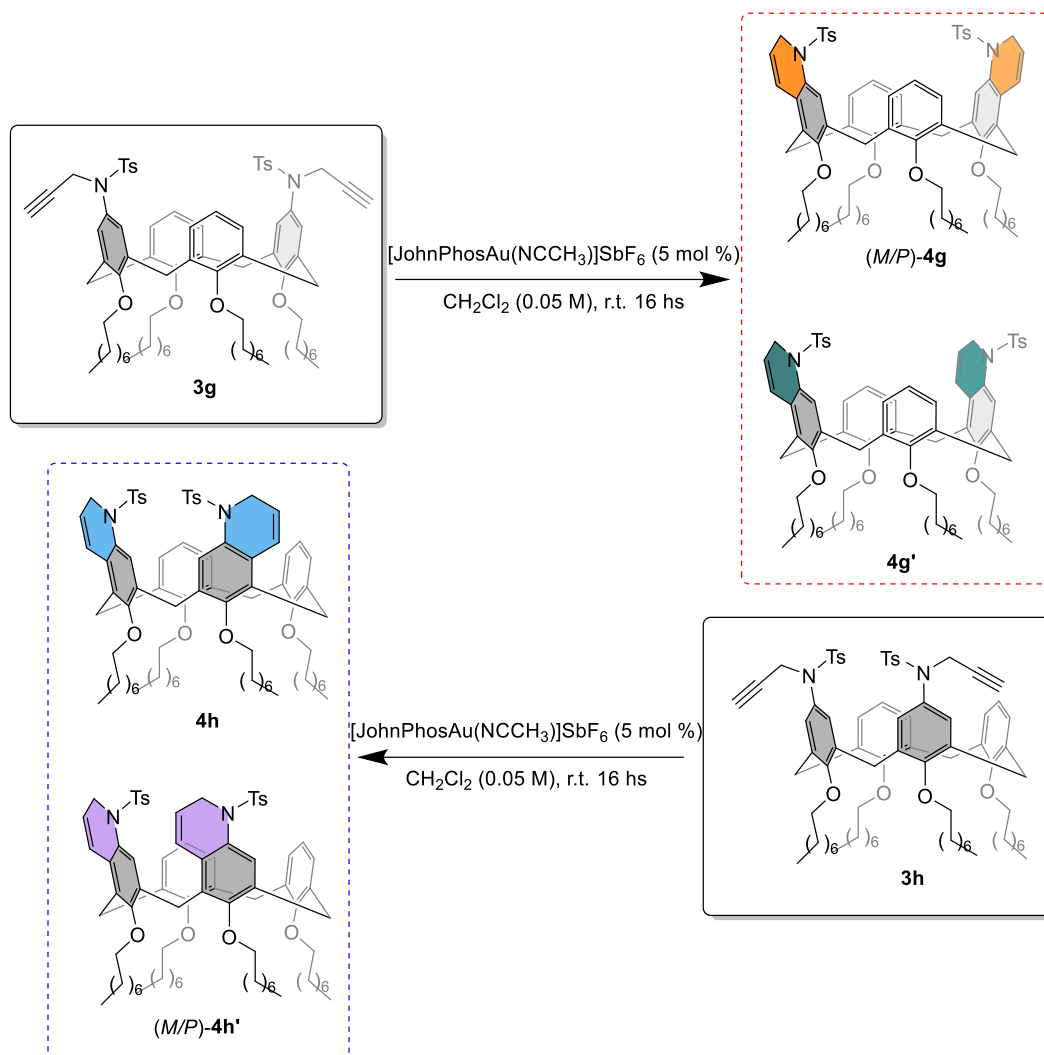
and **3b**, but their reactivities could be unlocked by running the catalysis at a higher temperature (80 °C, 1,2-dichloroethane as the solvent). Under these new reaction conditions, **4c-e** could all be delivered in high yields (Scheme 3.7, a). Noteworthy, sulfonyl groups could be deprotected under mild reaction conditions leading to the formation of the corresponding calix[4]quinoline scaffold **4f** in good yields (Scheme 3.7, b).^[13]



Scheme 3.7: a) Scope of the cycloarylation with differently substituted sulfonamide groups; b) Conversion of **4a** and **4b** ICCs into the quinoline-calix[4]arene derivative **4f**; conditions A: trifluoromethanesulfonic acid (2 eq.) and **4a** in 1,2-Dichloroethane (0.05 M) at 0 °C for 10 min.; conditions B: thiophenol (1.2 eq.), **4b** and K₂CO₃ in ACN (0.03 M) at r.t. for 18 hs.

To further investigate the regioselectivity of the transformation, bis-alkyne substrates **3g** and **3h** were subsequently synthesized from the corresponding 1,3- and 1,2-diamino calix[4]arene, respectively (Scheme 3.8).

Chapter 3



Scheme 3.8: Structure of the di-functionalized calix[4]arene substrates **3g** and **3h** and the relative structures of the respective hydroarylation reaction products (M/P)-**4g**, **4g'** and **4h**, (M/P)-**4h'**.

Hence, **3g** was subjected under the same optimized conditions for **3a**, delivering two different products in comparable yields ((M/P)-**4g**: 46 % and **4g'**: 40%) that could be easily isolated by column chromatography on silica gel. The structure of (M/P)-**4g** was assigned to a chiral compound, in its racemic form, with a C₂ symmetry axis while **4g'** was identified as an achiral *meso*-compound (Scheme 3.8 red box). Analogously, **3h** was converted into a mixture of products, the assignment of those was more challenging to realize due to the higher complexity of the system. The first compound was attributed to the *meso*-isomer **4h** (26 %), which is formed from the intramolecular hydroarylations of both alkyne fragments occurring at the diametral positions of the two adjacent phenolic rings. The second

Chapter 3

compound revealed to be the racemic, chiral compound (*M/P*)-**4h'** (43%) with C1 symmetry (Scheme 3.8 blue box).

The assignment of these structures was made possible by comparing the ¹H NMR spectra of each pair of products (Figure 3.6). The most important difference that could be observed between these (*M/P*)-**4g** and **4g'** is the presence of a single resonance at 3.67 ppm (orange \$) corresponding to the methylenes of the octyloxy groups appended at the unfunctionalised phenolic rings of the calix[4]arene. This signal shifts into two resonances at 3.72 and 3.61 ppm (green \$+\$') in the second isomer **4g'** suggesting the presence of a plane of symmetry passing through the unfunctionalised phenolic units.

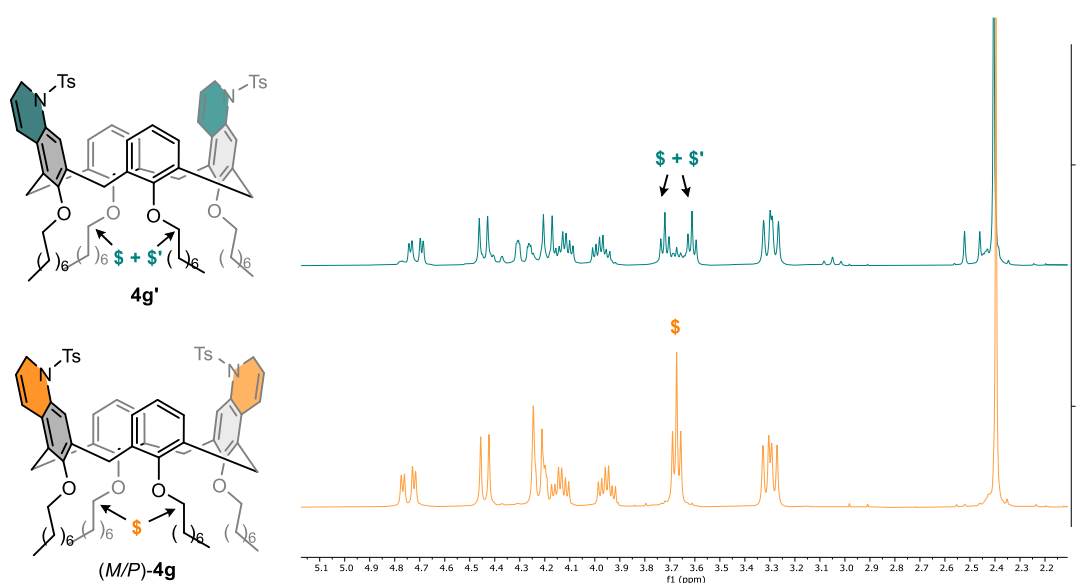


Figure 3.6: Detail of the stacked plot of ¹H NMR spectrum of (*M/P*)-**4g** and **4g'**.

Meanwhile, the most notable NMR features for **4h** and (*M/P*)-**4h'** are four doublets for the diastereotopic methylene C-H bonds (#, &) on the α -position of the dihydroquinoline scaffold (Figure 3.7). Unfortunately, these signals are located in the same densely populated region as the methylenes of the octyloxy groups and of the calix[4]arene scaffold, but it was still possible to appreciate that, in the case of **4h** these hydrogens generate two sets of signals, both integrating for two protons, while for (*M/P*)-**4h'** they have been splitted into four discrete signals, each integrating for one proton. Furthermore, 2D ROESY analysis was performed on product **4h**, where it was possible to see the interaction

Chapter 3

between the olefine protons H_{α} and the bridging methylene protons H_{α} and the interaction between the aromatic protons H_{β} and the bridging methylene protons H_{β} (Figure 3.8).

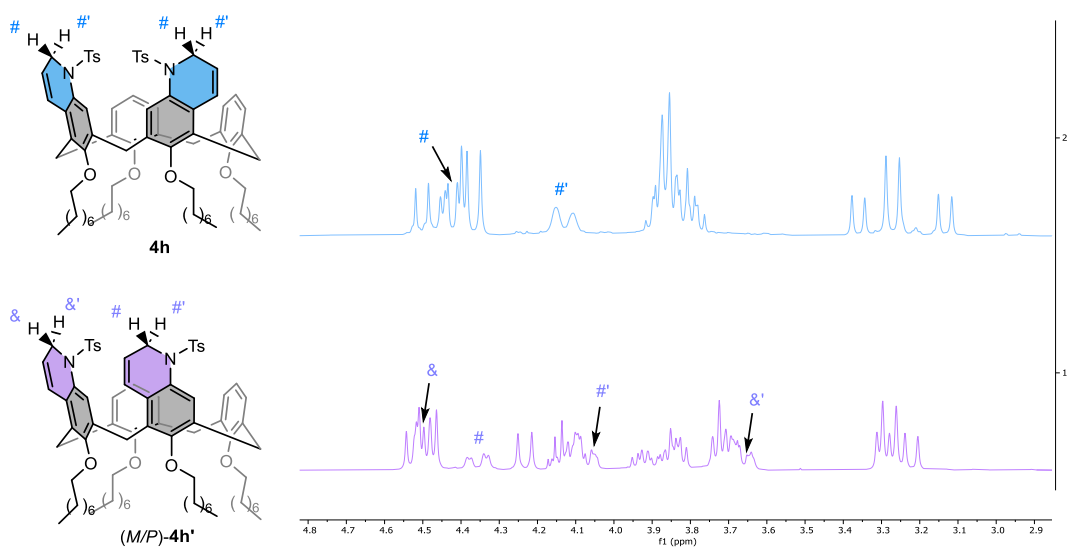


Figure 3.7: Detail of the stacked plot of the ^1H NMR spectrum of **4h** and **(M/P)-4h'**.

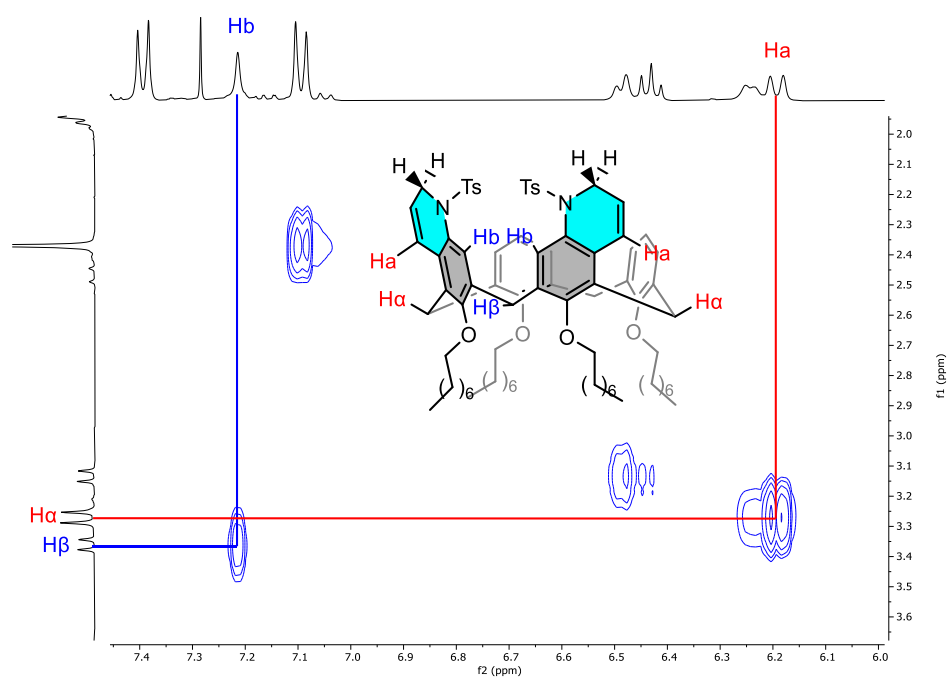


Figure 3.8: Detail of 2D ROESY of **4h** highlighting the interaction between H_{α} - H_{α} (red) and H_{β} - H_{β} (blue)

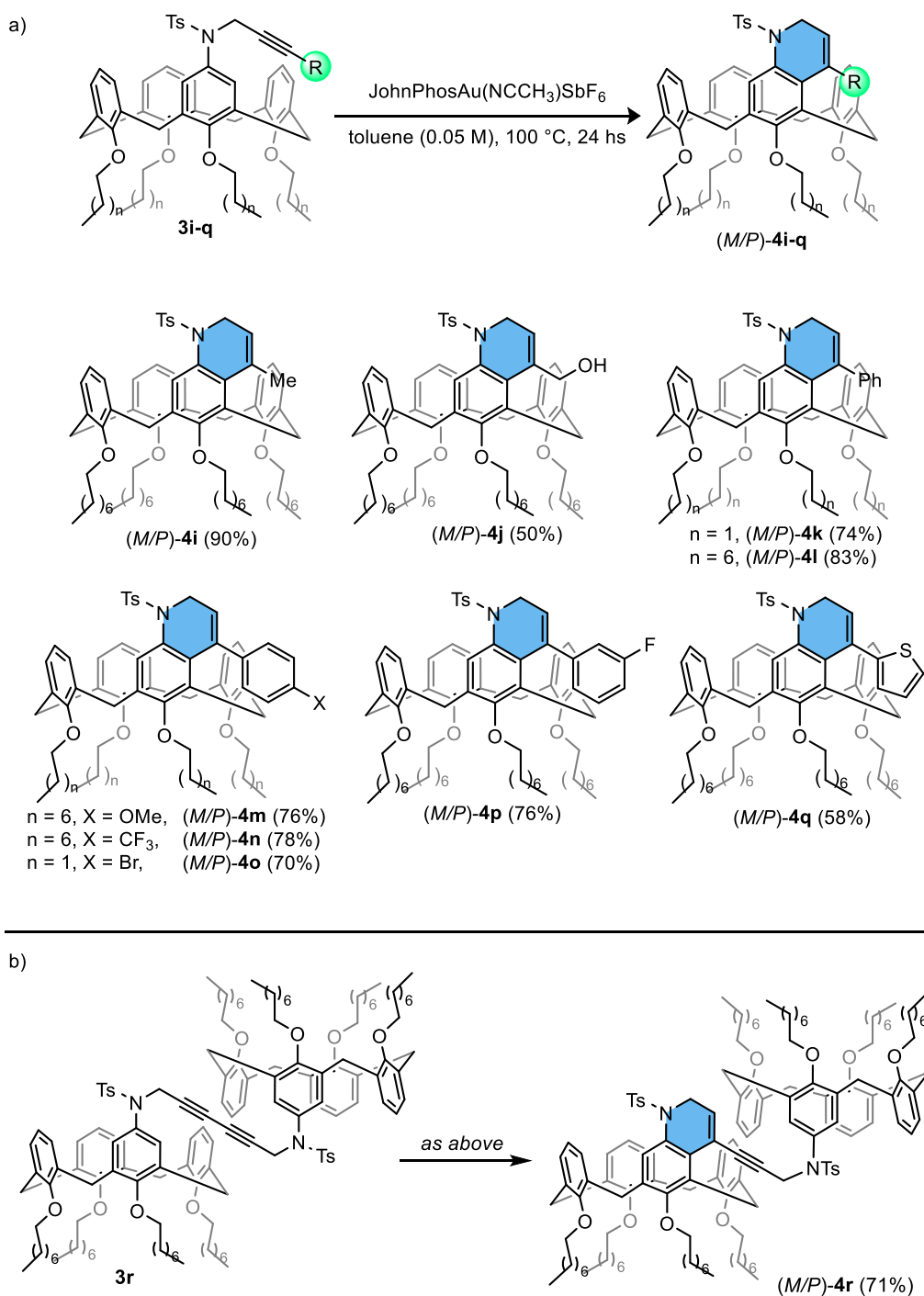
Chapter 3

Having acquired more detailed information about the reactivity of these compounds, new calix[4]arene derivatives were synthesized in order to further explore the versatility of this methodology. Firstly, internal alkyne derivatives were tested by subjecting them to the optimized conditions. Similarly to the sulfonamide-modified derivatives, an increase in temperature was necessary to achieve optimal performance (Scheme 3.9, a). In particular, a 2-butyne derivative (**3i**) could be easily converted into the corresponding product **4i** in good yields, while a propargylic alcohol analogue was converted into the corresponding product **4j** in moderate yields. Substitution with aryl groups was tolerated as well. Therefore, ICCs **4k-p** bearing an aryl ring functionalized with different electron-donating and withdrawing groups at the para and meta positions, were all delivered with high efficacy (50-90%). Noteworthy, the presence of a heterocyclic thiophene ring did not impact the outcome of the catalysis with product **4q** delivered in synthetically useful yields (58%). To prove the chemoselectivity of the transformation, a dimeric 1,3-diyne **3r** was synthesized and submitted to the catalysis (Scheme 3.9, b). Hence, the gold(I)-catalysed hydroarylation occurred selectively at only one of the alkyne fragments providing the highly functionalised macrocyclic structure **4r** in 71% yield. Disappointingly, the hydroarylation on the second alkyne fragment did not occur, probably due to the steric hindrance induced by the second calix[4]arene.

Next, the effect of the substitution on the methylene in the α -position of the alkyne was investigated, since upon this transformation a chiral centre would be generated. So, the chiral, racemic propargyl substrate **3s** was synthesized and then subjected to same condition as the internal alkyne derivatives (Figure 3.9, top). The NMR analysis of the crude reaction mixture revealed the formation of two diastereoisomeric products (*M/P*)-**4s** and (*M/P*)-**4s'** (1.6:1) with the phenyl ring pointing outside and inside the cavity, respectively (Figure 3.8, a). It was possible to easily separate the two compounds by column chromatography on silica gel ((*M/P*)-**4s**: 56% and (*M/P*)-**4s'**: 36%) and then compare their ^1H NMR spectra (Figure 3.9, bottom). A notable feature is represented by the different resonances of the C-H bonds in the α position of the heterocyclic ring. In fact, in compound (*M/P*)-**4s'**, δ' is downfield shifted of 0.2 ppm with respect δ , suggesting that this latter suffers a more shielded environment as a consequence of its proximity to the aromatic

Chapter 3

calix[4]arene cavity. This finding suggests that the macrocycle plays a role in influencing the stereochemical outcome of the gold(I)-catalysed hydroarylation.



Scheme 3.9: a) Scope of the catalytic reaction with internal alkynes. b) Hydroarylation reaction with dimeric diyne substrate **3r**.

Chapter 3

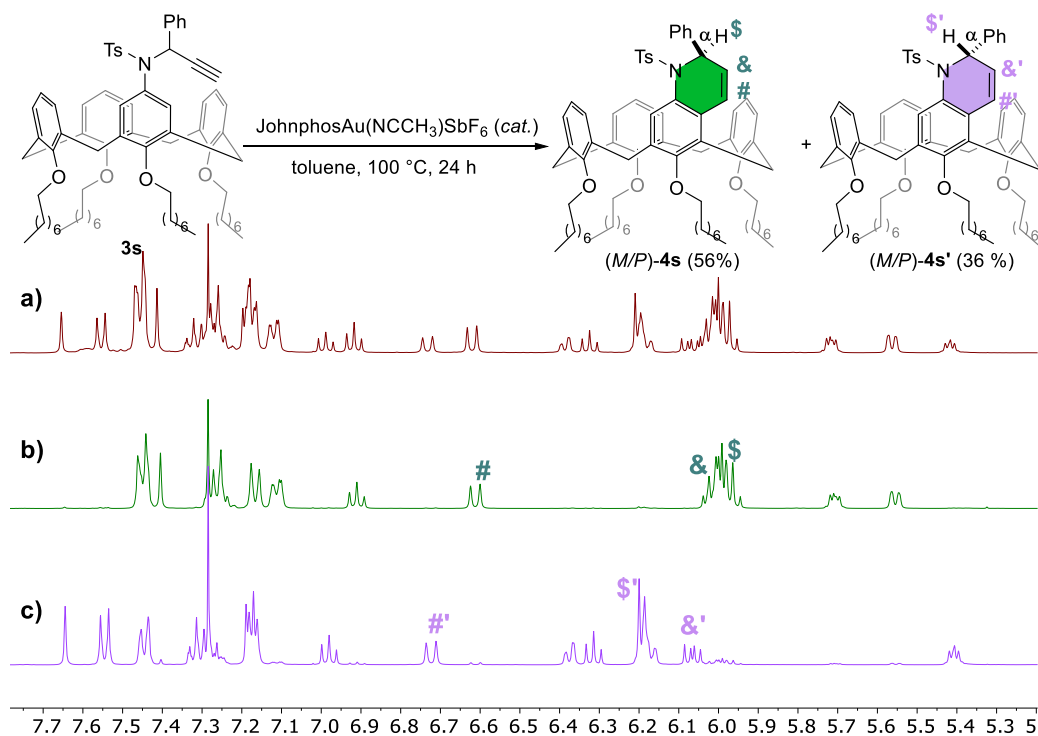
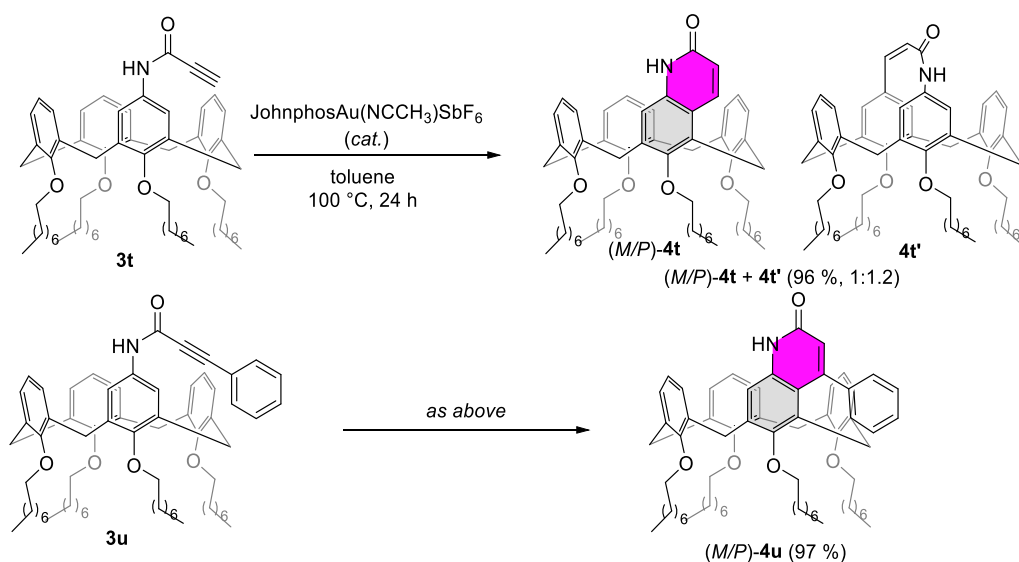


Figure 3.9: Reaction scheme for racemic substrate **3s** and detail of the stack plot of the ¹H NMR spectra of a) the crude of the catalytic reaction, b) product (M/P)-**4s** and c) product (M/P)-**4s'**.

At last, modification of nature of the tethering unit between the alkyne moiety and the calix[4]arene scaffold has been also evaluated by synthesizing the amide substrates **3t** and **3u** (Scheme 3.10).



Scheme 3.10: Hydroarylation reaction experiments with the amide-tethering substrates **3t** and **3u**.

Chapter 3

Submitting this type of substrate to the reaction condition led to the quantitative formation of an inseparable mixture of products, namely a chiral isoquinolone (*M/P*)-**4t** and its achiral isomer **4t'** (~ 1:1.2), which was confirmed by NMR analysis of the compound's mixture isolated by silica gel column chromatography (Figure 3.10).

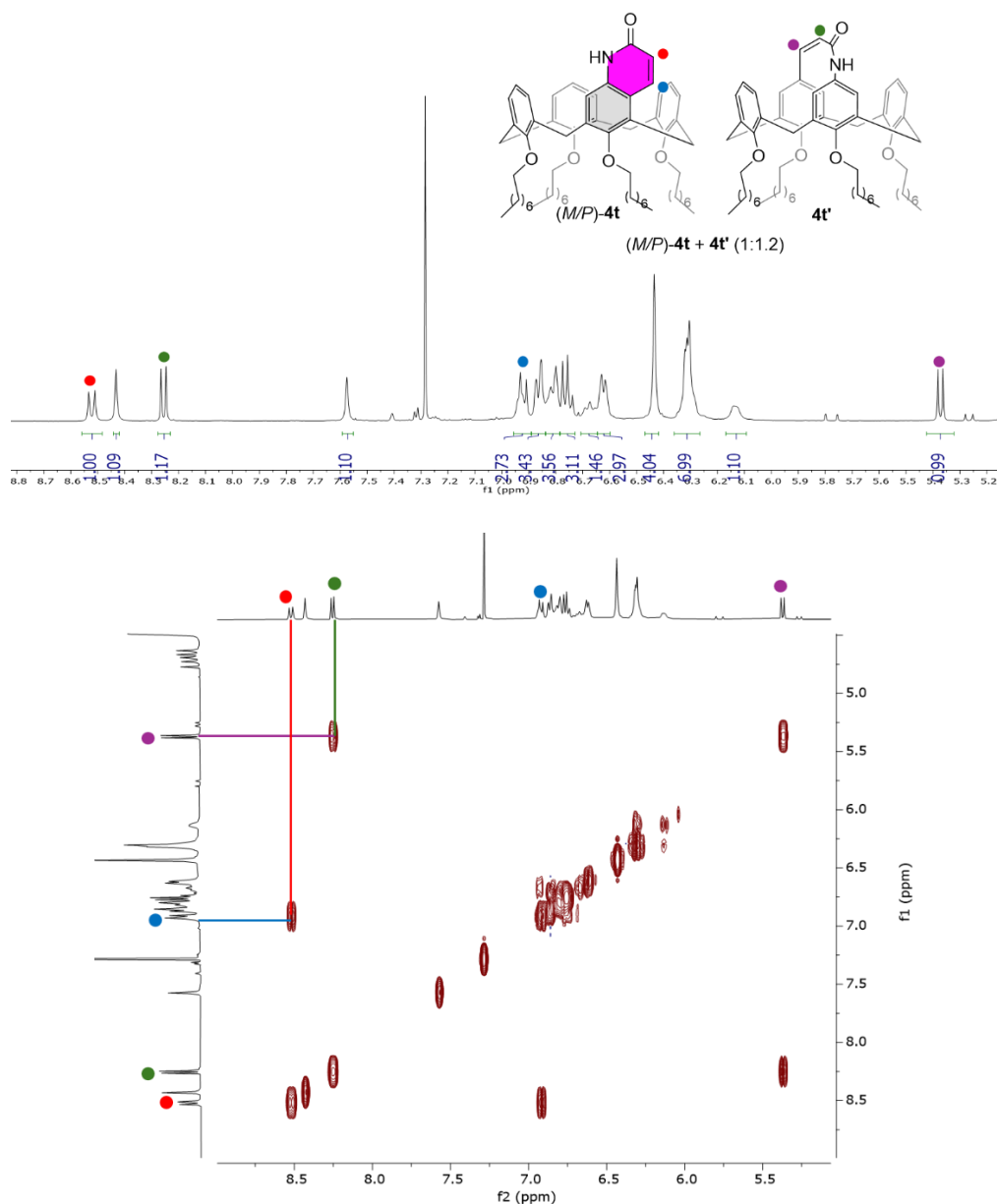
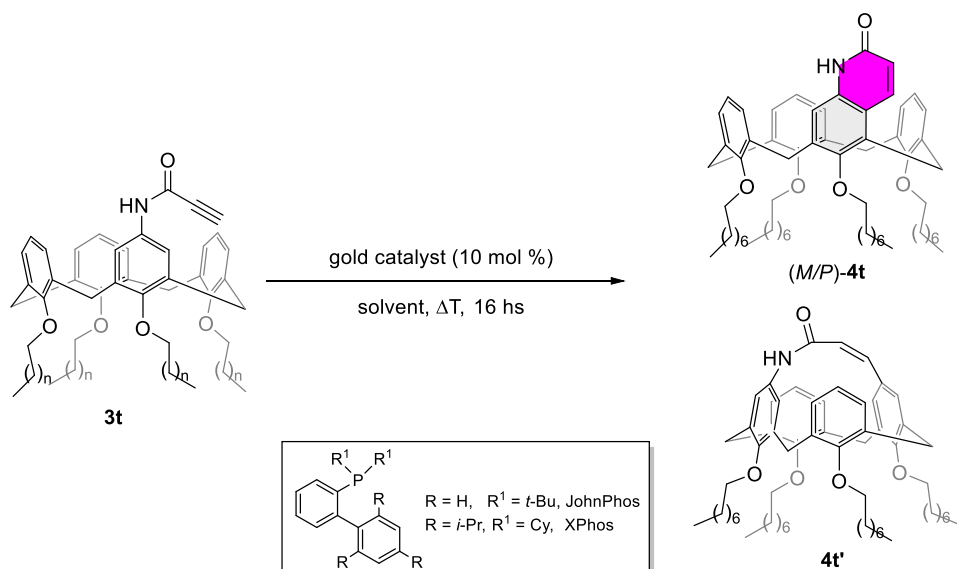


Figure 3.10: Detailed low-field expanded region of ^1H NMR of (*M/P*)-**4t** + **4t'** mixture (CDCl_3 , 400 MHz) showing the ^1H NMR resonances of olefinic protons (Top); Detailed low-field expanded region of 2D ^1H - ^1H COSY NMR (CDCl_3 , 400 MHz) spectrum of (*M/P*)-**4t** + **4t'** mixture showing the J-coupling correlation of olefinic protons (Bottom).

Chapter 3

To see if it was possible to modify the selectivity of the hydroarylation, to potentially obtain only one of the products, different gold(I) catalysts and modification of the key reaction parameters, such as solvent or temperature, were tested, but unfortunately did not lead to a substantial improvement in the regioselectivity of the gold-catalysed transformation (Table 3.2).



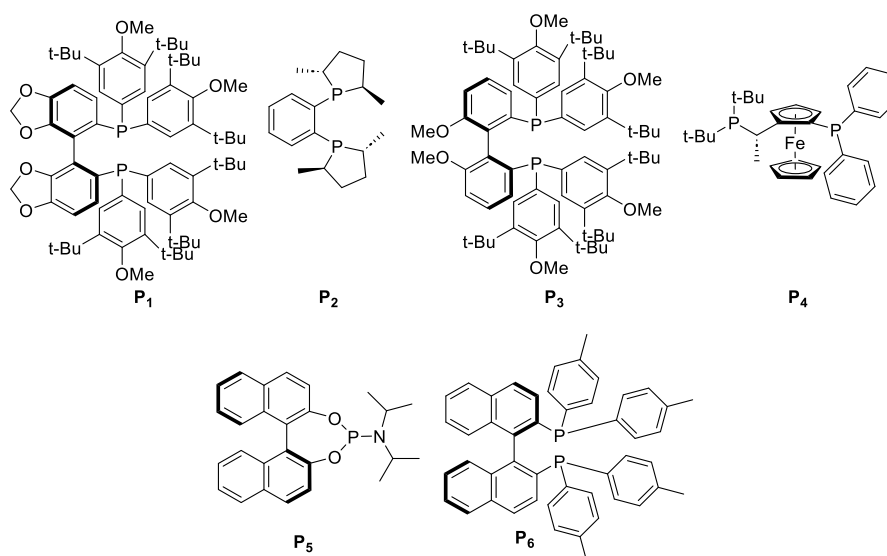
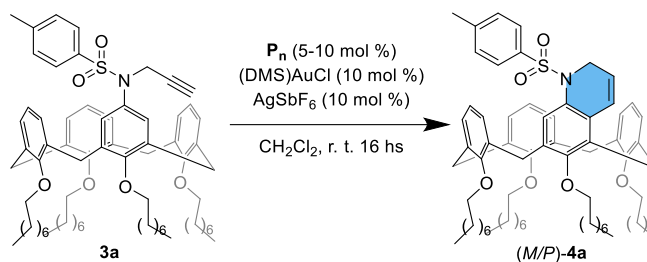
Entry	[Au] (10 mol %)	Solvent	T [°C]	Yield [%]	(M/P)-4t+4t'
1	[JohnPhosAu(I)ACN] ⁺ SbF ₆ ⁻	CH ₂ Cl ₂	25	40	1:1.1
2	XPhosAuCl/AgSbF ₆	CH ₂ Cl ₂	25	25	1.1: 1
3	[JohnPhosAu(I)ACN] ⁺ SbF ₆ ⁻	toluene	50	45	1:1
4	[JohnPhosAu(I)ACN] ⁺ SbF ₆ ⁻	DCE	80	75	1:1.1
5	XPhosAuCl/AgSbF ₆	toluene	100	67	1:1.2
6	PPh ₃ AuCl/AgSbF ₆	toluene	100	52	1:1.2
7	[JohnPhosAu(I)ACN] ⁺ SbF ₆ ⁻	toluene	100°C	96	1:1.2

Table 3.2: Tentative optimization of the reaction conditions for the transformation of **3t**.

This outcome underlines that, in principle, all the phenolic rings of the calix[4]arene scaffold are feasible for the functionalization and that the tethering unit is crucial to dictate the regioselectivity of the transformation. This issue could be overcome by increasing the steric hindrance of the alkyne fragment, as for substrate **3u** (Scheme 3.10, bottom). In this

Chapter 3

case, under virtually the same reaction conditions, the corresponding inherently chiral calix[4]isoquinolone (*M/P*)-**4u** was delivered in excellent yields.



Entry	P_n	Conversion (%)	Yield (<i>M/P</i>)- 4a (%)	e.r. ^a
1	P_1 (5 mol %)	100	84	49:51
2	P_2 (5 mol %)	15	11	44:56
3	P_3 (5 mol %)	100	82	45:55
4	P_4 (5 mol %)	30	26	47:53
5	P_5 (10 mol %)	100	98	36:64
6	P_6 (5 mol %)	59	46	45:55

a) Enantiomeric excess was determined by HPLC analysis using Lux® 5 μ m Cellulose 2, eluent: n-Hex:i-PrOH 98:2, flux: 1 ml/min.

Table 3.3: Preliminary experiment for the optimization of chiral control in the hydroarylation reaction of model substrate **3a**.

Chapter 3

Finally, we performed a few explorative experiments to stereoselectively control the construction of these chiral entities via gold(I) catalysis.^[14] To this end, a set of commercially available phosphine ligands was tested using model substrate **3a** and promising results were obtained only in the presence of the phosphoramidite ligand **P₅** (98%, e.r. = 36:64, Table 3.3 entry 5).

Although just preliminary, this finding opens new perspectives in designing new enantioselective, gold(I)-catalysed methods for ICCs.

Chapter 3

3.3 Conclusions

In summary, the first catalytic approach for synthesizing ICCs via gold(I) catalysis has been presented. Using commercially available catalysts, highly regioselective 6-endo-dig cyclizations were achieved to produce a diverse array of chiral macrocycles. This atom- and step-economical method provides a sustainable alternative to traditional stepwise synthetic routes, opening new avenues in the field. Notably, gold(I)-catalyzed functionalizations of unsaturated macrocyclic substrates could, in principle, be applied to the synthesis of novel chiral macrocyclic receptors with enhanced stereoinduction. These compounds, featuring pre-organized binding sites, are valuable for applications such as the recognition and enantioselective separation of chiral organic molecules. Additionally, their chiroptical properties hold potential for the design of novel organic materials in optoelectronic devices.

Chapter 3

3.4 Experimental section

- **General remarks and materials**

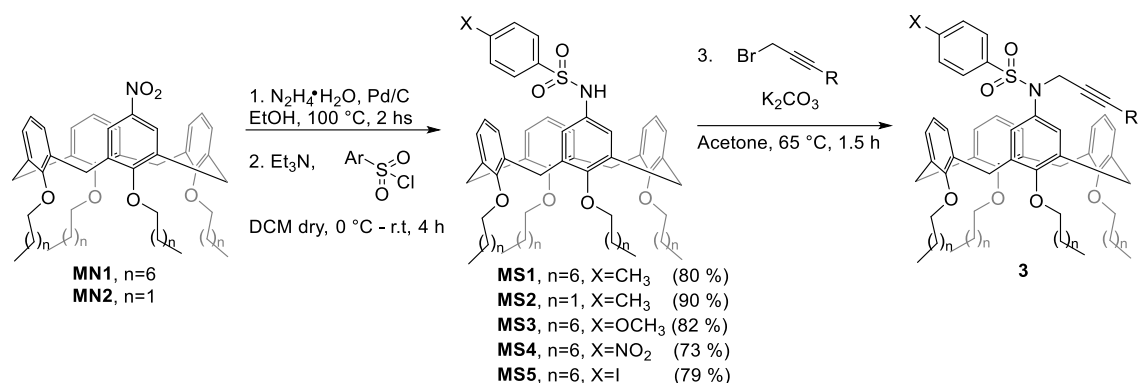
All chemicals those syntheses are not reported hereafter were purchased from commercial sources and used as received. Solvents were dried and stored over molecular sieves previously activated in an oven (450 °C overnight). Anhydrous CH₂Cl₂ for catalytic reactions was supplied by Fluka in Sureseal® bottles and used without any further purification. Melting points were measured with an Electrothermal apparatus and are uncorrected. Column chromatography was performed on silica gel 60 (70-230 mesh). NMR spectra were recorded on a Bruker 400 MHz and JEOL 600 MHz using solvents as internal standards (7.26 ppm for ¹H NMR and 77.00 ppm for ¹³C NMR for CDCl₃). The terms m, s, d, t, q and quint represent multiplet, singlet, doublet, triplet, quadruplet and quintuplet, respectively, and the term br means a broad signal. ¹³C DEPTQ NMR spectra are reported for substrates and corresponding products. Exact masses were recorded on an LTQ ORBITRAP XL Thermo Mass Spectrometer (ESI source).

Materials: **MN1** and **MN2** derivatives were synthesized according to known procedures.^[15] Substituted propargyl bromide derivatives were synthesized in variable yields (72-86%) from propargyl alcohol and commercially available aryl iodides following typical protocols. *Step 1:* Propargyl alcohol/aryl iodide/Bis-(triphenylphosphine)-palladium(II) chloride/CuI (1.1/1.0/0.02/0.04 equiv.), TEA (0.2 M), r.t., 4 hs;^[16] *Step 2:* substituted propargyl alcohol derivative/PPh₃/CBr₄ (1.0/1.5/1.5 eq.), CH₂Cl₂ (0.2 M), r.t., 2 hs.^[17]

Chapter 3

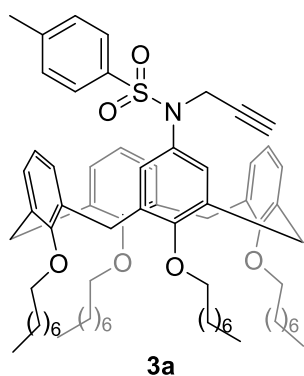
• Synthesis and Characterization of Substrates 3

General procedure for substrates 3:



In a two-necked round bottom flask, under nitrogen atmosphere, Pd/C (cat. amount) and hydrazine monohydrate (60 eq.) were added to a suspension of **MN** (200 mg, 0.22 mmol) in EtOH (20 mL). The reaction was heated to 100 °C and let react under reflux for 2 hrs. The reaction was monitored by TLC (n-Hex:EtOAc 9:1). Once the reaction was completed, the mixture was cooled to r.t. and filtered through celite and the solvent removed under low pressure. Water and DCM were added to the residue and the organic phase was recovered, washed with water (2 x 30 mL) and brine (30 mL), dried over Na_2SO_4 , filtered and the solvent removed under low pressure. The crude was used in the next step without further purification. The mono-amino derivative was then dissolved in dry DCM, under nitrogen atmosphere, and Et_3N (3 eq.) and the respective sulphonyl chloride (1 eq.) were added at 0 °C. The mixture was let warm up at r.t. and stirred for 4 h. The reaction was monitored by TLC (n-Hex:EtOAc 9:1). Once the reaction was completed, water was added to the mixture. The organic phase was separated and washed with water (2x 30 mL) and brine (30 mL), dried over Na_2SO_4 and the solvent removed under low pressure. The crude was purified by column chromatography on silica gel (n-Hex:EtOAc 9:1). Finally, the **MS** intermediate was dissolved in Acetone (10 mL) along with K_2CO_3 (2.5 eq.) and the respective propargyl bromide derivative (1.5 eq.). The mixture was warmed to 65 °C and stirred for 1.5 h. The reaction was monitored by TLC (n-Hex:EtOAc 9:1). Once the reaction was completed, water was added to the mixture. The organic phase was separated and washed with water (2x 30 mL) and brine (30 mL), dried over Na_2SO_4 and the solvent removed under low pressure. The crude was purified by column chromatography on silica gel (n-Hex:EtOAc 9:1), obtaining the desired substrate.

Chapter 3



General procedure was followed using **MS1** (229 mg, 0.22 mmol) and propargyl bromide (36 μ L, 1.5 eq.). Purification by column chromatography on silica gel (*n*-hexane/EtOAc 9:1) yielded **3a** (204 mg, 86 %) as a white solid, **M.p.** = 111 – 112 °C.

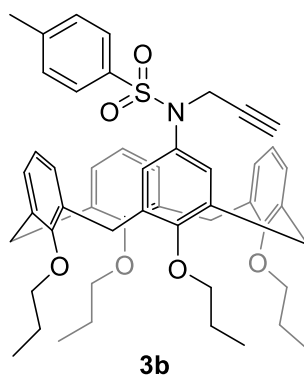
¹H NMR: (400 MHz, CDCl₃) δ = 7.61 (d, *J* = 8.2 Hz, 2H), 7.26 (d, *J* = 8.1 Hz, 2H), 6.75 (d, *J* = 7.4 Hz, 2H), 6.66 – 6.47 (m, 7H), 6.40 (dd, *J* = 7.5 Hz, 1.8 Hz, 2H), 4.45 (d, *J* = 13.2 Hz, 2H), 4.40 (d, *J* = 13.2 Hz, 2H), 4.17 (d, *J* = 2.5 Hz, 2H), 3.94 – 3.83 (m, 8H), 3.16 (d, *J* =

13.3 Hz, 2H), 3.06 (d, *J* = 13.3 Hz, 2H), 2.45 (s, 3H), 2.06 (t, *J* = 2.4 Hz, 1H), 1.96 – 1.89 (m, 8H), 1.49 – 1.31 (m, 40H), 0.94 – 0.90 (m, 12H).

¹³C NMR (101 MHz, CDCl₃) δ = 156.8 (C_q), 156.7 (C_q), 156.3 (C_q), 143.3 (C_q), 136.2 (C_q), 136.0 (C_q), 135.3 (C_q), 134.9 (C_q), 134.3 (C_q), 133.0 (C_q), 129.0 (CH), 128.5 (CH), 128.3 (CH), 128.3 (CH), 128.2 (CH), 128.0 (CH), 122.0 (CH), 121.9 (CH), 77.3 (CH), 75.4 (CH₂), 75.3 (CH₂), 75.2 (CH₂), 73.5 (C_q), 41.5 (CH₂), 32.0 (CH₂), 31.0 (CH₂), 30.9 (CH₂), 30.4 (CH₂), 30.3 (CH₂), 30.0 (CH₂), 29.9 (CH₂), 29.6 (CH₂), 29.6 (CH₂), 26.4 (CH₂), 26.3 (CH₂), 26.3 (CH₂), 22.7 (CH₂), 21.6 (CH₃), 14.1 (CH₃).

LC-MS: *m/z* [M+NH₄]⁺ calculated for C₇₀H₁₀₁N₂O₆S: 1097.74; found: 1097.42.

HR-MS (ESI) *m/z*: [M+H]⁺ calcd. for C₇₀H₉₈NO₆S 1080.7155; found 1080.7160.



General procedure was followed using **MS2** (236 mg, 0.31 mmol) and propargyl bromide (50 μ L, 1.5 eq.). Purification by column chromatography on silica gel (*n*-hexane/EtOAc 9:1) yielded **3b** (193 mg, 78 %) as a white solid, **M.p.** = 115-115 °C.

¹H NMR: (400 MHz, CDCl₃) δ = 8.28 (d, *J* = 8.4 Hz, 2H), 8.01 (d, *J* = 8.0 Hz, 2H), 6.76 (d, *J* = 7.2 Hz, 2H), 6.64 (t, *J* = 8.4 Hz, 3H), 6.57 – 6.49 (m, 4H), 6.39 (dd, *J* = 7.6 Hz, 2.0 Hz, 2H), 4.46 (d, *J* = 13.3 Hz,

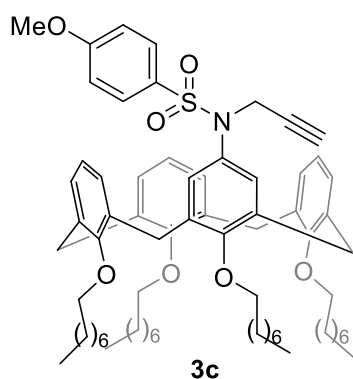
2H), 4.41 (d, *J* = 13.3 Hz, 2H), 4.17 (d, *J* = 2.4 Hz, 2H), 3.91 – 3.80 (m, 8H), 3.17 (d, *J* = 13.2 Hz, 2H), 3.07 (d, *J* = 13.2 Hz, 2H), 2.46 (s, 3H), 2.07 (t, *J* = 2.4 Hz, 1H), 1.99 – 1.89 (m, 8H), 1.04 – 0.97 (m, 12H).

Chapter 3

¹³C NMR: (101 MHz, CDCl₃) δ = 156.8 (C_q), 156.7 (C_q), 156.2 (C_q), 143.3 (C_q), 136.2 (C_q), 135.9 (C_q), 135.9 (C_q), 134.8 (C_q), 134.2 (C_q), 133.0 (C_q), 129.0 (CH), 128.5 (CH), 128.4 (CH), 128.3 (CH), 128.2 (CH), 128.0 (CH), 122.0 (CH), 121.9 (CH), 77.2 (CH), 76.9 (CH₂), 76.8 (CH₂), 76.7 (CH₂), 73.6 (C_q), 41.5 (CH₂), 31.0 (CH₂), 30.9 (CH₂), 23.3 (CH₂), 23.2 (CH₂), 21.6 (CH₂), 10.8 (CH₃), 10.3 (CH₃), 10.2 (CH₃).

LC-MS: *m/z* [M+NH₄]⁺ calculated for C₅₀H₆₁N₂O₆S: 817.43; found: 818.03.

HR-MS (ESI) *m/z*: [M+H]⁺ calcd. for C₅₀H₅₈NO₆S 800.3985; found 800.3991.



General procedure was followed using **MS3** (233 mg, 0.22 mmol) and propargyl bromide (36 μL, 1.5 eq.). Purification by column chromatography on silica gel (*n*-hexane/EtOAc 9:1) yielded **3c** (174 mg, 72 %) as a colourless oil.

¹H NMR: (400 MHz, CDCl₃) δ = 7.66 (d, *J* = 8.9 Hz, 2H), 6.94 (d, *J* = 8.9 Hz, 2H), 6.74 (d, *J* = 7.4 Hz, 2H), 6.63–6.58 (m, 5H), 6.53 (t, *J* = 7.4 Hz, 2H), 6.46–6.41 (m, 2H), 4.45 (d, *J* = 13.2 Hz,

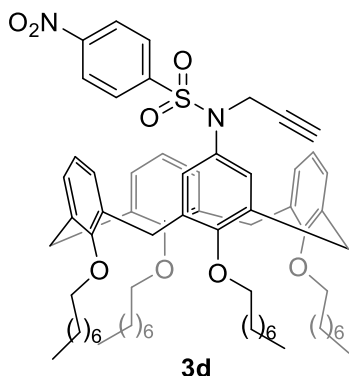
2H), 4.41 (d, *J* = 13.2 Hz, 2H), 4.16 (d, *J* = 2.5 Hz, 2H), 3.94–3.85 (m, 11H), 3.17 (d, *J* = 13.3 Hz, 2H), 3.07 (d, *J* = 13.3 Hz, 2H), 2.07 (t, *J* = 2.5 Hz, 1H), 1.97–1.90 (m, 8H), 1.42–1.32 (m, 40H), 0.95–0.91 (m, 12H).

¹³C NMR: (101 MHz, CDCl₃) δ = 162.9 (C_q), 156.8 (C_q), 156.7 (C_q), 156.3 (C_q), 135.9 (C_q), 135.2 (C_q), 135.0 (C_q), 134.4 (C_q), 133.2 (C_q), 130.9 (C_q), 130.4 (CH), 128.4 (CH), 128.3 (CH), 128.2 (CH), 128.0 (CH), 122.0 (CH), 121.9 (CH), 113.5 (CH), 77.4 (CH), 75.4 (CH₂), 75.3 (CH₂), 75.2 (CH₂), 73.5 (C_q), 35.6 (CH₃), 41.5 (CH₂), 32.0 (CH₂), 31.0 (CH₂), 30.9 (CH₂), 30.4 (CH₂), 30.3 (CH₂), 30.0 (CH₂), 29.9 (CH₂), 29.7 (CH₂), 26.5 (CH₂), 26.4 (CH₂), 26.3 (CH₂), 22.7 (CH₂), 14.2 (CH₃).

LC-MS: *m/z* [M+Na]⁺ calculated for C₇₀H₉₇NNaO₇S: 1118.69; found: 1118.17.

HR-MS (ESI) *m/z*: [M+H]⁺ calcd. for C₇₀H₉₈NO₇S 1096.7064; found 1096.7060.

Chapter 3



General procedure was followed using **MS4** (236 mg, 0.22 mmol) and propargyl bromide (36 μ L, 1.5 eq.). Purification by column chromatography on silica gel (*n*-hexane/EtOAc 9:1) yielded **3d** (203 mg, 83 %) as a yellowish oil.

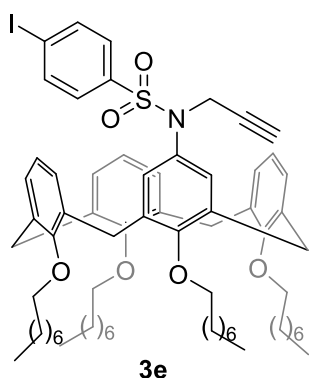
¹H NMR: (400 MHz, CDCl₃) δ = 8.28 (d, *J* = 8.8 Hz, 2H), 7.81 (d, *J* = 8.8 Hz, 2H), 6.82 (dd, *J* = 7.4 Hz, 1.9 Hz, 2H), 6.69–6.57 (m, 6H), 6.48–6.44 (m, 3H), 4.46 (d, *J* = 12.7 Hz, 2H), 4.42 (d,

J = 12.7 Hz, 2H), 4.07 (d, *J* = 2.5 Hz, 2H), 4.02–3.92 (m, 4H), 3.84 (dt, *J* = 14.9 Hz, 7.2 Hz, 4H), 3.18 (d, *J* = 13.2 Hz, 2H), 3.08 (d, *J* = 13.2 Hz, 2H), 2.01 (t, *J* = 2.4 Hz, 1H), 1.97–1.90 (m, 8H), 1.47–1.28 (m, 40H), 0.94–0.90 (m, 12H).

¹³C NMR: (101 MHz, CDCl₃) δ = 156.8 (C_q), 156.7 (C_q), 156.3 (C_q), 149.9 (C_q), 145.2 (C_q), 135.8 (C_q), 135.8 (C_q), 134.9 (C_q), 134.4 (C_q), 132.6 (C_q), 129.4 (CH), 128.7 (CH), 128.1 (CH), 128.0 (CH), 127.9 (CH), 123.5 (CH), 122.1 (CH), 121.9 (CH), 77.2 (CH), 75.6 (CH₂), 75.5 (CH₂), 75.2 (CH₂), 74.2 (C_q), 41.9 (CH₂), 32.0 (CH₂), 31.0 (CH₂), 30.9 (CH₂), 30.5 (CH₂), 30.2 (CH₂), 30.0 (CH₂), 29.9 (CH₂), 29.7 (CH₂), 29.6 (CH₂), 26.5 (CH₂), 26.4 (CH₂), 26.3 (CH₂), 22.7 (CH₂), 14.1 (CH₃).

LC-MS: *m/z* [M+K]⁺ calculated for C₆₉H₉₄KN₂O₈S: 1149.64; found: 1149.37.

HR-MS (ESI) *m/z*: [M+H]⁺ calcd. for C₆₉H₉₅N₂O₈S 1111.6809; found 1111.6802.



General procedure was followed using **MS5** (254 mg, 0.22 mmol) and propargyl bromide (36 μ L, 1.5 eq.). Purification by column chromatography on silica gel (*n*-hexane/EtOAc 9:1) yielded **3e** (207 mg, 79 %) as a colourless oil.

¹H NMR: (400 MHz, CDCl₃) δ = 7.82 (d, *J* = 8.4 Hz, 2H), 7.40 (d, *J* = 8.5 Hz, 2H), 6.72–6.59 (m, 6H), 6.57–6.52 (m, 5H), 4.46 (d, *J* = 13.1 Hz, 2H), 4.42 (d, *J* = 13.2 Hz, 2H), 4.11 (d, *J* = 2.5 Hz, 2H),

3.96–3.85 (m, 8H), 3.18 (d, *J* = 13.3 Hz, 2H), 3.08 (d, *J* = 13.3 Hz, 2H), 2.06 (t, *J* = 2.5 Hz, 1H), 1.97–1.90 (m, 8H), 1.42–1.29 (m, 40H), 0.96–0.91 (m, 12H).

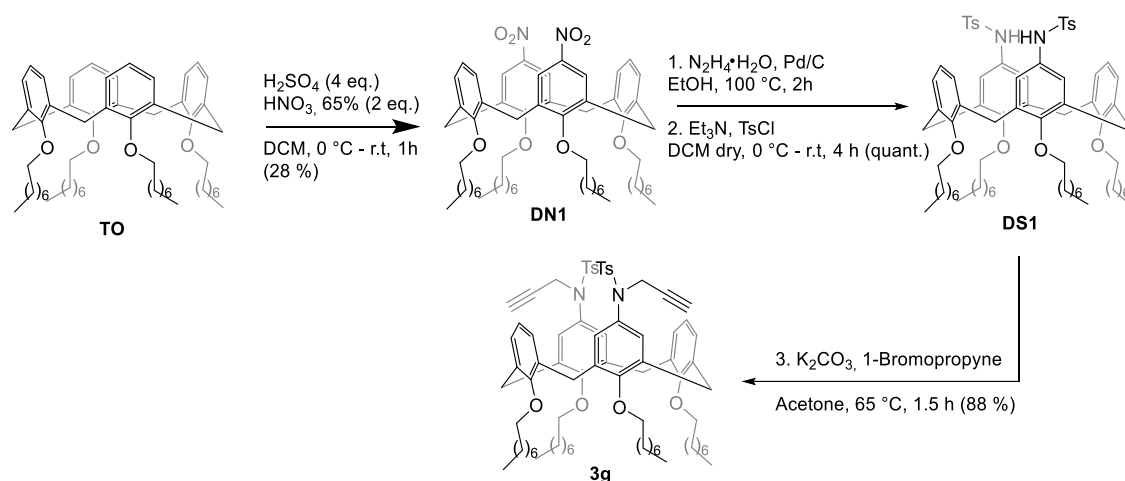
Chapter 3

¹³C NMR: (101 MHz, CDCl₃) δ = 156.6 (C_q), 156.6 (C_q), 138.9 (C_q), 137.6 (CH), 135.8 (C_q), 135.3 (C_q), 134.9 (C_q), 134.6 (C_q), 132.8 (C_q), 129.7 (CH), 128.4 (CH), 128.2 (CH), 128.0 (CH), 122.1 (CH), 121.9 (CH), 99.92 (C_q), 77.2 (CH), 75.4 (CH₂), 75.3 (CH₂), 75.2 (CH₂), 74.0 (C_q), 41.7 (CH₂), 32.0 (CH₂), 31.0 (CH₂), 30.9 (CH₂), 30.4 (CH₂), 30.4 (CH₂), 30.3 (CH₂), 30.0 (CH₂), 29.9 (CH₂), 29.7 (CH₂), 29.6 (CH₂), 26.4 (CH₂), 26.4 (CH₂), 22.8 (CH₂), 14.1 (CH₃).

LC-MS: *m/z* [M+NH₄]⁺ calculated for C₆₉H₉₈IN₂O₆S: 1209.62; found: 1209.05.

HR-MS (ESI) *m/z*: [M+H]⁺ calcd. for C₆₉H₉₅INO₆S 1192.5925; found 1192.5919.

Synthesis of substrate 3g:



Into a round bottom flask, H₂SO₄ (375 μL, 4 eq.) and HNO₃ (235 μL, 2 eq.) were added to a solution of **TO** (1 g, 1.69 mmol) in DCM (100 mL) at 0 °C. After 5 minutes the mixture was allowed to warm up to r.t. and left under magnetic stirring for 1 h. The reaction was monitored by TLC (*n*-hexane/EtOAc 95:5). Upon complete conversion of the starting material, the reaction was quenched with water (50 mL). The organic phase was separated and washed with water (2x 30 mL) and brine (30 mL), dehydrated with Na₂SO₄ and filtered. The crude was purified by column chromatography on silica gel (*n*-hexane/EtOAc 95:5) yielding **DN1** (350 mg, 28%) as a red waxy solid. Into a two-necked round bottom flask, under nitrogen atmosphere, Pd/C (cat. amount) and hydrazine monohydrate (940 μL, 60 eq.) were added to a suspension of **DN1** (200 mg, 0.21 mmol) in EtOH (20 mL). The reaction was heated to 100 °C and let react under reflux for 2 h. The reaction was monitored by TLC (*n*-Hex:EtOAc 9:1). Once the reaction was completed, the mixture was cooled to r.t. and filtered through celite and the solvent removed under low pressure. Water and DCM were added to the

Chapter 3

residue and the organic phase was recovered, washed with water (2 x 30 mL) and brine (30 mL), dehydrated with Na₂SO₄, filtered and the solvent removed under low pressure. The crude was used in the next step without further purification. The di-ammino derivative was then dissolved in dry DCM, under nitrogen atmosphere, and Et₃N (4 eq.) and p-toluensulfonyl chloride (2 eq.) were added at 0 °C. The mixture was let warm up at r.t. and stirred for 4 h. The reaction was monitored by TLC (n-Hex:EtOAc 9:1). Once the reaction was completed, water was added to the mixture. The organic phase was separated and washed with water (2x 30 mL) and brine (30 mL), dried over Na₂SO₄ and the solvent removed under low pressure. The crude was purified by column chromatography on silica gel (n-Hex:EtOAc 9:1). Finally, the **DS1** intermediate was dissolved in Acetone (10mL) along with K₂CO₃ (116 mg, 4 eq.) and propargyl bromide (70 µL, 3 eq.). The mixture was warmed to 65 °C and stirred for 1.5 h. The reaction was monitored by TLC (n-Hex:EtOAc 9:1). Once the reaction was completed, water was added to the mixture. The organic phase was separated and washed with water (2x 30 mL) and brine (30 mL), dried over Na₂SO₄ and the solvent removed under low pressure. The crude was purified by column chromatography on silica gel (n-Hex:EtOAc 9:1), yielding **3g** (249 mg, 88 %) as a colourless oil.

¹H NMR: (400 MHz, CDCl₃) δ = 7.70 (d, *J* = 8.3 Hz, 4H), 7.31 (d, *J* = 8.3 Hz, 4H), 7.04 (s, 4H), 6.24 (t, *J* = 7.6 Hz, 2H), 5.99 (d, *J* = 7.6 Hz, 4H), 4.52 (d, *J* = 2.5 Hz, 4H), 4.37 (d, *J* = 13.4 Hz, 4H), 4.10 – 4.02 (m, 4), 3.65 (t, *J* = 6.6 Hz, 4H), 3.04 (d, *J* = 13.4 Hz, 4H), 2.45 (s, 6H), 2.26 (t, *J* = 2.5 Hz, 2H), 1.99 – 1.79 (m, 8H), 1.60 – 1.49 (m, 4H), 1.42 – 1.20 (m, 36H), 0.96 – 0.88 (m, 12H).

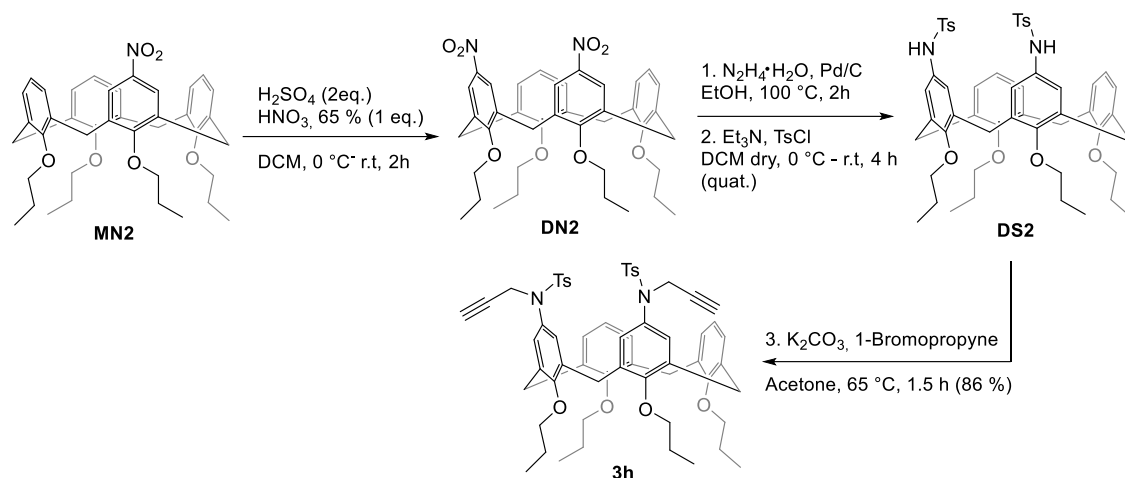
¹³C NMR: (101 MHz, CDCl₃) δ = 157.8 (C_q), 155.2 (C_q), 143.5 (C_q), 137.5 (2C_q), 135.9 (C_q), 132.7 (2C_q), 132.6 (C_q), 129.2 (CH), 128.9 (CH), 128.2 (CH), 127.5 (CH), 121.9 (CH), 77.2 (CH), 75.4 (CH₂), 75.1 (CH₂), 73.6 (C_q), 41.4 (CH₂), 32.0 (CH₂), 30.9 (CH₂), 30.5 (CH₂), 30.2 (CH₂), 30.1 (CH₂), 29.8 (CH₂), 29.7 (CH₂), 29.5 (CH₂), 26.7 CH₂), 26.0 (CH₂), 22.8 (CH₂), 22.7 (CH₂), 21.7 (CH₃), 14.1 (CH₃).

LC-MS: *m/z* [M+Na]⁺ calculated for C₈₀H₁₀₆N₂NaO₈S₂: 1309.73; found: 1309.26.

HR-MS (ESI) *m/z*: [M+H]⁺ calcd. for C₈₀H₁₀₇N₂O₈S₂ 1287.7469; found 1287.7466.

Chapter 3

Synthesis of substrate 3h:



Into a round bottom flask, H_2SO_4 (175 μL , 2 eq.) and HNO_3 (110 μL , 1 eq.) were added to a solution of **MN2** (1 g, 1.57 mmol) in DCM (100 mL) at 0 °C. After 5 minutes the mixture was allowed to warm up to r.t. and left under magnetic stirring for 1h. The reaction was monitored by TLC (*n*-hexane/EtOAc 95:5). Upon complete conversion of the starting material, the reaction was quenched with water (50 mL). The organic phase was separated and washed with water (2x 30 mL) and brine (30 mL), dried over Na_2SO_4 and filtered. The crude was purified by column chromatography on silica gel (*n*-hexane/EtOAc 95:5) yielding **DN2** (343 mg, 32%) as a red waxy solid. Into a two-necked round bottom flask, under nitrogen atmosphere, Pd/C (cat. amount) and hydrazine monohydrate (1300 μL , 60 eq.) were added to a suspension of **DN2** (200 mg, 0.29 mmol) in EtOH (20 mL). The reaction was heated to 100 °C and let react under reflux for 2 h. The reaction was monitored by TLC (*n*-Hex:EtOAc 9:1). Once the reaction was completed, the mixture was cooled to r.t. and filtered through celite and the solvent removed under low pressure. Water and DCM were added to the residue and the organic phase was recovered, washed with water (2 x 30 mL) and brine (30 mL), dehydrated with Na_2SO_4 , filtered and the solvent removed under low pressure. The crude was used in the next step without further purification. The di-ammino derivative was then dissolved in dry DCM, under nitrogen atmosphere, and Et_3N (4 eq.) and *p*-toluensulphonyl chloride (2 eq.) were added at 0 °C. The mixture was let warm up at r.t. and stirred for 4 h. The reaction was monitored by TLC (*n*-Hex:EtOAc 9:1). Once the reaction was completed, water was added to the mixture. The organic phase was separated and washed with water (2x 30 mL) and brine (30 mL), dried over Na_2SO_4 and the solvent removed under low pressure. The crude was purified by column chromatography on silica gel (*n*-Hex:EtOAc

Chapter 3

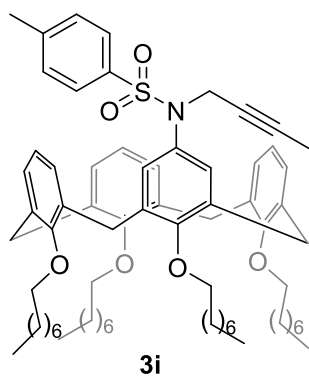
9:1). Finally, the **DS2** intermediate was dissolved in Acetone (10mL) along with K_2CO_3 (116 mg, 4 eq.) and 1-bromopropyne (70 μ L, 3 eq.). The mixture was warmed to 65 °C and stirred for 1.5 h. The reaction was monitored by TLC (n-Hex:EtOAc 9:1). Once the reaction was completed, water was added to the mixture. The organic phase was separated and washed with water (2x 30 mL) and brine (30 mL), dried over Na_2SO_4 and the solvent removed under low pressure. The crude was purified by column chromatography on silica gel (n-Hex:EtOAc 9:1), yielding **3h** (251 mg, 86 %) as a colourless oil.

1H NMR: (400 MHz, $CDCl_3$) δ = 7.59 (d, J = 8.4 Hz, 4H), 7.32 (d, J = 8.1 Hz, 4H), 6.68 (dd, J = 6.8 Hz, 2.4 Hz, 2H), 6.57 – 6.49 (m, 8H), 4.44 (d, J = 13.1 Hz, 1H), 4.40 (d, J = 13.1 Hz, 2H), 4.36 (d, J = 13.1 Hz, 1H), 4.24 (dd, J = 17.6 Hz, 2.5 Hz, 2H), 3.96 (dd, J = 17.7 Hz, 2.5 Hz, 2H), 3.89 – 3.81 (m, 8H), 3.15 (d, J = 13.2 Hz, 1H), 3.06 – 3.01 (m, 3H), 2.49 (s, 6H) 2.11 (t, J = 2.4 Hz, 2H), 1.98 – 1.91 (m, 8H), 1.04 – 0.98 (m, 12H).

^{13}C NMR: (101 MHz, $CDCl_3$) δ = 156.4 (C_q), 143.6 ($2C_q$), 136.1 (C_q), 135.6 (C_q), 135.2 (C_q), 134.9 (C_q), 134.4 (C_q), 133.3 (C_q), 129.2 (CH), 128.8 (CH), 128.5 (CH), 128.4 (CH), 128.2 (CH), 128.0 (CH), 122.1 (CH), 77.2 (CH), 76.9 (CH_2), 76.8 (CH_2), 74.0 (C_q), 41.7 (CH_2), 30.9 (CH_2), 30.9 (CH_2), 30.8 (CH_2), 23.2 (CH_2), 21.6 (CH_3), 10.3 (CH_3).

LC-MS: m/z $[M+Na]^+$ calculated for $C_{80}H_{106}N_2NaO_8S_2$: 1309.73; found: 1309.87.

HR-MS (ESI) m/z : $[M+H]^+$ calcd. for $C_{80}H_{107}N_2O_8S_2$ 1287.7469; found 1287.7474.



General procedure was followed using **MS1** (229 mg, 0.22 mmol) and 1-bromo-2-butyne (29 μ L, 1.5 eq.). Purification by column chromatography on silica gel (n-hexane/EtOAc 9:1) yielded **3i** (207 mg, 86 %) as a white solid, **M.p.** = 97 – 98 °C.

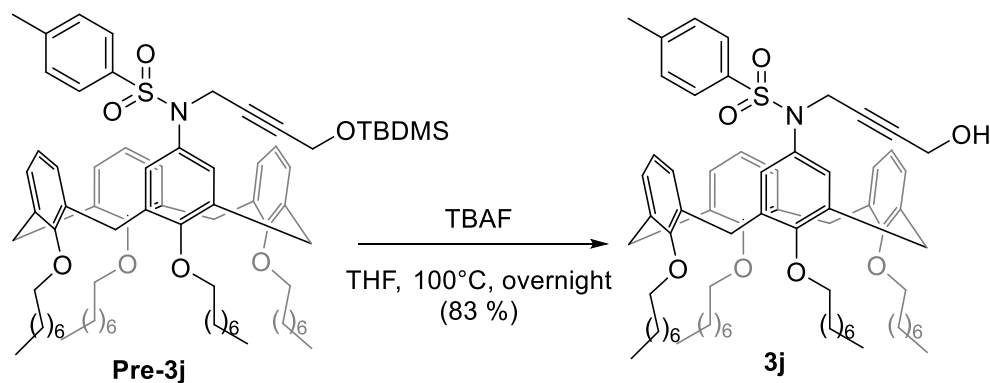
1H NMR: (400 MHz, $CDCl_3$) δ = 7.60 (d, J = 8.2 Hz, 2H), 7.26 (d, J = 7.2 Hz, 2H), 6.80 (d, J = 7.4 Hz, 2H), 6.69 (m, 3H), 6.54 – 6.44 (m, 4H), 6.36 (dd, J = 7.2 Hz, 2.0 Hz, 2H), 4.46 (d, J = 13.3 Hz, 2H), 4.41 (d, J = 13.3 Hz, 2H), 4.16 (d, J = 2.7 Hz, 2H), 3.96 (m, 4H), 3.84 (m, 4H), 3.16 (d, J = 13.4 Hz, 2H), 3.07 (d, J = 13.4, 2H), 2.45 (s, 3H), 1.93 (m, 8H), 1.69 (s, 3H), 1.54 – 1.23 (m, 40H), 0.95 – 0.91 (m, 12H).

Chapter 3

^{13}C NMR: (101 MHz, CDCl_3) δ = 157.0 (C_q), 156.7 (C_q), 156.1 (C_q), 143.0 (C_q), 136.4 (C_q), 136.0 (C_q), 135.6 (C_q), 134.7 (C_q), 134.2 (C_q), 133.5 (C_q), 128.8 (CH), 128.3 (CH), 128.0 (CH), 127.8 (CH), 122.0 (CH), 121.9 (CH), 81.1 (C_q), 75.3 (CH_2), 75.2 (CH_2), 75.1 (CH_2), 73.9 (C_q), 42.0 (CH_2), 32.0 (CH_2), 31.0 (CH_2), 30.9 (CH_2), 30.4 (CH_2), 30.3 (CH_2), 30.3 (CH_2), 30.0 (CH_2), 29.9 (CH_2), 29.7 (CH_2), 29.6 (CH_2), 26.5 (CH_2), 26.3 (CH_2), 26.3 (CH_2), 22.7 (CH_2), 21.6 (CH_3), 14.1 (CH_3), 3.6 (CH_3).

LC-MS: m/z $[\text{M}+\text{Na}]^+$ calculated for $\text{C}_{71}\text{H}_{99}\text{NNaO}_6\text{S}$: 1116.71; found: 1116.22.

HR-MS (ESI) m/z : $[\text{M}+\text{H}]^+$ calcd. for $\text{C}_{71}\text{H}_{100}\text{NO}_6\text{S}$ 1094.7271; found 1094.7277.



General procedure was followed using **MS1** (229 mg, 0.22 mmol) and [(4-bromobut-2-yn-1-yl)oxy](*t*-butyl)dimethylsilane (75.3 mg, 1.3 eq.). Purification by column chromatography on silica gel (*n*-hexane/EtOAc 9:1) yielded **Pre-3j** (205 mg, 76 %) as a colourless oil. Then the intermediate, under nitrogen atmosphere, was dissolved in THF (4 mL) and TBAF (44 mg, 1.5 eq.) was finally added. The mixture was heated to 100 °C and let stirring overnight. The reaction was monitored by TLC (*n*-Hex:EtOAc 8:2). Once the reaction was completed, water and EtOAc were added to the mixture. The organic phase was separated and washed with water (2x 30 mL) and brine (30 mL), dried over Na_2SO_4 and filtered. The crude was purified by column chromatography on silica gel (*n*-Hex:EtOAc 8:2) obtaining the desired product **3j** (157 mg, 83 %) as a colourless oil.

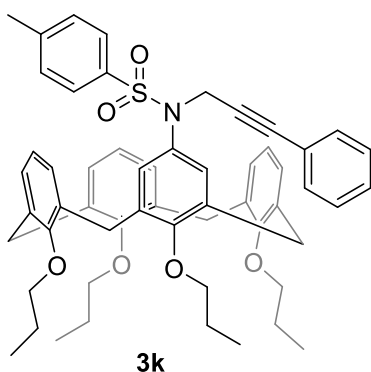
^1H NMR: (400 MHz, CDCl_3) δ = 7.59 (d, J = 8.3 Hz, 2H), 7.27 (d, J = 8.3 Hz, 2H), 6.71 (d, J = 7.4 Hz, 2H), 6.65 – 6.57 (m, 5H), 6.55 (t, J = 7.4 Hz, 2H), 6.46 (dd, J = 7.4 Hz, 1.8 Hz, 2H), 4.45 (d, J = 13.2 Hz, 2H), 4.41 (d, J = 13.2 Hz, 2H), 4.17 (s, 2H), 4.10 (s, 2H), 3.96 – 3.83 (m, 8H), 3.17 (d, J = 13.3 Hz, 2H), 3.07 (d, J = 13.3 Hz, 2H), 2.46 (s, 3H), 1.99 – 1.86 (m, 8H), 1.61 (bs, 1H), 1.47 – 1.23 (m, 40H), 0.97 – 0.87 (m, 12H).

Chapter 3

^{13}C NMR: (101 MHz, CDCl_3) δ = 156.8 (C_q), 156.6 (C_q), 156.4 (C_q), 143.3 (C_q), 136.4 (C_q), 135.8 (C_q), 135.2 (C_q), 135.1 (C_q), 134.5 (C_q), 133.4 (C_q), 128.9 (CH), 128.4 (CH), 128.3 (CH), 128.2 (CH), 127.9 (CH), 122.0 (CH), 83.2 (C_q), 80.7 (C_q), 75.4 (CH_2), 75.3 (CH_2), 75.2 (CH_2), 51.0 (CH_2), 41.8 (CH_2), 32.0 (CH_2), 31.0 (CH_2), 30.9 (CH_2), 30.4 (CH_2), 30.3 (CH_2), 30.3 (CH_2), 29.9 (CH_2), 29.9 (CH_2), 29.7 (CH_2), 26.4 (CH_2), 26.4 (CH_2), 26.3 (CH_2), 22.7 (CH_2), 21.6 (CH_3), 14.1 (CH_3).

LC-MS: m/z $[\text{M}+\text{Na}]^+$ calculated for $\text{C}_{71}\text{H}_{99}\text{NNaO}_7\text{S}$: 1132.70 ; found: 1132.16.

HR-MS (ESI) m/z : $[\text{M}+\text{H}]^+$ calcd. for $\text{C}_{71}\text{H}_{100}\text{NO}_7\text{S}$ 1110.7221; found 1110.7216.



General procedure was followed using **MS2** (236 mg, 0.31 mmol) and (3-bromo-1-propynyl)benzene (91 mg, 1.5 eq.). Purification by column chromatography on silica gel (*n*-hexane/EtOAc 9:1) yielded **3k** (230 mg, 85 %) as a colourless oil.

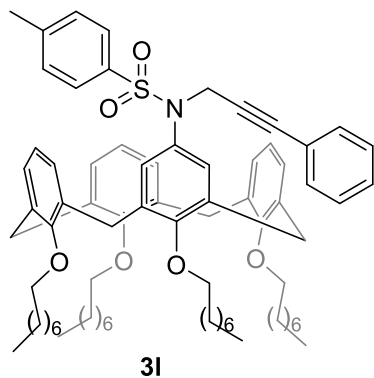
^1H NMR: (400 MHz, CDCl_3) δ = 7.64 (d, J = 8.3 Hz, 2H), 7.40 – 7.28 (m, 3H), 7.27 – 7.18 (m, 4H), 6.86 – 6.79 (m, 4H), 6.72 (dd, J = 8.1, 6.8 Hz, 1H), 6.49 (dd, J = 7.2, 2.2 Hz, 2H), 6.40 – 6.35 (m, 3H), 6.33 (d, J = 7.4 Hz, 1H), 4.52 – 4.39 (m, 6H), 3.99 – 3.88 (m, 4H), 3.87 – 3.77 (m, 4H), 3.18 (d, J = 13.3 Hz, 2H), 3.10 (d, J = 13.3 Hz, 2H), 2.42 (s, 3H), 2.04 – 1.88 (m, 8H), 1.13 – 0.96 (m, 12H).

^{13}C NMR: (101 MHz, CDCl_3) δ = 157.0 (C_q), 156.8 (C_q), 156.0 (C_q), 143.2 (C_q), 136.3 (C_q), 136.1 (C_q), 135.6 (C_q), 134.6 (C_q), 134.0 (C_q), 133.5 (C_q), 131.5 (CH), 129.1 (CH), 128.4 (CH), 128.3 (CH), 128.3 (CH), 128.2 (CH), 128.2 (CH), 128.1 (CH), 127.9 (CH), 122.8 (C_q), 122.2 (CH), 121.9 (CH), 85.2 (C_q), 84.2 (C_q), 76.9 (CH_2), 76.8 (CH_2), 76.7 (CH_2), 42.2 (CH_2), 31.0 (4 CH_2), 23.3 (2 CH_2), 23.2 (CH_2), 21.6 (CH_3), 10.5 (CH_3), 10.3 (CH_3), 10.2 (CH_3).

LC-MS: m/z $[\text{M}+\text{Na}]^+$ calculated for $\text{C}_{56}\text{H}_{61}\text{NNaO}_6\text{S}$: 898.41; found: 898.12.

HR-MS (ESI) m/z : $[\text{M}+\text{H}]^+$ calcd. for $\text{C}_{56}\text{H}_{62}\text{NO}_6\text{S}$ 876.4298; found 876.4294.

Chapter 3



3l

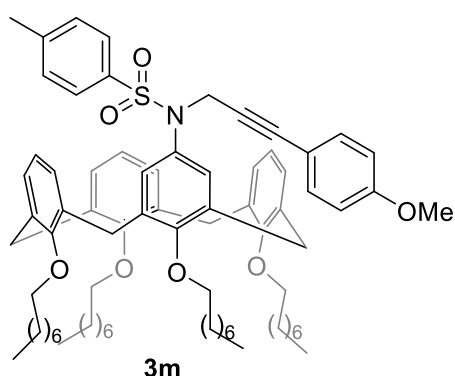
General procedure was followed using **MS1** (229 mg, 0.22 mmol) and (3-bromo-1-propynyl)benzene (64 mg, 1.5 eq.). Purification by column chromatography on silica gel (*n*-hexane/EtOAc 9:1) yielded **3l** (211 mg, 83 %) as a colourless oil.

¹H NMR: (400 MHz, CDCl₃) δ = 7.65 (d, *J* = 8.3 Hz, 2H), 7.37 – 7.31 (m, 3H), 7.24 – 7.21 (m, 4H), 6.83 (m, 4H), 6.73 (dd, *J* = 8.0 Hz, 6.8 Hz, 1H), 6.52 (dd, *J* = 7.2 Hz, 2.1 Hz, 2H), 6.40 (dd, *J* = 7.7 Hz, 2.2 Hz, 2H), 6.35 (t, *J* = 7.2 Hz, 2H), 4.54 – 4.40 (m, 6H), 4.03 – 3.92 (m, 4H), 3.90 – 3.86 (m, 4H), 3.19 (d, *J* = 13.3 Hz, 2H), 3.11 (d, *J* = 13.3 Hz, 2H), 2.42 (s, 3H), 2.00 – 1.94 (m, 8H), 1.62 – 1.50 (m, 4H), 1.43 – 1.35 (m, 36H), 0.97 – 0.94 (m, 12H).

¹³C NMR: (101 MHz, CDCl₃) δ = 157.0 (C_q), 156.8 (C_q), 156.1 (C_q), 143.2 (C_q), 136.4 (C_q), 136.1 (C_q), 135.6 (C_q), 134.7 (C_q), 134.1 (C_q), 133.6 (C_q), 131.5 (CH), 129.1 (CH), 128.3 (CH), 128.2 (CH), 128.1 (CH), 127.9 (CH), 122.8 (C_q), 122.2 (CH), 122.0 (CH), 85.3 (C_q), 84.2 (C_q), 75.4 (CH₂), 75.3 (CH₂), 42.2 (CH₂), 32.1 (CH₂), 31.0 (CH₂), 30.4 (3CH₂), 30.0 (CH₂), 29.9 (CH₂), 29.7 (2CH₂), 26.5 (CH₂), 26.4 (CH₂), 26.3 (CH₂), 22.6 (CH₂), 21.6 (CH₃), 14.3 (CH₃).

LC-MS: *m/z* [M+H]⁺ calculated for C₇₆H₁₀₁NO₆S⁺: 1157.75 ; found: 1157.70.

HR-MS (ESI) *m/z*: [M+H]⁺ calcd. for C₇₆H₁₀₂NO₆S 1156.7428; found 1156.7422.



3m

General procedure was followed using **MS1** (229 mg, 0.22 mmol) and (3-bromo-1-propynyl)4-methoxybenzene (74 mg, 1.5 eq.). Purification by column chromatography on silica gel (*n*-hexane/EtOAc 9:1) yielded **3m** (217 mg, 83 %) as a yellowish oil.

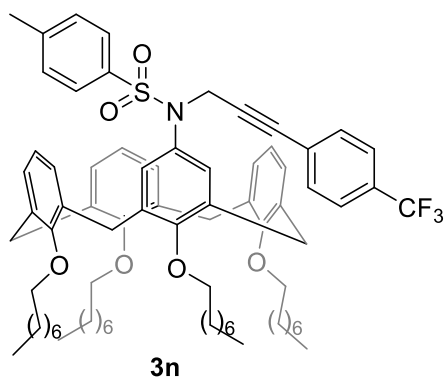
¹H NMR: (400 MHz, CDCl₃) δ = 7.62 (d, *J* = 8.3 Hz, 2H), 7.20 (d, *J* = 8.3 Hz, 2H), 7.14 (d, *J* = 8.8 Hz, 2H), 6.87 – 6.79 (m, 6H), 6.75 – 6.67 (m, 1H), 6.46 (t, *J* = 4.4 Hz, 2H), 6.33 (d, *J* = 5.0 Hz, 4H), 4.49 – 4.36 (m, 6H), 4.02 – 3.88 (m, 4H), 3.87 – 3.78 (m, 7H), 3.16 (d, *J* = 13.4 Hz, 2H), 3.07 (d, *J* = 13.4 Hz, 2H), 2.40 (s, 3H), 2.00 – 1.84 (m, 8H), 1.50 – 1.25 (m, 40H), 0.99 – 0.87 (m, 12H).

Chapter 3

¹³C NMR: (101 MHz, CDCl₃) δ = 159.6 (C_q), 157.0 (C_q), 156.8 (C_q), 156.0 (C_q), 143.0 (C_q), 136.3 (C_q), 136.1 (C_q), 135.7 (C_q), 134.6 (C_q), 134.0 (C_q), 133.5 (C_q), 133.0 (CH), 129.0 (CH), 128.4 (CH), 128.3 (CH), 128.2 (CH), 128.0 (CH), 127.8 (CH), 122.1 (CH), 121.9 (CH), 114.9 (C_q), 113.8 (CH), 85.1 (C_q), 82.7 (C_q), 75.3 (CH₂), 75.2 (CH₂), 75.2 (CH₂), 55.3 (CH₃), 42.3 (CH₂), 32.0 (CH₂), 31.0 (CH₂), 30.9 (CH₂), 30.4 (CH₂), 30.3 (2CH₂), 30.0 (CH₂), 29.9 (CH₂), 29.7 (CH₂), 29.6 (CH₂), 26.5 (CH₂), 26.3 (CH₂), 22.8 (CH₂), 21.6 (CH₃), 14.1 (CH₃).

LC-MS: *m/z* [M+H]⁺ calculated for C₇₇H₁₀₆NO₇S: 1186.76 ; found: 1186.54.

HR-MS (ESI) *m/z*: [M+H]⁺ calcd. for C₇₇H₁₀₄NO₇S 1186.7534; found 1186.7539.



General procedure was followed using **MS1** (229 mg, 0.22 mmol) and (3-bromo-1-propynyl)4-(trifluoromethyl)benzene (87 mg, 1.5 eq.). Purification by column chromatography on silica gel (*n*-hexane/EtOAc 9:1) yielded **3n** (202 mg, 75 %) as a colourless oil.

¹H NMR: (400 MHz, CDCl₃) δ = 7.61 (d, *J* = 8.3 Hz, 2H), 7.56 (d, *J* = 8.3 Hz, 2H), 7.27 (d, *J* = 8.3 Hz, 2H), 7.21 (d, *J* = 8.3 Hz, 2H), 6.76 (d, *J* = 7.5 Hz, 2H), 6.72 (s, 2H), 6.69 – 6.63 (m, 1H), 6.53 (dd, *J* = 7.4 Hz, 1.8 Hz, 2H), 6.40 (dd, *J* = 7.4 Hz, 1.8 Hz, 2H), 6.34 (t, *J* = 7.5 Hz, 2H), 4.50 – 4.38 (m, 6H), 3.99 – 3.80 (m, 8H), 3.16 (d, *J* = 13.3 Hz, 2H), 3.08 (d, *J* = 13.3 Hz, 2H), 2.41 (s, 3H), 2.00 – 1.86 (m, 8H), 1.48 – 1.26 (m, 40H), 0.99 – 0.86 (m, 12H).

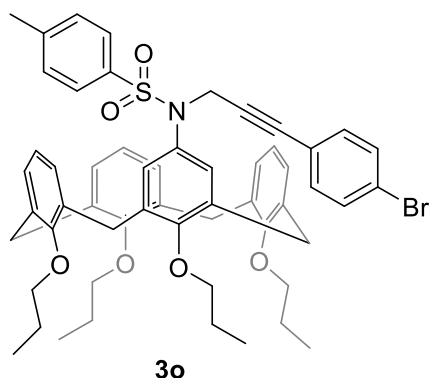
¹³C NMR: (101 MHz, CDCl₃) δ = 156.9 (C_q), 156.7 (C_q), 156.2 (C_q), 143.2 (C_q), 136.4 (C_q), 136.0 (C_q), 135.4 (C_q), 134.9 (C_q), 134.2 (C_q), 133.5 (C_q), 131.8 (CH), 129.9 (C_q), 129.1 (CH), 128.3 (CH), 128.2 (CH), 128.1 (CH), 128.0 (CH), 127.8 (CH), 126.5 (C_q), 125.1 (q, *J*_{C-F} = 3.8 Hz, CH), 124.0 (d, *J*_{C-F} = 272 Hz, C_q), 122.1 (CH), 121.9 (CH), 86.9 (C_q), 83.8 (C_q), 75.4 (CH₂), 75.3 (CH₂), 42.2 (CH₂), 32.0 (CH₂), 31.0 (CH₂), 30.4 (CH₂), 30.3 (CH₂), 30.0 (2CH₂), 29.9 (CH₂), 29.7 (CH₂), 29.6 (CH₂), 26.4 (CH₂), 26.3 (CH₂), 22.7 (CH₂), 21.6 (CH₃), 14.1 (CH₃).

¹⁹F NMR: (565 MHz, CDCl₃) δ = - 62.7.

ESI-MS: *m/z* [M+H₃O]⁺ calculated for C₇₇H₁₀₃F₃NO₇S: 1242.74; found: 1242.86.

HR-MS (ESI) *m/z*: [M+H]⁺ calcd. for C₇₇H₁₀₁F₃NO₆S 1224.7302; found 1224.7309.

Chapter 3



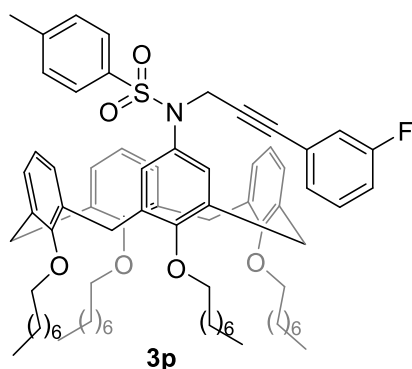
General procedure was followed using **MS2** (236 mg, 0.31 mmol) and 1-bromo-4-(3-bromoprop-1-yn-1-yl)benzene (129 mg, 1.5 eq.). Purification by column chromatography on silica gel (*n*-hexane/EtOAc 9:1) yielded **3o** (243 mg, 82 %) as a yellowish solid, **M.p.** = 94 – 95 °C.

¹H NMR: (400 MHz, CDCl₃) δ = 7.60 (d, *J* = 8.4 Hz, 2H), 7.43 (d, *J* = 8.6 Hz, 2H), 7.21 (d, *J* = 8.4 Hz, 2H), 7.03 (d, *J* = 8.6 Hz, 2H), 6.78 (d, *J* = 7.2 Hz, 2H), 6.72 (s, 2H), 6.71 – 6.63 (m, 1H), 6.51 (dd, *J* = 7.0 Hz, 2.4 Hz, 2H), 6.39 – 6.30 (m, 4H), 4.50 – 4.35 (m, 6H), 3.95 – 3.76 (m, 8H), 3.16 (d, *J* = 13.3 Hz, 2H), 3.07 (d, *J* = 13.3 Hz, 2H), 2.41 (s, 3H), 2.02 – 1.86 (m, 8H), 1.06 – 0.94 (m, 12H).

¹³C NMR: (101 MHz, CDCl₃) δ = 156.9 (C_q), 156.7 (C_q), 156.1 (C_q), 143.2 (C_q), 136.3 (C_q), 136.0 (C_q), 135.5 (C_q), 134.8 (C_q), 134.1 (C_q), 133.4 (C_q), 132.9 (CH), 131.4 (CH), 129.1 (CH), 128.3 (2CH), 128.1 (CH), 128.1 (CH), 127.8 (CH), 122.5 (C_q), 122.1 (CH), 121.9 (CH), 121.7 (C_q), 85.4 (C_q), 84.1 (C_q), 76.8 (CH₂), 76.8 (2CH₂), 76.8 (CH₂), 42.2 (CH₂), 31.0 (4CH₂), 23.3 (CH₂), 23.2 (2CH₂), 21.6 (CH₃), 10.4 (CH₃), 10.3 (CH₃), 10.2 (CH₃).

LC-MS: *m/z* [M+NH₄]⁺ calculated for C₅₆H₆₄BrN₂O₆S: 973.36; found: 973.56.

HR-MS: *m/z* [M+H]⁺ calculated for C₅₆H₆₁BrNO₆S: 954.3403; found: 954.3397.



General procedure was followed using **MS1** (229 mg, 0.22 mmol) and (3-bromo-1-propynyl)3-fluorobenzene (70 mg, 1.5 eq.). Purification by column chromatography on silica gel (*n*-hexane/EtOAc 9:1) yielded **3p** (207 mg, 80 %) as a colourless oil.

¹H NMR: (400 MHz, CDCl₃) δ = 7.60 (d, *J* = 8.3 Hz, 2H), 7.28 – 7.26 (m, 1H), 7.22 (d, *J* = 8.3 Hz, 2H), 7.05 (td, *J* = 8.4 Hz, 2.8 Hz, 1H), 6.98 (d, *J* = 7.7 Hz, 1H), 6.81 (dt, *J* = 9.4 Hz, 1.5 Hz, 1H), 6.73 (d, *J* = 7.3 Hz, 2H), 6.70 (s, 2H), 6.67 – 6.61 (m, 1H), 6.55 (d, *J* = 7.3 Hz, 2H), 6.42 (d, *J* = 7.5 Hz, 2H), 6.37 (t, *J* = 7.3 Hz, 2H), 4.50 – 4.35 (m, 6H), 3.98 – 3.81 (m, 8H), 3.16 (d, *J* = 13.3 Hz, 2H), 3.08 (d, *J* = 13.3 Hz, 2H), 2.42 (s, 3H), 2.01 – 1.84 (m, 8H), 1.48 – 1.25 (m, 40H), 0.99 – 0.86 (m, 12H).

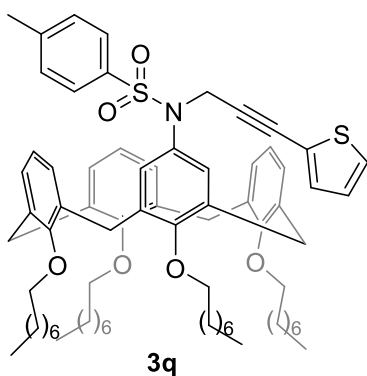
Chapter 3

¹³C NMR: (101 MHz, CDCl₃) δ = 162.4 (d, J_{C-F} = 247 Hz, C_q), 156.8 (C_q), 156.7 (C_q), 156.3 (C_q), 143.3 (C_q), 136.4 (C_q), 135.9 (C_q), 135.3 (C_q), 135.0 (C_q), 134.3 (C_q), 133.6 (C_q), 129.7 (d, J_{C-F} = 8.4 Hz, CH), 129.1 (CH), 128.3 (CH), 128.2 (CH), 128.2 (CH), 128.1 (CH), 127.9 (CH), 127.3 (d, J_{C-F} = 3.3 Hz, CH), 124.6 (d, J_{C-F} = 9.8 Hz, C_q), 122.1 (CH), 121.9 (CH), 118.3 (d, J_{C-F} = 23.0 Hz, CH), 118.6 (d, J_{C-F} = 21.2 Hz, CH), 85.2 (C_q), 83.9 (d, J_{C-F} = 3.3 Hz, C_q), 75.4 (CH₂), 75.3 (CH₂), 75.2 (CH₂), 42.1 (CH₂), 32.0 (CH₂), 31.0 (CH₂), 30.4 (CH₂), 30.4 (CH₂), 30.3 (CH₂), 30.0 (CH₂), 29.9 (CH₂), 29.7 (CH₂), 26.4 (CH₂), 26.3 (CH₂), 26.3 (CH₂), 22.7 (CH₂), 21.5 (CH₃), 14.1 (CH₃).

¹⁹F NMR: (565 MHz, CDCl₃) δ = - 62.5.

LC-MS: m/z [M+Na]⁺ calculated for C₇₆H₁₀₀FNNaO₆S: 1196.72; found: 1196.45.

HR-MS (ESI) m/z : [M+H]⁺ calcd. for C₇₆H₁₀₁FNO₆S 1174.7334; found 1174.7338.



General procedure was followed using **MS1** (229 mg, 0.22 mmol) and 2-(3-bromo-1-propynyl)thiophene (66 mg, 1.5 eq.). Purification by column chromatography on silica gel (*n*-hexane/EtOAc 9:1) yielded **3q** (194 mg, 76 %) as a yellowish solid, **M.p.** = 122 – 123 °C.

¹H NMR: (400 MHz, CDCl₃) δ = 7.61 (d, J = 8.3 Hz, 2H), 7.26 (dd, J = 5.1 Hz, 1.6 Hz, 1H), 7.22 (d, J = 8.3 Hz, 2H), 7.05 (dd, J = 3.6 Hz, 1.4 Hz, 1H), 6.99 (dd, J = 5.1 Hz, 3.5 Hz, 1H), 6.80 (d, J = 7.5 Hz, 2H), 6.74 (s, 2H), 6.71 – 6.65 (m, 1H), 6.53 – 6.47 (m, 2H), 6.42 – 6.35 (m, 4H), 4.50 – 4.36 (m, 6H), 3.99 – 3.89 (m, 4H), 3.88 – 3.79 (m, 4H), 3.16 (d, J = 13.3 Hz, 2H), 3.08 (d, J = 13.3 Hz, 2H), 2.40 (s, 3H), 2.00 – 1.85 (m, 8H), 1.49 – 1.26 (m, 40H), 0.98 – 0.88 (m, 12H).

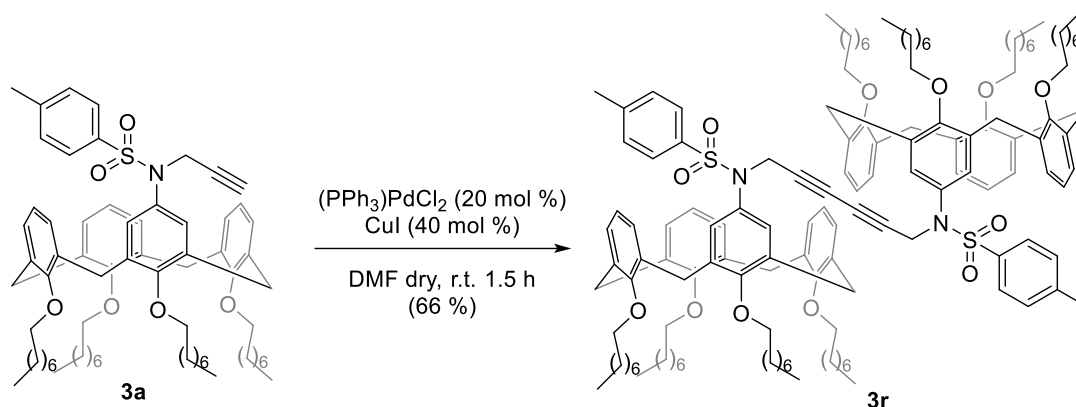
¹³C NMR: (101 MHz, CDCl₃) δ = 157.0 (C_q), 156.8 (C_q), 156.1 (C_q), 143.2 (C_q), 136.2 (C_q), 136.1 (C_q), 135.6 (C_q), 134.7 (C_q), 134.1 (C_q), 133.5 (C_q), 132.0 (CH), 129.1 (CH), 128.3 (CH), 128.2 (CH), 128.1 (CH), 128.1 (CH), 127.9 (CH), 127.0 (CH), 126.8 (CH), 122.7 (C_q), 122.1 (CH), 121.9 (CH), 88.1 (C_q), 78.5 (C_q), 75.3 (CH₂), 75.2 (CH₂), 42.4 (CH₂), 32.0 (CH₂), 31.0 (CH₂), 30.9 (CH₂), 30.4 (CH₂), 30.4 (CH₂), 30.3 (CH₂), 30.0 (CH₂), 29.9 (CH₂), 29.7 (CH₂), 29.6 (CH₂), 26.5 (CH₂), 26.3 (CH₂), 26.3 (CH₂), 22.7 (CH₂), 21.6 (CH₃), 14.1 (CH₃).

LC-MS: m/z [M+NH₄]⁺ calculated for C₇₄H₁₀₃N₂O₆S₂: 1179.73; found: 1179.52.

Chapter 3

HR-MS (ESI) m/z : $[M+H]^+$ calcd. for $C_{74}H_{100}NO_6S_2$ 1162.6992; found 1162.6988.

Synthesis of substrate **3r**:



In a two-necked round-bottom flask, under nitrogen atmosphere, bis(triphenylphosphine)Pd(II) dichloride (0.2 eq.), CuI (0.4 eq.) Et_3N (1.5 eq.) were added to a solution of **3a** (100 mg, 0.093 mmol) in DMF (4 mL). The reaction was stirred at r.t. for 1.5 h. The reaction was monitored by TLC (n-Hex:EtOAc 9:1). Once the reaction was completed, water and EtOAc were added to the mixture. The organic phase was separated and washed with water (2x 30 mL) and brine (30 mL), dried over Na_2SO_4 and filtered. Purified by column chromatography on silica gel (n-Hex:EtOAc 9:1), yielded **3r** (132 mg, 66 %) as a colourless oil.

1H NMR: (400 MHz, $CDCl_3$) δ = 7.59 (d, J = 8.1 Hz, 4H), 7.28 (d, J = 8.2 Hz, 4H), 6.79 (d, J = 7.5 Hz, 4H), 6.70 – 6.61 (m, 6H), 6.58 – 6.48 (m, 8H), 6.36 (dd, J = 7.2, 2.1 Hz, 4H), 4.45 (d, J = 13.2 Hz, 4H), 4.40 (d, J = 13.2 Hz, 4H), 4.31 (s, 4H), 3.97 – 3.77 (m, 16H), 3.16 (d, J = 13.3 Hz, 4H), 3.07 (d, J = 13.3 Hz, 4H), 2.44 (s, 6H), 1.99 – 1.88 (m, 16H), 1.48 – 1.25 (m, 80H), 0.99 – 0.88 (m, 24H).

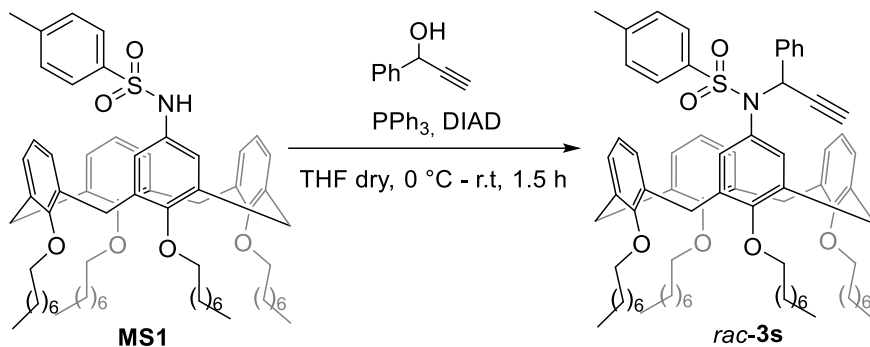
^{13}C NMR: (101 MHz, $CDCl_3$) δ = 156.9 (C_q), 156.8 (C_q), 156.1 (C_q), 143.6 (C_q), 136.3 (C_q), 135.8 (C_q), 135.6 (C_q), 134.7 (C_q), 134.00 (C_q), 133.1 (C_q), 129.2 (CH), 128.3 (CH), 128.2 (CH), 128.0 (CH), 127.9 (CH), 122.2 (CH), 121.9 (CH), 75.4 (CH_2), 75.3 (CH_2), 73.8 (C_q), 69.5 (C_q), 42.3 (CH_2), 32.0 (CH_2), 31.0 (CH_2), 30.9 (CH_2), 30.4 (CH_2), 30.3 (CH_2), 30.0 (CH_2), 29.9 (CH_2), 29.7 (CH_2), 29.6 (CH_2), 26.5 (CH_2), 26.3 (CH_2), 26.2 (CH_2), 22.7 (CH_2), 21.6 (CH_3), 14.1 (CH_3).

LC-MS: m/z $[M+2K]^{2+}$ calculated for $C_{140}H_{192}K_2N_2O_{12}S_2$: 1117.65; found: 1117.47.

Chapter 3

HR-MS (ESI) m/z : $[M+2K]^+$ calcd. for $C_{140}H_{192}K_2N_2O_{12}S_2$: 1117.6595; found: 1117.6590.

Synthesis of substrate *rac*-3s:



MS1 (229 mg, 0.22 mmol) was dissolved in dry THF (2mL) along with PPh_3 (69 mg, 1.2 eq.), DIAD (53 mg, 1.2 eq.) and 1-phenylprop-2-yn-1-ol (34 mg, 1.2 eq.). The mixture was let stirring at r.t. for 2.5 h. The reaction was monitored by TLC (n-Hex:EtOAc 9:1). Once the reaction was completed, water and EtOAc was added to the mixture. The organic phase was separated and washed with water (2x 30 mL) and brine (30 mL), dehydrated with Na_2SO_4 and the solvent removed under low pressure. Purification by column chromatography on silica gel (n-Hex:EtOAc 97:3), yielded *rac*-**3s** (221 mg, 87 %) as a white solid. **M.p.** = 104 – 105 $^\circ\text{C}$.

$^1\text{H NMR}$: (400 MHz, $CDCl_3$) δ = 7.77 (d, J = 8.3 Hz, 2H), 7.52 – 7.45 (m, 2H), 7.36 – 7.29 (m, 5H), 7.11 – 7.04 (m, 2H), 6.88 (t, J = 7.3 Hz, 1H), 6.83 (d, J = 2.6 Hz, 1H), 6.56 – 6.50 (m, 2H), 6.27 (t, J = 7.4 Hz, 1H), 6.20- 6.14 (m, 3H), 6.05 (dd, J = 7.6 Hz, 2.0 Hz, 1H), 5.30 (t, J = 4.4 Hz, 1H), 4.46 – 4.38 (m, 2H), 4.30 (d, J = 13.3 Hz, 1H), 4.25 (d, J = 13.3 Hz, 1H), 4.05 – 3.95 (m, 4H), 3.73 – 3.59 (m, 4H), 3.13 (d, J = 13.3 Hz, 2H), 2.90 (d, J = 13.3 Hz, 1H), 2.86 (d, J = 13.3 Hz, 1H), 2.48 (m, 4H), 1.99 – 1.77 (m, 8H), 1.56 – 1.48 (m, 4H), 1.44 – 1.18 (m, 36H), 0.99 – 0.86 (m, 12H).

$^{13}\text{C NMR}$: (101 MHz, $CDCl_3$) δ = 158.0 (C_q), 157.7 (C_q), 155.2 (C_q), 143.3 (C_q), 137.0 (C_q), 136.9 (C_q), 136.8 (C_q), 136.7 (C_q), 136.4 (C_q), 135.9 (C_q), 133.5 (C_q), 133.3 (C_q), 133.0 (CH), 132.9 (C_q), 132.7 (C_q), 130.7 (CH), 129.1 (CH), 128.8 (CH), 128.8 (CH), 128.7 (CH), 128.3 (CH), 128.2 (CH), 128.1 (CH), 127.5 (CH), 127.4 (CH), 127.3 (CH), 122.0 (CH), 121.9 (CH), 121.8 (CH), 77.2 (CH), 75.3 (C_q + CH_2), 75.2 (CH_2), 75.1 (CH_2), 75.0 (CH_2), 54.9 (CH), 32.1 (CH_2), 32.0 (CH_2), 31.0 (CH_2), 30.7 (CH_2), 30.6 (CH_2), 30.5 (CH_2), 30.4 (CH_2), 30.2 (CH_2), 30.1 (CH_2).

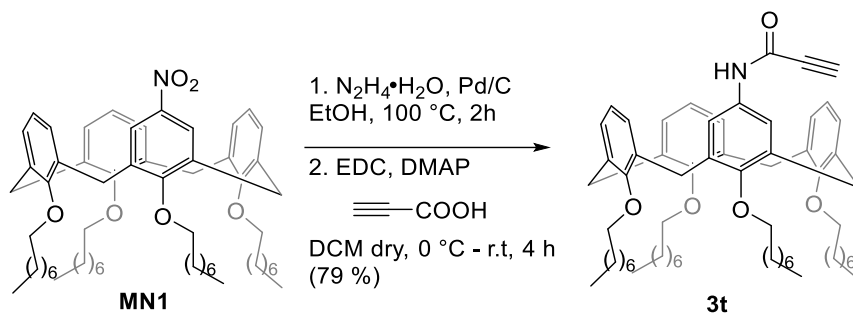
Chapter 3

30.0 (CH₂), 29.8 (CH₂), 29.7 (CH₂), 29.5 (CH₂), 26.6 (CH₂), 26.5 (CH₂), 26.1 (CH₂), 22.8 (CH₂), 22.7 (CH₂), 22.7 (CH₂), 21.7 (CH₃), 14.1 (CH₃).

ESI-MS: m/z [M+NH₄]⁺ calculated for C₇₆H₁₀₅N₂O₆S: 1173.77; found: 1173.64.

HR-MS (ESI) m/z : [M+H]⁺ calcd. for C₇₆H₁₀₂NO₆S₂ 1156.7428; found 1156.7422.

Synthesis of substrate 3t:



In a two-necked round bottom flask, under nitrogen atmosphere, Pd/C (cat. amount) and hydrazine monohydrate (60 eq.) were added to a suspension of **MN1** (200 mg, 0.22 mmol) in EtOH (20 mL). The reaction was heated to 100 °C and let react under reflux for 2 h. The reaction was monitored by TLC (n-Hex:EtOAc 9:1). Once the reaction was completed, the mixture was cooled to r.t. and filtered through celite and the solvent removed under low pressure. Water and DCM were added to the residue and the organic phase was recovered, washed with water (2 x 30 mL) and brine (30 mL), dried over Na₂SO₄, filtered and the solvent removed under low pressure. The crude was used in the next step without further purification. The mono-ammino derivative was then dissolved in dry DCM, under nitrogen atmosphere, and EDC (1.3 eq.), DMAP (cat.) and 3-propionic acid (1.3 eq.) were added at 0 °C. The mixture was let warm up at r.t. and stirred for 4 h. The reaction was monitored by TLC (n-Hex:EtOAc 9:1). Once the reaction was completed, water was added to the mixture. The organic phase was separated and washed with water (2x 30 mL) and brine (30 mL), dried over Na₂SO₄ and the solvent removed under low pressure. The crude was purified by column chromatography on silica gel (n-Hex:EtOAc 9:1), obtaining the desired substrate **3t** (163 mg, 79 %) as a colourless oil.

¹H NMR: (400 MHz, CDCl₃) δ = 7.00 (s, 1H), 6.84 – 6.77 (m, 4H), 6.72 (t, *J* = 7.4 Hz, 2H), 6.52 (s, 2H), 6.47 (s, 3H), 4.46 (d, *J* = 13.3 Hz, 2H), 4.44 (d, *J* = 13.3 Hz, 2H), 3.97 – 3.94 (m, 2H), 3.82 (q, *J* = 7.0 Hz, 4H), 3.18 (d, *J* = 13.2 Hz, 2H), 3.14 (d, *J* = 13.2 Hz, 2H), 2.84 (s, 1H), 1.97 – 1.84 (m, 8H), 1.55 – 1.24 (m, 40H), 0.96 – 0.88 (m, 12H).

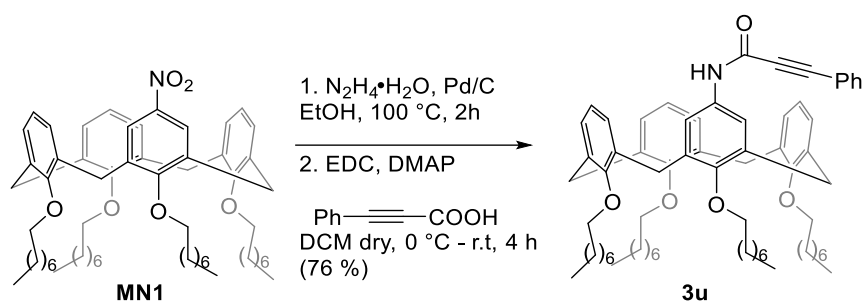
Chapter 3

¹³C NMR: (101 MHz, CDCl₃) δ = 157.1 (C_q), 156.3 (C_q), 153.9 (C_q), 149.0 (C_q), 135.9 (C_q), 135.5 (C_q), 135.4 (C_q), 134.6 (C_q), 130.5 (C_q), 128.6 (CH), 128.4 (CH), 127.8 (CH), 122.0 (CH), 121.4 (CH), 120.1 (CH), 76.8 (CH), 75.2 (CH₂), 75.2 (CH₂), 75.2 (CH₂), 73.3 (C_q), 32.0 (CH₂), 31.1 (CH₂), 31.0 (CH₂), 30.4 (CH₂), 30.3 (CH₂), 30.3 (CH₂), 30.0 (CH₂), 29.9 (CH₂), 29.9 (CH₂), 29.7 (CH₂), 29.6 (CH₂), 29.6 (CH₂), 26.5 (CH₂), 26.4 (CH₂), 26.2 (CH₂), 22.7 (CH₂), 22.7 (CH₂), 14.1 (CH₃).

LC-MS: *m/z* [M+NH₄]⁺ calculated for C₆₃H₉₃N₂O₅: 957.71; found: 957.45.

HR-MS (ESI) *m/z*: [M+H]⁺ calcd. for C₆₃H₉₀NO₅ 940.6819; found 940.6816.

Synthesis of substrate 3u:



In a two-necked round bottom flask, under nitrogen atmosphere, Pd/C (cat. amount) and hydrazine monohydrate (60 eq.) were added to a suspension of **MN1** (200 mg, 0.22 mmol) in EtOH (20 mL). The reaction was heated to 100 °C and let react under reflux for 2 h. The reaction was monitored by TLC (n-Hex:EtOAc 9:1). Once the reaction was completed, the mixture was cooled to r.t. and filtered through celite and the solvent removed under low pressure. Water and DCM were added to the residue and the organic phase was recovered, washed with water (2 x 30 mL) and brine (30 mL), dehydrated with Na₂SO₄, filtered and the solvent removed under low pressure. The crude was used in the next step without further purification. The mono-ammino derivative was then dissolved in dry DCM, under nitrogen atmosphere, and EDC (1.3 eq.), DMAP (cat.) and 3-phenylpropionic acid (1.3 eq.) were added at 0 °C. The mixture was let warm up at r.t. and stirred for 4 h. The reaction was monitored by TLC (n-Hex:EtOAc 9:1). Once the reaction was completed, water was added to the mixture. The organic phase was separated and washed with water (2x 30 mL) and brine (30 mL), dehydrated with Na₂SO₄ and the solvent removed under low pressure. The crude was purified by column chromatography on silica gel (n-Hex:EtOAc 9:1), obtaining the desired substrate **7b** (170 mg, 76 %) as a colourless oil.

Chapter 3

¹H NMR: (400 MHz, CDCl₃) δ = 7.61 – 7.54 (m, 2H), 7.49 – 7.30 (m, 3H), 7.08 (s, 1H), 6.85 – 6.77 (m, 3H), 6.72 (t, *J* = 7.4 Hz, 2H), 6.59 (s, 2H), 6.55 – 6.45 (m, 2H), 4.47 (d, *J* = 13.3 Hz, 2H), 4.45 (d, *J* = 13.3 Hz, 2H), 4.00 – 3.89 (m, 4H), 3.89 – 3.79 (m, 4H), 3.18 (d, *J* = 13.4 Hz, 2H), 3.17 (d, *J* = 13.4 Hz, 2H), 1.99 – 1.84 (m, 8H), 1.48 – 1.23 (m, 40H), 0.96 – 0.88 (m, 12H).

¹³C NMR: (101 MHz, CDCl₃) δ = 157.1 (C_q), 156.4 (C_q), 153.8 (C_q), 150.4 (C_q), 135.9 (C_q), 135.5 (C_q), 135.4 (C_q), 134.7 (C_q), 132.6 (CH), 131.0 (C_q), 130.1 (CH), 128.6 (CH), 128.4 (CH), 127.9 (CH), 122.0 (CH), 121.5 (CH), 120.2 (C_q), 120.1 (CH), 85.0 (C_q), 83.7 (C_q), 75.2 (CH₂), 75.1 (CH₂), 32.0 (CH₂), 31.1 (CH₂), 31.0 (CH₂), 30.4 (CH₂), 30.4 (CH₂), 30.3 (CH₂), 30.0 (CH₂), 29.9 (CH₂), 29.8 (CH₂), 29.7 (CH₂), 29.6 (CH₂), 26.5 (CH₂), 26.4 (CH₂), 26.3 (CH₂), 22.7 (CH₂), 14.1 (CH₃).

LC-MS: *m/z* [M+NH₄]⁺ calculated for C₆₉H₉₇N₂O₅: 1033.74; found: 1033.46.

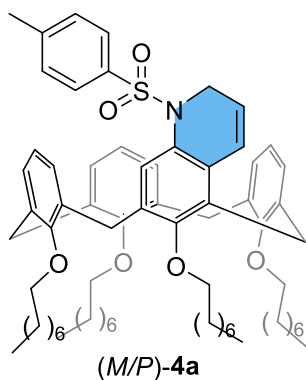
HR-MS (ESI) *m/z*: [M+H]⁺ calcd. for C₆₉H₉₄NO₅ 1016.7132; found 1016.7128.

Chapter 3

• Characterization of Products 4

General Procedure for catalytic reactions

Into a Schlenk flask, under nitrogen atmosphere, the corresponding substrate **3** (50.0 mg) and [JohnPhosAu(I)ACN]⁺SbF₆⁻ (5-10 mol %) were dissolved in a dry solvent (1.0 mL) and the mixture stirred at the desired temperature for 16 hrs. After completion, the mixture was diluted with CH₂Cl₂ (10 ml) and filtered through a pad of celite that was washed with an additional 20 ml of CH₂Cl₂. The solvent was removed under low pressure and the crude was purified by column chromatography on silica gel (n-Hex: EtOAc 95:5), obtaining the desired product.



Representative procedure was followed using **3a** (50 mg, 0.046 mmol), [JohnPhosAu(I)ACN]⁺SbF₆⁻ (5 mol %), CH₂Cl₂ (1.0 ml) as the solvent and stirring the reaction at 25 °C. Purification by column chromatography on silica gel (n-Hexane/EtOAc 95:5) yielded (M/P)-**4a** (47.6 mg, 95 %) as a white solid. **M.p.** = 142 – 143 °C.

¹H NMR: (400 MHz, CDCl₃) δ = 7.58 (s, 1H), 7.44 (d, *J* = 8.1 Hz, 2H), 7.18 – 7.06 (m, 4H), 6.92 (t, *J* = 7.4 Hz, 1H), 6.45 – 6.39 (m,

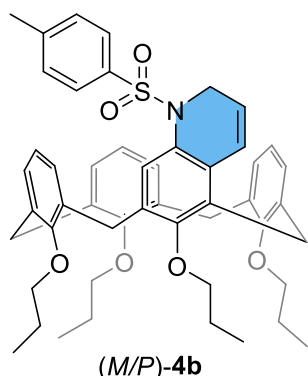
2H), 6.36 (t, *J* = 7.4 Hz, 1H), 6.27 – 6.18 (m, 3H), 5.68 (dt, *J* = 9.3, 4.3 Hz, 1H), 5.62 – 5.53 (m, 1H), 4.71 (dd, *J* = 17.9, 5.0 Hz, 1H), 4.53 – 4.40 (m, 3H), 4.30 – 4.17 (m, 2H), 4.14 (td, *J* = 11.0, 5.4 Hz, 1H), 4.10 – 4.03 (m, 2H), 3.96 (td, *J* = 10.9, 5.5 Hz, 1H), 3.75 (td, *J* = 6.7, 3.2 Hz, 2H), 3.70 (t, *J* = 6.7 Hz, 2H), 3.34 – 3.25 (m, 2H), 3.23 – 3.12 (m, 2H), 2.38 (s, 3H), 2.16 – 1.76 (m, 8H), 1.66 – 1.48 (m, 4H), 1.48 – 1.18 (m, 36H), 0.93 (t, *J* = 6.6 Hz, 12H).

¹³C NMR: (101 MHz, CDCl₃) δ = 157.8 (C_q), 156.4 (C_q), 155.5 (C_q), 155.4 (C_q), 143.1 (C_q), 137.0 (C_q), 136.9 (C_q), 136.6 (C_q), 136.6 (C_q), 133.5 (C_q), 133.4 (C_q), 133.1 (C_q), 132.9 (C_q), 132.8 (C_q), 129.2 (C_q), 129.0 (CH), 128.9 (CH), 128.7 (CH), 127.8 (CH), 127.7 (CH), 127.6 (CH), 127.0 (C_q), 127.0 (CH), 126.8 (CH), 123.9 (CH), 123.1 (CH), 122.0 (CH), 121.9 (CH), 121.7 (CH), 75.5 (CH₂), 75.3 (CH₂), 75.2 (CH₂), 75.0 (CH₂), 45.1 (CH₂), 32.0 (2CH₂), 31.1 (2CH₂), 31.0 (CH₂), 30.6 (CH₂), 30.5 (CH₂), 30.2 (CH₂), 30.1 (2CH₂), 29.8 (2CH₂), 29.5 (2CH₂), 26.7 (CH₂), 26.6 (CH₂), 26.2 (CH₂), 26.1 (CH₂), 24.5 (CH₂), 22.8 (CH₂), 22.7 (2CH₂), 21.6 (CH₃), 14.1 (2CH₃).

LC-MS: *m/z* [M+NH₄]⁺ calculated for C₇₀H₁₀₁N₂O₆S: 1097.74; found: 1097.49.

Chapter 3

HR-MS (ESI) m/z : $[M+K]^+$ calcd. for $C_{70}H_{97}KNO_6S$ 1118.6674; found 1118.6682.



Representative procedure was followed using **3b** (50.0 mg, 0.062 mmol), $[JohnPhosAu(I)ACN]^+SbF_6^-$ (5 mol %), CH_2Cl_2 (1.0 ml) as the solvent and stirring the reaction at 25 °C. Purification by column chromatography on silica gel (n-Hexane/EtOAc 95:5) yielded (*M/P*)-**4b** (47.1 mg, 94 %) as a white solid. **M.p.** = 148 – 149 °C.

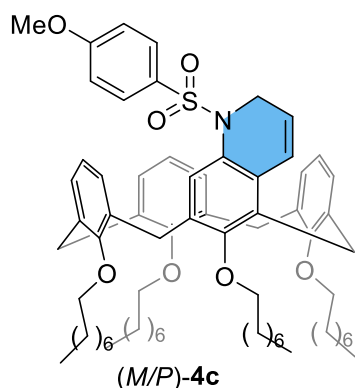
1H NMR: (400 MHz, $CDCl_3$) δ = 7.58 (s, 1H), 7.44 (d, J = 8.3 Hz, 2H), 7.17 – 7.07 (m, 4H), 6.92 (t, J = 7.4 Hz, 1H), 6.44 – 6.39 (m, 2H), 6.36 (t, J = 7.4 Hz, 1H), 6.29 – 6.18 (m, 3H), 5.73 – 5.64 (m, 1H), 5.57 (t, J = 4.7 Hz, 1H), 4.75 – 4.65 (m, 1H), 4.52 – 4.38 (m, 3H), 4.26 (d, J = 14.1 Hz, 1H), 4.20 (ddd, J = 17.9, 3.6, 2.1 Hz, 1H), 4.10 (td, J = 10.6, 5.6 Hz, 1H), 4.05 – 3.99 (m, 2H), 3.92 (td, J = 10.6, 5.8 Hz, 1H), 3.73 (td, J = 6.9, 3.4 Hz, 2H), 3.67 (t, J = 6.8 Hz, 2H), 3.35 – 3.24 (m, 2H), 3.23 – 3.14 (m, 2H), 2.38 (s, 3H), 2.09 – 1.80 (m, 8H), 1.13 (t, J = 7.4 Hz, 3H), 1.09 (t, J = 7.4 Hz, 3H), 0.99 – 0.88 (m, 6H).

^{13}C NMR: (101 MHz, $CDCl_3$) δ = 157.9 (C_q), 156.5 (C_q), 155.4 (C_q), 155.3 (C_q), 143.1 (C_q), 136.9 (C_q), 136.8 (C_q), 136.6 (C_q), 136.5 (C_q), 133.5 (C_q), 133.4 (C_q), 133.1 (C_q), 132.9 (C_q), 132.8 (C_q), 129.2 (C_q), 129.0 (CH), 128.9 (CH), 128.7 (CH), 127.8 (CH), 127.7 (CH), 127.6 (CH), 127.5 (CH), 127.0 (C_q), 127.0 (CH), 126.8 (CH), 123.8 (CH), 123.1 (CH), 122.0 (CH), 121.9 (CH), 121.8 (CH), 76.8 (CH_2), 76.5 (CH_2), 45.1 (CH_2), 31.1 (CH_2), 31.0 (CH_2), 30.9 (CH_2), 24.5 (CH_2), 23.5 (CH_2), 23.4 (CH_2), 23.0 (CH_2), 22.9 (CH_2), 21.6 (CH_3), 10.8 (CH_3), 10.7 (CH_3), 10.0 (CH_3), 9.9 (CH_3).

LC-MS: m/z $[M+Na]^+$ calculated for $C_{50}H_{57}NNaO_6S$: 822.38; found: 822.86.

HR-MS (ESI) m/z : $[M+K]^+$ calcd. for $C_{50}H_{57}KNO_6S$ 838.3544; found 838.3538.

Chapter 3



Representative procedure was followed using **3c** (50.0 mg, 0.046 mmol), [JohnPhosAu(I)ACN]⁺SbF₆⁻ (5 mol %), 1,2-dichloroethane (1.0 ml) as the solvent and stirring the reaction at 80 °C. Purification by column chromatography on silica gel (n-Hexane/EtOAc 95:5) yielded (M/P)-**4c** (42.6 mg, 85 %) as a yellowish oil.

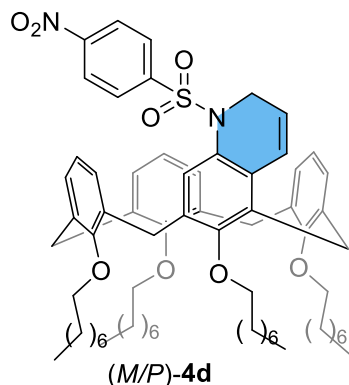
¹H NMR: (400 MHz, CDCl₃) δ = 7.56 (s, 1H), 7.48 (d, *J* = 8.9 Hz, 2H), 7.10 (dd, *J* = 7.4, 1.7 Hz, 1H), 7.08 (dd, *J* = 7.4, 1.7 Hz, 1H), 6.91 (t, *J* = 7.4 Hz, 1H), 6.79 (d, *J* = 8.9 Hz, 2H), 6.45 (d, *J* = 9.8 Hz, 1H), 6.41 – 6.31 (m, 2H), 6.28 – 6.18 (m, 3H), 5.74 – 5.65 (m, 1H), 5.60 (dd, *J* = 6.6, 2.7 Hz, 1H), 4.68 (dd, *J* = 17.9, 5.0 Hz, 1H), 4.50 – 4.41 (m, 3H), 4.30 – 4.17 (m, 2H), 4.12 (td, *J* = 11.0, 5.5 Hz, 1H), 4.08 – 4.01 (m, 2H), 3.95 (td, *J* = 10.9, 5.5 Hz, 1H), 3.81 (s, 3H), 3.74 (td, *J* = 6.7, 3.5 Hz, 2H), 3.69 (t, *J* = 6.7 Hz, 2H), 3.34 – 3.23 (m, 2H), 3.22 – 3.13 (m, 2H), 2.12 – 1.79 (m, 8H), 1.66 – 1.48 (m, 4H), 1.47 – 1.21 (m, 36H), 0.96 – 0.87 (m, 12H).

¹³C NMR: (101 MHz, CDCl₃) δ = 162.8 (C_q), 157.8 (C_q), 156.4 (C_q), 155.4 (C_q), 155.3 (C_q), 137.0 (C_q), 136.9 (C_q), 136.6 (C_q), 133.5 (C_q), 133.5 (C_q), 133.2 (C_q), 132.9 (C_q), 132.8 (C_q), 131.3 (C_q), 129.8 (CH), 129.3 (C_q), 128.9 (CH), 128.7 (CH), 127.7 (CH), 127.6 (CH), 127.5 (CH), 127.0 (CH), 126.9 (C_q), 126.8 (CH), 123.9 (CH), 123.1 (CH), 122.0 (CH), 121.9 (CH), 121.8 (CH), 113.4 (CH), 75.5 (CH₂), 75.3 (CH₂), 75.2 (CH₂), 75.0 (CH₂), 55.5 (CH₃), 45.1 (CH₂), 32.0 (2CH₂), 31.1 (CH₂), 31.0 (CH₂), 30.6 (CH₂), 30.5 (CH₂), 30.2 (CH₂), 30.1 (CH₂), 30.1 (CH₂), 29.8 (CH₂), 29.7 (CH₂), 29.5 (CH₂), 29.4 (CH₂), 26.7 (CH₂), 26.6 (CH₂), 26.2 (CH₂), 26.1 (CH₂), 24.5 (CH₂), 22.8 (CH₂), 22.7 (CH₂), 22.7 (CH₂), 14.1 (2CH₃).

LC-MS: *m/z* [M+Na]⁺ calculated for C₅₀H₅₇NaO₇S: 1118.69; found: 1118.59.

HR-MS (ESI) *m/z*: [M+K]⁺ calcd. for C₇₀H₉₇KNO₇S 1134.6623; found 1134.6618.

Chapter 3



Representative procedure was followed using **3d** (50.0 mg, 0.045 mmol), [JohnPhosAu(I)ACN]⁺SbF₆⁻ (5 mol %), 1,2-dichloroethane (1.0 ml) as the solvent and stirring the reaction at 80 °C. Purification by column chromatography on silica gel (n-Hexane/EtOAc 95:5) yielded (M/P)-**4d** (37.2 mg, 74 %) as a yellowish oil.

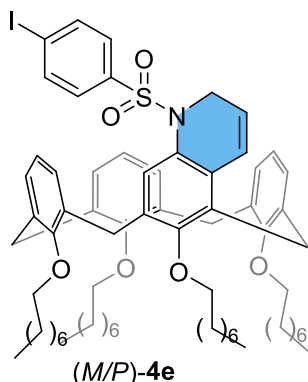
¹H NMR: (400 MHz, CDCl₃) δ = 8.15 (d, *J* = 8.8 Hz, 2H), 7.66 (d, *J* = 8.8 Hz, 2H), 7.51 (s, 1H), 7.07 (dd, *J* = 7.4, 1.7 Hz, 1H), 7.03 (dd, *J* = 7.4, 1.7 Hz, 1H), 6.89 (t, *J* = 7.4 Hz, 1H), 6.49 – 6.37 (m, 3H), 6.36 – 6.23 (m, 3H), 5.70 – 5.58 (m, 2H), 4.57 (dd, *J* = 18.0, 4.6 Hz, 1H), 4.53 – 4.41 (m, 3H), 4.33 (ddd, *J* = 17.9, 4.1, 1.8 Hz, 1H), 4.27 (d, *J* = 14.0 Hz, 1H), 4.14 (td, *J* = 10.7, 5.4 Hz, 1H), 4.03 (m, 2H), 3.97 (dt, *J* = 10.7, 5.4 Hz, 1H), 3.84 – 3.73 (m, 2H), 3.71 (t, *J* = 6.8 Hz, 2H), 3.34 – 3.23 (m, 2H), 3.23 – 3.14 (m, 2H), 1.93 (m, 8H), 1.66 – 1.24 (m, 40H), 0.92 (m, 12H).

¹³C NMR: (101 MHz, CDCl₃) δ = 157.6 (C_q), 157.0 (C_q), 155.6 (C_q), 155.5 (C_q), 149.8 (C_q), 145.1 (C_q), 136.9 (C_q), 136.7 (C_q), 136.6 (C_q), 134.0 (C_q), 133.9 (C_q), 133.4 (C_q), 132.7 (C_q), 132.7 (C_q), 128.9 (CH), 128.8 (CH), 128.6 (CH), 128.2 (C_q), 128.1 (CH), 128.0 (CH), 127.4 (CH), 127.0 (CH), 126.8 (C_q), 126.6 (CH), 124.3 (CH), 123.4 (CH), 122.7 (CH), 122.1 (CH), 122.0 (CH), 121.7 (CH), 75.6 (CH₂), 75.4 (CH₂), 75.3 (CH₂), 75.3 (CH₂), 45.3 (CH₂), 32.0 (CH₂), 32.0 (CH₂), 31.1 (CH₂), 31.0 (CH₂), 30.9 (CH₂), 30.6 (CH₂), 30.4 (CH₂), 30.2 (CH₂), 30.1 (CH₂), 30.0 (CH₂), 29.8 (CH₂), 29.7 (CH₂), 29.5 (CH₂), 29.4 (CH₂), 26.6 (CH₂), 26.5 (CH₂), 26.2 (CH₂), 26.1 (CH₂), 24.9 (CH₂), 22.8 (CH₂), 22.7 (CH₂), 22.7 (CH₂), 14.1 (2CH₃).

LC-MS: *m/z* [M+H]⁺ calculated for C₆₉H₉₅N₂O₈S: 1111.68; found: 1111.20.

HR-MS (ESI) *m/z*: [M+K]⁺ calcd. for C₆₉H₉₄KN₂O₈S 1149.6368; found 1149.6362.

Chapter 3



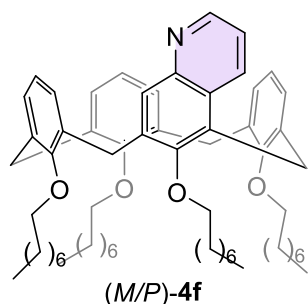
Representative procedure was followed using **3e** (50.0 mg, 0.042 mmol), [JohnPhosAu(I)ACN]⁺SbF₆⁻ (5 mol %), 1,2-dichloroethane (1.0 ml) as the solvent and stirring the reaction at 80 °C. Purification by column chromatography on silica gel (n-Hexane/EtOAc 95:5) yielded (M/P)-**4e** (36.4 mg, 73 %), as a colourless oil.

¹H NMR: (400 MHz, CDCl₃) δ = 7.66 (d, *J* = 8.5 Hz, 2H), 7.54 (s, 1H), 7.23 (d, *J* = 8.4 Hz, 2H), 7.14 – 7.05 (m, 2H), 6.91 (t, *J* = 7.4 Hz, 1H), 6.49 – 6.42 (m, 1H), 6.40 – 6.32 (m, 3H), 6.32 – 6.22 (m, 2H), 5.74 – 5.66 (m, 1H), 5.59 (dd, *J* = 7.6, 1.7 Hz, 1H), 4.66 (dd, *J* = 17.9, 4.9 Hz, 1H), 4.51 – 4.41 (m, 3H), 4.30 – 4.18 (m, 2H), 4.13 (td, *J* = 10.8, 5.4 Hz, 1H), 4.09 – 4.02 (m, 2H), 3.96 (td, *J* = 10.8, 5.5 Hz, 1H), 3.78 – 3.72 (m, 2H), 3.70 (t, *J* = 6.8 Hz, 2H), 3.35 – 3.25 (m, 2H), 3.22 – 3.14 (m, 2H), 2.07 – 1.80 (m, 8H), 1.62 – 1.47 (m, 4H), 1.47 – 1.20 (m, 36H), 1.01 – 0.85 (m, 12H).

¹³C NMR: (101 MHz, CDCl₃) δ = 157.7 (C_q), 156.7 (C_q), 155.4 (2C_q), 139.1 (C_q), 137.5 (CH), 136.9 (C_q), 136.8 (C_q), 136.8 (C_q), 133.7 (C_q), 133.6 (C_q), 133.4 (C_q), 132.8 (C_q), 132.8 (C_q), 129.1 (CH), 128.9 (CH), 128.7 (C_q), 128.7 (CH), 127.8 (CH), 127.7 (CH), 127.5 (CH), 126.9 (C_q), 126.9 (CH), 126.7 (CH), 124.2 (CH), 122.9 (CH), 122.0 (CH), 121.9 (CH), 99.7 (C_q), 75.5 (CH₂), 75.3 (CH₂), 75.3 (CH₂), 75.1 (CH₂), 45.2 (CH₂), 32.0 (2CH₂), 31.1 (2CH₂), 31.0 (CH₂), 30.6 (CH₂), 30.5 (CH₂), 30.2 (CH₂), 30.1 (2CH₂), 29.8 (CH₂), 29.5 (CH₂), 29.5 (CH₂), 26.7 (CH₂), 26.6 (CH₂), 26.2 (CH₂), 26.1 (CH₂), 24.6 (CH₂), 22.8 (CH₂), 22.7 (CH₂), 22.7 (CH₂), 14.1 (2CH₃).

LC-MS: *m/z* [M+H₃O]⁺ calculated for C₆₉H₉₇NIO₇S: 1210.60; found: 1210.05.

HR-MS (ESI) *m/z*: [M+K]⁺ calcd. for C₆₉H₉₄IKNO₆S 1230.5484; found 1230.5488.



4f. Method A: Into a Schlenk, trifluoromethanesulphonic acid (2 eq., 0.093 mmol) was added to a solution of **4a** (50 mg, 0.046 mmol) in 1,2-DCE (1 ml) at 0 °C. After 10 minutes, the ice-bath was removed, and the mixture was left stirring at r.t. overnight. The reaction was monitored by TLC (n-Hex:EtOAc 9:1). Once the reaction was completed, water and DCM were added to the

residue, the organic phase was separated and washed with water (2x 30 mL) and brine (30 mL), dried over Na₂SO₄ and filtered. The crude was purified by column chromatography on

Chapter 3

silica gel (n-Hex:EtOAc 9:1), obtaining the desired product **4f** (30.1 mg, 71 %) as a colourless oil.

4f. Method B: Into a two-necked round bottom flask, under nitrogen atmosphere, thiophenol (1.2 eq., 0.054 mmol) was added to a suspension of **4d** (50.0 mg, 0.045 mmol) and K₂CO₃ (3 eq., 0.130 mmol) in dry acetonitrile (1.5 mL). The mixture was left stirring at r.t. overnight. The reaction was monitored by TLC (n-Hex:EtOAc 9:1). Once the reaction was completed, the solvent was removed under reduced pressure. Water and EtOAc were added to the residue, the organic phase was separated and washed with water (2x 30 mL) and brine (30 mL), dried over Na₂SO₄ and filtered. The crude was purified by column chromatography on silica gel (n-Hex:EtOAc 9:1), obtaining the desired product **4f** (24.3 mg, 59 %) as a colourless oil.

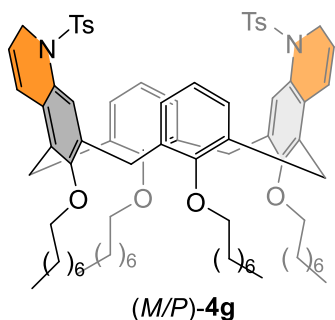
¹H NMR: (400 MHz, CDCl₃) δ = 8.81 (dd, *J* = 4.2, 1.5 Hz, 1H), 8.44 (dd, *J* = 8.8, 1.6 Hz, 1H), 7.81 (s, 1H), 7.37 (dd, *J* = 8.6, 4.2 Hz, 1H), 7.00 (dd, *J* = 7.5, 1.7 Hz, 1H), 6.91 (d, *J* = 7.4 Hz, 1H), 6.76 (t, *J* = 7.4 Hz, 1H), 6.29 – 6.15 (m, 5H), 6.05 – 5.97 (m, 1H), 4.70 – 4.59 (m, 2H), 4.53 – 4.42 (m, 2H), 4.20 (td, *J* = 10.7, 5.6 Hz, 1H), 4.13 – 4.00 (m, 3H), 3.96 (d, *J* = 14.2 Hz, 1H), 3.89 – 3.74 (m, 4H), 3.46 (d, *J* = 13.3 Hz, 1H), 3.17 (d, *J* = 13.4 Hz, 2H), 2.06 – 1.84 (m, 8H), 1.62 – 1.50 (m, 4H), 1.47 – 1.23 (m, 36H), 1.01 – 0.85 (m, 12H).

¹³C NMR: (101 MHz, CDCl₃) δ = 157.6 (C_q), 156.0 (C_q), 155.7 (C_q), 155.6 (C_q), 147.9 (CH), 145.4 (C_q), 144.4 (C_q), 141.2 (C_q), 136.8 (C_q), 136.7 (C_q), 133.9 (2C_q), 133.3 (C_q), 132.4 (C_q), 132.0 (CH), 130.2 (C_q), 128.8 (CH), 128.7 (CH), 128.5 (CH), 127.8 (CH), 127.7 (CH), 127.6 (CH), 126.9 (CH), 122.1 (CH), 122.1 (CH), 121.8 (CH), 120.1 (CH), 75.5 (CH₂), 75.4 (CH₂), 75.3 (CH₂), 75.0 (CH₂), 32.0 (CH₂), 32.0 (CH₂), 31.7 (CH₂), 31.1 (CH₂), 31.0 (CH₂), 30.6 (CH₂), 30.5 (CH₂), 30.2 (CH₂), 30.2 (CH₂), 30.1 (CH₂), 30.0 (CH₂), 29.8 (CH₂), 29.8 (CH₂), 29.8 (CH₂), 29.7 (CH₂), 29.5 (CH₂), 29.5 (CH₂), 26.6 (CH₂), 26.6 (CH₂), 26.2 (CH₂), 26.2 (CH₂), 24.3 (CH₂), 22.8 (CH₂), 22.7 (2CH₂), 14.1 (2CH₃).

LC-MS: *m/z* [M+Na]⁺ calculated for C₆₃H₈₉NNaO₄: 946.67; found: 946.83.

HR-MS: *m/z* [M+K]⁺ calculated for C₆₃H₈₉KNO₄: 962.6429; found: 964.6423

Chapter 3



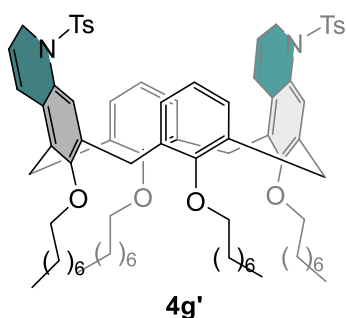
Representative procedure was followed using **3g** (50.0 mg, 0.039 mmol), [JohnPhosAu(I)ACN]⁺SbF₆⁻ (5 mol %), CH₂Cl₂ (1.0 ml) as the solvent and stirring the reaction at 25 °C. Purification by column chromatography on silica gel (n-Hexane/EtOAc 95:5) yielded (M/P)-**4g** (23.1 mg, 46 %) as a colourless oil.

¹H NMR: (400 MHz, CDCl₃) δ = 7.64 (s, 2H), 7.45 (d, *J* = 8.1 Hz, 4H), 7.15 (d, *J* = 8.1 Hz, 4H), 6.47 – 6.38 (m, 4H), 6.29 (t, *J* = 7.6 Hz, 2H), 5.75 – 5.65 (m, 2H), 5.59 (dd, *J* = 7.6, 1.7 Hz, 2H), 4.75 (dd, *J* = 18.0, 5.1 Hz, 2H), 4.44 (d, *J* = 13.2 Hz, 2H), 4.28 – 4.18 (m, 4H), 4.14 (td, *J* = 11.1, 5.2 Hz, 2H), 3.95 (td, *J* = 11.0, 5.4 Hz, 2H), 3.67 (t, *J* = 6.6 Hz, 4H), 3.35 – 3.25 (m, 4H), 2.40 (s, 6H), 2.10 – 1.99 (m, 2H), 1.99 – 1.90 (m, 2H), 1.90 – 1.80 (m, 4H), 1.54 (t, *J* = 7.7 Hz, 4H), 1.44 – 1.22 (m, 36H), 0.92 (td, *J* = 6.7, 4.1 Hz, 12H).

¹³C NMR: (101 MHz, CDCl₃) δ = 156.5 (C_q), 155.3 (C_q), 143.2 (C_q), 136.7 (C_q), 136.6 (C_q), 133.3 (C_q), 132.9 (C_q), 132.8 (C_q), 129.2 (C_q), 128.9 (CH), 127.8 (CH), 127.7 (CH), 127.1 (CH), 127.1 (C_q), 126.8 (CH), 123.7 (CH), 123.4 (CH), 121.8 (CH), 75.4 (CH₂), 75.3 (CH₂), 45.1 (CH₂), 32.0 (CH₂), 32.0 (CH₂), 31.2 (CH₂), 30.6 (CH₂), 30.1 (CH₂), 30.1 (CH₂), 29.8 (CH₂), 29.8 (CH₂), 29.5 (CH₂), 26.7 (CH₂), 26.1 (CH₂), 24.1 (CH₂), 22.8 (CH₂), 22.7 (CH₂), 21.7 (CH₃), 14.1 (CH₃).

LC-MS: *m/z* [M+H]⁺ calculated for C₈₀H₁₀₇N₂O₈S₂: 1287.75; found: 1287.27.

HR-MS: *m/z* [M+K]⁺ calculated for C₈₀H₁₀₆KN₂O₈S₂: 1325.7028; found: 1325.7024.



Representative procedure was followed using **3g** (50.0 mg, 0.039 mmol), [JohnPhosAu(I)ACN]⁺SbF₆⁻ (5 mol %), CH₂Cl₂ (1.0 ml) as the solvent and stirring the reaction at 25 °C. Purification by column chromatography on silica gel (n-Hexane/EtOAc 95:5) yielded **4g'** (19.8 mg, 40 %) as a colourless oil.

¹H NMR: (400 MHz, CDCl₃) δ = 7.64 (s, 2H), 7.47 (d, *J* = 8.3 Hz, 4H), 7.16 (d, *J* = 8.2 Hz, 4H), 6.45 (d, *J* = 9.8 Hz, 2H), 6.34 (m, 3H), 6.15 (t, *J* = 7.6 Hz, 1H), 5.72 (dt, *J* = 9.4, 4.3 Hz, 2H), 5.57 (d, *J* = 7.6 Hz, 2H), 4.71 (dd, *J* = 18.0, 4.9 Hz, 2H), 4.45 (d, *J* = 13.3 Hz, 2H), 4.29 (ddd, *J* = 18.0, 3.8, 2.0 Hz, 2H), 4.19 (d, *J* = 14.0 Hz, 2H), 4.12 (td, *J* = 11.0, 5.3 Hz, 2H), 3.97 (td, *J* = 11.0, 5.5

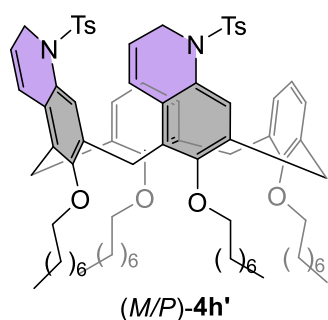
Chapter 3

Hz, 2H), 3.72 (t, $J = 6.5$ Hz, 2H), 3.61 (t, $J = 6.5$ Hz, 2H), 3.35 – 3.24 (m, 4H), 2.40 (s, 6H), 2.08 – 1.76 (m, 8H), 1.57 – 1.47 (m, 4H), 1.44 – 1.22 (m, 36H), 0.92 (m, 12H).

^{13}C NMR: (101 MHz, CDCl_3) $\delta = 156.6$ (C_q), 155.4 (C_q), 155.2 (C_q), 143.0 (C_q), 136.8 (C_q), 136.7 (C_q), 133.4 (C_q), 133.0 (C_q), 132.7 (C_q), 129.2 (C_q), 128.8 (CH), 127.8 (CH), 127.6 (CH), 127.2 (CH), 126.9 (C_q), 126.7 (CH), 123.6 (CH), 123.4 (CH), 122.0 (CH), 121.7 (CH), 75.5 (CH_2), 75.2 (CH_2), 45.1 (CH_2), 32.0 (CH_2), 32.0 (CH_2), 31.1 (CH_2), 30.7 (CH_2), 30.5 (CH_2), 30.1 (CH_2), 30.1 (CH_2), 29.8 (CH_2), 29.8 (CH_2), 29.7 (CH_2), 29.5 (CH_2), 29.4 (CH_2), 26.7 (CH_2), 26.6 (CH_2), 26.1 (CH_2), 24.2 (CH_2), 22.8 (CH_2), 22.7 (CH_2), 22.7 (CH_2), 21.6 (CH_3), 14.1 (CH_3).

LC-MS: m/z $[\text{M}+\text{H}]^+$ calculated for $\text{C}_{80}\text{H}_{107}\text{N}_2\text{O}_8\text{S}_2^+$: 1287.75; found: 1287.34.

HR-MS: m/z $[\text{M}+\text{K}]^+$ calculated for $\text{C}_{80}\text{H}_{106}\text{KN}_2\text{O}_8\text{S}_2$: 1325.7028; found: 1325.7021.



Representative procedure was followed using **3h** (50.0 mg, 0.039 mmol), $[\text{JohnPhosAu}(\text{I})\text{ACN}]^+\text{SbF}_6^-$ (5 mol %), CH_2Cl_2 (1.0 ml) as the solvent and stirring the reaction at 25 °C. Purification by column chromatography on silica gel (n-Hexane/EtOAc 95:5) yielded (M/P)-**4h'** (21.5 mg, 43 %) as colourless oil.

^1H NMR: (400 MHz, CDCl_3) $\delta = 7.23$ – 7.15 (m, 5H), 7.11 – 7.01 (m, 5H), 6.99 (d, $J = 7.4$ Hz, 1H), 6.87 (t, $J = 7.4$ Hz, 1H), 6.81 (s, 1H), 6.43 (dd, $J = 7.6, 1.8$ Hz, 1H), 6.36 (t, $J = 7.5$ Hz, 1H), 6.24 (dd, $J = 9.8, 2.4$ Hz, 1H), 6.18 (d, $J = 9.8$ Hz, 1H), 5.92 (d, $J = 7.4$ Hz, 1H), 5.41 – 5.30 (m, 2H), 4.57 – 4.44 (m, 4H), 4.36 (dd, $J = 17.7, 4.9$ Hz, 1H), 4.23 (d, $J = 14.5$ Hz, 1H), 4.18 – 4.03 (m, 3H), 3.97 – 3.80 (m, 3H), 3.76 – 3.62 (m, 4H), 3.33 – 3.25 (m, 3H), 3.22 (d, $J = 13.4$ Hz, 1H), 2.39 (s, 3H), 2.34 (s, 3H), 1.92 (m, 8H), 1.12 (t, $J = 7.4$ Hz, 3H), 1.05 (t, $J = 7.4$ Hz, 3H), 0.96 (t, $J = 7.5$ Hz, 3H), 0.90 (t, $J = 7.4$ Hz, 3H).

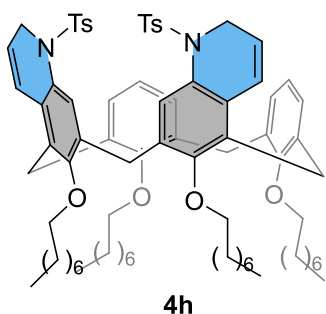
^{13}C NMR: (101 MHz, CDCl_3) $\delta = 157.3$ (C_q), 156.3 (C_q), 156.0 (C_q), 155.2 (C_q), 143.2 (C_q), 143.1 (C_q), 136.7 (C_q), 136.6 (C_q), 136.3 (C_q), 135.4 (C_q), 134.2 (C_q), 134.1 (C_q), 133.7 (C_q), 133.3 (C_q), 132.7 (C_q), 132.6 (C_q), 129.7 (C_q), 129.1 (CH), 128.9 (CH), 128.8 (C_q), 128.8 (CH), 128.6 (CH), 128.2 (CH), 128.0 (CH), 127.5 (CH), 127.1 (CH), 126.9 (CH), 126.9 (C_q), 126.8 (CH), 126.5 (C_q), 124.4 (CH), 123.3 (CH), 122.7 (CH), 122.5 (CH), 121.5 (CH), 121.4 (CH), 76.9 (CH_2), 76.7 (CH_2), 76.3 (CH_2), 44.7 (CH_2), 44.3 (CH_2), 31.2 (CH_2), 30.7 (CH_2), 28.7 (CH_2), 25.4

Chapter 3

(CH₂), 23.4 (CH₂), 23.3 (CH₂), 23.1 (CH₂), 22.5 (CH₂), 21.6 (CH₃), 10.8 (CH₃), 10.6 (CH₃), 10.1 (CH₃), 9.9 (CH₃).

LC-MS: m/z [M+H]⁺ calculated for C₈₀H₁₀₇N₂O₈S₂: 1287.75; found: 1287.33.

HR-MS: m/z [M+K]⁺ calculated for C₈₀H₁₀₆KN₂O₈S₂: 1325.7028; found: 1325.7034.



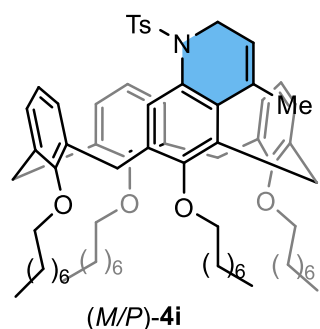
Representative procedure was followed using **3h** (50.0 mg, 0.039 mmol), [JohnPhosAu(I)ACN]⁺SbF₆⁻ (5 mol %), CH₂Cl₂ (1.0 ml) as the solvent and stirring the reaction at 25 °C. Purification by column chromatography on silica gel (n-Hexane/EtOAc 95:5) yielded **4h** (13.2 mg, 26% as a white solid. **M.p.**: 140 – 141 °C.

¹H NMR : (400 MHz, CDCl₃) δ = 7.39 (d, J = 8.2 Hz, 4H), 7.21 (s, 2H), 7.09 (d, J = 8.1 Hz, 4H), 6.52 – 6.46 (m, 2H), 6.43 (t, J = 7.4 Hz, 2H), 6.28 – 6.22 (m, 2H), 6.19 (d, J = 9.9 Hz, 2H), 5.46 (dt, J = 9.3, 4.3 Hz, 2H), 4.50 (d, J = 13.4 Hz, 1H), 4.47 – 4.39 (m, 3H), 4.37 (d, J = 14.0 Hz, 2H), 4.18 – 4.08 (m, 2H), 3.94 – 3.72 (m, 8H), 3.36 (d, J = 13.4 Hz, 1H), 3.27 (d, J = 14.1 Hz, 2H), 3.13 (d, J = 14.0 Hz, 1H), 2.37 (s, 6H), 1.99 – 1.90 (m, 4H), 1.90 – 1.80 (m, 4H), 1.04 (t, J = 7.4 Hz, 6H), 0.96 (t, J = 7.4 Hz, 6H).

¹³C NMR (101 MHz, CDCl₃) δ = 156.7 (C_q), 155.7 (C_q), 142.8 (C_q), 136.7 (C_q), 135.2 (C_q), 134.1 (C_q), 133.9 (C_q), 131.2 (C_q), 129.7 (C_q), 128.7 (2 x CH), 127.9 (CH), 127.8 (CH), 127.0 (C_q), 126.9 (CH), 124.1 (CH), 121.6 (CH), 121.3 (CH), 77.2 (CH₂), 76.3 (CH₂), 44.8 (CH₂), 31.4 (CH₂), 30.9 (CH₂), 27.0 (CH₂), 23.3 (CH₂), 22.8 (CH₂), 21.6 (CH₃), 10.4 (CH₃), 10.2 (CH₃).

LC-MS: m/z [M+H]⁺ calculated for C₈₀H₁₀₇N₂O₈S₂: 1287.75; found: 1287.42.

HR-MS: m/z [M+K]⁺ calculated for C₈₀H₁₀₆KN₂O₈S₂: 1325.7028; found: 1325.7021.



Representative procedure was followed using **3i** (50.0 mg, 0.046 mmol), [JohnPhosAu(I)ACN]⁺SbF₆⁻ (10 mol %), toluene (1.0 ml) as the solvent and stirring the reaction at 100 °C. Purification by column chromatography on silica gel (n-Hexane/EtOAc 95:5) yielded (*M/P*)-**4i** (44.9 mg, 90 %) as a yellowish solid. **M.p.** = 100 – 101 °C.

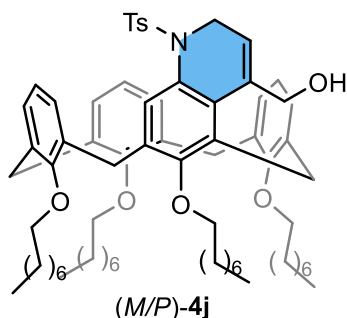
Chapter 3

¹H NMR: (400 MHz, CDCl₃) δ = 7.55 (s, 1H), 7.37 (d, *J* = 8.2 Hz, 2H), 7.18 – 7.06 (m, 4H), 6.92 (t, *J* = 7.4 Hz, 1H), 6.36 – 6.21 (m, 2H), 6.15 – 6.07 (m, 2H), 5.99 (dd, *J* = 7.7, 1.7 Hz, 1H), 5.54 (dd, *J* = 7.6, 1.7 Hz, 1H), 5.43 – 5.35 (m, 1H), 4.46 – 4.33 (m, 4H), 4.29 (d, *J* = 14.3 Hz, 1H), 4.17 – 3.98 (m, 5H), 3.70 (td, *J* = 6.5, 2.9 Hz, 2H), 3.64 (t, *J* = 6.5 Hz, 2H), 3.47 (d, *J* = 14.4 Hz, 1H), 3.26 (d, *J* = 13.6 Hz, 1H), 3.20 – 3.08 (m, 2H), 2.35 (s, 3H), 1.89 (m 8H), 1.62 (s, 3H), 1.56 (m, 4H), 1.46 – 1.17 (m, 36H), 0.96 – 0.84 (m, 12H).

¹³C NMR: (101 MHz, CDCl₃) δ = 158.3 (C_q), 158.1 (C_q), 155.2 (C_q), 155.2 (C_q), 142.8 (C_q), 137.3 (C_q), 137.2 (C_q), 136.9 (C_q), 136.3 (C_q), 134.1 (C_q), 133.6 (C_q), 133.4 (C_q), 133.4 (C_q), 133.0 (C_q), 132.5 (C_q), 131.6 (C_q), 130.5 (C_q), 128.9 (CH), 128.8 (CH), 128.7 (CH), 127.9 (CH), 127.8 (CH), 127.5 (CH), 127.3 (CH), 127.2 (CH), 126.2 (CH), 122.8 (CH), 122.2 (CH), 122.1 (CH), 121.8 (CH), 75.3 (CH₂), 75.2 (CH₂), 75.1 (CH₂), 74.8 (CH₂), 45.4 (CH₂), 32.1 (CH₂), 32.0 (CH₂), 31.1 (CH₂), 31.0 (CH₂), 30.8 (CH₂), 30.6 (CH₂), 30.5 (CH₂), 30.1 (CH₂), 30.1 (CH₂), 30.1 (CH₂), 29.8 (CH₂), 29.7 (CH₂), 29.5 (CH₂), 29.5 (CH₂), 27.6 (CH₂), 26.7 (CH₂), 26.6 (CH₂), 26.3 (CH₂), 26.1 (CH₂), 22.8 (CH₂), 22.8 (CH₂), 22.7 (CH₂), 22.7 (CH₂), 22.0 (CH₃), 21.5 (CH₃), 14.1 (CH₃).

LC-MS: (ESI) *m/z*: [M+H]⁺ calcd. for C₇₁H₁₀₀NO₆S 1094.72; found 1099.79.

HR-MS (ESI) *m/z*: [M+K]⁺ calcd. for C₇₁H₉₉KNO₆S 1132.6830; found 1132.6827.



Representative procedure was followed using **3j** (50.0 mg, 0.045 mmol), [JohnPhosAu(I)ACN]⁺SbF₆⁻ (10 mol %), toluene (1.0 ml) as the solvent and stirring the reaction at 100 °C. Purification by column chromatography on silica gel (n-Hexane/EtOAc 95:5) yielded (*M/P*)-**4j** (24.8 mg, 50 %) as a yellowish oil.

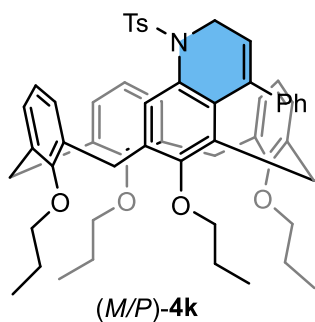
¹H NMR: (400 MHz, CDCl₃) δ = 7.58 (s, 1H), 7.40 (d, *J* = 8.2 Hz, 2H), 7.18 (d, *J* = 8.2 Hz, 2H), 7.14 (dd, *J* = 7.5, 1.7 Hz, 1H), 7.10 (dd, *J* = 7.5, 1.7 Hz, 1H), 6.93 (t, *J* = 7.4 Hz, 1H), 6.35 – 6.26 (m, 2H), 6.18 – 6.07 (m, 2H), 6.02 (dd, *J* = 7.7, 1.7 Hz, 1H), 5.85 – 5.78 (m, 1H), 5.58 (dd, *J* = 7.6, 1.7 Hz, 1H), 4.67 (dd, *J* = 17.1, 6.1 Hz, 1H), 4.51 – 4.33 (m, 4H), 4.17 – 3.99 (m, 7H), 3.78 – 3.68 (m, 2H), 3.65 (t, *J* = 6.6 Hz, 2H), 3.30 (d, *J* = 13.5 Hz, 1H), 3.24 – 3.09 (m, 3H), 2.42 (s, 3H), 2.06 – 1.78 (m, 8H), 1.63 – 1.50 (m, 4H), 1.41 – 1.21 (m, 36H), 1.00 – 0.85 (m, 12H).

Chapter 3

^{13}C NMR (101 MHz, CDCl_3) δ = 158.4 (C_q), 158.0 (C_q), 155.2 (2C_q), 143.5 (C_q), 138.3 (C_q), 137.5 (C_q), 137.3 (C_q), 137.1 (C_q), 136.8 (C_q), 133.8 (C_q), 133.5 (C_q), 133.5 (C_q), 133.3 (C_q), 132.3 (C_q), 130.2 (C_q), 129.1 (C_q), 128.9 (CH), 128.8 (CH), 128.8 (CH), 128.3 (CH), 127.9 (CH), 127.6 (CH), 127.4 (CH), 127.1 (CH), 126.0 (CH), 122.6 (CH), 122.2 (CH), 122.1 (CH), 121.8 (CH), 75.3 (CH_2), 75.2 (CH_2), 75.1 (CH_2), 74.9 (CH_2), 64.2 (CH_2), 45.1 (CH_2), 32.1 (CH_2), 32.0 (CH_2), 31.0 (CH_2), 30.8 (CH_2), 30.6 (CH_2), 30.5 (CH_2), 30.2 (CH_2), 30.1 (CH_2), 30.1 (CH_2), 29.8 (CH_2), 29.8 (CH_2), 29.8 (CH_2), 29.5 (CH_2), 27.9 (CH_2), 26.7 (CH_2), 26.6 (CH_2), 26.3 (CH_2), 26.1 (CH_2), 22.8 (CH_2), 22.8 (CH_2), 22.7, (CH_2) 21.4 (CH_3), 14.1 (CH_3).

LC-MS: m/z $[\text{M}+\text{H}]^+$ calculated for $\text{C}_{71}\text{H}_{100}\text{NO}_7\text{S}$: 1110.72; found: 1110.59.

HR-MS: m/z $[\text{M}+\text{K}]^+$ calculated for $\text{C}_{71}\text{H}_{99}\text{KNO}_7\text{S}$: 1148.6779; found: 1148.6772.



Representative procedure was followed using **3k** (50.0 mg, 0.057 mmol), $[\text{JohnPhosAu}(\text{I})\text{ACN}]^+\text{SbF}_6^-$ (10 mol %), toluene (1.0 ml) as the solvent and stirring the reaction at 100 °C. Purification by column chromatography on silica gel (n-Hexane/EtOAc 95:5) yielded (M/P)-**4k** (36.8 mg, 74 %), as a colourless oil.

^1H NMR: (400 MHz, CDCl_3) δ = 7.62 (s, 1H), 7.48 – 7.41 (m, 1H), 7.38 (d, J = 8.3 Hz, 2H), 7.34 – 7.29 (m, 1H), 7.21 – 7.12 (m, 2H), 7.10 (dd, J = 7.4, 1.7 Hz, 1H), 7.03 (dd, J = 7.4, 1.7 Hz, 1H), 6.96 – 6.85 (m, 3H), 6.38 – 6.31 (m, 2H), 6.15 (dd, J = 5.9, 3.5 Hz, 1H), 6.08 (t, J = 7.6 Hz, 1H), 5.94 (dd, J = 7.7, 1.7 Hz, 1H), 5.69 (dd, J = 6.6, 3.7 Hz, 1H), 5.56 (dd, J = 7.7, 1.7 Hz, 1H), 5.01 (dd, J = 16.9, 6.6 Hz, 1H), 4.50 (d, J = 13.4 Hz, 1H), 4.44 (d, J = 13.3 Hz, 1H), 4.32 (d, J = 13.5 Hz, 1H), 4.13 – 3.88 (m, 5H), 3.77 – 3.68 (m, 2H), 3.64 (d, J = 14.6 Hz, 1H), 3.52 – 3.43 (m, 1H), 3.33 (d, J = 13.5 Hz, 1H), 3.20 – 3.12 (m, 2H), 3.05 (d, J = 13.6 Hz, 1H), 2.56 (d, J = 14.6 Hz, 1H), 2.20 (s, 3H), 2.01 – 1.86 (m, 6H), 1.67 – 1.53 (m, 2H), 1.14 (t, J = 7.4 Hz, 3H), 1.00 (t, J = 7.5 Hz, 3H), 0.95 – 0.82 (m, 6H).

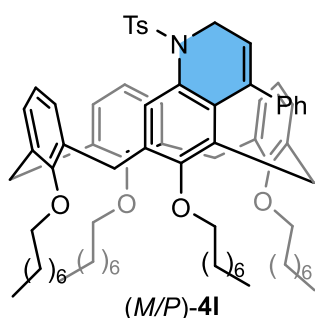
^{13}C NMR (101 MHz, CDCl_3) δ = 158.6 (C_q), 158.1 (C_q), 155.2 (C_q), 155.0 (C_q), 143.0 (C_q), 141.1 (C_q), 139.3 (C_q), 137.1 (C_q), 137.0 (C_q), 136.8 (C_q), 136.8 (C_q), 135.1 (C_q), 133.7 (C_q), 133.5 (C_q), 133.3 (C_q), 132.5 (C_q), 131.1 (C_q), 130.3 (C_q), 129.6 (CH), 129.0 (CH), 128.8 (CH), 128.7 (CH), 127.8 (CH), 127.7 (CH), 127.6 (CH), 127.2 (CH), 127.1 (CH), 126.8 (CH), 126.5 (CH), 125.7 (CH), 122.8 (CH), 122.3 (CH), 122.0 (CH), 121.7 (CH), 76.9 (CH_2), 76.5 (CH_2), 76.5

Chapter 3

(CH₂), 76.2 (CH₂), 45.7 (CH₂), 31.0 (CH₂), 30.9 (CH₂), 30.8 (CH₂), 29.4 (CH₂), 29.4 (CH₂), 23.5 (CH₂), 23.2 (CH₂), 23.0 (CH₂), 23.0 (CH₂), 21.3 (CH₃), 10.9 (CH₃), 10.8 (CH₃), 10.4 (CH₃), 9.9 (CH₃).

LC-MS: m/z [M+Na]⁺ calculated for C₅₆H₆₁NNaO₆S: 898.41; found: 898.73.

HR-MS: m/z [M+H]⁺ calculated for C₅₆H₆₁NKO₆S: 914.3857; found: 914.3863.



Representative procedure was followed using **3I** (50.0 mg, 0.043 mmol), [JohnPhosAu(I)ACN]⁺SbF₆⁻ (10 mol %), toluene (1.0 ml) as the solvent and stirring the reaction at 100 °C. Purification by column chromatography on silica gel (n-Hexane/EtOAc 95:5) yielded (*M/P*)-**4I** (41.4 mg, 83 %) as a colourless oil.

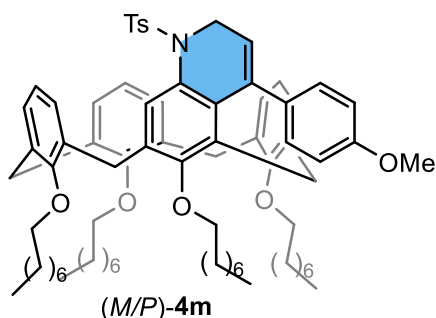
¹H NMR: (400 MHz, CDCl₃) δ = 7.62 (s, 1H), 7.38 (d, *J* = 8.2 Hz, 2H), 7.20 – 7.07 (m, 5H), 7.03 (dd, *J* = 7.5, 1.7 Hz, 1H), 6.95 – 6.86 (m, 4H), 6.37 – 6.30 (m, 2H), 6.15 (dd, *J* = 6.3, 3.1 Hz, 1H), 6.07 (t, *J* = 7.6 Hz, 1H), 5.94 (dd, *J* = 7.7, 1.7 Hz, 1H), 5.69 (dd, *J* = 6.6, 3.7 Hz, 1H), 5.56 (dd, *J* = 7.5, 1.7 Hz, 1H), 5.02 (dd, *J* = 16.9, 6.6 Hz, 1H), 4.48 (d, *J* = 13.4 Hz, 1H), 4.43 (d, *J* = 13.3 Hz, 1H), 4.31 (d, *J* = 13.5 Hz, 1H), 4.17 – 3.90 (m, 5H), 3.74 (td, *J* = 6.6, 2.9 Hz, 2H), 3.63 (d, *J* = 14.6 Hz, 1H), 3.49 (dt, *J* = 9.4, 6.3 Hz, 1H), 3.33 (d, *J* = 13.5 Hz, 1H), 3.23 – 3.13 (m, 2H), 3.05 (d, *J* = 13.6 Hz, 1H), 2.55 (d, *J* = 14.6 Hz, 1H), 2.20 (s, 3H), 1.98 – 1.82 (m, 8H), 1.67 – 1.51 (m, 4H), 1.51 – 1.17 (m, 36H), 0.97 – 0.90 (m, 12H).

¹³C NMR: (101 MHz, CDCl₃) δ = 158.3 (C_q), 158.1 (C_q), 155.3 (C_q), 155.1 (C_q), 143.0 (C_q), 141.1 (C_q), 139.2 (C_q), 137.1 (C_q), 137.1 (C_q), 137.0 (C_q), 136.8 (C_q), 135.3 (C_q), 133.7 (C_q), 133.5 (C_q), 133.3 (C_q), 132.5 (C_q), 131.1 (C_q), 130.3 (C_q), 128.9 (CH), 128.8 (CH), 128.7 (CH), 127.6 (CH), 127.6 (CH), 127.6 (CH), 127.1 (CH), 127.0 (CH), 126.9 (CH), 126.8 (CH), 125.7 (CH), 122.8 (CH), 122.3 (CH), 122.0 (CH), 121.7 (CH), 75.3 (CH₂), 75.0 (CH₂), 74.8 (CH₂), 74.5 (CH₂), 45.7 (CH₂), 32.1 (CH₂), 32.0 (CH₂), 32.0 (CH₂), 31.0 (CH₂), 30.9 (CH₂), 30.9 (CH₂), 30.6 (CH₂), 30.2 (CH₂), 30.1 (CH₂), 30.0 (CH₂), 29.9 (CH₂), 29.8 (CH₂), 29.8 (CH₂), 29.8 (CH₂), 29.6 (CH₂), 29.5 (2CH₂), 29.5 (CH₂), 26.7 (CH₂), 26.5 (CH₂), 26.3 (CH₂), 26.1 (CH₂), 22.8 (CH₂), 22.7 (CH₂), 21.3 (CH₃), 14.2 (CH₃), 14.2 (CH₃), 14.1 (CH₃), 14.1 (CH₃).

LC-MS: m/z [M+NH₄]⁺ calculated for C₇₆H₁₀₅N₂O₆S: 1173.77; found: 1173.33.

Chapter 3

HR-MS: m/z $[M+K]^+$ calculated for $C_{76}H_{101}KNO_6S$: 1194.6987; found: 1194.6994.



Representative procedure was followed using **3m** (50.0 mg, 0.042 mmol), $[JohnPhosAu(I)ACN]^+SbF_6^-$ (10 mol %), toluene (1.0 ml) as the solvent and stirring the reaction at 100 °C. Purification by column chromatography on silica gel (n-Hexane/EtOAc 95:5) yielded (M/P)-**4m** (38.2 mg, 76 %) as a yellowish oil.

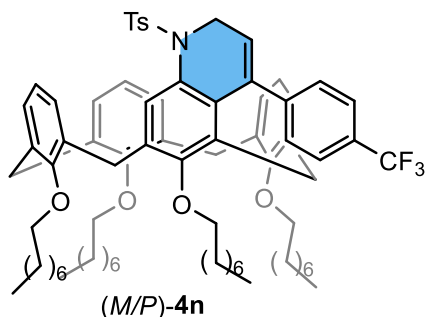
1H NMR: (400 MHz, $CDCl_3$) δ = 7.60 (s, 1H), 7.37 (d, J = 8.2 Hz, 2H), 7.09 (dd, J = 7.4, 1.7 Hz, 1H), 7.02 (dd, J = 7.5, 1.7 Hz, 1H), 6.95 – 6.86 (m, 3H), 6.72 – 6.66 (m, 3H), 6.39 – 6.29 (m, 3H), 6.16 (dd, J = 6.6, 2.7 Hz, 1H), 6.08 (t, J = 7.6 Hz, 1H), 5.95 (dd, J = 7.8, 1.7 Hz, 1H), 5.62 (dd, J = 6.6, 3.8 Hz, 1H), 5.57 (dd, J = 7.6, 1.7 Hz, 1H), 4.98 (dd, J = 16.8, 6.6 Hz, 1H), 4.48 (d, J = 13.5 Hz, 1H), 4.43 (d, J = 13.3 Hz, 1H), 4.32 (d, J = 13.5 Hz, 1H), 4.12 – 3.94 (m, 4H), 3.80 (s, 3H), 3.78 – 3.71 (m, 2H), 3.67 (d, J = 14.5 Hz, 1H), 3.51 (dt, J = 9.4, 6.3 Hz, 1H), 3.32 (d, J = 13.5 Hz, 1H), 3.24 (dt, J = 9.4, 6.6 Hz, 2H), 3.17 (d, J = 13.4 Hz, 1H), 3.05 (d, J = 13.6 Hz, 1H), 2.64 (d, J = 14.5 Hz, 1H), 2.21 (s, 3H), 1.98 – 1.84 (m, 8H), 1.67 – 1.54 (m, 4H), 1.39 – 1.21 (m, 36H), 0.97 – 0.88 (m, 12H).

^{13}C NMR: (101 MHz, $CDCl_3$) δ = 158.7 (C_q), 158.3 (C_q), 158.0 (C_q), 155.3 (C_q), 155.1 (C_q), 142.8 (C_q), 138.7 (C_q), 137.1 (C_q), 137.0 (C_q), 136.8 (C_q), 136.8 (C_q), 135.3 (C_q), 133.7 (C_q), 133.7 (C_q), 133.5 (C_q), 133.4 (C_q), 132.5 (C_q), 131.2 (C_q), 130.4 (C_q), 128.9 (CH), 128.8 (CH), 128.7 (CH), 127.9 (CH), 127.6 (CH), 127.6 (CH), 127.6 (CH), 127.2 (CH), 127.0 (CH), 125.8 (CH), 122.3 (CH), 122.0 (CH), 121.7 (CH), 121.7 (CH), 113.1 (CH), 75.3 (CH_2), 75.0 (CH_2), 74.8 (CH_2), 74.6 (CH_2), 55.2 (CH_3), 45.7 (CH_2), 32.1 (CH_2), 32.0 (CH_2), 32.0 (CH_2), 32.0 (CH_2), 31.0 (CH_2), 31.0 (CH_2), 30.8 (CH_2), 30.6 (CH_2), 30.2 (CH_2), 30.2 (CH_2), 30.1 (CH_2), 30.0 (CH_2), 30.0 (CH_2), 29.8 (CH_2), 29.8 (CH_2), 29.8 (CH_2), 29.6 (CH_2), 29.5 (CH_2), 29.5 (CH_2), 29.3 (CH_2), 26.7 (CH_2), 26.5 (CH_2), 26.4 (CH_2), 26.1 (CH_2), 22.8 (CH_2), 22.7 (CH_2), 21.3 (CH_3), 14.1 (CH_3).

LC-MS: m/z $[M+NH_4]^+$ calculated for $C_{77}H_{107}N_2O_7S$: 1203.78; found: 1204.23.

HR-MS: m/z $[M+K]^+$ calculated for $C_{77}H_{103}KNO_7S$: 1224.7092; found: 1224.7088.

Chapter 3



Representative procedure was followed using **3n** (50.0 mg, 0.041 mmol), [JohnPhosAu(I)ACN]⁺SbF₆⁻ (10 mol %), toluene (1.0 ml) as the solvent and stirring the reaction at 100 °C. Purification by column chromatography on silica gel (n-Hexane/EtOAc 95:5) yielded (*M/P*)-**3n** (39.2 mg, 78 %) as a white solid. **M.p.** = 152 – 153 °C.

¹H NMR: (400 MHz, CDCl₃) δ = 7.62 (s, 1H), 7.43 (d, *J* = 8.1 Hz, 2H), 7.38 (d, *J* = 8.1 Hz, 2H), 7.09 (dd, *J* = 7.5, 1.7 Hz, 1H), 7.01 (dd, *J* = 7.5, 1.7 Hz, 1H), 6.95 – 6.86 (m, 4H), 6.40 – 6.32 (m, 3H), 6.19 (dd, *J* = 5.6, 3.8 Hz, 1H), 6.09 (t, *J* = 7.6 Hz, 1H), 5.98 (dd, *J* = 7.7, 1.7 Hz, 1H), 5.76 (dd, *J* = 6.6, 3.8 Hz, 1H), 5.55 (dd, *J* = 7.6, 1.7 Hz, 1H), 5.04 (dd, *J* = 17.0, 6.6 Hz, 1H), 4.50 (d, *J* = 13.4 Hz, 1H), 4.44 (d, *J* = 13.3 Hz, 1H), 4.32 (d, *J* = 13.5 Hz, 1H), 4.16 – 3.90 (m, 5H), 3.82 – 3.72 (m, 2H), 3.69 (d, *J* = 14.4 Hz, 1H), 3.52 (dt, *J* = 9.5, 6.4 Hz, 1H), 3.34 (d, *J* = 13.5 Hz, 1H), 3.24 – 3.14 (m, 2H), 3.06 (d, *J* = 13.6 Hz, 1H), 2.44 (d, *J* = 14.5 Hz, 1H), 2.18 (s, 3H), 1.97 – 1.83 (m, 8H), 1.66 – 1.52 (m, 4H), 1.52 – 1.20 (m, 36H), 1.03 – 0.88 (m, 12H).

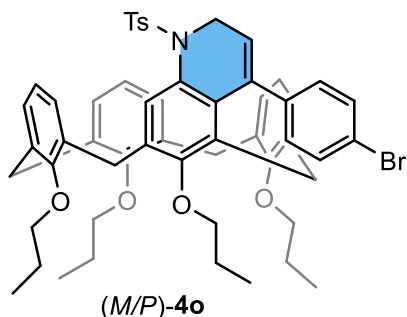
¹³C NMR: (101 MHz, CDCl₃) δ = 158.4 (C_q), 158.0 (C_q), 155.3 (C_q), 155.1 (C_q), 144.6 (d, *J*_{C-F} = 1.4 Hz, C_q), 143.1 (C_q), 138.0 (C_q), 137.5 (C_q), 137.0 (C_q), 136.9 (C_q), 136.9 (C_q), 134.8 (C_q), 133.6 (C_q), 133.6 (C_q), 133.2 (C_q), 132.4 (C_q), 131.2 (C_q), 129.5 (C_q), 129.2 (C_q), 129.0 (CH), 128.8 (CH), 128.6 (CH), 127.8 (CH), 127.8 (CH), 127.6 (CH), 127.3 (CH), 127.2 (CH), 126.9 (CH), 125.6 (CH), 124.7 (2CH), 124.1 (q, *J*_{C-F} = 271 Hz, C_q), 122.3 (CH), 122.0 (CH), 121.8 (CH), 75.3 (CH₂), 75.1 (CH₂), 74.9 (CH₂), 74.7 (CH₂), 45.6 (CH₂), 32.1 (CH₂), 32.0 (CH₂), 32.0 (CH₂), 31.9 (CH₂), 31.0 (CH₂), 31.0 (2CH₂), 30.6 (CH₂), 30.2 (CH₂), 30.2 (CH₂), 30.2 (CH₂), 30.0 (CH₂), 30.0 (CH₂), 29.9 (CH₂), 29.8 (CH₂), 29.8 (CH₂), 29.7 (CH₂), 29.6 (CH₂), 29.5 (CH₂), 29.4 (CH₂), 26.7 (CH₂), 26.5 (CH₂), 26.4 (CH₂), 26.1 (CH₂), 22.8 (CH₂), 22.7 (CH₂), 22.7 (2CH₂), 21.2 (CH₃), 14.1 (2CH₃), 14.1 (CH₃), 14.1 (CH₃).

¹⁹F NMR: (565 MHz, CDCl₃) δ = -62.5.

LC-MS: *m/z* [M+Na]⁺ calculated for C₇₇H₁₀₀F₃NNaO₆S: 1246.71; found: 1246.31.

HR-MS: *m/z* [M+K]⁺ calculated for C₇₇H₁₀₀F₃KNO₆S: 1262.6861; found: 1262.6866.

Chapter 3



Representative procedure was followed using **3o** (50.0 mg, 0.040 mmol), [JohnPhosAu(I)ACN]⁺SbF₆⁻ (10 mol %), toluene (1.0 ml) as the solvent and stirring the reaction at 100 °C. Purification by column chromatography on silica gel (n-Hexane/EtOAc 95:5) yielded (M/P)-**4o** (35.0 mg, 70 %) as an orange solid. **M.p.** = 127 – 128 °C.

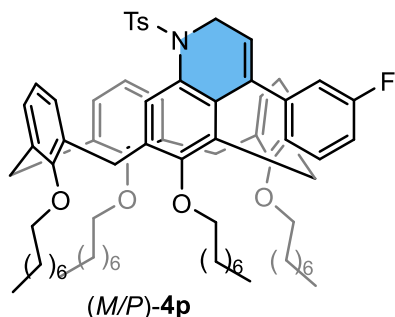
¹H NMR: (400 MHz, CDCl₃) δ = 7.59 (s, 1H), 7.36 (d, *J* = 8.4 Hz, 2H), 7.30 (d, *J* = 8.8 Hz, 2H), 7.08 (dd, *J* = 7.4, 1.7 Hz, 1H), 7.01 (dd, *J* = 7.4, 1.8 Hz, 1H), 6.93 (d, *J* = 8.1 Hz, 2H), 6.89 (t, *J* = 7.4 Hz, 1H), 6.39 – 6.31 (m, 4H), 6.18 (t, *J* = 4.7 Hz, 1H), 6.08 (t, *J* = 7.6 Hz, 1H), 5.97 (dd, *J* = 7.7, 1.7 Hz, 1H), 5.68 (dd, *J* = 6.6, 3.8 Hz, 1H), 5.58 – 5.50 (m, 1H), 5.00 (dd, *J* = 16.9, 6.7 Hz, 1H), 4.50 (d, *J* = 13.5 Hz, 1H), 4.44 (d, *J* = 13.3 Hz, 1H), 4.33 (d, *J* = 13.5 Hz, 1H), 4.11 – 4.01 (m, 1H), 4.01 – 3.89 (m, 4H), 3.78 – 3.66 (m, 3H), 3.54 (dt, *J* = 9.5, 6.5 Hz, 1H), 3.33 (d, *J* = 13.5 Hz, 1H), 3.23 (dt, *J* = 9.6, 6.8 Hz, 1H), 3.18 (d, *J* = 13.5 Hz, 1H), 3.07 (d, *J* = 13.6 Hz, 1H), 2.53 (d, *J* = 14.5 Hz, 1H), 2.23 (s, 3H), 2.02 – 1.82 (m, 8H), 1.72 – 1.54 (m, 4H), 1.13 (t, *J* = 7.4 Hz, 3H), 1.01 (t, *J* = 7.5 Hz, 3H), 0.94 (t, *J* = 7.4 Hz, 3H), 0.90 (t, *J* = 7.5 Hz, 3H).

¹³C NMR: (101 MHz, CDCl₃) δ = 158.6 (C_q), 158.0 (C_q), 155.2 (C_q), 155.1 (C_q), 143.1 (C_q), 140.0 (C_q), 138.1 (C_q), 137.1 (C_q), 137.0 (C_q), 136.9 (C_q), 136.8 (C_q), 134.8 (C_q), 133.6 (C_q), 133.5 (C_q), 133.4 (C_q), 132.4 (C_q), 131.2 (C_q), 130.9 (CH), 129.8 (C_q), 129.0 (CH), 128.8 (CH), 128.7 (CH), 128.3 (CH), 127.7 (CH), 127.6 (CH), 127.3 (CH), 127.2 (CH), 125.7 (CH), 123.5 (CH), 122.3 (CH), 122.0 (CH), 121.7 (CH), 120.7 (C_q), 76.9 (CH₂), 76.6 (CH₂), 76.5 (CH₂), 76.3 (CH₂), 45.6 (CH₂), 31.0 (CH₂), 31.0 (CH₂), 30.8 (CH₂), 29.7 (CH₂), 29.6 (CH₂), 23.5 (CH₂), 23.3 (CH₂), 23.2 (CH₂), 23.1 (CH₂), 23.0 (CH₂), 21.3 (CH₃), 10.8 (CH₃), 10.7 (CH₃), 10.4 (CH₃), 9.9 (CH₃).

LC-MS: *m/z* [M+Na]⁺ calculated for C₅₆H₆₀BrNNaO₆S: 976.32; found: 976.67.

HR-MS: *m/z* [M+K]⁺ calculated for C₅₆H₆₀BrKNO₆S: 992.2962; found: 992.2968.

Chapter 3



Representative procedure was followed using **3p** (50.0 mg, 0.043 mmol), [JohnPhosAu(I)ACN]⁺SbF₆⁻ (10 mol %), toluene (1.0 ml) as the solvent and stirring the reaction at 100 °C. Purification by column chromatography on silica gel (n-Hexane/EtOAc 95:5) yielded (M/P)-**4p** (38.1 mg, 76 %) as a colourless oil.

¹H NMR: (400 MHz, CDCl₃) δ = 7.64 (s, 1H), 7.36 (d, *J* = 8.3 Hz, 2H), 7.17 – 7.06 (m, 3H), 7.03 (dd, *J* = 7.5, 1.7 Hz, 1H), 6.97 – 6.85 (m, 5H), 6.36 – 6.30 (m, 2H), 6.15 (dd, *J* = 5.6, 3.8 Hz, 1H), 6.07 (t, *J* = 7.6 Hz, 1H), 5.95 (dd, *J* = 7.8, 1.7 Hz, 1H), 5.73 (dd, *J* = 6.6, 3.8 Hz, 1H), 5.54 (dd, *J* = 7.7, 1.7 Hz, 1H), 5.04 (dd, *J* = 16.9, 6.6 Hz, 1H), 4.49 (d, *J* = 13.4 Hz, 1H), 4.43 (d, *J* = 13.3 Hz, 1H), 4.32 (d, *J* = 13.5 Hz, 1H), 4.16 – 3.91 (m, 4H), 3.78 – 3.66 (m, 4H), 3.52 (dt, *J* = 9.4, 6.3 Hz, 1H), 3.33 (d, *J* = 13.5 Hz, 1H), 3.25 – 3.20 (m, 1H), 3.17 (d, *J* = 13.6 Hz, 1H), 3.05 (d, *J* = 13.5 Hz, 1H), 2.52 (d, *J* = 14.5 Hz, 1H), 2.22 (s, 3H), 1.98 – 1.84 (m, 8H), 1.68 – 1.54 (m, 4H), 1.39 – 1.20 (m, 36H), 0.97 – 0.87 (m, 12H).

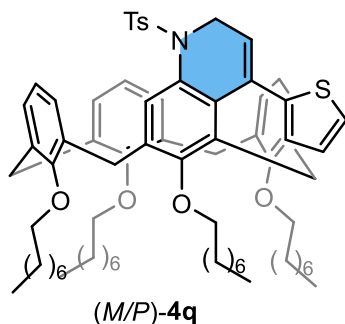
¹³C NMR: (101 MHz, CDCl₃) δ = 161.2 (d, *J*_{C-F} = 249 Hz, C_q), 158.4 (C_q), 158.1 (C_q), 155.3 (C_q), 155.1 (C_q), 143.4 (d, *J*_{C-F} = 8 Hz, C_q), 143.3 (C_q), 138.2 (d, *J*_{C-F} = 3 Hz, C_q), 137.4 (C_q), 137.1 (C_q), 137.0 (C_q), 136.7 (C_q), 135.1 (C_q), 133.5 (C_q), 133.4 (C_q), 133.4 (C_q), 132.4 (C_q), 131.0 (C_q), 129.8 (C_q), 129.4 (CH), 128.9 (CH), 128.8 (CH), 128.7 (CH), 127.7 (d, *J*_{C-F} = 2 Hz, CH), 127.7 (CH), 127.6 (CH), 127.2 (CH), 127.1 (d, *J*_{C-F} = 4 Hz, CH), 125.6 (CH), 123.6 (CH), 122.3 (CH), 122.2 (d, *J*_{C-F} = 24 Hz, CH), 121.7 (CH), 113.6 (d, *J*_{C-F} = 21 Hz, CH), 75.3 (CH₂), 75.1 (CH₂), 74.8 (CH₂), 74.6 (CH₂), 45.7 (CH₂), 32.1 (CH₂), 32.0 (CH₂), 32.0 (CH₂), 32.0 (CH₂), 31.0 (CH₂), 30.9 (CH₂), 30.9 (CH₂), 30.6 (CH₂), 30.2 (CH₂), 30.1 (CH₂), 30.1 (CH₂), 30.0 (CH₂), 29.9 (CH₂), 29.8 (CH₂), 29.8 (2CH₂), 29.7 (CH₂), 29.6 (CH₂), 29.5 (CH₂), 29.4 (CH₂), 26.7 (CH₂), 26.5 (CH₂), 26.3 (CH₂), 26.1 (CH₂), 22.8 (CH₂), 22.7 (2CH₂), 22.7 (CH₂), 21.1 (CH₃), 14.2 (CH₃), 14.1 (CH₃), 14.1 (CH₃).

¹⁹F NMR: (565 MHz, CDCl₃) δ = -113.7.

LC-MS: *m/z* [M+H]⁺ calculated for C₇₆H₁₀₁FNO₆S: 1174.73; found: 1175.12.

HR-MS: *m/z* [M+K]⁺ calculated for C₇₆H₁₀₀FKNO₆S: 1212.6892; found: 1212.6896.

Chapter 3



Representative procedure was followed using **3q** (50.0 mg, 0.043 mmol), [JohnPhosAu(I)ACN]⁺SbF₆⁻ (10 mol %), toluene (1.0 ml) as the solvent and stirring the reaction at 100 °C. Purification by column chromatography on silica gel (n-Hexane/EtOAc 95:5) yielded (M/P)-**4q** (28.8 mg, 58 %) as a yellowish oil.

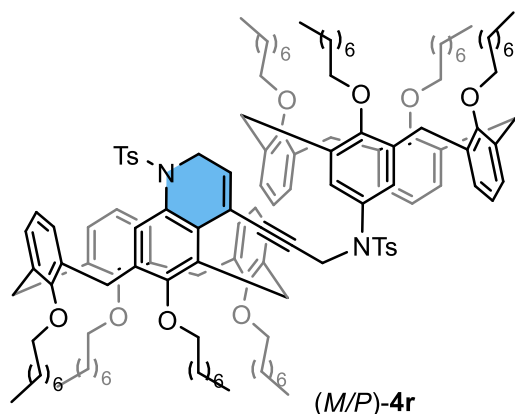
¹H NMR: (400 MHz, CDCl₃) δ = 7.57 (s, 1H), 7.37 (d, *J* = 8.3 Hz, 2H), 7.13 – 7.06 (m, 2H), 7.02 (dd, *J* = 7.5, 1.7 Hz, 1H), 6.94 (d, *J* = 8.1 Hz, 2H), 6.89 (t, *J* = 7.4 Hz, 1H), 6.83 (dd, *J* = 5.1, 3.5 Hz, 1H), 6.45 (dd, *J* = 3.6, 1.2 Hz, 1H), 6.39 – 6.31 (m, 2H), 6.18 (dd, *J* = 6.5, 3.0 Hz, 1H), 6.08 (t, *J* = 7.6 Hz, 1H), 5.96 (dd, *J* = 7.8, 1.7 Hz, 1H), 5.72 (dd, *J* = 6.6, 4.0 Hz, 1H), 5.57 (dd, *J* = 7.6, 1.7 Hz, 1H), 4.93 (dd, *J* = 16.9, 6.7 Hz, 1H), 4.49 (d, *J* = 13.3 Hz, 1H), 4.44 (d, *J* = 13.3 Hz, 1H), 4.34 (d, *J* = 13.4 Hz, 1H), 4.17 (td, *J* = 10.4, 6.2 Hz, 1H), 4.09 – 3.91 (m, 4H), 3.89 (d, *J* = 14.4 Hz, 1H), 3.74 (td, *J* = 6.7, 3.8 Hz, 2H), 3.56 (dt, *J* = 9.4, 6.3 Hz, 1H), 3.38 – 3.27 (m, 2H), 3.17 (d, *J* = 13.4 Hz, 1H), 3.07 (d, *J* = 13.6 Hz, 1H), 2.84 (d, *J* = 14.5 Hz, 1H), 2.21 (s, 3H), 2.01 – 1.83 (m, 8H), 1.73 – 1.52 (m, 4H), 1.47 – 1.27 (m, 36H), 1.02 – 0.89 (m, 12H).

¹³C NMR: (101 MHz, CDCl₃) δ = 158.5 (C_q), 158.0 (C_q), 155.3 (C_q), 155.2 (C_q), 143.5 (C_q), 143.1 (C_q), 137.2 (C_q), 137.1 (C_q), 137.0 (C_q), 136.8 (C_q), 135.2 (C_q), 133.6 (C_q), 133.6 (C_q), 133.4 (C_q), 132.5 (C_q), 132.4 (C_q), 131.1 (C_q), 130.2 (C_q), 129.0 (CH), 128.8 (CH), 128.7 (CH), 127.7 (CH), 127.5 (CH), 127.3 (CH), 127.2 (CH), 127.1 (CH), 126.3 (CH), 125.8 (CH), 124.6 (CH), 124.1 (CH), 122.7 (CH), 122.3 (CH), 122.0 (CH), 121.7 (CH), 75.3 (CH₂), 75.0 (2CH₂), 74.6 (CH₂), 45.5 (CH₂), 32.1 (CH₂), 32.0 (CH₂), 31.1 (CH₂), 31.0 (CH₂), 30.8 (CH₂), 30.6 (CH₂), 30.3 (CH₂), 30.1 (CH₂), 30.0 (CH₂), 29.8 (CH₂), 29.7 (CH₂), 29.7 (CH₂), 29.7 (CH₂), 29.5 (CH₂), 29.5 (CH₂), 26.7 (CH₂), 26.5 (CH₂), 26.3 (CH₂), 26.1 (CH₂), 22.8 (CH₂), 22.8 (CH₂), 22.7 (CH₂), 21.4 (CH₃), 14.2 (CH₃), 14.2 (CH₃), 14.1 (CH₃).

LC-MS: *m/z* [M+NH₄]⁺ calculated for C₇₄H₁₀₃N₂O₆S₂: 1179.73; found: 1179.64.

HR-MS: *m/z* [M+K]⁺ calculated for C₇₄H₉₉KNO₆S₂: 1200.6551; found: 1200.6557.

Chapter 3



Representative procedure was followed using **3r** (50.0 mg, 0.023 mmol), [JohnPhosAu(I)ACN]⁺SbF₆⁻ (10 mol %), toluene (1.0 ml) as the solvent and stirring the reaction at 100 °C. Purification by column chromatography on silica gel (n-Hexane/EtOAc 95:5) yielded (M/P)-**4r** (35.5mg, 71 %) as a colourless oil.

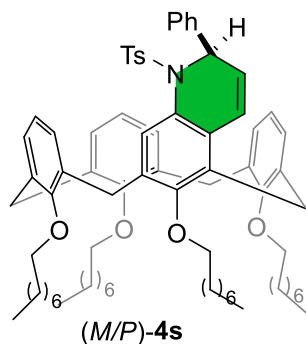
¹H NMR: (400 MHz, CDCl₃) δ = 7.47 (d, *J* = 8.1 Hz, 2H), 7.42 (d, *J* = 5.9 Hz, 2H), 7.39 (s, 1H), 7.18 (d, *J* = 8.0 Hz, 2H), 7.13 (d, *J* = 8.0 Hz, 2H), 7.04 (d, *J* = 7.2 Hz, 1H), 7.02 – 6.92 (m, 3H), 6.87 (d, *J* = 7.4 Hz, 1H), 6.85 – 6.77 (m, 2H), 6.74 (d, *J* = 2.7 Hz, 1H), 6.41 – 6.36 (m, 1H), 6.36 – 6.26 (m, 6H), 6.24 – 6.15 (m, 2H), 6.10 – 6.04 (m, 2H), 5.83 (d, *J* = 7.2 Hz, 1H), 5.75 (t, *J* = 5.1 Hz, 1H), 4.52 – 4.42 (m, 6H), 4.38 (dd, *J* = 13.3, 3.4 Hz, 2H), 4.33 – 4.18 (m, 6H), 4.10 – 3.94 (m, 8H), 3.82 – 3.59 (m, 8H), 3.26 (d, *J* = 13.6 Hz, 1H), 3.22 – 3.11 (m, 5H), 2.99 (d, *J* = 10.3 Hz, 1H), 2.96 (d, *J* = 10.3 Hz, 1H), 2.41 (s, 3H), 2.38 (s, 3H), 2.05 – 1.77 (m, 16H), 1.61 – 1.45 (m, 8H), 1.41 – 1.26 (m, 72H), 0.97 – 0.88 (m, 24H).

¹³C NMR: (101 MHz, CDCl₃) δ = 157.8 (C_q), 157.5 (C_q), 157.5 (C_q), 157.2 (C_q), 155.7 (C_q), 155.6 (C_q), 155.6 (C_q), 155.5 (C_q), 143.5 (C_q), 143.3 (C_q), 137.2 (C_q), 136.9 (C_q), 136.8 (2C_q), 136.4 (C_q), 136.0 (C_q), 135.7 (C_q), 134.7 (C_q), 134.0 (C_q), 133.9 (C_q), 133.5 (C_q), 133.3 (C_q), 133.1 (C_q), 133.1 (C_q), 132.9 (C_q), 132.7 (C_q), 132.0 (CH), 130.0 (C_q), 129.2 (CH), 128.7 (CH), 128.6 (CH), 128.2 (CH), 128.1 (CH), 127.8 (CH), 127.8 (CH), 127.7 (CH), 127.6 (CH), 127.4 (CH), 127.3 (CH), 127.0 (CH), 126.6 (C_q), 122.1 (CH), 122.0 (CH), 121.9 (CH), 121.9 (CH), 121.8 (CH), 121.6 (CH), 120.2 (C_q), 86.1 (C_q), 83.7 (C_q), 75.4 (CH₂), 75.3 (CH₂), 75.3 (CH₂), 75.3 (CH₂), 75.1 (CH₂), 75.0 (CH₂), 45.1 (CH₂), 41.9 (CH₂), 32.0 (CH₂), 32.0 (CH₂), 31.1 (CH₂), 31.0 (CH₂), 30.9 (CH₂), 30.6 (CH₂), 30.5 (CH₂), 30.3 (CH₂), 30.2 (CH₂), 30.2 (CH₂), 30.1 (CH₂), 30.1 (3CH₂), 29.9 (CH₂), 29.9 (CH₂), 29.8 (CH₂), 29.8 (CH₂), 29.8 (CH₂), 29.6 (CH₂), 29.6 (CH₂), 29.5 (CH₂), 26.7 (CH₂), 26.6 (CH₂), 26.6 (CH₂), 26.3 (CH₂), 26.2 (CH₂), 26.2 (CH₂), 26.1 (CH₂), 22.8 (CH₂), 22.7 (CH₂), 22.7 (CH₂), 21.6 (CH₃), 14.1 (CH₃), 14.1 (CH₃).

LC-MS: *m/z* [M+2K]²⁺ calculated for C₁₄₀H₁₉₂K₂N₂O₁₂S₂: 1117.65; found: 1117.82.

HR-MS (ESI) *m/z*: [M+2K]⁺ calcd. for C₁₄₀H₁₉₂K₂N₂O₁₂S₂: 1117.6595; found: 1117.6588.

Chapter 3



Representative procedure was followed using **3s** (50.0 mg, 0.043 mmol), [JohnPhosAu(I)ACN]⁺SbF₆⁻ (10 mol %), toluene (1.0 ml) as the solvent and stirring the reaction at 100 °C. Purification by column chromatography on silica gel (n-Hexane/EtOAc 95:5) yielded (*M/P*)-**4s** (27.9 mg, 56 %) as a waxy oil.

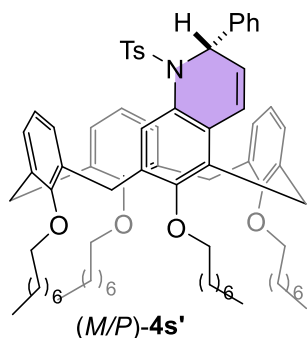
¹H NMR: (400 MHz, CDCl₃) δ = 7.48 – 7.42 (m, 4H), 7.40 (s, 1H), 7.28 – 7.23 (m, 3H), 7.17 (d, *J* = 8.1 Hz, 2H), 7.11 (dd, *J* = 7.4, 2.2 Hz, 2H), 6.91 (t, *J* = 7.4 Hz, 1H), 6.61 (d, *J* = 9.5 Hz, 1H), 6.05 – 5.93 (m, 6H), 5.71 (dd, *J* = 6.0, 3.4 Hz, 1H), 5.55 (dd, *J* = 7.6, 1.9 Hz, 1H), 4.45 – 4.35 (m, 3H), 4.25 (d, *J* = 13.7 Hz, 1H), 4.16 (td, *J* = 10.8, 5.4 Hz, 1H), 4.07 – 3.94 (m, 3H), 3.72 – 3.61 (m, 4H), 3.32 (d, *J* = 13.6 Hz, 1H), 3.17 (d, *J* = 13.5 Hz, 1H), 3.12 (d, *J* = 13.3 Hz, 2H), 2.43 (s, 3H), 2.05 – 1.90 (m, 4H), 1.90 – 1.79 (m, 4H), 1.64 – 1.52 (m, 4H), 1.47 – 1.17 (m, 36H), 0.99 – 0.87 (m, 12H).

¹³C NMR: (101 MHz, CDCl₃) δ = 157.9 (C_q), 157.2 (C_q), 155.1 (C_q), 154.9 (C_q), 143.1 (C_q), 138.8 (C_q), 137.3 (C_q), 137.2 (C_q), 136.8 (C_q), 136.7 (C_q), 133.2 (2C_q), 132.4 (C_q), 132.2 (C_q), 129.9 (CH), 129.0 (CH), 128.9 (CH), 128.8 (CH), 128.1 (CH), 127.6 (CH), 127.5 (CH), 127.4 (CH), 127.3 (CH), 127.3 (CH), 127.2 (C_q), 127.1 (C_q), 127.0 (CH), 126.8 (CH), 126.5 (CH), 123.6 (CH), 122.1 (CH), 121.9 (CH), 121.7 (CH), 75.2 (CH₂), 75.2 (CH₂), 75.1 (CH₂), 74.8 (CH₂), 56.3 (CH), 32.1 (CH₂), 32.0 (2CH₂), 31.0 (CH₂), 31.0 (CH₂), 30.8 (CH₂), 30.6 (CH₂), 30.2 (CH₂), 30.1 (CH₂), 30.0 (CH₂), 29.8 (CH₂), 29.8 (CH₂), 29.5 (2CH₂), 26.7 (CH₂), 26.6 (CH₂), 26.2 (CH₂), 26.1 (CH₂), 24.6 (CH₂), 22.8 (CH₂), 22.8 (CH₂), 22.7 (CH₂), 22.7 (CH₂), 21.6 (CH₃), 14.1 (CH₃), 14.1 (2CH₃).

LC-MS: *m/z* [M+NH₄]⁺ calculated for C₇₆H₁₀₅N₂O₆S: 1173.77; found: 1174.22.

HR-MS: *m/z* [M+K]⁺ calculated for C₇₆H₁₀₁KNO₆S: 1194.6987; found: 1194.6883.

Chapter 3



Representative procedure was followed using *rac*-**3s** (50.0 mg, 0.043 mmol), [JohnPhosAu(I)ACN]⁺SbF₆⁻ (10 mol %), toluene (1.0 ml) as the solvent and stirring the reaction at 100 °C. Purification by column chromatography on silica gel (n-Hexane/EtOAc 95:5) yielded (*M/P*)-**4s'** (18.1 mg, 36 %) as a white solid. **M.p.** = 160 – 161 °C.

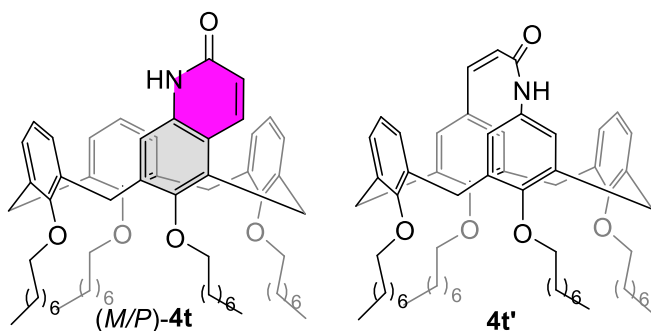
¹H NMR: (400 MHz, CDCl₃) δ = 7.64 (s, 1H), 7.55 (d, *J* = 8.3 Hz, 2H), 7.49 – 7.42 (m, 2H), 7.34 – 7.29 (m, 2H), 7.28 – 7.24 (m, 1H), 7.18 (dd, *J* = 7.8, 3.5 Hz, 4H), 6.98 (t, *J* = 7.4 Hz, 1H), 6.72 (d, *J* = 9.8 Hz, 1H), 6.38 (dd, *J* = 7.7, 1.8 Hz, 1H), 6.31 (t, *J* = 7.5 Hz, 1H), 6.22 – 6.14 (m, 4H), 6.07 (dd, *J* = 9.8, 6.2 Hz, 1H), 5.41 (dd, *J* = 5.5, 3.8 Hz, 1H), 4.50 – 4.42 (m, 2H), 4.37 (d, *J* = 13.2 Hz, 1H), 4.22 (d, *J* = 14.0 Hz, 1H), 4.14 – 4.03 (m, 3H), 3.88 (td, *J* = 11.1, 5.3 Hz, 1H), 3.74 – 3.61 (m, 4H), 3.37 (d, *J* = 14.0 Hz, 1H), 3.24 – 3.14 (m, 3H), 2.39 (s, 3H), 2.08 – 1.91 (m, 4H), 1.91 – 1.78 (m, 4H), 1.66 – 1.50 (m, 4H), 1.45 – 1.16 (m, 36H), 0.99 – 0.85 (m, 12H).

¹³C NMR: (101 MHz, CDCl₃) δ = 158.0 (C_q), 156.2 (C_q), 155.3 (C_q), 155.2 (C_q), 143.1 (C_q), 138.8 (C_q), 137.2 (C_q), 137.2 (C_q), 137.0 (C_q), 136.3 (C_q), 133.3 (C_q), 133.1 (C_q), 133.1 (C_q), 132.9 (C_q), 132.7 (C_q), 129.1 (CH), 129.0 (CH), 128.8 (CH), 128.3 (2CH), 127.8 (CH), 127.7 (CH), 127.6 (CH), 127.5 (CH), 127.5 (CH), 127.4 (CH), 127.0 (C_q), 126.6 (CH), 126.0 (C_q), 125.8 (CH), 123.5 (CH), 121.9 (CH), 121.8 (CH), 121.7 (CH), 75.4 (CH₂), 75.3 (CH₂), 75.1 (CH₂), 75.0 (CH₂), 56.3 (CH), 32.0 (CH₂), 31.2 (CH₂), 31.1 (CH₂), 30.9 (CH₂), 30.6 (CH₂), 30.6 (CH₂), 30.2 (CH₂), 30.1 (CH₂), 30.1 (CH₂), 29.8 (CH₂), 29.8 (2CH₂), 29.7 (CH₂), 29.5 (CH₂), 29.4 (CH₂), 26.7 (CH₂), 26.6 (CH₂), 26.1 (CH₂), 26.0 (CH₂), 24.0 (CH₂), 22.7 (CH₂), 22.7 (CH₂), 21.6 (CH₃), 14.1 (CH₃).

LC-MS: *m/z* [M+H]⁺ calculated for C₇₆H₁₀₂NO₆S: 1156.74; found: 1156.32.

HR-MS: *m/z* [M+K]⁺ calculated for C₇₆H₁₀₁KNO₆S: 1194.6987; found: 1194.6892.

Chapter 3



Representative procedure was followed using **3t** (50.0 mg, 0.053 mmol), [JohnPhosAu(I)ACN]⁺SbF₆⁻ (10 mol %), toluene (1.0 ml) as the solvent and stirring the reaction at 100 °C. Purification by column chromatography on silica gel (n-

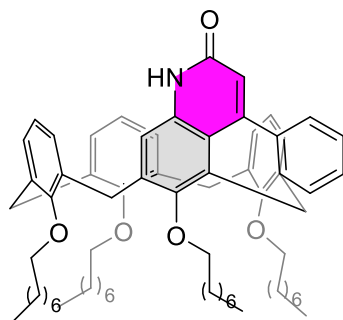
Hexane/EtOAc 95:5) yielded (M/P)-**4t** + **4t'** (47.8 mg, 96%, (M/P)-**4t**/**4t'** 1:1.2) as a colourless oil.

(M/P)-**4t**: ¹H NMR (400 MHz, CDCl₃) δ = 8.52 (d, *J* = 9.1 Hz, 1H), 8.43 (s, 1H), 7.58 (s, 1H), 6.92 (d, *J* = 9.0 Hz, 1H), 6.88 – 6.85 (m, 2H), 6.83 – 6.78 (m, 1H), 6.67 (t, *J* = 7.4 Hz, 1H), 6.43 (s, 2H), 6.34 – 6.27 (m, 2H), 6.13 (d, *J* = 6.7 Hz, 1H), 4.79 – 4.61 (m, 2H), 4.51 – 4.41 (m, 2H), 4.18 (td, *J* = 10.5, 5.7 Hz, 1H), 4.10 – 3.99 (m, 3H), 3.99 – 3.88 (m, 1H), 3.88 – 3.76 (m, 3H), 3.42 (d, *J* = 13.3 Hz, 1H), 3.24 – 3.12 (m, 3H), 2.10 – 1.84 (m, 8H), 1.65 – 1.25 (m, 40H), 0.97 – 0.84 (m, 12H). ¹³C NMR (101 MHz, CDCl₃) δ = 157.5 (C_q), 157.2 (C_q), 156.0 (C_q), 155.7 (C_q), 153.1 (C_q), 142.5 (C_q), 142.1 (C_q), 136.9 (CH), 136.5 (C_q), 136.4 (C_q), 135.7 (C_q), 134.3 (C_q), 134.2 (C_q), 133.2 (C_q), 131.9 (C_q), 128.6 (CH), 128.4 (CH), 127.8 (CH), 127.6 (CH), 127.2 (CH), 127.0 (CH), 122.2 (CH), 122.2 (CH), 121.8 (CH), 121.8 (CH), 110.0 (CH), 75.6 (CH₂), 75.4 (CH₂), 75.3 (CH₂), 75.0 (CH₂), 32.0 (CH₂), 32.0 (CH₂), 31.6 (CH₂), 31.1 (CH₂), 30.6 (CH₂), 30.5 (CH₂), 30.4 (CH₂), 30.4 (CH₂), 30.1 (CH₂), 30.0 (CH₂), 30.0 (CH₂), 29.6 (CH₂), 29.6 (CH₂), 29.6 (CH₂), 29.5 (CH₂), 26.6 (CH₂), 26.6 (CH₂), 26.5 (CH₂), 26.5 (CH₂), 25.2 (CH₂), 22.7 (CH₂), 14.1 (CH₃).

4t': ¹H NMR (400 MHz, CDCl₃) δ = 8.26 (d, *J* = 7.4 Hz, 1H), 6.92 (s, 1H), 6.83 – 6.78 (m, 2H), 6.76 (t, *J* = 7.3 Hz, 2H), 6.64 – 6.61 (m, 2H), 6.43 (s, 1H), 6.34 – 6.27 (m, 3H), 5.37 (d, *J* = 7.4 Hz, 1H), 4.51 – 4.41 (m, 4H), 3.99 – 3.88 (m, 4H), 3.88 – 3.76 (m, 4H), 3.24 – 3.12 (m, 4H), 2.10 – 1.84 (m, 8H), 1.65 – 1.25 (m, 40H), 0.97 – 0.84 (m, 12H). ¹³C NMR (101 MHz, CDCl₃) δ = 162.3 (C_q), 156.3 (C_q), 155.9 (C_q), 155.4 (C_q), 142.9 (CH), 142.5 (C_q), 136.4 (C_q), 135.9 (C_q), 135.3 (C_q), 134.7 (C_q), 128.7 (CH), 128.4 (CH), 128.0 (CH), 128.0 (CH), 127.8 (CH), 127.6 (CH), 125.6 (C_q), 121.9 (CH), 121.6 (CH), 120.0 (CH), 113.7 (C_q), 106.7 (CH), 75.2 (CH₂), 75.1 (CH₂), 75.1 (CH₂), 65.9 (C_q), 64.9 (C_q), 32.0 (CH₂), 31.0 (CH₂), 30.3 (CH₂), 30.3 (2CH₂), 30.2 (CH₂), 29.9 (CH₂), 29.9 (CH₂), 29.8 (CH₂), 29.8 (CH₂), 29.7 (CH₂), 29.7 (CH₂), 26.3 (CH₂), 26.2 (CH₂), 26.2 (CH₂), 22.7 (CH₂), 14.1 (CH₃).

LC-MS of the mixture: *m/z* [M+K]⁺ calculated for C₆₃H₈₉KNO₅: 978.64; found: 978.75.

Chapter 3



(*M/P*)-**4u**

Representative procedure was followed using **3u** (50.0 mg, 0.049 mmol), [JohnPhosAu(I)ACN]⁺SbF₆⁻ (10 mol %), toluene (1.0 ml) as the solvent and stirring the reaction at 100 °C. Purification by column chromatography on silica gel (n-Hexane/EtOAc 95:5) yielded (*M/P*)-**4u** (48.6 mg, 97 %), isolated as a colourless oil.

¹H NMR: (400 MHz, CDCl₃) δ = 7.56–7.51 (m, 1H), 7.46–7.37 (m, 4H), 7.33 (d, *J* = 7.4 Hz, 1H), 7.14 (dd, *J* = 7.5, 1.7 Hz, 1H), 7.10 (dd, *J* = 7.5, 1.7 Hz, 1H), 6.93 (t, *J* = 7.4 Hz, 1H), 6.67 (s, 1H), 6.29–6.22 (m, 2H), 6.08 (dd, *J* = 6.3, 3.0 Hz, 1H), 6.03 (t, *J* = 7.6 Hz, 1H), 5.87 (dd, *J* = 7.8, 1.6 Hz, 1H), 5.49 (dd, *J* = 7.6, 1.6 Hz, 1H), 4.52 (d, *J* = 13.1 Hz, 1H), 4.42 (d, *J* = 13.3 Hz, 1H), 4.34 (d, *J* = 13.4 Hz, 1H), 4.11 (td, *J* = 10.9, 5.4 Hz, 1H), 4.07–3.95 (m, 3H), 3.90 (d, *J* = 14.8 Hz, 1H), 3.70 (t, *J* = 6.5 Hz, 2H), 3.50 (dt, *J* = 9.4, 6.3 Hz, 1H), 3.37 (d, *J* = 13.2 Hz, 1H), 3.22–3.12 (m, 2H), 3.06 (d, *J* = 13.6 Hz, 1H), 2.84 (d, *J* = 14.9 Hz, 1H), 2.11–1.75 (m, 8H), 1.73–1.63 (m, 2H), 1.63–1.54 (m, 2H), 1.51–1.27 (m, 36H), 1.04–0.85 (m, 12H).

¹³C NMR: (101 MHz, CDCl₃) δ = 158.2 (C_q), 155.9 (C_q), 155.1 (2C_q), 154.9 (C_q), 141.8 (C_q), 141.7 (C_q), 137.4 (C_q), 137.3 (C_q), 135.3 (C_q), 135.0 (C_q), 134.0 (C_q), 133.4 (C_q), 133.1 (2C_q), 131.4 (C_q), 129.3 (2CH), 128.8 (2CH), 128.2 (CH), 128.0 (CH), 127.9 (CH), 127.7 (CH), 127.1 (CH), 127.0 (CH), 126.8 (CH), 125.6 (CH), 122.3 (CH), 122.2 (CH), 121.7 (CH), 119.5 (C_q), 116.6 (CH), 75.7 (CH₂), 75.3 (CH₂), 75.0 (CH₂), 74.5 (CH₂), 32.0 (CH₂), 32.0 (CH₂), 32.0 (CH₂), 31.0 (CH₂), 31.0 (CH₂), 30.8 (CH₂), 30.6 (CH₂), 30.3 (CH₂), 30.1 (2CH₂), 30.1 (CH₂), 29.8 (CH₂), 29.7 (CH₂), 29.5 (CH₂), 29.5 (CH₂), 28.1 (CH₂), 26.7 (CH₂), 26.6 (CH₂), 26.2 (CH₂), 26.0 (CH₂), 22.8 (CH₂), 22.8 (CH₂), 22.7 (CH₂), 22.7 (CH₂), 14.1 (CH₃), 14.1 (CH₃).

LC-MS: *m/z* [M+NH₄]⁺ calculated for C₆₉H₉₇N₂O₅: 1033.74; found: 1033.37.

HR-MS (ESI) *m/z*: [M+K]⁺ calcd. for C₆₉H₉₃KNO₅ 1054.6691; found 1054.6685.

Chapter 3

3.5 Bibliography

- [1] C. Gutsche, *Calixarenes: An Introduction*, Cambridge: RSC Publishing, Cambridge, **2008**.
- [2] A. Dalla Cort, L. Mandolini, C. Pasquini, L. Schiaffino, *New J. Chem.*, **2004**, 28, 1198–1199.
- [3] Y.-D. Cao, J. Luo, Q.-Y. Zheng, C.-F. Chen, M.-X. Wang, Z.-T. Huang, *J. Org. Chem.*, **2004**, 69, 206–208.
- [4] a) S. Shirakawa, S. Shimizu, *Eur. J. Org. Chem.*, **2009**, 12, 1916–1924; b) S. Shirakawa, T. Kimura, S. I. Murata, S. Shimizu, *J. Org. Chem.*, **2009**, 74, 1288–1296.
- [5] a) O. Middel, Z. Greff, N. J. Taylor, W. Verboom, D. N. Reinhoudt, V. Snieckus, *J. Org. Chem.*, **2000**, 65, 667–675; b) F.-J. An, W.-Q. Xu, S. Zheng, S.-K. Ma, S.-Y. Li, R.-L. Wang, J.-M. Liu, *Eur. J. Org. Chem.*, **2016**, 5, 1012–1016.
- [6] P. Lhoták, *Org. Biomol. Chem.*, **2022**, 20, 7377–7390.
- [7] Z.-X. Xu, C. Zhang, Q.-Y. Zheng, C.-F. Chen, Z.-T. Huang, *Org. Lett.*, **2007**, 9, 4447–4450.
- [8] K. Flídrova, S. Böhm, H. Dvořáková, V. Eigner, P. Lhoták, *Org. Lett.*, **2014**, 16, 138–141
- [9] a) M. Mastalerz, W. Heggenberg, G. Dyker, *Eur. J. Org. Chem.*, **2006**, 17, 3977–3987; b) W. Heggenberg, A. Seper, I. M. Oppel, G. Dyker, *Eur. J. Org. Chem.*, **2010**, 35, 6786–6797; c) O. G. Barton, B. Neumann, H.-G. Stammler, J. Mattay, *Org. Biomol. Chem.*, **2008**, 6, 104–111.
- [10] a) Y.-Z. Zhang, M.-M. Xu, X.-G. Si, J.-L. Hou and Q. Cai, *J. Am. Chem. Soc.*, **2022**, 144, 22858; b) X. Zhang, S. Tong, J. Zhu and M.-X. Wang, *Chem. Sci.*, **2023**, 14, 827–832.
- [11] a) R. Dorel, A. M. Echavarren, *Chem. Rev.*, **2015**, **115**, 9028; b) A. Kumar, N. T. Patil, *ACS Sustainable Chem. Eng.*, **2022**, 10, 6900.
- [12] a) L. Alonso-Marañón, M. Montserrat Martínez, M.; L. A. Sarandesesa, and J. P. Sestelo, *Org. Biomol. Chem.*, **2015**, 13, 379; b) K. Komeyama, R. Igawa and K. Takaki, *Chem. Commun.*, **2010**, 46, 1748.
- [13] a) M. Tlustý, V. Eigner, H. Dvořáková and P. Lhoták, *Molecules*, **2022**, 27, 8545; b) R. Miao, Q.-Y. Zheng, C.-F. Chen and Z.-T. Huang, *J. Org. Chem.*, **2005**, 70, 7662.
- [14] W. Zi and F. D. Toste, *Chem. Rev.*, **2016**, 45, 4567.
- [15] C. D. Jurisch, and G. E. Arnott, *Beilstein J. Org. Chem.*, **2019**, 15, 1996–2002.

Chapter 3

- [16] Z. Chen, P. Liang, F. Xu, Z. Deng, L. Long, G. Luo and M. Ye, *J. Org. Chem.*, **2019**, *84*, 12639–12647.
- [17] D. Lim and S. B. Park, *Chem. Eur. J.*, **2013**, *19*, 7100 – 7108.

Chapter 4. Regioselective functionalization of calix[4]arenes via Iridium-catalyzed C-H Borylations

4.1 Introduction

Calix[4]arenes are a class of macrocycles that have been widely exploited in supramolecular chemistry for the preparation of receptors, prototypes of molecular machines and in catalysis.^[1] One of the main advantages of these derivatives is the possibility to easily functionalized the cavity scaffold for the insertion of different functionalities, in other to properly tune the property of the final cavitand.^[2] On this matter, many methodology have been developed in order to obtain regioselective functionalization of the upper- and lower-rim and simultaneously maintain the calix[4]arene scaffold in the cone conformation, preserving the shape of cavity.^[3] In the early stages of calix[4]arene chemistry, methodologies selective functionalization of the lower-rim were characterized by sequential multi-step reaction, like the one reported by Arduini for the preparation of bis-crown-ether type calix[4]arene derivative (Figure 4.1).^[4]

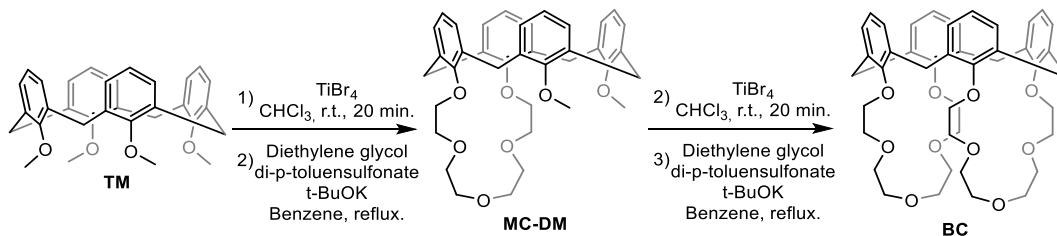


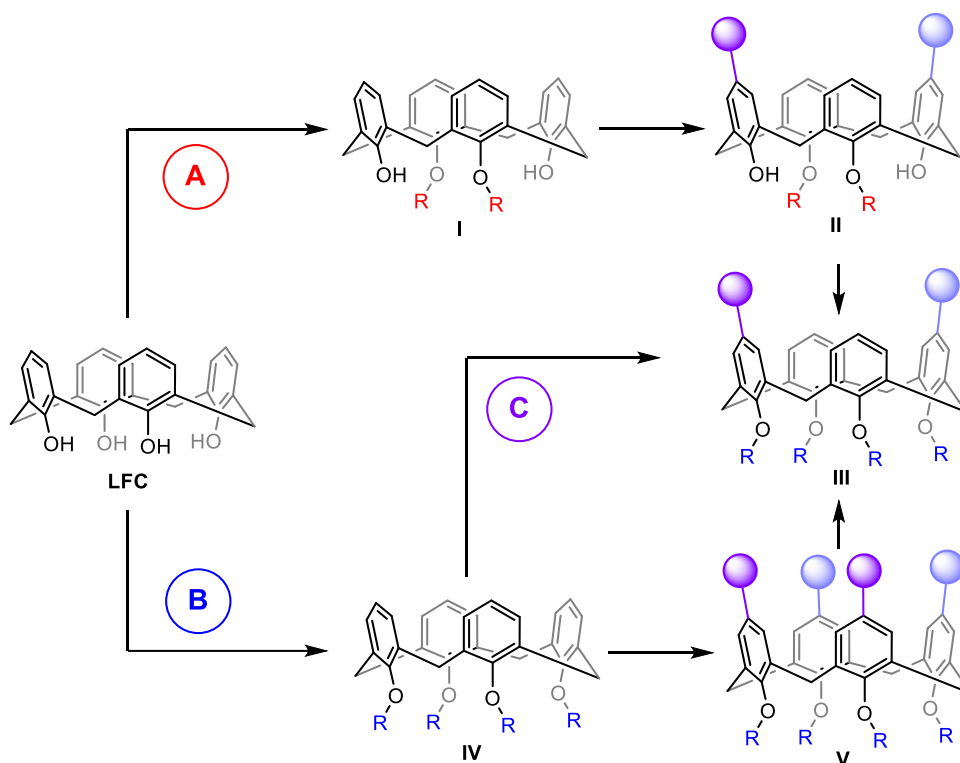
Figure 4.1: Synthetic pathway for the preparation of bis-crown-calix[4]arene derivative **BC**.

Later, the same research group developed a methodology for the regioselective distal 1,3-dialkylation of the lower rim, using stoichiometric amounts of a mild base and the desired alkyl bromide or tosylate (Scheme 4.1, A).^[5]

These procedures not only lead to the formation of the described calix[4]arene derivatives, but represent also a methodology to selectively functionalized the upper-rim. In fact, by alkylation of the phenols in the lower-rim it was possible to simultaneously deactivate the *para*-position of the corresponding aromatic rings, guiding the functionalization onto the more reactive non-protected ones. This strategy remained one of the main route to the

Chapter 4

preparation of *proximal* 5,11- and *distal* 5,17-functionalized calix[4]arene derivatives (from now on referred to as 1,2- and 1,3-difunctionalized),^[6] with the main disadvantage of requiring multiple step of alkylation or de-alkylation in order to introduce the desired substituents.



Scheme 4.1: Schematic representation of the main reported strategies for the selective functionalization of the calix[4]arene's upper-rim.

Another strategy was developed, starting with the tertaalkoxy-calix[4]arene, that saw the perfunctionalization of *para*-positions of the macrocyclic scaffold, followed by controlled desymmetrisation for the selective removal on the undesired “extra” substituents (Scheme 4.1, B).^[7]

The optimal methodology would be the direct regioselective functionalization of the upper-rim, however these strategies are characterized by the formation of mono-, di- and tri-substituted derivatives that lead to tedious purification procedures and lower yields (Scheme 4.1, C).^[8]

Chapter 4

The project discussed in this chapter will present the published results^[9] for a novel catalytic approach for the preparation of a versatile di-functionalized tetraalkoxy-calix[4]arene derivative on the upper-rim employing the known Ir-catalyzed C-H borylation reaction on macrocyclic compounds (Figure 4.2).^[10]

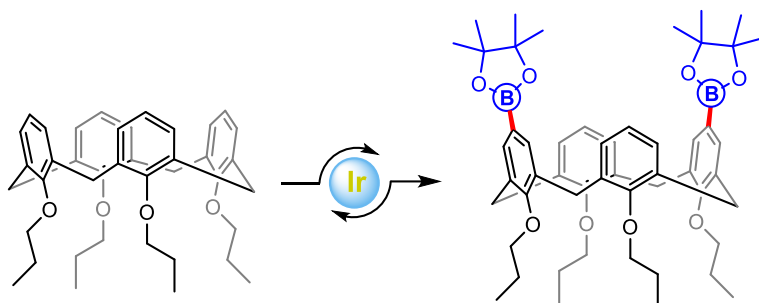
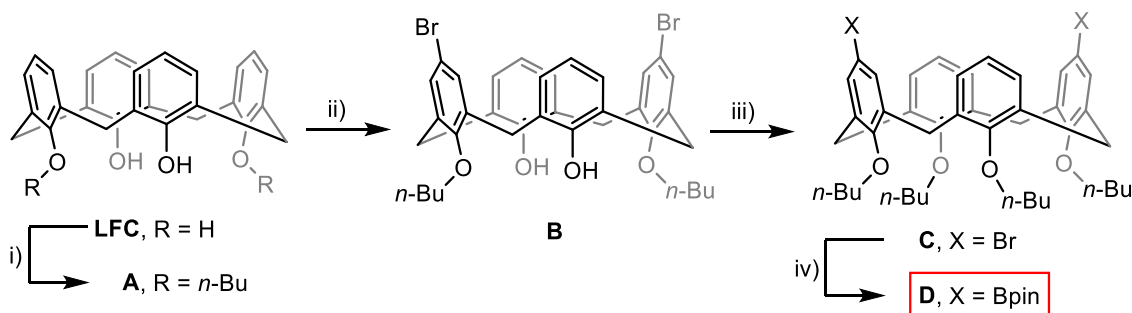


Figure 4.2: Direct 1,3-regioselective functionalization of the upper-rim by Iridium-catalyzed C-H borylation reaction.

The synthesis for this type of calix[4]arene intermediate was already reported (Scheme 4.2) but it required a long multi-step reaction pathway that made it not so easily accessible and less attractive, even considered his high potential for further more “exotic” functionalization of the macrocyclic scaffold.^[11]

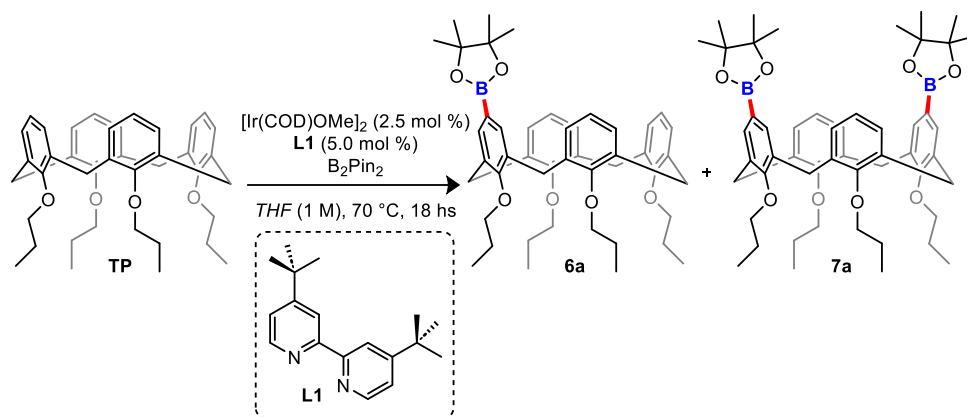


Scheme 5.2: Multi-step synthetic pathway for 1,3-di-functionalized calix[4]arene derivative **D**: i) BuBr, K₂CO₃, DMF, reflux; ii) Br₂, CHCl₃, 0 °C to r.t.; iii) BuBr, NaH, DMF, reflux; iv) Pd(dppf)Cl₂, [B(Pin)]₂, CH₃COOK, dioxane, 110 °C.

Chapter 4

4.2 Results and discussion

The study began by exploring the well-known tetrapropoxycalix[4]arene (TP) in the presence of various commercially available ligands previously shown to be effective for C–H borylations (Scheme 4.3).



Scheme 4.3: Initial investigation for the direct C–H borylation reaction on model substrate TP.

Initially, TP was reacted with $[\text{Ir}(\text{COD})\text{OMe}]_2$ as the catalyst, 4,4'-di-tert-butyl-2,2'-bipyridine (L1) as the ligand, and bis(pinacolato)diboron (B_2pin_2 , 1.0 eq.) as the boron source in THF at 70 °C. Under these conditions, two new compounds were isolated after chromatographic purification. NMR analysis confirmed these products as the mono- and di-borylated calix[4]arenes (Figure 4.3).

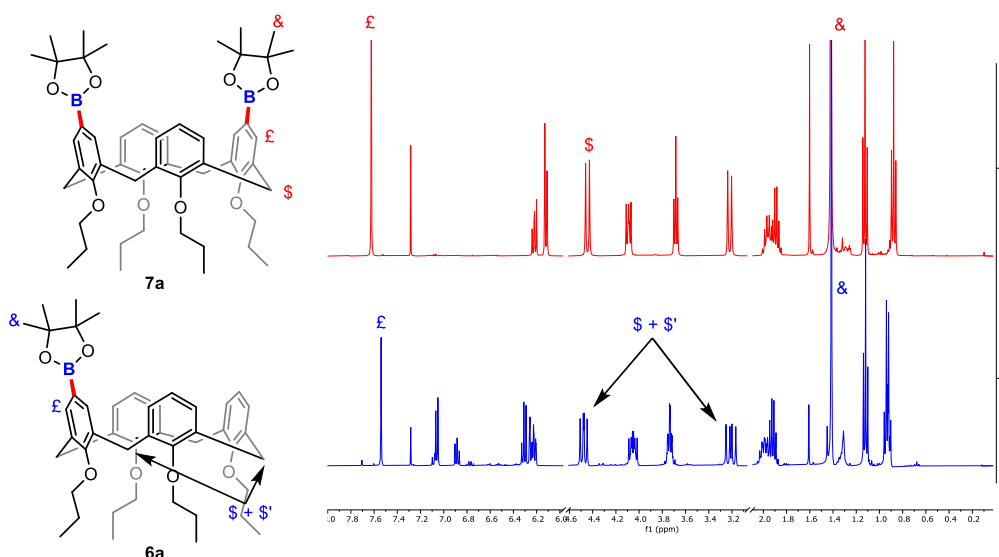


Figure 4.3: ^1H NMR spectra stack plot of derivatives 6a and 7a.

Chapter 4

The main identifiable features were the splitting patterns of the signals corresponding to the bridging methylene protons (Figure 4.3, \$ and \$'): in compound **6a**, these protons appeared as two sets of doublets at 4.5 and 3.2 ppm, each integrating for 2 protons, indicating that the macromolecule exhibited C_1 symmetry due to mono-functionalization at the upper rim. For compound **7a**, only two doublets were observed in the same region, but each integrated for 4 protons, indicating a C_2 symmetry and a selective functionalization at the distal 1,3-positions. Other notable signals included singlets at 7.54 and 7.62 ppm (Figure 4.3, £), integrating for 2 protons in **6a** and 4 protons in **7a**, along with a singlet at 1.41 and 1.42 ppm (Figure 4.3, &), confirming proper installation of the Bpin groups.

These structural assignments were further confirmed by X-ray diffraction analysis (Figure 4.4). Notably, no other regioisomers were detected in the reaction mixture.

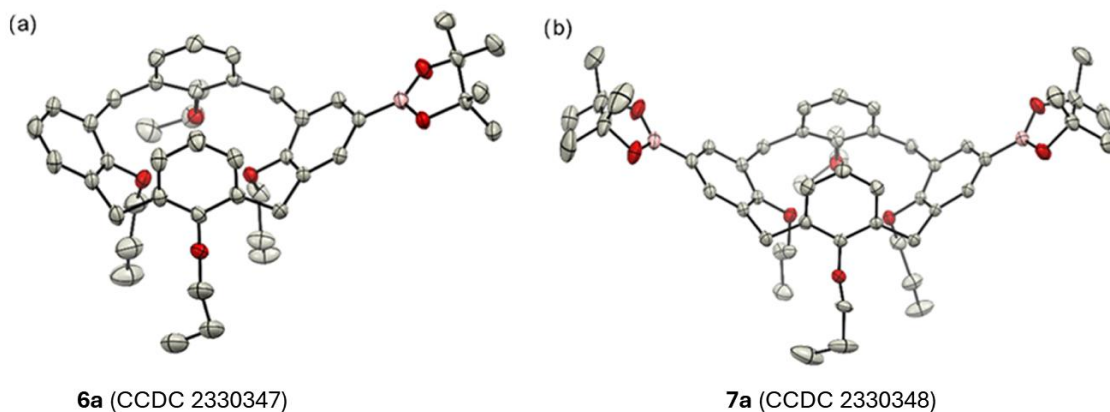


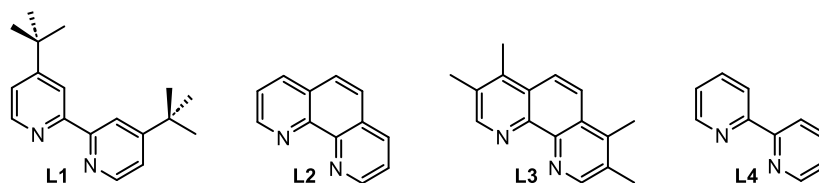
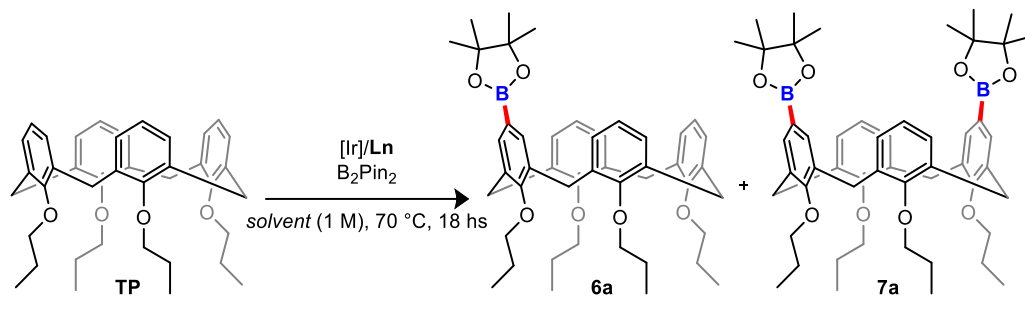
Figure 4.4: X-ray diffraction structures for **6a** (a) and **7a** (b).

To optimize reaction conditions, additional experiments were conducted, adjusting the ligand, catalyst, and solvent (Table 4.1). A control reaction without a catalyst resulted in no transformation, confirming the critical role of Iridium catalysts in facilitating the B_2pin_2 addition (Table 4.1, entry 2). The impact of various ligands was then assessed: in the absence of a ligand or with alternative ligands commonly used for C-H borylations, such as **L2** and **L3**, no transformation was observed (Table 4.1 entries 3–5). However, using the simpler 2,2'-bipyridine ligand **L4** led to the isolation of products **6a** and **7a** with moderate yields (40% and 20%, respectively).

Exploration of other solvents showed that cyclohexane and 1,4-dioxane had minimal impact on yields or product distribution, while toluene proved unsuitable, likely due to

Chapter 4

competitive C-H borylation of the toluene itself (Table 4.1, entries 7–9). Finally, substituting $[\text{Ir}(\text{COD})\text{OMe}]_2$ with $[\text{Ir}(\text{COD})\text{Cl}]_2$ adversely affected the C-H borylation, further underscoring the need for careful catalyst selection (Table 4.1, entry 10).



Entry	Ln	[Ir]	Solvent	6a/7a [%]
1	L1	$[\text{Ir}(\text{COD})\text{OMe}]_2$	THF	35/7
2	--	--	THF	--
3	--	$[\text{Ir}(\text{COD})\text{OMe}]_2$	THF	--
4	L2	$[\text{Ir}(\text{COD})\text{OMe}]_2$	THF	--
5	L3	$[\text{Ir}(\text{COD})\text{OMe}]_2$	THF	--
6	L4	$[\text{Ir}(\text{COD})\text{OMe}]_2$	THF	44/20
7	L4	$[\text{Ir}(\text{COD})\text{OMe}]_2$	Cylohexane	41/15
8	L4	$[\text{Ir}(\text{COD})\text{OMe}]_2$	1,4-dioxane	40/22
9	L4	$[\text{Ir}(\text{COD})\text{OMe}]_2$	Toluene	--
10	L4	$[\text{Ir}(\text{COD})\text{Cl}]_2$	THF	--
11 ^b	L4	$[\text{Ir}(\text{COD})\text{OMe}]_2$	THF	20/52
12 ^c	L4	$[\text{Ir}(\text{COD})\text{OMe}]_2$	THF	25/56
13 ^d	L4	$[\text{Ir}(\text{COD})\text{OMe}]_2$	THF	21/61

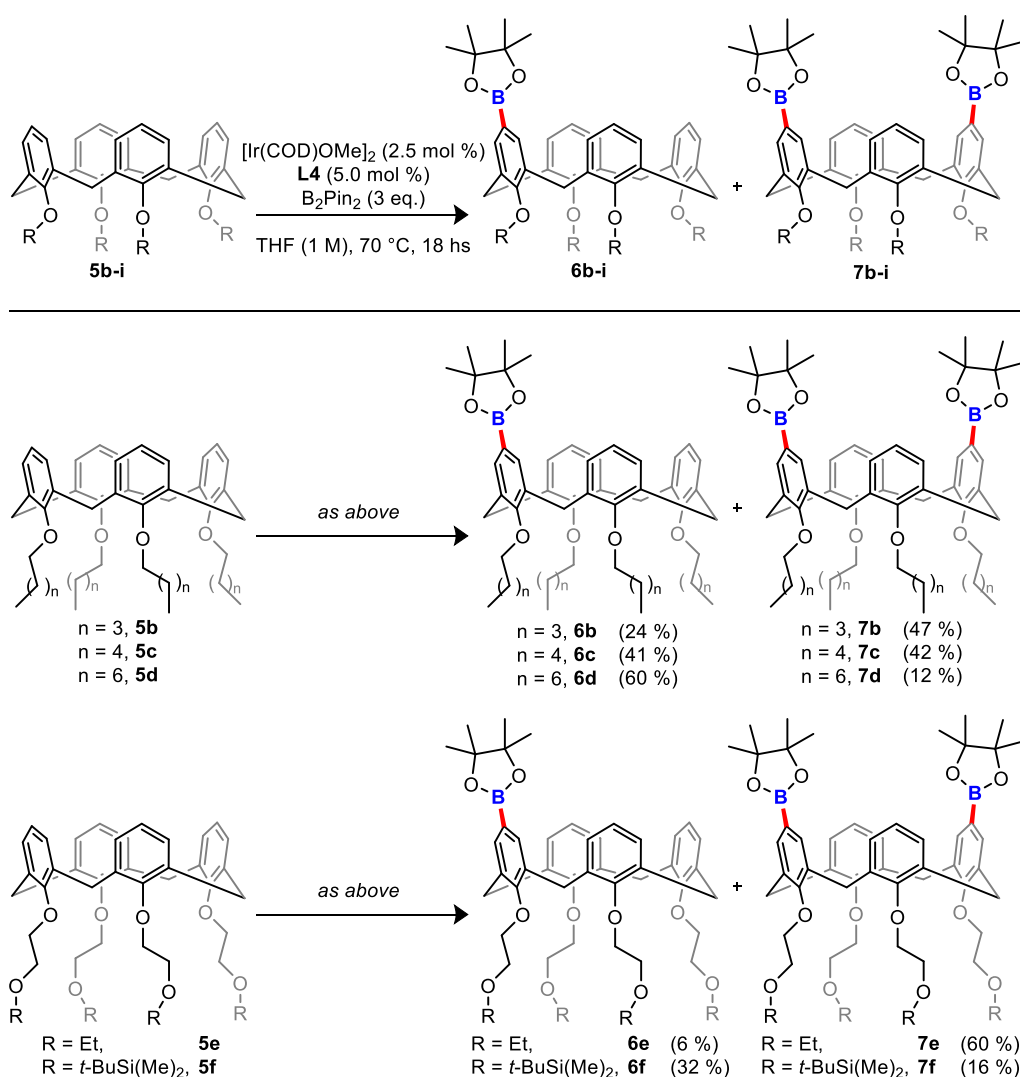
Reaction conditions: TP (0.3 mmol), [Ir] (2.5 mol %), Ln (5.0 mol %), B_2Pin_2 (1.0 eq.) and solvent (1 M) at 70 °C for 18 hs; b) B_2Pin_2 (2.0 eq.); c) B_2Pin_2 (3.0 eq.); d) TP (1.0 mmol), [Ir] (2.5 mol %), Ln (5.0 mol %), B_2Pin_2 (3.0 eq.) and THF (1 M) at 70 °C for 18 hs

Table 4.1: Table of optimization of the reaction conditions.

Chapter 4

Increasing the amount of bis(pinacolato)-diboron to 2.0 and 3.0 equivalents improved the overall catalytic yields (Table 4.1, entries 11-12). Additionally, this adjustment shifted selectivity toward the formation of product **7a**, which was obtained in good yields (52% and 56%, respectively).

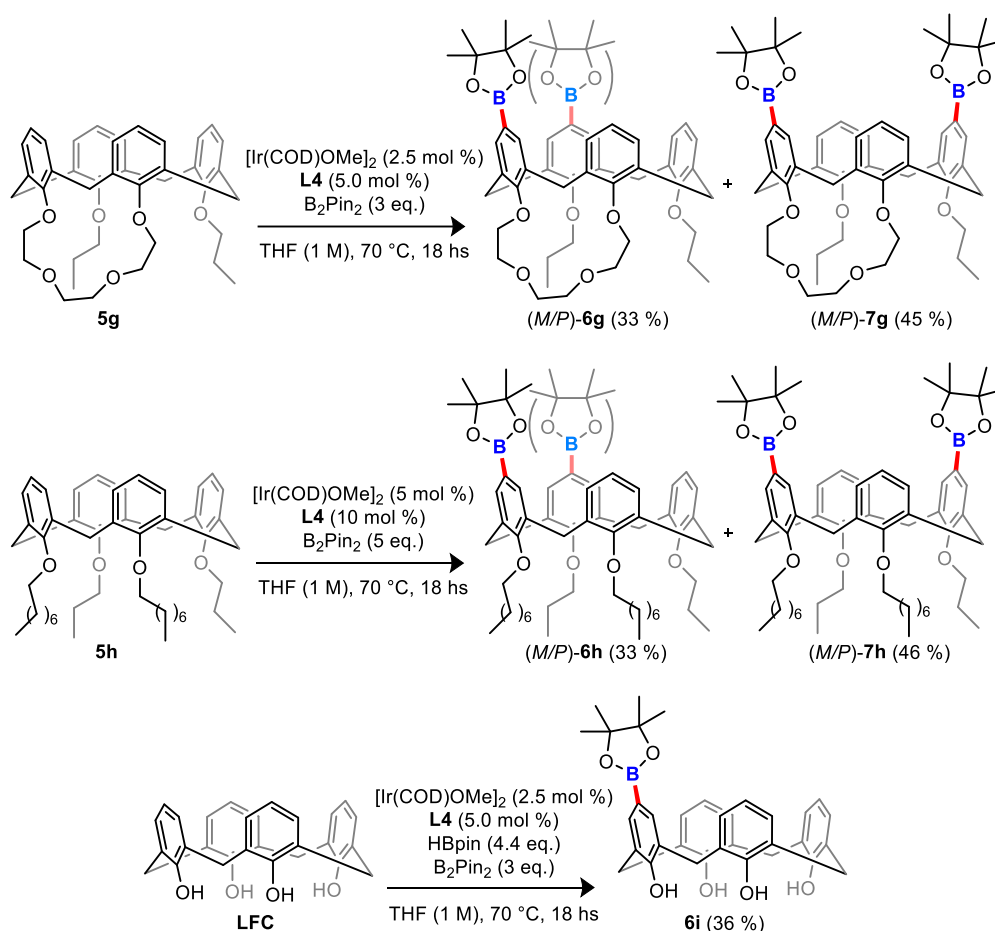
With the optimized conditions established, a series of calix[4]arene derivatives were tested to assess the influence of various substituents on the lower rim of the macrocycle (Scheme 4.4).



Scheme 4.4: Scope of the C-H borylation reaction with lower-rim substituted calix[4]arene derivatives.

Chapter 4

Tetrapentyl-, tetrahexyl-, and tetraoctyl-oxy calix[4]arene derivatives **5b-d** were subjected to the catalytic conditions, resulting in the formation of their corresponding mono- and difunctionalized products with good efficiency. A trend was observed in the yields of the di-borylated products **7b-d**, which decreased as the alkyl chain length increased. Specifically, **7b** and **7c** were isolated in satisfactory yields (47% and 42%, respectively), while **7d** was obtained in only 12% yield, with the mono-borylated product **6d** being predominant (60% yield). The reaction with substrate **5e** primarily yielded **7e** (60%), whereas the silyl-protected calix[4]arene **5f** formed the mono-borylated product **6f** in moderate yield.

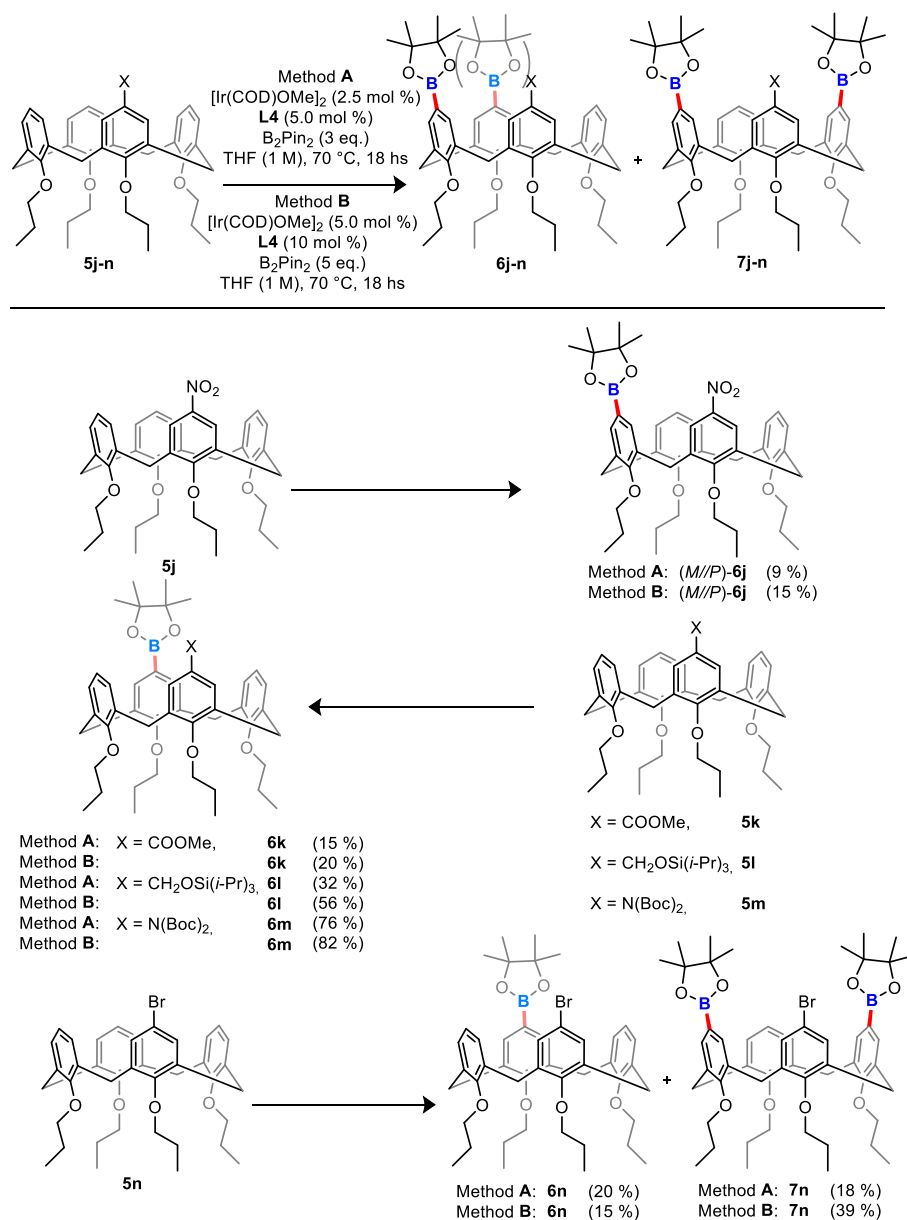


Scheme 4.5: Scope of the C-H borylation reaction with differently lower-rim functionalized calix[4]arene derivatives **5g** and **5h** and directly on **LFC**.

Compounds **5g-h**, featuring a symmetry plane bisecting the molecule due to varied substituents on the lower rim, also proved to be suitable substrates (Scheme 4.5). Inherently chiral di-borylated compounds (M/P)-**7g-h** were efficiently produced in the

Chapter 4

reaction mixture, with isolated yields of 45% and 46%, respectively. The mono-borylated analogues **6g-h**, however, were isolated only as inseparable regioisomeric mixtures, making them less synthetically useful (Scheme 4.5, in brackets). Notably, direct C-H borylation on calix[4]arene **LFC** was achieved only with the assistance of HBpin as a temporary protecting group, yielding product **6i** in modest amounts. Following this, the impact of upper-rim functionalization on the reactivity of the calix[4]arene scaffold was examined (Scheme 4.6).



Scheme 4.6: Scope of the C-H borylation reaction with upper-rim functionalized calix[4]arene derivatives **5j-n**.

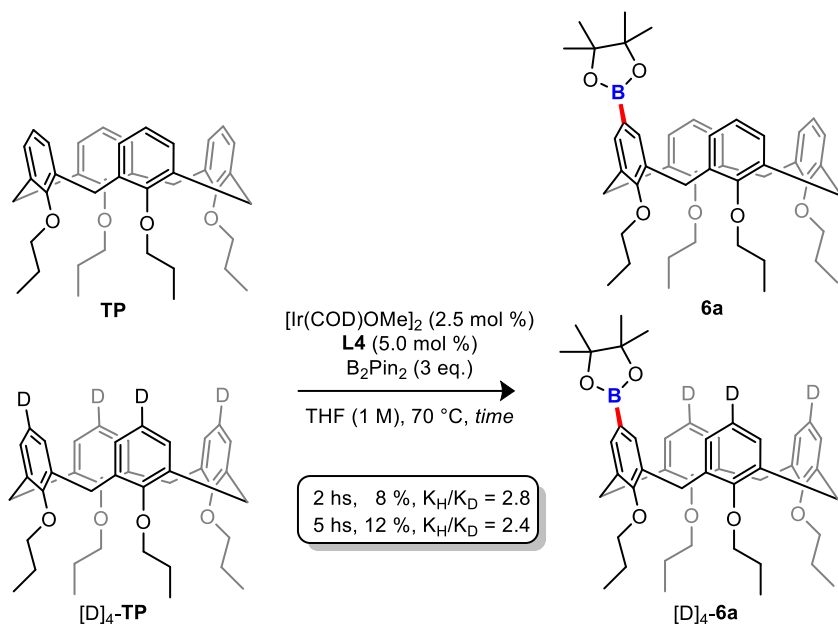
Chapter 4

When calix[4]arenes bearing electron-withdrawing groups, such as nitro- and methylcarboxylate ester derivatives (**5j-k**), were subjected to both reaction conditions, they proved to be challenging substrates, even with increased catalyst loading (Scheme 4.6, method B). The iridium-catalyzed C–H borylation of these compounds produced the mono-borylated products **6j-k** in low yields. Notably, for compound **5j**, C–H borylation selectively targeted the proximal phenolic ring, resulting in an inherently chiral macrocycle in a streamlined manner.

Compounds with silyl-protected hydroxymethyl (**5l**) and bis-carbamate-protected amino (**5m**) groups were also compatible with the protocol, yielding only the mono-borylated products **6l-m** in high yields. This regioselectivity is attributed to the steric bulk of the upper-rim functional groups, which likely hinders reactivity at the adjacent phenolic rings. Conversely, the bromo-substituted calix[4]arene **5n** produced both mono- and di-borylated products (**6n** and **7n**) under standard conditions, with 2-fold C–H borylation occurring preferentially at positions proximal to the bromo-substituted phenolic ring. Enhanced selectivity for **7n** was achieved by increasing both the catalyst loading and the amount of bis(pinacolato)-diboron (Method B).

Following these transformations, preliminary mechanistic experiments were conducted to gain insights into the catalyst's mode of action (Scheme 4.7).

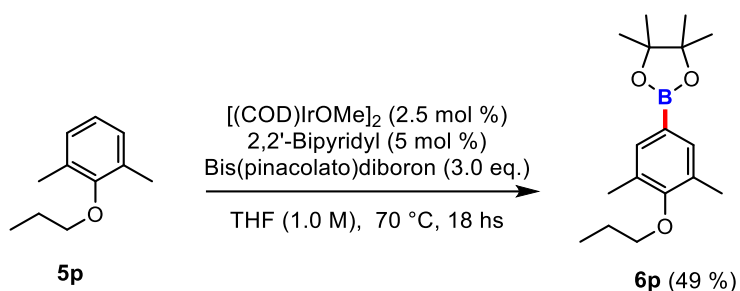
Chapter 4



Scheme 4.7: Kinetic Isotope Effect (KIE) experiments.

Intermolecular competition experiments between **TP** and its tetra-deuterated analogue $[\text{D}]_4\text{-TP}$ revealed a primary kinetic isotope effect, indicating that the C-H activation step is likely rate- or product-determining in the catalytic cycle.^[12] This observation is consistent with previous mechanistic findings in iridium-catalyzed C-H borylation of arenes.^[13]

Subsequently, a monomeric analogue of calix[4]arene **TP** was synthesized and subjected to the optimized catalytic conditions (Scheme 4.8).

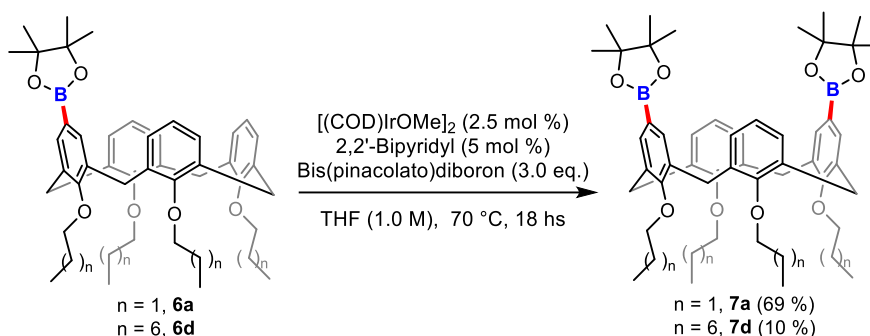


Scheme 4.8: Direct C-H borylation reaction performed on monomeric substrate **5p**.

This reaction produced compound **6p** as a single regioisomer, mirroring the selectivity observed at each phenolic ring of the macrocyclic calix[4]arenes. This outcome suggests that a significant steric influence governs the regioselectivity in iridium-catalyzed C-H borylation.

Chapter 4

At last, the effect of the length of the alkyl chain on 2-fold C–H borylations was considered (Scheme 4.9).

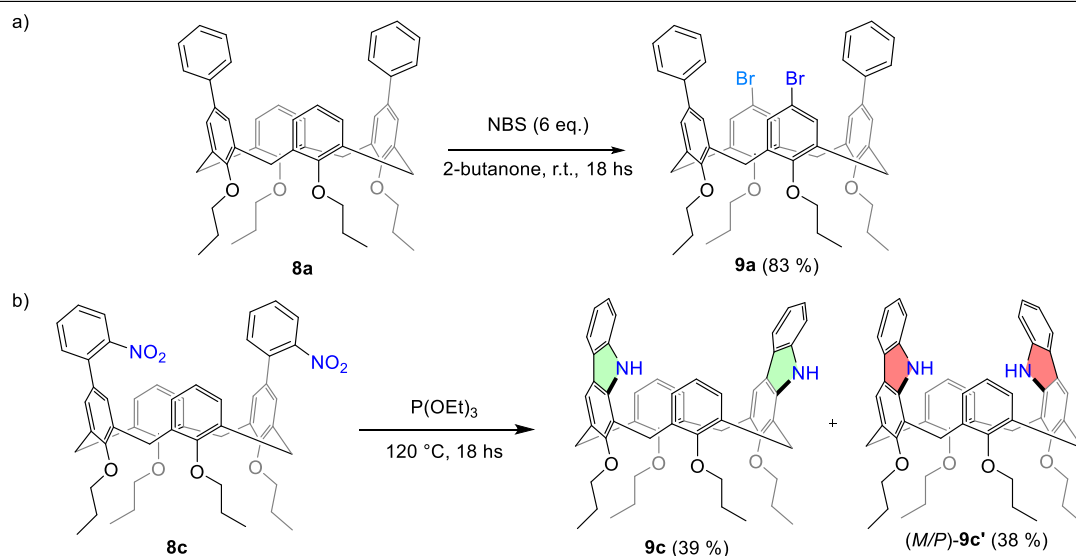
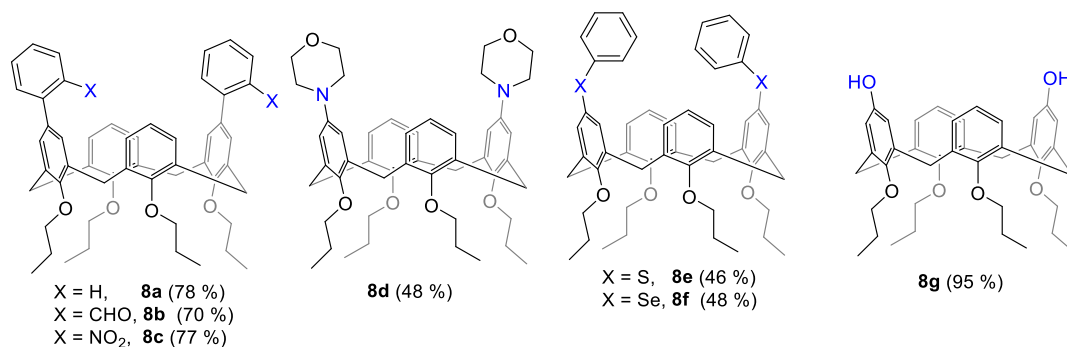


Scheme 4.9: Evaluation of the effect of the lower-rim chain's length in the C–H borylation reaction of mono-borylated compounds **6a** and **6d**.

Mono-borylated compounds **6a** and **6d** were next subjected to standard C–H borylation conditions. While **6a** efficiently produced the di-borylated product **7a** in high yield, **6d** was significantly less reactive, forming **7d** only in very low yield. This result further underscores the influence of calix[4]arene rigidity in determining the selectivity between mono- and di-borylated products. Mechanistically, additional details are still needed to fully clarify the (regio)selectivity of the catalyst. At this stage, we hypothesize that a bulky [Ir(bpy)(Bpin)₃]^[14] complex may preferentially approach the less hindered, distal phenolic unit of **6a** from the outside of the macrocycle, thus facilitating formation of the di-borylated product **7a**. However, in longer O-alkylated calix[4]arenes, conformational strain may inhibit the second C–H borylation event.

Finally, a broad range of C–B functionalizations was applied to compound **7a**, highlighting the versatility of the C–H borylation protocol (Scheme 4.10).

Chapter 4



Scheme 4.10: C-B functionalizations of di-borylated derivative **7a**.

Palladium-catalyzed Suzuki–Miyaura couplings were successfully performed with various bromoarenes. Using bromobenzene as a model substrate, compound **8a** was synthesized and then selectively transformed into **9a** through a standard bromination protocol with high site- and regioselectivity (Scheme 4.10, a). Remarkably, ortho-nitrobromobenzene also served effectively as a substrate, yielding **8c**, which was subsequently subjected to a Cadogan reaction^[15] to form carbazole-fused calix[4]arenes **9c**/*(M/P)*-**9c'** (Scheme 4.10, a).^[16] Importantly, meso-(**9c**) and chiral (**9c'**) forms of calix[4]arene were successfully separated from the reaction mixture. Additionally, copper-mediated Chan-Lam couplings^[17] were utilized to create novel macrocycles, forming new C–N bonds with morpholine as a coupling partner, yielding **8d** in moderate yield. Sulfur- and selenium-containing calix[4]arenes (**8e** and **8f**) were obtained in synthetically valuable yields via copper-mediated sulfenylation and selenylation of aryl boronates. Finally, a transition-metal-free hydroxylation of boronate ester **7a** produced versatile calix[4]arene **8g** in high yield.

Chapter 4

4.3 Conclusions

A novel methodology employing direct C–H borylation of cavitands for the regioselective functionalizations of calix[4]arene macrocycles has been developed. The method was exploited to synthesize a broad family of borylated calix[4]arenes with overall good yields and easy purification procedures. The synthetic versatility of these borylated compounds was further demonstrated with the synthesis of highly decorated calix[4]arenes by the application of established C–B functionalization protocols. This work, which exploits the power of iridium catalysis, opens new perspectives in the field of macrocycles. In fact, the application of iridium-catalyzed C–H borylations could boost the programmed synthesis of sophisticated supramolecular entities in the most atom- and step-economical manner

Chapter 4

4.4 Experimental section

- **General materials and remarks**

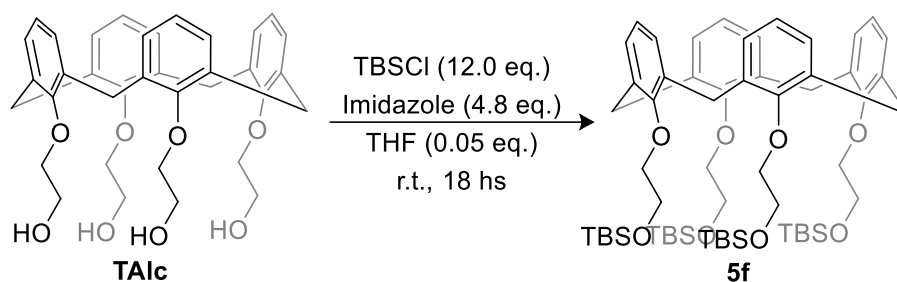
All chemicals those syntheses are not reported hereafter were purchased from commercial sources and used as received. Solvents were dried and stored over molecular sieves previously activated in an oven (450 °C overnight). THF for catalytic reactions was dried passing through alumina columns using an Inert[®] system and stored under nitrogen. Melting points were measured with an Electrothermal apparatus and are uncorrected. Column chromatography was performed on silica gel 60 (70-230 mesh). NMR spectra were recorded on a Bruker 400 MHz and JEOL 600 MHz using solvents as internal standards (7.26 ppm for ¹H NMR and 77.00 ppm for ¹³C NMR for CDCl₃). The terms m, s, d, t, q and quint represent multiplet, singlet, doublet, triplet, quadruplet and quintuplet, respectively, and the term br means a broad signal. ¹³C DEPTQ NMR spectra are reported for substrates and corresponding products. Exact masses were recorded on an LTQ ORBITRAP XL Thermo Mass Spectrometer (ESI source). Structural assignments were made with additional information from gCOSY, gHSQC, and gHMBC experiments.

Materials: Derivatives, **TP**,^[18] **5b**,^[19] **5c**,^[20] **5d**,^[21] **5e**,^[22] **TAlc**,^[23] **MC3**,^[24] **DPr**,^[25] **1j**,^[26] **MAc**,^[27] **MAld**,^[27] **MAm**,^[26] **5n**,^[28] were synthesized according to known procedures.

Chapter 4

- Synthesis and characterization of substrates 5

Substrate 5f:



Into a round-bottom flask, *tert*-butyl dimethyl silyl chloride (0.34 mL, 2.0 eq.) and imidazole (163 mg, 3.0 eq.) were added to a solution of **TAlc** (495 mg, 0.8 mmol) in THF (0.2 M). The mixture was left under magnetic stirring overnight. The reaction was monitored by TLC (*n*-Hexane:EtOAc 9:1). After completion, the mixture was quenched by addition of water (15 mL) and extracted with EtOAc (15 mL). The combined organic layers were separated, washed with water (15 mL) and brine (15 mL), dried over Na₂SO₄, filtered and the solvent removed under reduced pressure. The crude was purified by column chromatography on silica gel (*n*-Hexane:EtOAc 95:5) yielding **5f** as a white solid (535 mg, 90%). **M.p.**: 80 – 82 °C.

¹H NMR (400 MHz, CDCl₃) δ = 6.65 – 6.55 (m, 12H), 4.53 (d, *J* = 13.4 Hz, 4H), 4.09 – 3.98 (m, 16H), 3.15 (d, *J* = 13.5 Hz, 4H), 0.90 (s, 36H), 0.06 (s, 24H).

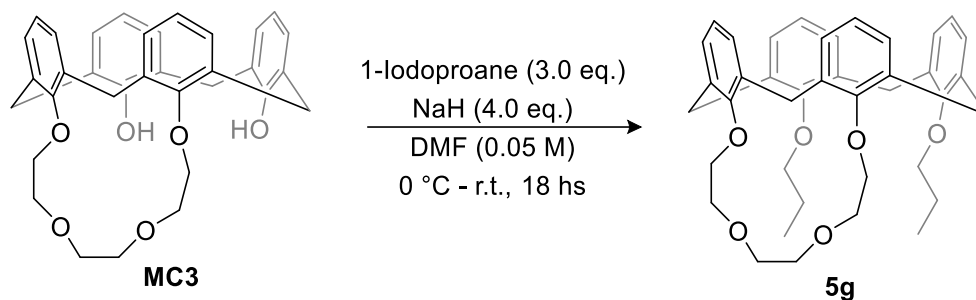
¹³C NMR (101 MHz, CDCl₃) δ = 156.7 (C_q), 135.0 (C_q), 128.1 (CH), 122.0 (CH), 75.7 (CH₂), 62.4 (CH₂), 31.1 (CH₂), 25.9 (CH₃), 18.2 (C_q), -5.2 (CH₃).

LC-MS: *m/z* [M + Na]⁺ calculated for C₆₀H₉₆NaO₈Si₄: 1079.61; found: 1079.84.

HR-MS (ESI): *m/z* [M + Na]⁺ calculated for C₆₀H₉₆NaO₈Si₄: 1079.6152; found: 1079.6155.

Chapter 4

Substrate 5g:



Into a two-necked round-bottom flask, under N₂ atmosphere, NaH (108 mg, 50 %, 4.0 eq.) and 1-iodopropane (0.164 mL, 3.0 eq.) were added to a solution of **MC3** (302 mg, 0.56 mmol) in DMF (0.05 M), cooled to 0 °C via an iced bath. After 10 minutes, the mixture was allowed to warm up to r.t. and was left under magnetic stirring overnight. After 18 hs, analysis by TLC (*n*-Hexane:EtOAc 85:15) showed complete consumption of **MC3**. The mixture was quenched by the addition of HCl 10 % (40 mL) and extracted with EtOAc. The combined organic layers were washed with water (20 mL) and brine (20 mL), dried over Na₂SO₄, filtered and the solvent removed under reduced pressure. The crude was purified by column chromatography on silica gel (*n*-Hexane:EtOAc 85:15) yielding **5g** as a white solid (260 mg, 73%). **M.p.**: 124 – 126 °C.

¹H NMR (400 MHz, CDCl₃) δ = 6.72 – 6.55 (m, 12H), 4.99 (d, *J* = 13.0 Hz, 1H), 4.52 – 4.40 (m, 3H), 4.33 – 4.27 (m, 2H), 4.20 (ddd, *J* = 11.0, 8.3, 2.8 Hz, 2H), 4.02 – 3.79 (m, 10H), 3.79 – 3.67 (m, 2H), 3.26 – 3.11 (m, 4H), 2.04 – 1.89 (m, 4H), 1.03 (t, *J* = 7.4 Hz, 6H)

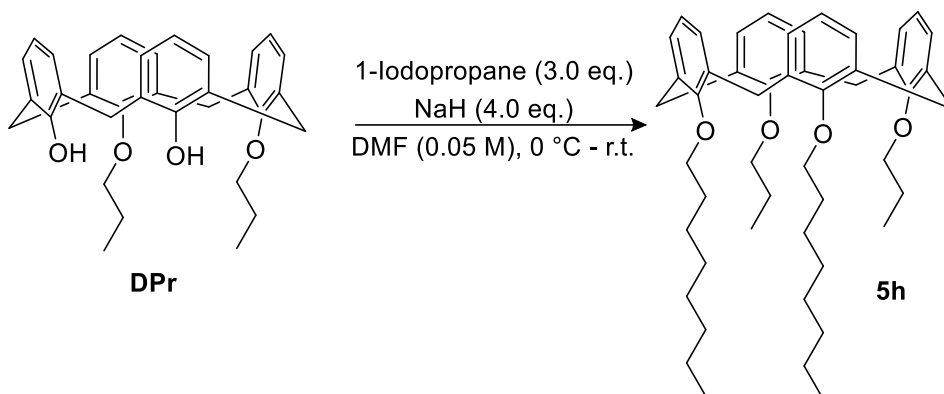
¹³C NMR (101 MHz, CDCl₃) δ = 156.5 (C_q), 156.1 (C_q), 135.8 (C_q), 135.1 (C_q), 135.0 (C_q), 134.7 (C_q), 128.2 (CH), 128.2 (CH), 128.2 (CH), 128.1 (CH), 122.2 (CH), 122.0 (CH), 76.7 (CH₂), 73.3 (CH₂), 70.8 (CH₂), 70.3 (CH₂), 31.1 (CH₂), 30.9 (CH₂), 30.0 (CH₂), 23.3 (CH₂), 10.4 (CH₃).

LC-MS: *m/z* [M + Na]⁺ calculated for C₄₀H₄₆NaO₆: 645.34; found: 645.53.

HR-MS (ESI): *m/z* [M + Na]⁺ calculated for C₄₀H₄₆NaO₆: 645.3367; found: 645.3363.

Chapter 4

Substrate 5h:



Into a two-necked round-bottom flask, under N₂ atmosphere, NaH (151 mg, 50 %, 4.0 eq.) and 1-iodooctane (0.41 mL, 3.0 eq.) were added to a solution of **DPr** (510 mg, 0.79 mmol) in DMF (0.05 M) cooled to 0 °C via an iced bath. After 10 minutes, the mixture was allowed to warm up to r.t. and was left under magnetic stirring overnight. After 18 hs, analysis by TLC (*n*-Hexane:EtOAc 95:5) showed complete consumption of **MC3**. The mixture was quenched by addition of HCl 10 % (40 mL) and extracted with EtOAc. The combined organic layers were washed with water (20 mL) and brine (20 mL), dried over Na₂SO₄, filtered and the solvent removed under reduced pressure. The crude was purified by column chromatography on silica gel (*n*-Hexane:EtOAc 85:15) yielding **5h** as a white solid (538 mg, 93%). **M.p.**: 88 – 90 °C.

¹H NMR (400 MHz, CDCl₃) δ = 6.66 – 6.55 (m, 12H), 4.51 – 4.45 (m, 4H), 3.90 (t, *J* = 7.6 Hz, 4H), 3.87 (t, *J* = 7.6 Hz, 4H), 3.17 (d, *J* = 13.3 Hz, 4H), 2.01 – 1.88 (m, 8H), 1.47 – 1.27 (m, 20H), 1.02 (t, *J* = 7.4 Hz, 6H), 0.95 – 0.90 (m, 6H).

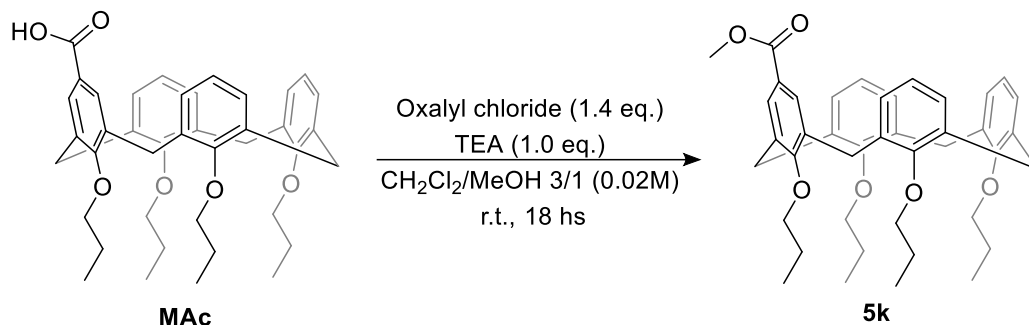
¹³C NMR (101 MHz, CDCl₃) δ = 156.7 (C_q), 156.6 (C_q), 135.2 (4 x C_q), 128.1 (4 x CH), 121.9 (CH), 121.9 (CH), 76.7 (CH₂), 75.2 (CH₂), 31.9 (CH₂), 31.0 (CH₂), 30.3 (CH₂), 29.8 (CH₂), 29.5 (CH₂), 26.3 (CH₂), 23.3 (CH₂), 22.7 (CH₂), 14.1 (CH₃), 10.4 (CH₃).

LC-MS: *m/z* [M + Na]⁺ calculated for C₅₀H₆₈NaO₄: 755.52; found: 755.67.

HR-MS (ESI): *m/z* [M + Na]⁺ calculated for C₅₀H₆₈NaO₄: 755.5190; found: 755.5195.

Chapter 4

Substrate 5k:



Into a two-necked round-bottom flask, under N_2 atmosphere, triethylamine (0.078 mL, 1.0 eq.) and oxalyl chloride (0.069 mL, 1.4 eq.) were added to a solution of **MAc** (356 mg, 0.56 mmol) in $CH_2Cl_2/MeOH$ 3/1 (0.02 M). The mixture was left under magnetic stirring at r.t. for 18 hs. After 18 hs, analysis by TLC (*n*-Hexane:EtOAc 9:1) showed complete consumption of **MAc**. The mixture was quenched with the addition of water (20 mL). The organic layers were extracted, washed with water (2 x 15 mL) and brine (15 mL), dried over Na_2SO_4 , filtered and the solvent removed under reduced pressure. The crude was purified by column chromatography on silica gel (*n*-Hexane:EtOAc 9:1) yielding **5k** as a white solid (281 mg, 77%). **M.p.**: 114 – 116 °C.

1H NMR (400 MHz, $CDCl_3$) δ = 7.40 (s, 2H), 6.67 (d, J = 7.4 Hz, 2H), 6.59 – 6.53 (m, 7H), 4.49 (d, J = 13.4 Hz, 2H), 4.47 (d, J = 13.4 Hz, 2H), 3.97 (t, J = 7.5 Hz, 2H), 3.93 – 3.80 (m, 9H), 3.23 (d, J = 13.5 Hz, 2H), 3.18 (d, J = 13.5 Hz, 2H), 2.01 – 1.87 (m, 8H), 1.08 – 0.97 (m, 12H).

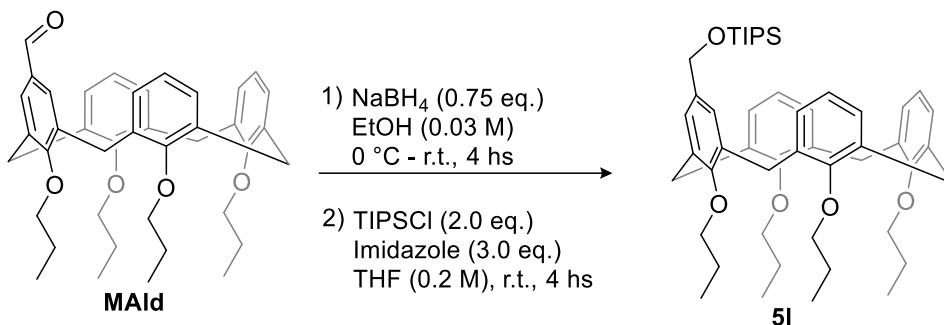
^{13}C NMR (101 MHz, $CDCl_3$) δ = 167.3 (C_q), 161.2 (C_q), 156.8 (C_q), 156.3 (C_q), 135.7 (C_q), 135.4 (C_q), 135.0 (C_q), 134.1 (C_q), 129.9 (CH), 128.3 (CH), 128.3 (CH), 128.1 (CH), 123.5 (C_q), 122.1 (CH), 121.8 (CH), 76.8 (CH_2), 76.7 (CH_2), 76.6 (CH_2), 51.7 (CH_3), 31.0 (CH_2), 31.0 (CH_2), 23.2 (3 x CH_2), 10.4 (CH_3), 10.3 (CH_3), 10.3 (CH_3).

LC-MS: m/z [$M + Na$] $^+$ calculated for $C_{42}H_{50}NaO_6$: 673.37; found: 673.48.

HR-MS (ESI): m/z [$M + Na$] $^+$ calculated for $C_{42}H_{50}NaO_6$: 673.3680; found: 673.3685.

Chapter 4

Substrate 5I:



Into a two-necked round-bottom flask, under N₂ atmosphere, NaBH₄ (25 mg, 0.75 eq.) was added to a solution of **MAld** (538 mg, 0.87 mmol) in EtOH (0.02 M), cooled at 0 °C via an iced-bath. After 10 minutes, the mixture was allowed to warm up to r.t. and was left under magnetic stirring for 4 hs. After 4 hs, analysis by TLC (*n*-Hexane:EtOAc 85:15) showed complete consumption of **MAld**. The mixture was quenched by addition of water (10 mL) and extracted with EtOAc. The organic layers were separated, washed with water (15 mL) and brine (15 mL), dried over Na₂SO₄, filtered and the solvent removed under reduced pressure. Subsequently, the crude was dissolved in THF (0.2 M) and TIPSCl (0.34 mL, 2.0 eq.) and imidazole (163 mg, 3.0 eq.) were added to this mixture. The reaction was left under magnetic stirring for 4 hs. After 4 hs, analysis by TLC (*n*-Hexane:EtOAc 95:5) showed complete consumption of the starting material. The mixture was quenched by addition of water (15 mL) and extracted by EtOAc (15 mL). The combined organic layers were washed with water (15 mL) and brine (15 mL), dried over Na₂SO₄, filtered and the solvent removed under reduced pressure. Product **5I** was isolated from the crude by column chromatography on silica gel (*n*-Hexane:EtOAc 95:5) as a wax-like solid (550 mg, 88%).

¹H NMR (400 MHz, CDCl₃) δ = 6.69 – 6.62 (m, 4H), 6.61 – 6.51 (m, 7H), 4.52 (s, 2H), 4.48 (d, *J* = 13.3 Hz, 2H), 4.46 (d, *J* = 13.3 Hz, 2H), 3.91 – 3.81 (m, 8H), 3.17 (d, *J* = 13.4 Hz, 2H), 3.15 (d, *J* = 13.4 Hz, 2H), 2.01 – 1.89 (m, 8H), 1.11 – 1.06 (m, 18H), 1.06 – 0.98 (m, 15H).

¹³C NMR (101 MHz, CDCl₃) δ = 156.7 (C_q), 156.6 (C_q), 155.4 (C_q), 135.3 (C_q), 135.2 (C_q), 135.1 (C_q), 134.7 (C_q), 134.6 (C_q), 128.3 (CH), 128.1 (2 x CH), 125.6 (CH), 121.9 (CH), 121.6 (CH),

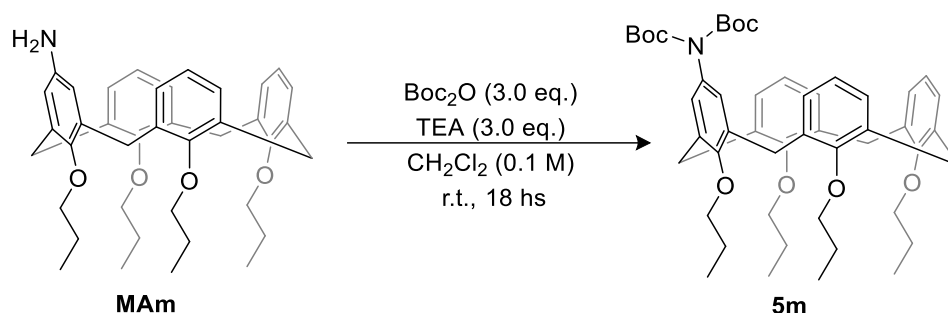
Chapter 4

76.7 (CH₂), 76.7 (CH₂), 76.7 (CH₂), 64.8 (CH₂), 31.1 (CH₂), 31.0 (CH₂), 23.3 (2 x CH₂), 23.3 (CH₂), 18.1 (CH₃), 12.1 (CH), 10.4 (CH₃), 10.4 (CH₃), 10.3 (CH₃).

LC-MS: m/z [M + Na]⁺ calculated for C₅₀H₇₀NaO₅Si: 801.49; found: 801.57.

HR-MS (ESI): m/z [M + Na]⁺ calculated for C₅₀H₇₀NaO₅Si: 801.4993; found: 801.4989.

Substrate 5m:



Into a two-necked round-bottom flask, under N₂ atmosphere, di-*tert*-butyl dicarbonate (367 mg, 3.0 eq.) and triethylamine (0.234 mL, 3.0 eq.) were added to a solution of **MAm** (396 mg, 0.56 mmol) in CH₂Cl₂ (0.1 M). The mixture was left under magnetic stirring at r.t. for 18 hs. After 18 hs, analysis by TLC (*n*-Hexane:EtOAc 9:1) showed complete consumption of **MAm**. The mixture was quenched with the addition of water (20 mL). The organic layers were extracted, washed with water (2 x 15 mL) and brine (15 mL), dried over Na₂SO₄, filtered and the solvent removed under reduced pressure. The crude was purified by column chromatography on silica gel (*n*-Hexane:EtOAc 9:1) yielding **5m** as a white solid (378 mg, 83%). **M.p.:** 188 – 190 °C.

¹H NMR (400 MHz, CDCl₃) δ = 7.15 (d, *J* = 7.4 Hz, 2H), 6.95 (t, *J* = 7.4 Hz, 1H), 6.92 (s, 2H), 6.21 – 6.09 (m, 6H), 4.47 (d, *J* = 13.3 Hz, 4H), 4.11 – 4.00 (m, 4H), 3.74 – 3.64 (m, 4H), 3.17 (d, *J* = 13.3 Hz, 2H), 3.13 (d, *J* = 13.3 Hz, 2H), 2.05 – 1.85 (m, 8H), 1.48 (s, 18H), 1.13 (t, *J* = 7.4 Hz, 6H), 0.91 (t, *J* = 7.5, 3H), 0.90 (t, *J* = 7.5, 3H).

¹³C NMR (101 MHz, CDCl₃) δ = 158.0 (C_q), 157.2 (C_q), 155.2 (C_q), 152.2 (C_q), 137.3 (C_q), 137.1 (C_q), 133.3 (C_q), 133.0 (C_q), 132.7 (C_q), 129.0 (CH), 128.1 (CH), 127.4 (CH), 127.3 (CH), 121.8

Chapter 4

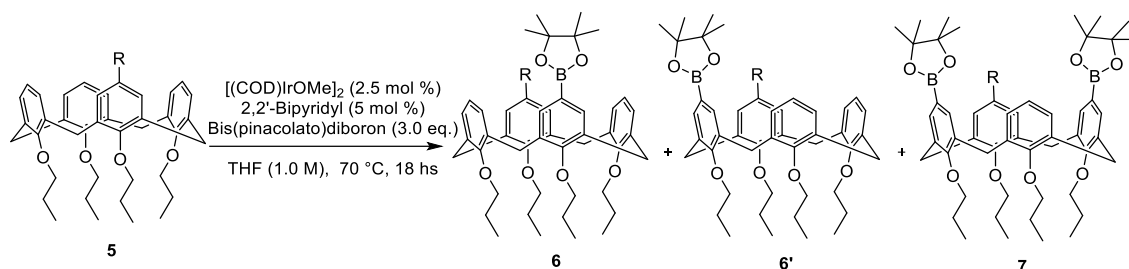
(CH), 121.8 (CH), 82.2 (C_q), 77.0 (CH₂), 76.4 (CH₂), 76.4 (CH₂), 31.0 (CH₂), 30.8 (CH₂), 28.0 (CH₃), 23.5 (CH₂), 23.0 (CH₂), 23.0 (CH₂), 10.9 (CH₃), 10.0 (CH₃), 9.8 (CH₃).

LC-MS: m/z [M + Na]⁺ calculated for C₅₀H₆₅NNaO₈: 830.47; found: 830.48.

HR-MS (ESI): m/z [M + Na]⁺ calculated for C₅₀H₆₅NNaO₈: 830.4710; found: 830.4716.

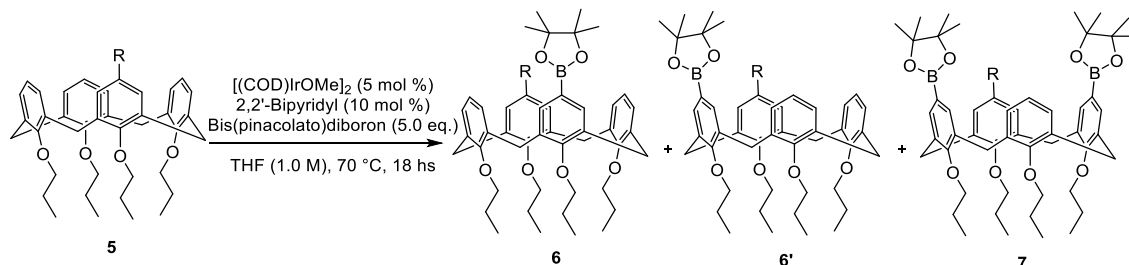
- **General Procedures for catalytic reactions**

Method A:



To a stirred solution of [(COD)IrOMe]₂ (2.5 mol %), 2,2'-bipyridyl (5.0 mol %) and substrate **5** (0.3 mmol) in anhydrous THF (0.3 mL, 1.0 M), bis(pinacolato)diboron (0.9 mmol, 3.0 eq.) was added in a single portion under nitrogen atmosphere. Then, the mixture was placed in a pre-heated oil bath at 70 °C. After stirring for 18 hs, the reaction was cooled down at room temperature, diluted with CH₂Cl₂ (4 mL) and filtered through a pad of celite. After washing with additional CH₂Cl₂ (3 x 5 mL), the combined organic extracts were concentrated under reduced pressure. The crude was purified by column chromatography on silica gel (*n*-Hexane/EtOAc).

Method B:



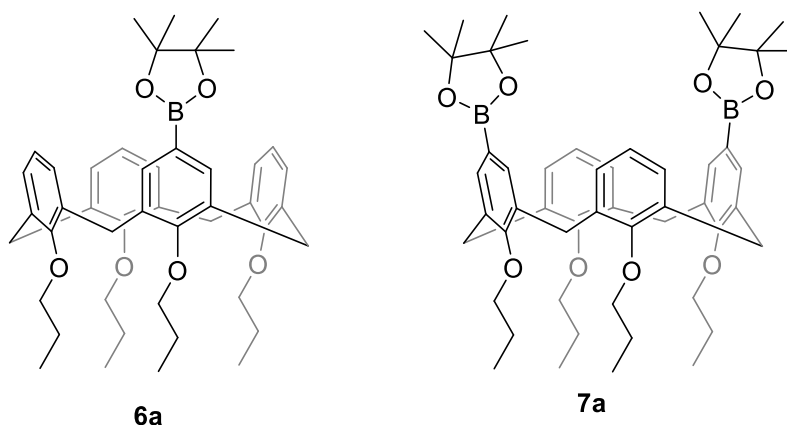
To a stirred solution of [(COD)IrOMe]₂ (5.0 mol %), 2,2'-bipyridyl (10.0 mol %) and substrate **5** (0.3 mmol) in anhydrous THF (0.3 mL, 1.0 M), bis(pinacolato)diboron (1.5 mmol, 5.0 eq.)

Chapter 4

was added in a single portion under nitrogen atmosphere. Then, the mixture was placed in a pre-heated oil bath at 70 °C. After stirring for 18 hs, the reaction was cooled down at room temperature, diluted with CH₂Cl₂ (4 mL) and filtered through a pad of celite. After washing with additional CH₂Cl₂ (3 x 5 ml), the combined organic extracts were concentrated under reduced pressure. The crude was purified by column chromatography on silica gel (*n*-Hexane/EtOAc).

- **Synthesis and characterizations of borylated products 2 and 3**

Products 6a+7a



Method **A** was followed using substrate **TP** (178 mg, 0.3 mmol). Purification by column chromatography on silica gel (*n*-Hexane:EtOAc 95:5) allowed to isolate **6a** (54.4 mg, 25%) as a white solid and **7a** (142.1 mg, 56%) as a white solid.

6a. M.p.: 208 – 210 °C. **¹H NMR** (400 MHz, CDCl₃) δ = 7.54 (s, 2H), 7.06 (d, *J* = 7.4 Hz, 2H), 6.91 – 6.85 (m, 1H), 6.31 (t, *J* = 7.5 Hz, 2H), 6.27 – 6.24 (m, 2H), 6.22 (dd, *J* = 7.4, 2.0 Hz, 2H), 4.50 (d, *J* = 13.4 Hz, 2H), 4.46 (d, *J* = 13.4 Hz, 2H), 4.11 – 4.00 (m, 4H), 3.74 (td, *J* = 7.0, 2.1 Hz, 4H), 3.23 (d, *J* = 13.5 Hz, 2H), 3.18 (d, *J* = 13.4 Hz, 2H), 2.05 – 1.86 (m, 8H), 1.41 (s, 12H), 1.12 (t, *J* = 7.4 Hz, 6H), 0.97 – 0.89 (m, 6H).

¹³C NMR (101 MHz, CDCl₃) δ = 160.9 (C_q), 157.8 (C_q), 155.3 (C_q), 136.8 (C_q), 136.3 (C_q), 135.6 (CH), 133.4 (C_q), 133.4 (C_q), 128.8 (CH), 127.7 (CH), 127.4 (CH), 122.0 (CH), 121.7 (CH), 83.5 (C_q), 76.9 (CH₂), 76.5 (CH₂), 76.4 (CH₂), 31.0 (CH₂), 30.8 (CH₂), 25.0 (CH₃), 23.5 (CH₂), 23.1 (CH₂), 23.0 (CH₂), 10.8 (CH₃), 9.9 (CH₃), 9.9 (CH₃). The carbon directly attached to the boron

Chapter 4

atom was not detected due to quadrupolar broadening.^[29]

LC-MS: m/z $[M + Na]^+$ calculated for $C_{46}H_{59}BNaO_6$: 741.43; found: 741.64.

HR-MS (ESI): m/z $[M + Na]^+$ calculated for $C_{46}H_{59}BNaO_6$: 741.4318; found: 741.4321.

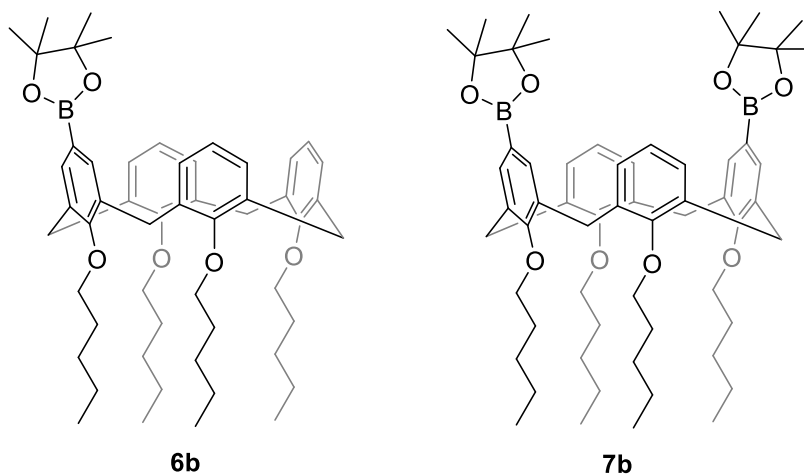
7a. M.p.: (Decomp.) **1H NMR** (400 MHz, $CDCl_3$) δ = 7.62 (s, 4H), 6.23 (d, J = 7.0 Hz, 1H), 6.21 (d, J = 7.4 Hz, 1H), 6.12 (d, J = 7.5 Hz, 4H), 4.44 (d, J = 13.4 Hz, 4H), 4.13 – 4.06 (m, 4H), 3.68 (t, J = 6.7 Hz, 4H), 3.22 (d, J = 13.4 Hz, 4H), 2.02 – 1.84 (m, 8H), 1.42 (s, 24H), 1.12 (t, J = 7.4 Hz, 6H), 0.88 (t, J = 7.5 Hz, 6H).

^{13}C NMR (101 MHz, $CDCl_3$) δ = 161.2 (C_q), 155.0 (C_q), 136.7 (C_q), 135.7 (CH), 133.0 (C_q), 127.5 (CH), 122.1 (CH), 83.6 (C_q), 76.9 (CH_2), 76.4 (CH_2), 30.8 (CH_2), 25.0 (CH_3), 23.6 (CH_2), 23.0 (CH_2), 10.9 (CH_3), 9.8 (CH_3). The carbons directly attached to the boron atom were not detected due to quadrupolar broadening.^[29]

LC-MS: m/z $[M + Na]^+$ calculated for $C_{52}H_{70}B_2NaO_8$: 867.52; found: 867.75.

HR-MS (ESI): m/z $[M + K]^+$ calculated for $C_{46}H_{59}BKO_6$: 883.4925; found: 883.4922.

Product 6b+7b



Method **A** was followed using substrate **5b** (212 mg, 0.3 mmol). Purification by column chromatography on silica gel (*n*-Hexane:EtOAc 95:5) allowed to isolate **6b** as a white solid (60.2 mg, 24%) and **7b** (133.6 mg, 47%) as a white solid.

Chapter 4

6b. M.p.: 163 – 165 °C **¹H NMR** (400 MHz, CDCl₃) δ = 7.53 (s, 2H), 7.05 (d, *J* = 7.4 Hz, 2H), 6.88 (t, *J* = 7.4 Hz, 1H), 6.29 (t, *J* = 7.5 Hz, 2H), 6.25 – 6.21 (m, 2H), 6.19 (dd, *J* = 7.4, 1.9 Hz, 2H), 4.47 (d, *J* = 13.3 Hz, 2H), 4.44 (d, *J* = 13.3 Hz, 2H), 4.13 – 4.04 (m, 4H), 3.75 (td, *J* = 6.8, 1.2 Hz, 4H), 3.22 (d, *J* = 13.4 Hz, 2H), 3.17 (d, *J* = 13.5 Hz, 2H), 2.00 – 1.84 (m, 8H), 1.57 – 1.50 (m, 4H), 1.47 – 1.36 (m, 20H), 1.30 – 1.22 (m, 4H), 1.00 – 0.94 (m, 12H).

¹³C NMR (101 MHz, CDCl₃) δ = 160.9 (C_q), 157.8 (C_q), 155.4 (C_q), 136.9 (C_q), 136.4 (C_q), 135.5 (CH), 133.5 (C_q), 133.4 (C_q), 128.8 (CH), 127.7 (CH), 127.4 (CH), 122.0 (CH), 121.8 (CH), 83.5 (C_q), 75.3 (CH₂), 75.0 (CH₂), 74.9 (CH₂), 31.0 (CH₂), 30.9 (CH₂), 30.2 (CH₂), 29.8 (2 x CH₂), 28.7 (CH₂), 28.2 (CH₂), 28.1 (CH₂), 25.0 (CH₃), 22.9 (CH₂), 22.9 (CH₂), 22.7 (CH₂), 14.3 (CH₃), 14.3 (CH₃), 14.1 (CH₃). The carbon directly attached to the boron atom was not detected due to quadrupolar broadening.^[29]

LC-MS: *m/z* [M + Na]⁺ calculated for C₅₄H₇₅BNaO₆: 853.56; found: 853.73.

HR-MS (ESI): *m/z* [M + Na]⁺ calculated for C₅₄H₇₅BNaO₆: 853.5657; found: 853.5662.

7b. M.p.: 240 – 242 °C. **¹H NMR** (400 MHz, CDCl₃) δ = 7.63 (s, 4H), 6.22 (dd, *J* = 8.2, 6.8 Hz, 2H), 6.12 (d, *J* = 7.5 Hz, 4H), 4.44 (d, *J* = 13.3 Hz, 4H), 4.18 – 4.10 (m, 4H), 3.71 (t, *J* = 6.5 Hz, 4H), 3.22 (d, *J* = 13.4 Hz, 4H), 2.00 – 1.83 (m, 8H), 1.63 – 1.54 (m, 4H), 1.51 – 1.35 (m, 32H), 1.28 – 1.16 (m, 4H), 0.97 (t, *J* = 7.3 Hz, 6H), 0.95 (t, *J* = 7.3 Hz, 6H).

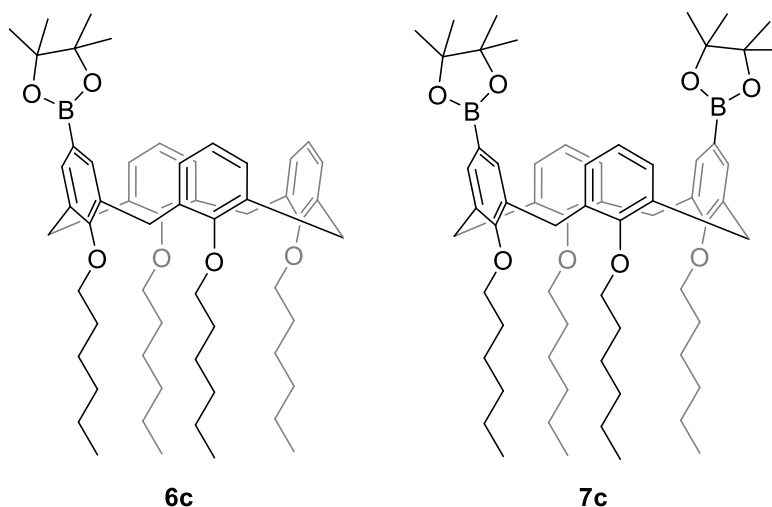
¹³C NMR (101 MHz, CDCl₃) δ = 161.2 (C_q), 155.1 (C_q), 136.7 (C_q), 135.7 (CH), 133.0 (C_q), 127.5 (CH), 122.1 (CH), 83.6 (C_q), 75.3 (CH₂), 74.9 (CH₂), 30.8 (CH₂), 30.3 (CH₂), 29.7 (CH₂), 28.7 (CH₂), 28.1 (CH₂), 25.0 (CH₃), 22.9 (CH₂), 22.7 (CH₂), 14.3 (CH₃), 14.1 (CH₃). The carbons directly attached to the boron atom were not detected due to quadrupolar broadening.^[29]

LC-MS: *m/z* [M + Na]⁺ calculated for C₆₀H₈₆B₂NaO₈: 979.65; found: 979.81.

HR-MS (ESI): *m/z* [M + Na]⁺ calculated for C₆₀H₈₆B₂NaO₈: 979.6509; found: 979.6512.

Chapter 4

Product 6c+7c:



Method **A** was followed using substrate **5c** (228 mg, 0.3 mmol). Purification by column chromatography on silica gel (*n*-Hexane:EtOAc 95:5) allowed to isolate **6c** (59.7 mg, 41%) as a white solid and **7c** (127.3 mg, 42%) as a white solid.

6c. M.p.: 87 – 89 °C **¹H NMR** (400 MHz, CDCl₃) δ = 7.54 (s, 2H), 7.06 (d, *J* = 7.4 Hz, 2H), 6.88 (t, *J* = 7.4 Hz, 1H), 6.29 (t, *J* = 7.5 Hz, 2H), 6.26 – 6.22 (m, 2H), 6.20 (dd, *J* = 7.4, 1.9 Hz, 2H), 4.48 (d, *J* = 13.3 Hz, 2H), 4.44 (d, *J* = 13.3 Hz, 2H), 4.14 – 4.03 (m, 4H), 3.78 – 3.71 (m, 4H), 3.22 (d, *J* = 13.4 Hz, 2H), 3.17 (d, *J* = 13.4 Hz, 2H), 2.03 – 1.85 (m, 8H), 1.61 – 1.53 (m, 4H), 1.43 – 1.34 (m, 28H), 1.31 – 1.24 (m, 4H), 1.00 – 0.91 (m, 12H).

¹³C NMR (101 MHz, CDCl₃) δ = 160.9 (C_q), 157.8 (C_q), 155.4 (C_q), 136.9 (C_q), 136.4 (C_q), 135.5 (CH), 133.5 (C_q), 133.4 (C_q), 128.8 (CH), 127.7 (CH), 127.4 (CH), 122.0 (CH), 121.8 (CH), 83.5 (C_q), 75.3 (CH₂), 75.1 (CH₂), 75.0 (CH₂), 32.2 (CH₂), 32.2 (CH₂), 32.0 (CH₂), 31.0 (CH₂), 30.9 (CH₂), 30.5 (CH₂), 30.1 (2 x CH₂), 26.2 (CH₂), 25.7 (CH₂), 25.7 (CH₂), 25.0 (CH₃), 23.0 (CH₂), 22.9 (CH₂), 22.8 (CH₂), 14.2 (CH₃), 14.1 (2 x CH₃). The carbon directly attached to the boron atom was not detected due to quadrupolar broadening.^[29]

LC-MS: *m/z* [M + Na]⁺ calculated for C₅₈H₈₃BNaO₆: 909.62; found: 909.84.

HR-MS (ESI): *m/z* [M + Na]⁺ calculated for C₅₈H₈₃BNaO₆: 909.6204; found: 979.6213.

7c. M.p.: 109 – 111 °C. **¹H NMR** (400 MHz, CDCl₃) δ = 7.63 (s, 4H), 6.22 (dd, *J* = 8.2, 6.8 Hz, 2H), 6.12 (d, *J* = 7.5 Hz, 4H), 4.44 (d, *J* = 13.3 Hz, 4H), 4.17 – 4.09 (m, 4H), 3.71 (t, *J* = 6.5 Hz,

Chapter 4

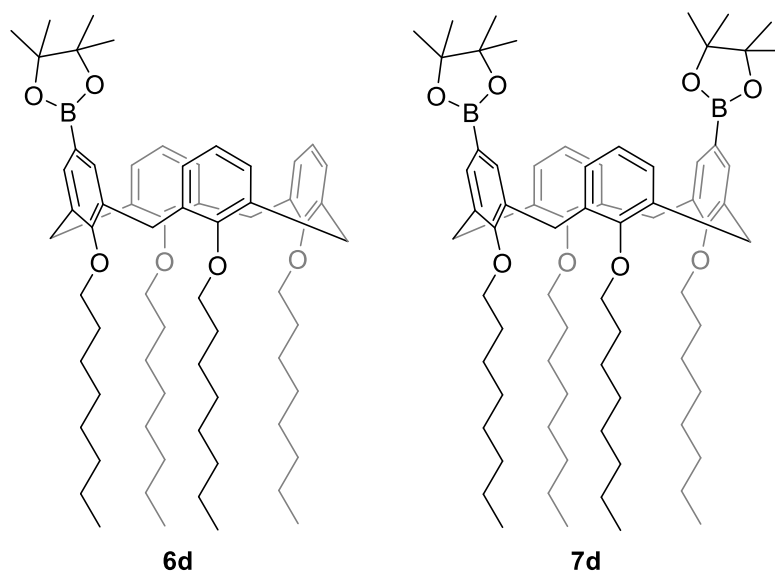
4H), 3.22 (d, $J = 13.4$ Hz, 4H), 1.99 – 1.83 (m, 8H), 1.64 – 1.56 (m, 4H), 1.44 – 1.32 (m, 40H), 1.28 – 1.18 (m, 4H), 0.94 (t, $J = 6.8$ Hz, 6H), 0.93 (t, $J = 6.8$ Hz, 6H).

$^{13}\text{C NMR}$ (101 MHz, CDCl_3) $\delta = 161.2$ (C_q), 155.1 (C_q), 136.8 (C_q), 135.7 (CH), 133.0 (C_q), 127.5 (CH), 122.1 (CH), 83.6 (C_q), 75.3 (CH_2), 75.0 (CH_2), 32.2 (CH_2), 31.9 (CH_2), 30.8 (CH_2), 30.6 (CH_2), 30.1 (CH_2), 26.3 (CH_2), 25.6 (CH_2), 25.0 (CH_3), 23.0 (CH_2), 22.7 (CH_2), 14.2 (CH_3), 14.1 (CH_3). The carbons directly attached to the boron atom were not detected due to quadrupolar broadening.^[29]

LC-MS: m/z $[\text{M} + \text{Na}]^+$ calculated for $\text{C}_{64}\text{H}_{94}\text{B}_2\text{NaO}_8$: 1035.71; found: 1035.87.

HR-MS (ESI): m/z $[\text{M} + \text{Na}]^+$ calculated for $\text{C}_{64}\text{H}_{94}\text{B}_2\text{NaO}_8$: 1035.7135; found: 1035.7139.

Product 6d+7d:



Method **A** was followed using substrate **5d** (262 mg, 0.3 mmol). Purification by column chromatography on silica gel (n -Hexane:EtOAc 95:5) allowed to isolate **6d** (60.2 mg, 60%) as a white solid and **7d** (38.8mg, 12%) as a white solid.

6d. M.p.: 60 – 62 °C $^1\text{H NMR}$ (400 MHz, CDCl_3) $\delta = 7.56$ (s, 2H), 7.07 (d, $J = 7.4$ Hz, 2H), 6.90 (t, $J = 7.4$ Hz, 1H), 6.31 (t, $J = 7.4$ Hz, 2H), 6.27 – 6.24 (m, 2H), 6.22 (dd, $J = 7.3, 1.9$ Hz, 2H), 4.50 (d, $J = 13.3$ Hz, 2H), 4.46 (d, $J = 13.3$ Hz, 2H), 4.16 – 4.05 (m, 4H), 3.76 (td, $J = 6.7, 1.5$

Chapter 4

Hz, 4H), 3.24 (d, $J = 13.4$ Hz, 2H), 3.19 (d, $J = 13.4$ Hz, 2H), 2.06 – 1.85 (m, 8H), 1.64 – 1.52 (m, 4H), 1.45 – 1.29 (m, 48H), 0.98 – 0.91 (m, 12H).

^{13}C NMR (101 MHz, CDCl_3) $\delta = 160.9$ (C_q), 157.8 (C_q), 155.4 (C_q), 136.9 (C_q), 136.4 (C_q), 133.5 (C_q), 133.4 (C_q), 128.8 (CH), 128.1 (CH), 127.7 (CH), 127.4 (CH), 122.0 (CH), 121.7 (CH), 83.5 (C_q), 75.3 (CH_2), 75.2 (CH_2), 75.1 (CH_2), 75.0 (CH_2), 32.0 (CH_2), 31.0 (CH_2), 30.9 (CH_2), 30.6 (CH_2), 30.4 (CH_2), 30.2 (CH_2), 30.1 (CH_2), 30.0 (2 x CH_2), 29.8 (CH_2), 29.8 (CH_2), 29.8 (CH_2), 29.7 (CH_2), 29.5 (CH_2), 26.6 (CH_2), 26.4 (CH_2), 26.1 (CH_2), 25.0 (CH_3), 22.8 (CH_2), 22.7 (CH_2), 14.1 (3 x CH_3). The carbon directly attached to the boron atom was not detected due to quadrupolar broadening.^[29]

LC-MS: m/z $[\text{M} + \text{Na}]^+$ calculated for $\text{C}_{66}\text{H}_{99}\text{BNaO}_6$: 1021.75; found: 1021.91.

HR-MS (ESI): m/z $[\text{M} + \text{Na}]^+$ calculated for $\text{C}_{66}\text{H}_{99}\text{BNaO}_6$: 1021.7535; found: 1021.7539.

7d. M.p.: 88 – 90 °C **^1H NMR** (400 MHz, CDCl_3) $\delta = 7.63$ (s, 4H), 6.23 (dd, $J = 8.2, 6.8$ Hz, 2H), 6.13 (d, $J = 7.5$ Hz, 4H), 4.44 (d, $J = 13.3$ Hz, 4H), 4.17 – 4.11 (m, 4H), 3.71 (t, $J = 6.5$ Hz, 4H), 3.23 (d, $J = 13.4$ Hz, 4H), 2.01 – 1.83 (m, 8H), 1.64 – 1.55 (m, 4H), 1.43 (s, 24H), 1.42 – 1.27 (m, 32H), 1.28 – 1.19 (m, 4H), 0.97 – 0.89 (m, 12H).

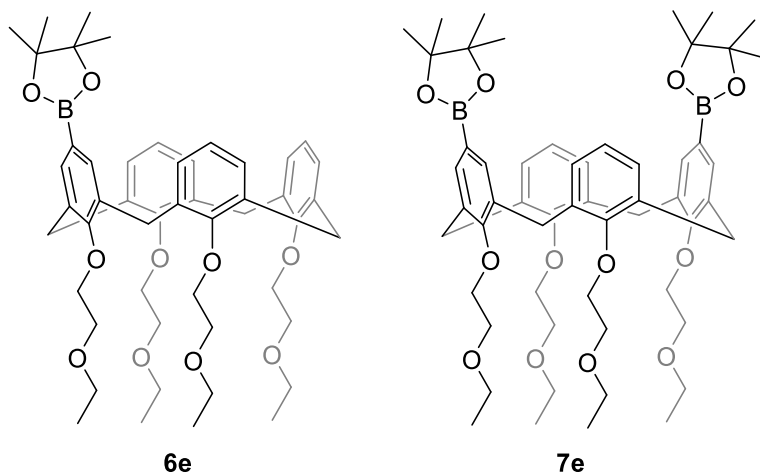
^{13}C NMR (101 MHz, CDCl_3) $\delta = 161.2$ (C_q), 155.1 (C_q), 136.7 (C_q), 135.7 (CH), 133.1 (C_q), 127.5 (CH), 122.1 (CH), 83.6 (C_q), 75.3 (CH_2), 75.0 (CH_2), 32.0 (CH_2), 32.0 (CH_2), 30.8 (CH_2), 30.6 (CH_2), 30.2 (CH_2), 30.1 (CH_2), 29.8 (2 x CH_2), 29.5 (CH_2), 26.7 (CH_2), 26.1 (CH_2), 25.0 (CH_3), 22.8 (CH_2), 22.7 (CH_2), 14.1 (2 x CH_3). The carbon directly attached to the boron atom was not detected due to quadrupolar broadening.^[29]

LC-MS: m/z $[\text{M} + \text{Na}]^+$ calculated for $\text{C}_{72}\text{H}_{110}\text{B}_2\text{NaO}_8$: 1147.83; found: 1147.95.

HR-MS (ESI): m/z $[\text{M} + \text{Na}]^+$ calculated for $\text{C}_{72}\text{H}_{110}\text{B}_2\text{NaO}_8$: 1147.8387; found: 1147.8392.

Chapter 4

Product 6e+7e:



Method **A** was followed using substrate **5e** (214 mg, 0.3 mmol). Purification by column chromatography on silica gel (*n*-Hexane:EtOAc 95:5) allowed to isolate **6e** (14.3 mg, 6%) as a white solid and **7e** (173.2 mg, 60%) as a white solid.

6e. M.p.: 183 – 185 °C **¹H NMR** (400 MHz, CDCl₃) δ = 7.53 (s, 2H), 7.05 (d, *J* = 7.4 Hz, 2H), 6.88 (t, *J* = 7.4 Hz, 1H), 6.33 – 6.22 (m, 6H), 4.52 (d, *J* = 13.4 Hz, 2H), 4.50 (d, *J* = 13.4 Hz, 2H), 4.32 (q, *J* = 6.9 Hz, 4H), 3.98 (t, *J* = 5.1 Hz, 4H), 3.92 (q, *J* = 6.8 Hz, 4H), 3.81 (t, *J* = 5.1 Hz, 4H), 3.64 – 3.49 (m, 8H), 3.22 (d, *J* = 13.4 Hz, 2H), 3.17 (d, *J* = 13.4 Hz, 2H), 1.40 (s, 12H), 1.26 (t, *J* = 7.0 Hz, 6H), 1.20 (t, *J* = 7.0 Hz, 3H), 1.18 (t, *J* = 7.0 Hz, 3H).

¹³C NMR (101 MHz, CDCl₃) δ = 160.9 (C_q), 157.8 (C_q), 154.8 (C_q), 136.6 (C_q), 136.1 (C_q), 135.5 (CH), 133.5 (C_q), 133.5 (C_q), 128.7 (CH), 127.9 (CH), 127.6 (CH), 122.3 (CH), 122.1 (CH), 83.5 (C_q), 73.8 (CH₂), 72.5 (CH₂), 72.5 (CH₂), 69.7 (CH₂), 69.7 (2 x CH₂), 66.5 (CH₂), 66.2 (2 x CH₂), 30.9 (CH₂), 30.7 (CH₂), 25.0 (CH₃), 15.4 (2 x CH₃), 15.3 (CH₃). The carbon directly attached to the boron atom was not detected due to quadrupolar broadening.^[29]

LC-MS: *m/z* [M + Na]⁺ calculated for C₅₂H₆₇BNaO₈: 861.48; found: 861.56.

HR-MS (ESI): *m/z* [M + Na]⁺ calculated for C₅₂H₆₇BNaO₈: 861.4827; found: 861.4831.

7e. M.p.: 246 – 248 °C **¹H NMR** (400 MHz, CDCl₃) δ = 7.61 (s, 4H), 6.25 (dd, *J* = 8.4, 6.5 Hz, 2H), 6.17 (d, *J* = 7.5 Hz, 4H), 4.51 (d, *J* = 13.3 Hz, 4H), 4.36 (t, *J* = 6.5 Hz, 4H), 3.95 (dd, *J* = 5.9, 4.0 Hz, 4H), 3.91 (t, *J* = 6.5 Hz, 4H), 3.79 (dd, *J* = 5.9, 4.0 Hz, 4H), 3.60 (q, *J* = 7.0 Hz, 4H), 3.51

Chapter 4

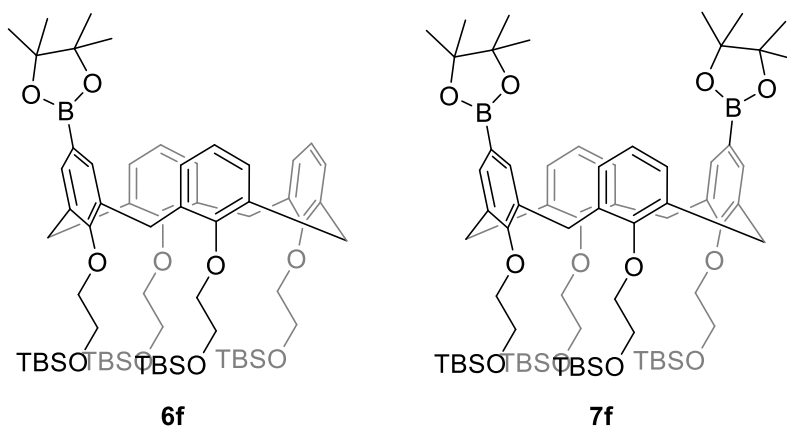
(q, $J = 7.0$ Hz, 4H), 3.22 (d, $J = 13.5$ Hz, 4H), 1.42 (s, 24H), 1.26 (t, $J = 7.0$ Hz, 6H), 1.18 (t, $J = 7.0$ Hz, 6H).

$^{13}\text{C NMR}$ (101 MHz, CDCl_3) $\delta = 161.3$ (C_q), 154.5 (C_q), 136.4 (C_q), 135.6 (CH), 133.2 (C_q), 127.7 (CH), 122.3 (CH), 83.6 (C_q), 73.9 (CH_2), 72.5 (CH_2), 69.7 (CH_2), 69.6 (CH_2), 66.5 (CH_2), 66.2 (CH_2), 30.7 (CH_2), 25.0 (CH_3), 15.4 (CH_3), 15.3 (CH_3). The carbon directly attached to the boron atom was not detected due to quadrupolar broadening.^[29]

LC-MS: m/z $[\text{M} + \text{Na}]^+$ calculated for $\text{C}_{56}\text{H}_{78}\text{B}_2\text{NaO}_{12}$: 987.56; found: 987.65.

HR-MS (ESI): m/z $[\text{M} + \text{Na}]^+$ calculated for $\text{C}_{56}\text{H}_{78}\text{B}_2\text{NaO}_{12}$: 987.5586; found: 987.5589.

Product 6f+7f:



Method **A** was followed using substrate **5f** (318 mg, 0.3 mmol). Purification by column chromatography on silica gel (*n*-Hexane:EtOAc 95:5) allowed to isolate **6f** (115.3 mg, 32%) as a white solid and **7f** (64.4 mg, 16%) as a white solid.

6f. M.p.: 90 – 92 °C. $^1\text{H NMR}$ (400 MHz, CDCl_3) $\delta = 7.49$ (s, 2H), 7.01 (d, $J = 7.4$ Hz, 2H), 6.84 (t, $J = 7.4$ Hz, 1H), 6.29 (t, $J = 7.5$ Hz, 2H), 6.26 – 6.21 (m, 2H), 6.19 (dd, $J = 7.4, 1.9$ Hz, 2H), 4.53 (d, $J = 13.4$ Hz, 2H), 4.49 (d, $J = 13.4$ Hz, 2H), 4.24 – 4.15 (m, 4H), 4.07 – 3.97 (m, 8H), 3.89 (t, $J = 5.9$ Hz, 4H), 3.20 (d, $J = 13.5$ Hz, 2H), 3.15 (d, $J = 13.5$ Hz, 2H), 1.40 (s, 12H), 0.92 (s, 18H), 0.86 (s, 9H), 0.85 (s, 9H), 0.09 (s, 12H), 0.02 (s, 12H).

$^{13}\text{C NMR}$ (101 MHz, CDCl_3) $\delta = 161.2$ (C_q), 158.0 (C_q), 155.0 (C_q), 136.5 (C_q), 135.9 (C_q), 135.5 (CH), 133.4 (C_q), 133.4 (C_q), 128.7 (CH), 127.8 (CH), 127.5 (CH), 122.2 (CH), 121.8 (CH), 83.5

Chapter 4

(C_q), 76.1 (CH₂), 75.4 (CH₂), 75.2 (CH₂), 62.7 (CH₂), 62.4 (CH₂), 62.1 (CH₂), 31.1 (CH₂), 30.9 (CH₂), 25.9 (2 x CH₃), 25.8 (CH₃), 25.8 (CH₃), 24.9 (CH₃), 18.3 (2 x C_q), 18.1 (C_q), -5.2 (2 x CH₃). The carbon directly attached to the boron atom was not detected due to quadrupolar broadening.^[29]

LC-MS: m/z [M + Na]⁺ calculated for C₆₆H₁₀₇BNaO₁₀Si₄: 1205.70; found: 1205.94.

HR-MS (ESI): m/z [M + Na]⁺ calculated for C₆₆H₁₀₇BNaO₁₀Si₄: 1205.7034; found: 1205.7037.

7f. M.p.: 103 – 105 °C. **¹H NMR** (400 MHz, CDCl₃) δ = 7.58 (s, 4H), 6.22 (dd, J = 8.3, 6.8 Hz, 2H), 6.12 (d, J = 7.5 Hz, 4H), 4.49 (d, J = 13.5 Hz, 4H), 4.23 (t, J = 6.2 Hz, 4H), 4.02 (t, J = 6.2 Hz, 4H), 3.98 (t, J = 5.8 Hz, 4H), 3.86 (t, J = 5.8 Hz, 4H), 3.20 (d, J = 13.5 Hz, 4H), 1.42 (s, 24H), 0.92 (s, 18H), 0.84 (s, 18H), 0.10 (s, 12H), 0.01 (s, 12H).

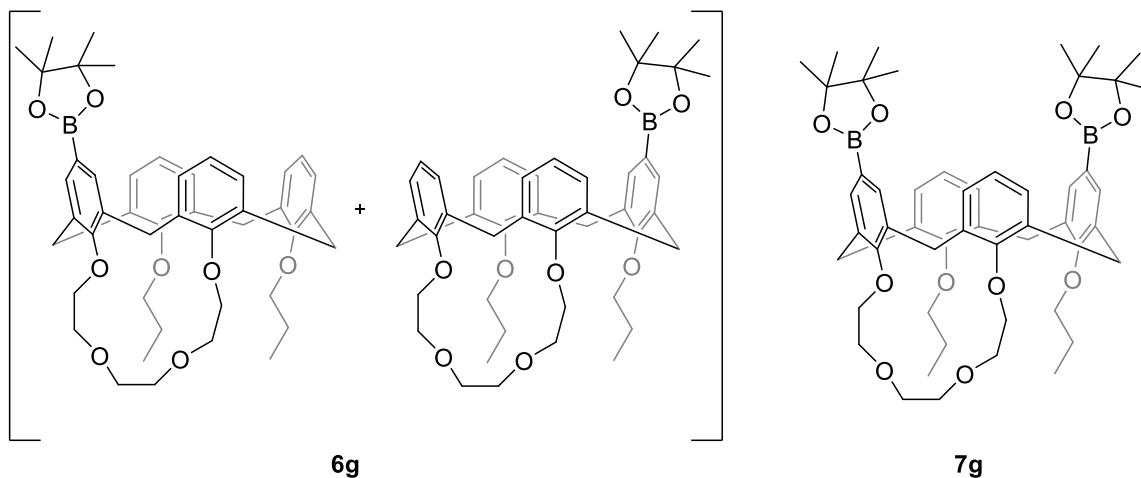
¹³C NMR (101 MHz, CDCl₃) δ = 161.6 (C_q), 154.6 (C_q), 136.2 (C_q), 135.6 (CH), 133.1 (C_q), 127.6 (CH), 122.3 (CH), 83.5 (C_q), 76.2 (CH₂), 75.2 (CH₂), 62.5 (CH₂), 62.0 (CH₂), 30.8 (CH₂), 25.9 (CH₃), 25.8 (CH₃), 25.0 (CH₃), 18.3 (C_q), 18.1 (C_q), -5.2 (2 x CH₃). The carbon directly attached to the boron atom was not detected due to quadrupolar broadening.^[29]

LC-MS: m/z [M + Na]⁺ calculated for C₇₂H₁₁₈B₂NaO₁₂Si₄: 1332.78; found: 1332.92.

HR-MS (ESI): m/z [M + K]⁺ calculated for C₇₂H₁₁₈B₂KO₁₂Si₄: 1347.7554; found: 1347.7560.

Chapter 4

Product 6g +7g:



Method **A** was followed using substrate **5g** (187 mg, 0.3 mmol). Purification by column chromatography on silica gel (*n*-Hexane:EtOAc 95:5) allowed to isolate **6g** as an inseparable mixture of regioisomers (74.1 mg, 33%) and **7g** as a white solid (115.6 mg, 45%).

6g. ¹H NMR (400 MHz, CDCl₃) δ = 7.54 – 7.48 (m, 4H), 7.09 – 6.99 (m, 4H), 6.86 (td, *J* = 7.4, 5.6 Hz, 2H), 6.35 – 6.22 (m, 8H), 6.20 (s, 2H), 6.17 (dd, *J* = 7.1, 2.0 Hz, 2H), 4.95 (t, *J* = 13.4 Hz, 2H), 4.76 – 4.64 (m, 2H), 4.47 – 4.37 (m, 5H), 4.37 – 4.28 (m, 3H), 4.13 (td, *J* = 10.5, 5.6 Hz, 2H), 4.09 – 3.94 (m, 6H), 3.93 – 3.82 (m, 8H), 3.81 – 3.65 (m, 12H), 3.27 – 3.08 (m, 8H), 2.06 – 1.94 (m, 4H), 1.88 (h, *J* = 7.2 Hz, 4H), 1.37 (d, *J* = 3.6 Hz, 24H), 1.08 (td, *J* = 7.4, 1.7 Hz, 6H), 0.95 – 0.86 (m, 6H).

LC-MS: *m/z* [M + Na]⁺ calculated for C₄₆H₅₇BNaO₈: 771.41; found: 771.47.

HR-MS (ESI): *m/z* [M + Na]⁺ calculated for C₄₆H₅₇BNaO₈: 771.4146; found: 771.4151.

7g. M.p.: 147 – 149 °C. ¹H NMR (400 MHz, CDCl₃) δ = 7.66 – 7.57 (m, 4H), 6.32 – 6.26 (m, 1H), 6.24 – 6.18 (m, 3H), 6.18 – 6.09 (m, 2H), 4.96 (d, *J* = 13.0 Hz, 1H), 4.84 (dtd, *J* = 11.8, 5.2, 3.4 Hz, 1H), 4.51 – 4.38 (m, 3H), 4.35 (d, *J* = 13.6 Hz, 1H), 4.19 (td, *J* = 10.9, 5.8 Hz, 1H), 4.11 – 3.97 (m, 3H), 3.95 – 3.86 (m, 3H), 3.84 – 3.65 (m, 7H), 3.30 – 3.14 (m, 4H), 2.09 – 1.84 (m, 4H), 1.41 (s, 24H), 1.12 (t, *J* = 7.4 Hz, 3H), 0.90 (t, *J* = 7.5 Hz, 3H).

¹³C NMR (101 MHz, CDCl₃) δ = 161.2 (C_q), 161.1 (C_q), 155.0 (C_q), 154.2 (C_q), 137.2 (C_q), 136.7 (C_q), 136.5 (C_q), 136.0 (CH), 135.8 (CH), 135.6 (CH), 135.6 (C_q), 135.3 (CH), 133.9 (C_q), 133.1

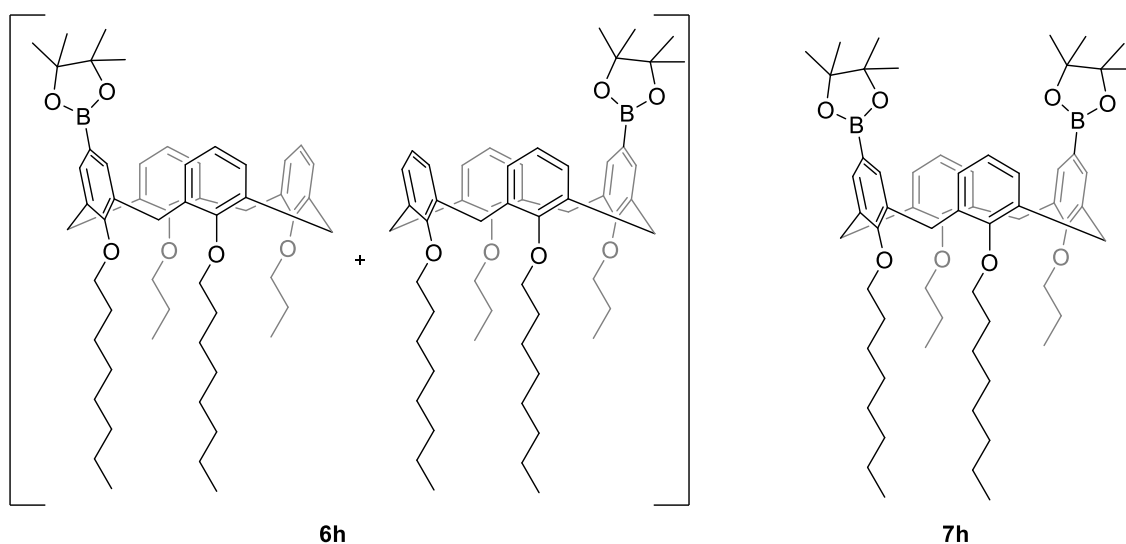
Chapter 4

(C_q), 133.0 (C_q), 132.7 (C_q), 128.1 (CH), 127.7 (CH), 127.6 (CH), 127.4 (CH), 122.3 (CH), 122.2 (CH), 83.6 (C_q), 83.5 (C_q), 77.1 (CH₂), 76.3 (CH₂), 73.4 (CH₂), 73.2 (CH₂), 71.4 (CH₂), 70.8 (CH₂), 70.8 (CH₂), 69.2 (CH₂), 31.0 (CH₂), 30.8 (CH₂), 30.8 (CH₂), 29.8 (CH₂), 25.0 (CH₃), 25.0 (CH₃), 25.0 (CH₃), 23.6 (CH₂), 23.0 (CH₂), 10.9 (CH₃), 9.9 (CH₃). The carbons directly attached to the boron atom were not detected due to quadrupolar broadening.^[29]

LC-MS: m/z [M + Na]⁺ calculated for C₅₂H₆₈B₂NaO₁₀: 897.50; found: 897.61.

HR-MS (ESI): m/z [M + Na]⁺ calculated for C₅₂H₆₈B₂NaO₁₀: 897.4999; found: 897.4994.

Product 6h+7h:



Method **A** and Method **B** were followed using substrate **5h** (220 mg, 0.3 mmol). Purification by column chromatography on silica gel (*n*-Hexane:EtOAc 95:5) allowed to isolate **6h** (method **A**: 125.8 mg, 49%; method **B**: 88.2 mg, 34%) as an inseparable mixture of regioisomers and **7h** (method **A**: 36.1 mg, 12%; method **B**: 146.4 mg, 49%) as a white solid.

6h. ¹H NMR (400 MHz, CDCl₃) δ = 7.52 (s, 4H), 7.04 (d, *J* = 7.4 Hz, 4H), 6.87 (t, *J* = 7.4 Hz, 2H), 6.28 (t, *J* = 7.5 Hz, 4H), 6.24 – 6.20 (m, 4H), 6.18 (dd, *J* = 7.3, 1.9 Hz, 4H), 4.50 – 4.40 (m, 8H), 4.14 – 3.97 (m, 8H), 3.78 – 3.66 (m, 8H), 3.18 (dd, *J* = 20.5, 13.4 Hz, 8H), 2.02 – 1.82 (m, 16H), 1.43 – 1.24 (m, 64H), 1.10 (t, *J* = 7.4 Hz, 6H), 0.94 – 0.87 (m, 18H).

LC-MS: m/z [M + Na]⁺ calculated for C₅₆H₇₉BNaO₆: 881.60; found: 881.67.

Chapter 4

HR-MS (ESI): m/z $[M + Na]^+$ calculated for $C_{56}H_{79}BNaO_6$: 881.5970; found: 881.5975.

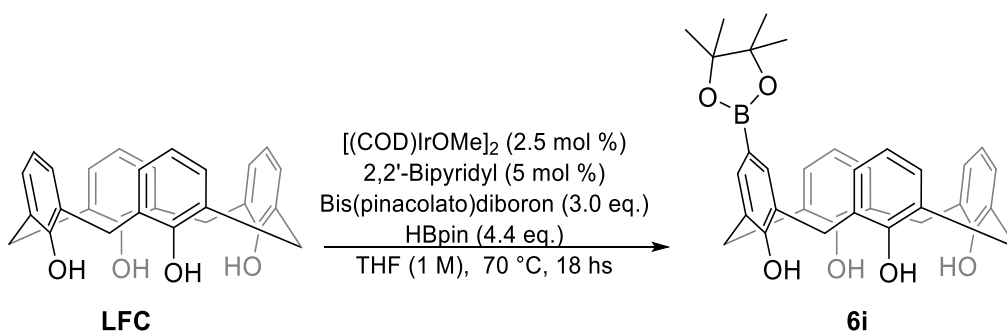
7h. M.p.: 151 – 153 C. **1H NMR** (400 MHz, $CDCl_3$) δ = 7.63 (s, 4H), 6.22 (dd, J = 8.2, 6.8 Hz, 2H), 6.12 (d, J = 7.5 Hz, 4H), 4.47 – 4.40 (m, 4H), 4.17 – 4.05 (m, 4H), 3.71 (t, J = 6.6 Hz, 2H), 3.69 (t, J = 6.6 Hz, 2H), 3.22 (d, J = 13.4 Hz, 4H), 2.00 – 1.82 (m, 8H), 1.64 – 1.54 (m, 2H), 1.42 (s, 24H), 1.39 – 1.28 (m, 16H), 1.27 – 1.20 (m, 2H), 1.13 (t, J = 7.4 Hz, 3H), 0.96 – 0.90 (m, 6H), 0.87 (t, J = 7.5 Hz, 3H).

^{13}C NMR (101 MHz, $CDCl_3$) δ = 161.3 (C_q), 161.2 (C_q), 155.1 (C_q), 155.0 (C_q), 136.7 (C_q), 136.7 (3 x C_q), 135.7 (3 x CH), 135.7 (CH), 133.1 (C_q), 133.1 (C_q), 133.0 (2 x C_q), 127.5 (4 x CH), 122.1 (2 x CH), 83.6 (2 x C_q), 76.9 (CH_2), 76.4 (CH_2), 75.3 (CH_2), 75.1 (CH_2), 32.0 (2 x CH_2), 31.9 (2 x CH_2), 30.8 (2 x CH_2), 30.6 (CH_2), 30.0 (CH_2), 29.8 (CH_2), 29.7 (CH_2), 29.6 (CH_2), 29.4 (CH_2), 26.6 (CH_2), 25.9 (CH_2), 25.0 (2 x CH_3), 23.6 (CH_2), 23.0 (CH_2), 22.7 (2 x CH_2), 14.1 (CH_3), 14.1 (CH_3), 10.9 (CH_3), 9.8 (CH_3). The carbons directly attached to the boron atom were not detected due to quadrupolar broadening.^[29]

LC-MS: m/z $[M + Na]^+$ calculated for $C_{62}H_{90}B_2NaO_8$: 1007.67; found: 1007.77.

HR-MS (ESI): m/z $[M + Na]^+$ calculated for $C_{62}H_{90}B_2NaO_8$: 1007.6822; found: 1007.6826.

Product 6i:



Into a Schlenk tube, under N_2 atmosphere, HBpin (0.192 mL, 4.4 eq.) was added to a solution of **LFC** (127 mg, 0.3 mmol) in THF (1.0 M) and the mixture was left stirring for 20 minutes at r.t. Then, $[(COD)IrOMe]_2$ (2.5 mol %), 2,2'-Bipyridyl (5.0 mol %) and Bis(pinacolato)diboron (3.0 eq.) were added. The mixture was placed into an oil bath and left stirring at 70 °C for 18 hs. After stirring for 18 hs, the reaction was cooled down at room

Chapter 4

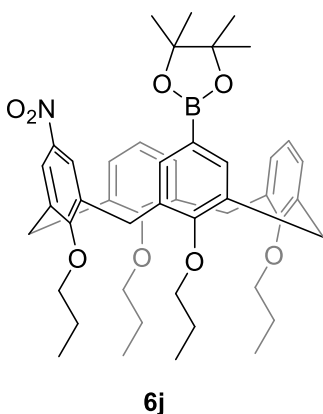
temperature, diluted with CH₂Cl₂ (4 mL) and filtered through a pad of celite. After washing with additional CH₂Cl₂ (3x5 mL), the combined organic extracts were concentrated under reduced pressure. The crude was purified by column chromatography on silica gel (*n*-Hexane:EtOAc 8:2) yielding **6i** as a white solid (60.3 mg, 36%). **M.p.:** (decomp.).

¹H NMR (400 MHz, CDCl₃) δ = 10.23 (s, 4H), 7.54 (s, 2H), 7.16 (dd, *J* = 7.6, 1.6 Hz, 2H), 7.11 – 7.03 (m, 4H), 6.80 – 6.69 (m, 3H), 4.30 (bs, 4H), 3.64 (bs, 4H), 1.30 (s, 12H).

¹³C NMR (101 MHz, CDCl₃) δ = 159.3 (C_q), 151.8 (C_q), 148.7 (C_q), 148.6 (C_q), 135.9 (CH), 129.3 (CH), 128.9 (2 x CH), 128.2 (C_q), 128.1 (C_q), 127.6 (C_q), 122.3 (2 x CH), 83.6 (C_q), 31.7 (CH₂), 31.5 (CH₂), 24.8 (CH₃). The carbon directly attached to the boron atom was not detected due to quadrupolar broadening.^[29]

LC-MS: *m/z* [M + Na]⁺ calculated for C₃₄H₃₅BNaO₆: 573.24; found: 573.33.

HR-MS (ESI): *m/z* [M + NH₄]⁺ calculated for C₃₄H₃₉BNO₆: 568.2870; found: 568.2886.



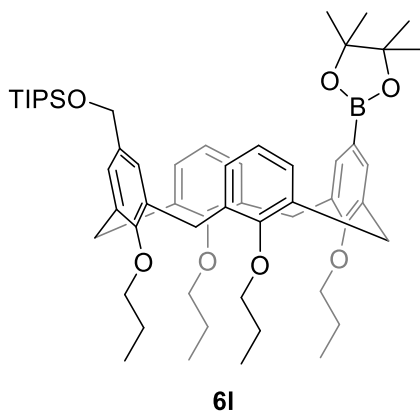
Method **A** and Method **B** were followed using substrate **5j** (191 mg, 0.3 mmol). Product **6j** was isolated by column chromatography on silica gel (*n*-Hexane:EtOAc 95:5) as a yellowish solid (method **A**: 20.1 mg, 9%; method **B**: 34.3 mg, 15%). **M.p.:** 171 – 173 °C.

¹H NMR (400 MHz, CDCl₃) δ = 7.63 (s, 1H), 7.62 (s, 1H), 7.18 (s, 1H), 7.16 (s, 1H), 7.01 (t, *J* = 7.4 Hz, 1H), 6.95 (d, *J* = 2.9 Hz, 1H), 6.92 (d, *J* = 2.9 Hz, 1H), 6.10 – 6.02 (m, 3H), 4.54 – 4.39 (m, 4H),

4.14 – 4.02 (m, 2H), 4.01 – 3.90 (m, 2H), 3.78 (t, *J* = 6.7 Hz, 2H), 3.69 (td, *J* = 6.7, 1.9 Hz, 2H), 3.30 – 3.13 (m, 4H), 1.97 – 1.84 (m, 8H), 1.44 (s, 12H), 1.18 – 1.06 (m, 6H), 0.90 (t, *J* = 7.4 Hz, 3H), 0.88 (t, *J* = 7.4 Hz, 3H).

¹³C NMR (101 MHz, CDCl₃) δ = 160.8 (C_q), 160.7 (C_q), 157.8 (C_q), 155.3 (C_q), 142.8 (C_q), 137.4 (C_q), 136.8 (C_q), 136.5 (CH), 135.8 (2 x C_q), 135.5 (CH), 135.4 (C_q), 135.3 (C_q), 133.3 (C_q), 133.2 (C_q), 129.8 (CH), 128.9 (CH), 127.7 (CH), 127.4 (CH), 123.1 (CH), 123.1 (CH), 122.5 (CH), 121.6 (CH), 83.7 (C_q), 77.1 (CH₂), 77.1 (CH₂), 76.8 (CH₂), 76.6 (CH₂), 76.4 (CH₂), 31.1 (CH₂), 31.0 (CH₂), 30.8 (CH₂), 25.0 (CH₃), 23.5 (CH₂), 23.5 (CH₂), 23.0 (2 x CH₂), 10.8 (CH₃),

Chapter 4



Method **A** and Method **B** were followed using substrate **5l** (234 mg, 0.3 mmol). Product **6l** was isolated by column chromatography on silica gel (*n*-Hexane:EtOAc 95:5) as a wax-like solid (method **A**: 87.9 mg, 32%; method **B**: 152.4 mg, 56%).

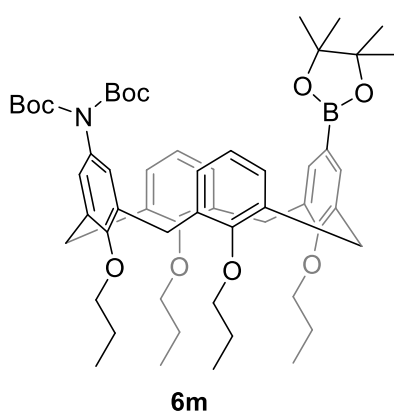
¹H NMR (400 MHz, CDCl₃) δ = 7.61 (s, 2H), 7.12 (s, 2H), 6.21 (t, *J* = 7.5 Hz, 2H), 6.16–6.11 (m, 4H), 4.85 (s, 2H), 4.45 (dd, *J* = 13.3, 6.6 Hz, 4H), 4.10–4.00 (m, 4H), 3.68

(td, *J* = 6.7, 1.6 Hz, 4H), 3.22 (d, *J* = 13.4 Hz, 2H), 3.15 (d, *J* = 13.3 Hz, 2H), 2.02–1.85 (m, 8H), 1.41 (d, *J* = 5.0 Hz, 12H), 1.27–1.07 (m, 26H), 0.92–0.86 (m, 7H)

¹³C NMR (101 MHz, CDCl₃) δ = 161.2 (C_q), 157.0 (C_q), 155.1 (C_q), 136.6 (C_q), 136.6 (C_q), 135.7 (CH), 134.8 (C_q), 133.1 (C_q), 133.1 (C_q), 127.5 (CH), 127.4 (CH), 126.7 (CH), 122.0 (CH), 83.5 (C_q), 76.9 (CH₂), 76.5 (CH₂), 76.4 (CH₂), 65.2 (CH₂), 31.1 (CH₂), 30.8 (CH₂), 25.0 (CH₃), 23.5 (CH₂), 23.0 (CH₂), 23.0 (CH₂), 18.1 (CH₃), 12.2 (CH), 10.8 (CH₃), 9.8 (CH₃), 9.8 (CH₃). The carbon directly attached to the boron atom was not detected due to quadrupolar broadening.^[29]

LC-MS: *m/z* [M + Na]⁺ calculated for C₅₆H₈₁BNaO₇Si: 927.58; found: 927.71.

HR-MS (ESI): *m/z* [M + Na]⁺ calculated for C₅₆H₈₁BNaO₇Si: 927.5845; found: 927.5851.



Method **A** and Method **B** were followed using substrate **5m** (242 mg, 0.3 mmol). Product **6m** was isolated by column chromatography on silica gel (*n*-Hexane:EtOAc 95:5) as a white solid (method **A**: 214.3 mg, 76%, method **B**: 230.8 mg, 82%). **M.p.**: 98–100 °C.

¹H NMR (400 MHz, CDCl₃) δ = 7.62 (s, 2H), 6.93 (s, 2H), 6.21–6.08 (m, 6H), 4.46 (d, *J* = 13.3 Hz, 2H), 4.43 (d, *J* = 13.3 Hz, 2H), 4.12–4.02 (m, 4H), 3.77–3.58 (m, 4H), 3.22

(d, *J* = 13.4 Hz, 2H), 3.13 (d, *J* = 13.4 Hz, 2H), 2.02–1.83 (m, 8H), 1.41 (s, 12H), 1.29 (s, 18H), 1.12 (t, *J* = 7.4 Hz, 6H), 0.89 (dt, *J* = 10.2, 7.4 Hz, 6H).

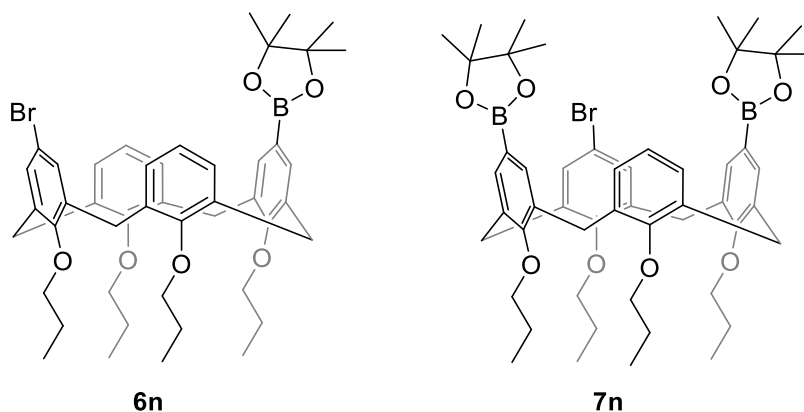
Chapter 4

^{13}C NMR (101 MHz, CDCl_3) δ = 161.2 (C_q), 157.2 (C_q), 155.1 (C_q), 152.2 (C_q), 137.3 (C_q), 136.6 (C_q), 135.7 (CH), 133.2 (C_q), 133.0 (C_q), 132.6 (C_q), 128.1 (CH), 127.6 (CH), 127.3 (CH), 121.8 (CH), 83.6 (C_q), 82.2 (C_q), 77.0 (CH_2), 76.4 (CH_2), 76.3 (CH_2), 30.8 (2 x CH_2), 28.0 (CH_3), 25.0 (CH_3), 23.5 (CH_2), 23.0 (2 x CH_2), 10.9 (CH_3), 9.9 (CH_3), 9.8 (CH_3). The carbon directly attached to the boron atom was not detected due to quadrupolar broadening.^[29]

LC-MS: m/z [$\text{M} + \text{Na}$]⁺ calculated for $\text{C}_{56}\text{H}_{76}\text{BNNaO}_{10}$: 956.55; found: 956.72.

HR-MS (ESI): m/z [$\text{M} + \text{K}$]⁺ calculated for $\text{C}_{56}\text{H}_{81}\text{BKO}_7\text{Si}$: 972.5194; found: 972.5199.

Product 6n+7n:



Method **A** and Method **B** were followed using substrate **5n** (202 mg, 0.3 mmol). Purification by column chromatography on silica gel (*n*-Hexane:EtOAc 95:5) allowed to isolate **6n** (method **A**: 48.0 mg, 20%; method **B**: 44.0 mg, 18%) as a white solid and **7n** (method **A**: 30.2 mg, 11%; method **B**: 106.8 mg, 39%) as a white solid.

6n. M.p.: 226 – 228 °C- **^1H NMR** (400 MHz, CDCl_3) δ = 7.58 (s, 2H), 7.21 (s, 2H), 6.32 (t, J = 7.5 Hz, 2H), 6.24 (dd, J = 7.8, 1.9 Hz, 2H), 6.20 (dd, J = 7.5, 1.8 Hz, 2H), 4.44 (d, J = 13.4 Hz, 4H), 4.10 – 3.98 (m, 4H), 3.76 – 3.62 (m, 4H), 3.23 (d, J = 13.4 Hz, 2H), 3.12 (d, J = 13.5 Hz, 2H), 2.02 – 1.86 (m, 8H), 1.41 (s, 12H), 1.11 (t, J = 7.5 Hz, 6H), 0.93 (t, J = 7.5 Hz, 3H), 0.90 (t, J = 7.5 Hz, 3H).

^{13}C NMR (101 MHz, CDCl_3) δ = 160.9 (C_q), 157.1 (C_q), 155.2 (C_q), 139.0 (C_q), 136.2 (C_q), 135.6 (CH), 133.5 (C_q), 132.4 (C_q), 131.2 (CH), 128.0 (CH), 127.4 (CH), 122.2 (CH), 114.2 (C_q), 83.6 (C_q), 77.0 (CH_2), 76.6 (CH_2), 76.5 (CH_2), 30.8 (2 x CH_2), 25.0 (CH_3), 23.5 (CH_2), 23.1 (CH_2),

Chapter 4

22.9 (CH₂), 10.8 (CH₃), 9.9 (2 x CH₃). The carbon directly attached to the boron atom was not detected due to quadrupolar broadening.^[29]

LC-MS: m/z [M + Na]⁺ calculated for C₄₆H₅₈BBrNaO₆: 819.34; found: 819.54.

HR-MS (ESI): m/z [M + Na]⁺ calculated for C₄₆H₅₈BBrNaO₆: 819.3432; found: 819.3442.

7n. M.p.: (Decomp.) **¹H NMR** (400 MHz, CDCl₃) δ = 7.65 (d, J = 1.6 Hz, 2H), 7.58 (d, J = 1.6 Hz, 2H), 6.45 (t, J = 7.6 Hz, 1H), 6.16 (s, 2H), 6.09 (d, J = 7.6 Hz, 2H), 4.45 (d, J = 13.5 Hz, 2H), 4.38 (d, J = 13.5 Hz, 2H), 4.14 – 3.96 (m, 4H), 3.70 (t, J = 6.6 Hz, 2H), 3.65 (t, J = 6.7 Hz, 2H), 3.25 (d, J = 13.6 Hz, 2H), 3.16 (d, J = 13.7 Hz, 2H), 1.96 – 1.83 (m, 8H), 1.43 (s, 24H), 1.13 (t, J = 7.2 Hz, 3H), 1.11 (t, J = 7.2, 3H), 0.85 (t, J = 7.5 Hz, 6H).

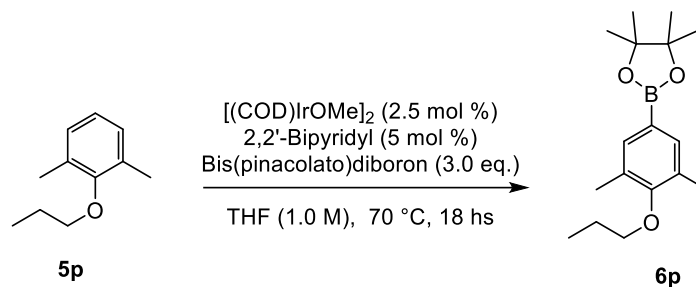
¹³C NMR (101 MHz, CDCl₃) δ = 161.2 (C_q), 155.0 (C_q), 154.4 (C_q), 136.9 (C_q), 136.2 (CH), 135.9 (C_q), 135.6 (C_q), 135.5 (CH), 133.0 (C_q), 130.1 (CH), 127.5 (CH), 122.3 (CH), 115.1 (C_q), 83.7 (C_q), 76.8 (CH₂), 76.7 (CH₂), 76.5 (CH₂), 30.9 (CH₂), 30.7 (CH₂), 25.0 (CH₃), 23.6 (CH₂), 23.5 (CH₂), 23.0 (CH₂), 10.9 (CH₃), 10.8 (CH₃), 9.7 (CH₃). The carbons directly attached to the boron atom were not detected due to quadrupolar broadening.^[29]

LC-MS: m/z [M + Na]⁺ calculated for C₅₂H₆₉B₂BrNaO₈: 945.43; found: 945.61.

HR-MS (ESI): m/z [M + Na]⁺ calculated for C₅₂H₆₉B₂BrNaO₈: 945.4362; found: 945.4368.

Chapter 4

Site-selectivity for C-H borylation of monomer



To a stirred solution of $[(\text{COD})\text{IrOMe}]_2$ (2.5 mol %), 2,2'-bipyridyl (5.0 mol %) and substrate **5p** (0.3 mmol) in anhydrous THF (0.3 mL, 1.0 M), bis(pinacolato)diboron (0.9 mmol, 3.0 eq.) was added in a single portion under nitrogen atmosphere. Then, the mixture was placed in a pre-heated oil bath at 70 °C. After stirring for 18 hs, the reaction was cooled down at room temperature, diluted with CH_2Cl_2 (4 mL) and filtered through a pad of celite. After washing with additional CH_2Cl_2 (3 x 5 mL), the combined organic extracts were concentrated under reduced pressure. The crude product was purified by column chromatography on silica gel (*n*-Hexane:EtOAc 95:5) yielding **6p** as a white solid (42.2 mg, 49%). **M.p.**: 67 – 69 °C.

¹H NMR (400 MHz, CDCl_3) δ = 7.52 (s, 2H), 3.76 (t, *J* = 6.6 Hz, 2H), 2.31 (s, 6H), 1.86 (h, *J* = 7.1 Hz, 2H), 1.36 (s, 12H), 1.10 (t, *J* = 7.4 Hz, 3H).

¹³C NMR (101 MHz, CDCl_3) δ = 159.0 (C_q), 135.6 (CH), 130.4 (C_q), 83.6 (C_q), 73.8 (CH_2), 24.9 (CH_3), 23.7 (CH_2), 16.1 (CH_3), 10.7 (CH_3). The carbon directly attached to the boron atom was not detected due to quadrupolar broadening.^[29]

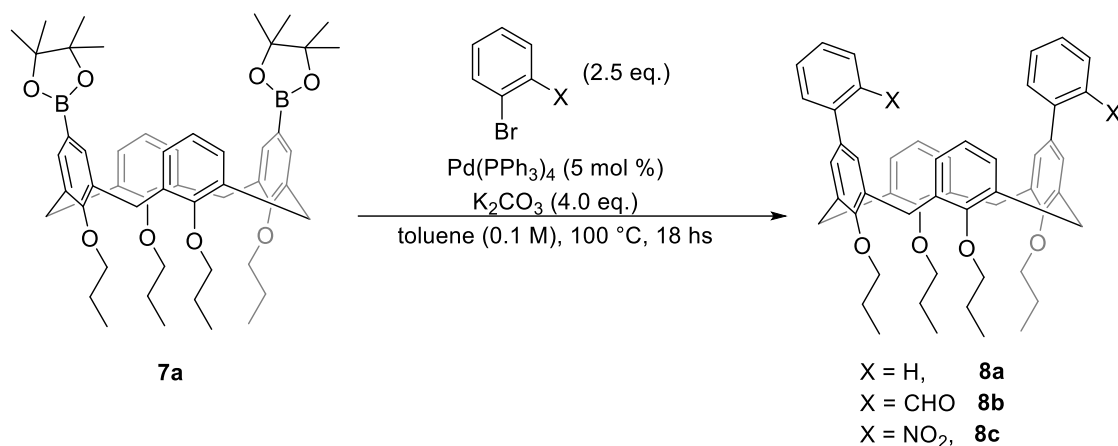
LC-MS: *m/z* $[\text{M} + \text{Na}]^+$ calculated for $\text{C}_{17}\text{H}_{27}\text{BNaO}_3$: 313.20; found: 313.31.

HR-MS (ESI): *m/z* $[\text{M} + \text{Na}]^+$ calculated for $\text{C}_{17}\text{H}_{27}\text{BNaO}_3$: 313.2053; found: 313.2061.

Chapter 4

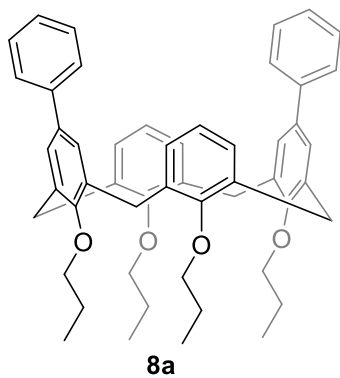
- Synthetic diversifications of calix[4]arene **7a**

Suzuki coupling



Into a glass tube, under nitrogen atmosphere, the corresponding bromobenzene derivative (2.5 eq.) was added to solution of **7a** (0.3 mmol, 1.0 eq.), K₂CO₃ (166 mg, 4.0 eq.) and Pd(PPh₃) (17.3 mg, 5 mol %) in toluene (0.1 M) under magnetic stirring. The mixture was placed into an oil-bath and the reaction was left stirring at 100 °C overnight. After 18 hs, analysis by TLC (n-hexane:EtOAc 95:5) showed complete consumption of **7a**. The reaction was quenched by addition of water (15 mL) and DCM (10 mL). The organic layers were extracted, washed with water (2 x 15 mL) and brine (15 mL), dried over Na₂SO₄, and filtered. The solvent was removed under reduced pressure and the crude purified by column chromatography on silica gel.

Chapter 4



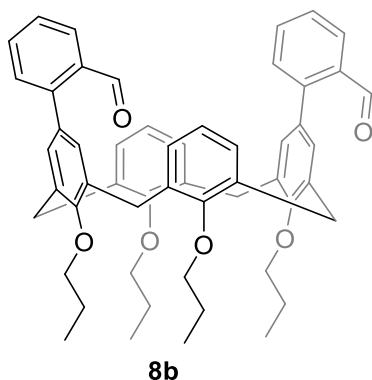
The general procedure was followed using **7a** (253 mg, 0.3 mmol) and bromobenzene (0.078 mL, 2.5 eq.). Product **8a** was isolated from the crude via precipitation in EtOAc as a white solid (174 mg, 78%). **M.p.:** 262 – 264 °C.

¹H NMR (400 MHz, CDCl₃) δ = 7.42 – 7.37 (m, 4H), 7.31 – 7.25 (m, 4H), 7.26 – 7.19 (m, 2H), 7.11 (s, 4H), 6.53 – 6.44 (m, 6H), 4.54 (d, *J* = 13.3 Hz, 4H), 4.04 – 3.96 (m, 4H), 3.85 (t, *J* = 7.2 Hz, 4H), 3.25 (d, *J* = 13.3 Hz, 4H), 2.06 – 1.94 (m, 8H), 1.10 (t, *J* = 7.4 Hz, 6H), 1.00 (t, *J* = 7.5 Hz, 6H).

¹³C NMR (101 MHz, CDCl₃) δ = 156.9 (C_q), 155.9 (C_q), 141.1 (C_q), 136.1 (C_q), 134.7 (C_q), 134.1 (C_q), 128.4 (CH), 127.9 (CH), 127.1 (CH), 126.7 (CH), 126.3 (CH), 122.2 (CH), 76.9 (CH₂), 76.8 (CH₂), 31.2 (CH₂), 23.4 (CH₂), 23.2 (CH₂), 10.6 (CH₃), 10.2 (CH₃).

LC-MS: *m/z* [M + Na]⁺ calculated for C₅₂H₅₆NaO₄: 767.41; found: 767.53.

HR-MS (ESI): *m/z* [M + Na]⁺ calculated for C₅₂H₅₆NaO₄: 767.4179; found: 767.4183.



The general procedure was followed using **7a** (253 mg, 0.3 mmol) and 2-bromobenzaldehyde (139 mg, 2.5 eq.). Product **8b** was isolated by column chromatography on silica gel (*n*-Hexane:EtOAc 95:5) as a white solid (169 mg, 70%). **M.p.:** 251 – 253 °C.

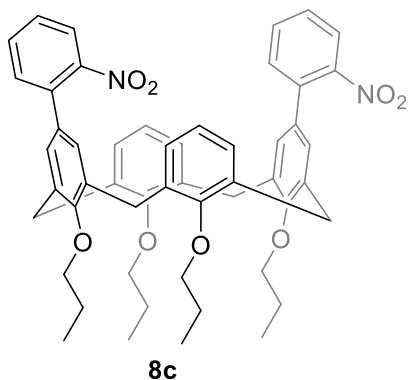
¹H NMR (400 MHz, CDCl₃) δ = 8.07 (bs, 2H), 7.34 – 7.29 (m, 2H), 7.16 (d, *J* = 7.5 Hz, 4H), 7.10 – 7.02 (m, 6H), 6.95 (t, *J* = 7.5 Hz, 2H), 6.42 (s, 4H), 4.57 (d, *J* = 13.1 Hz, 4H), 4.20 – 4.10 (m, 4H), 3.79 (t, *J* = 6.9 Hz, 4H), 3.27 (d, *J* = 13.1 Hz, 4H), 2.19 – 2.05 (m, 4H), 1.98 (h, *J* = 7.2 Hz, 4H), 1.15 (t, *J* = 7.4 Hz, 6H), 0.98 (t, *J* = 7.5 Hz, 6H).

¹³C NMR (101 MHz, CDCl₃) δ = 190.9 (CH), 157.0 (C_q), 155.6 (C_q), 144.5 (C_q), 136.4 (C_q), 134.0 (C_q), 132.9 (CH), 132.7 (C_q), 130.6 (C_q), 130.1 (CH), 130.0 (CH), 129.1 (CH), 127.2 (CH), 126.3 (CH), 123.0 (CH), 77.6 (CH₂), 76.7 (CH₂), 31.0 (CH₂), 23.5 (CH₂), 23.0 (CH₂), 10.8 (CH₃), 9.9 (CH₃).

Chapter 4

LC-MS: m/z $[M + Na]^+$ calculated for $C_{54}H_{56}NaO_6$: 823.41; found: 823.61.

HR-MS (ESI): m/z $[M + Na]^+$ calculated for $C_{54}H_{56}NaO_6$: 823.4077; found: 823.4083.



The general procedure was followed using **7a** (253 mg, 0.3 mmol) and 2-nitrobromobenzene (152 mg, 2.5 eq.). Product **8c** was isolated by column chromatography on silica gel (*n*-Hexane:EtOAc 95:5) as a yellow solid (194 mg, 77%). **M.p.:** 272 – 274 °C.

1H NMR (400 MHz, $CDCl_3$) δ = 7.78 – 7.72 (m, 2H), 7.40 – 7.35 (m, 4H), 7.22 – 7.14 (m, 2H), 6.88 (s, 4H), 6.50 (dd, J = 8.3, 6.6 Hz, 2H), 6.41 (d, J = 7.4 Hz, 4H), 4.51 (d, J = 13.3 Hz, 4H), 4.05 – 3.97 (m, 4H), 3.81 (t, J = 7.1 Hz, 4H), 3.19 (d, J = 13.4 Hz, 4H), 2.06 – 1.91 (m, 8H), 1.09 (t, J = 7.4 Hz, 6H), 1.00 (t, J = 7.5 Hz, 6H).

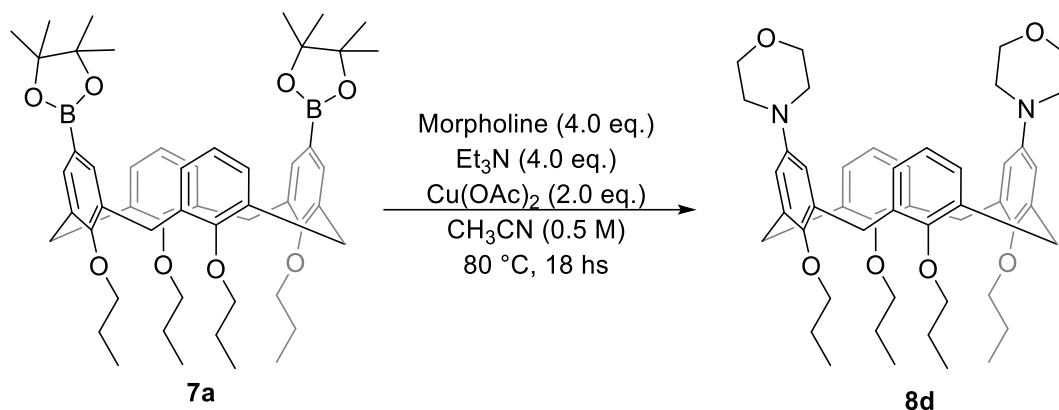
^{13}C NMR (101 MHz, $CDCl_3$) δ = 157.7 (C_q), 155.8 (C_q), 149.4 (C_q), 136.4 (C_q), 136.2 (C_q), 133.7 (C_q), 131.8 (2 x CH), 130.3 (C_q), 128.1 (CH), 128.0 (CH), 127.3 (CH), 123.7 (CH), 122.5 (CH), 76.8 (CH_2), 76.7 (CH_2), 31.0 (CH_2), 23.4 (CH_2), 23.2 (CH_2), 10.6 (CH_3), 10.1 (CH_3).

LC-MS: m/z $[M + Na]^+$ calculated for $C_{52}H_{54}N_2NaO_8$: 857.39; found: 857.54.

HR-MS (ESI): m/z $[M + Na]^+$ calculated for $C_{52}H_{54}N_2NaO_8$: 857.3880; found: 857.3884.

Chapter 4

Product 8d:



Into a Schlenk tube, under air atmosphere, triethylamine (0.084 mL, 4.0 eq.) and morpholine (0.052 mL, 4.0 eq.) were added to a solution of **7a** (127 mg, 0.15 mmol) and $\text{Cu}(\text{OAc})_2$ (55 mg, 2.0 eq.) in acetonitrile (0.5 M). The mixture was placed into an oil bath and left under magnetic stirring at 80 °C overnight. After completion, the mixture was diluted with CH_2Cl_2 (3 x 5 mL) filtered through celite and the solvent was removed under reduced pressure. The organic residue was extracted with EtOAc (10 mL), washed with water (2 x 10 mL) and brine (10 mL), dried over Na_2SO_4 , filtered and the solvent removed under reduced pressure. Product **8d** was isolated by column chromatography on silica gel (*n*-Hexane:EtOAc 9:1) as a white solid (55 mg, 48%). **M.p.:** (Decomp.).

$^1\text{H NMR}$ (400 MHz, CDCl_3) δ = 6.49 (s, 4H), 6.40 (s, 6H), 4.45 (d, J = 13.2 Hz, 4H), 3.92 – 3.84 (m, 12H), 3.77 (t, J = 7.1 Hz, 4H), 3.10 (d, J = 13.2 Hz, 4H), 3.03 (dd, J = 5.8, 3.8 Hz, 8H), 2.00 – 1.87 (m, 8H), 1.07 (t, J = 7.4 Hz, 6H), 0.94 (t, J = 7.5 Hz, 6H).

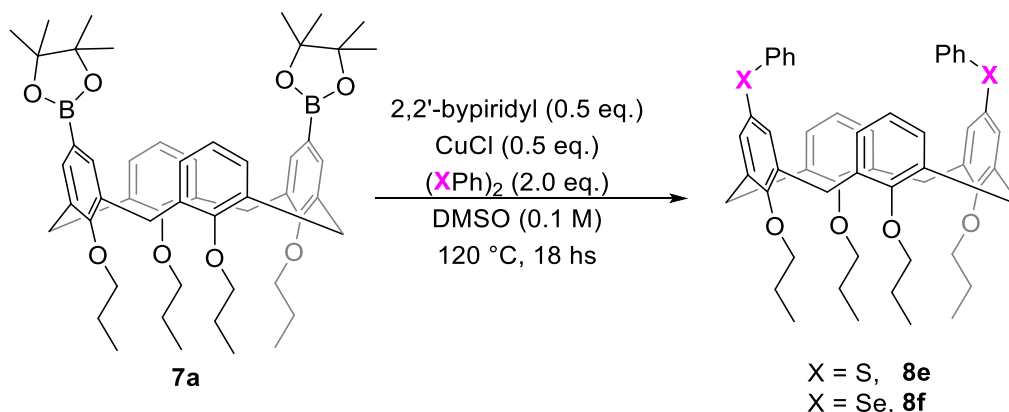
$^{13}\text{C NMR}$ (101 MHz, CDCl_3) δ = 155.8 (C_q), 151.3 (C_q), 145.9 (C_q), 136.3 (C_q), 134.0 (C_q), 127.6 (CH), 122.0 (CH), 116.3 (CH), 76.8 (CH_2), 76.6 (CH_2), 67.0 (CH_2), 50.3 (CH_2), 31.4 (CH_2), 23.4 (CH_2), 23.0 (CH_2), 10.6 (CH_3), 10.1 (CH_3).

LC-MS: m/z [$\text{M} + \text{Na}$] $^+$ calculated for $\text{C}_{48}\text{H}_{62}\text{N}_2\text{NaO}_6$: 785.45; found: 785.61.

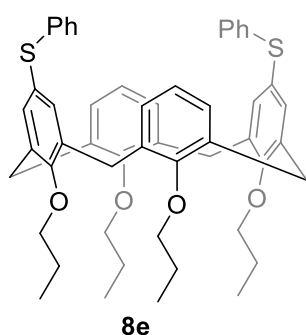
HR-MS (ESI): m/z [$\text{M} + \text{Na}$] $^+$ calculated for $\text{C}_{48}\text{H}_{62}\text{N}_2\text{NaO}_6$: 785.4608; found: 785.4612.

Chapter 4

General procedure for Cham-Lam coupling



Into a Schlenk tube, 2,2'-bipyridyl (11.7 mg, 0.5 eq.), CuCl (7.4 mg, 0.5 eq.) and (XPh)₂ (2.0 eq.) were added to a solution of **7a** (127 mg, 0.15 mmol) in DMSO (0.1 M). The mixture was placed into an oil bath and left under magnetic stirring at 120 °C overnight. After completion, the mixture was diluted with CH₂Cl₂ (3 x 5 ml) filtered through celite and solvent was removed under reduced pressure. The organic residue was extracted with EtOAc (10 mL), washed with water (2 x 10 mL) and brine (10 mL), dried over Na₂SO₄, filtered and the solvent removed under reduced pressure. The product was isolated by column chromatography on silica gel (*n*-Hexane:EtOAc).



The Cham-Lam coupling procedure was followed using **7a** (127 mg, 0.15 mmol) and (SPh)₂ (65.5 mg, 2.0 eq.). Product **8e** was isolated by column chromatography on silica gel (*n*-Hexane:EtOAc 95:5) as a white solid (39 mg, 32%). **M.p.**: 108 – 110 °C.

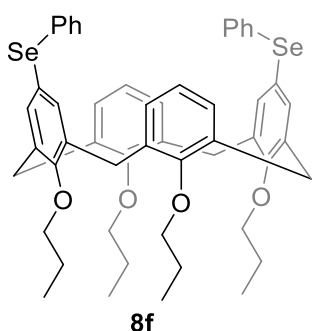
¹H NMR (400 MHz, CDCl₃) δ = 7.26 (d, *J* = 7.5 Hz, 4H), 7.21 – 7.13 (m, 6H), 7.04 (s, 4H), 6.52 – 6.45 (m, 2H), 6.45 – 6.40 (m, 4H), 4.46 (d, *J* = 13.3 Hz, 4H), 4.03 – 3.94 (m, 4H), 3.78 (t, *J* = 7.2 Hz, 4H), 3.15 (d, *J* = 13.3 Hz, 4H), 2.05 – 1.89 (m, 8H), 1.07 (t, *J* = 7.5 Hz, 6H), 1.00 (t, *J* = 7.4 Hz, 6H).

Chapter 4

^{13}C NMR (101 MHz, CDCl_3) δ = 157.5 (C_q), 155.8 (C_q), 138.6 (C_q), 137.2 (C_q), 133.7 (C_q), 133.4 (CH), 128.9 (CH), 128.4 (CH), 128.0 (CH), 125.7 (C_q), 125.6 (CH), 122.3 (CH), 76.9 (CH_2), 76.9 (CH_2), 30.9 (CH_2), 23.4 (CH_2), 23.2 (CH_2), 10.6 (CH_3), 10.1 (CH_3).

LC-MS: m/z [$\text{M} + \text{Na}$] $^+$ calculated for $\text{C}_{52}\text{H}_{56}\text{NaO}_4\text{S}_2$: 831.35; found: 831.51.

HR-MS (ESI): m/z [$\text{M} + \text{Na}$] $^+$ calculated for $\text{C}_{52}\text{H}_{56}\text{NaO}_4\text{S}_2$: 831.3512; found: 831.3542.



The Cham-Lam coupling procedure was followed using **7a** (127 mg, 0.15 mmol) and $(\text{SePh})_2$ (93.6 mg, 2.0 eq.). Product **8f** was isolated by column chromatography on silica gel (*n*-Hexane:EtOAc 95:5) as a white solid (65 mg, 48%). **M.p.:** 117 – 119 °C.

^1H NMR (400 MHz, CDCl_3) δ = 7.32 – 7.29 (m, 4H), 7.27 – 7.21 (m, 6H), 7.12 (s, 4H), 6.50 – 6.44 (m, 2H), 6.43 – 6.39 (m, 4H), 4.44 (d, J = 13.2 Hz, 4H), 4.01 – 3.92 (m, 4H), 3.77 (t, J = 7.2 Hz, 4H), 3.13 (d, J = 13.3 Hz, 4H), 2.05 – 1.85 (m, 8H), 1.05 (t, J = 7.4 Hz, 6H), 0.99 (t, J = 7.5 Hz, 6H).

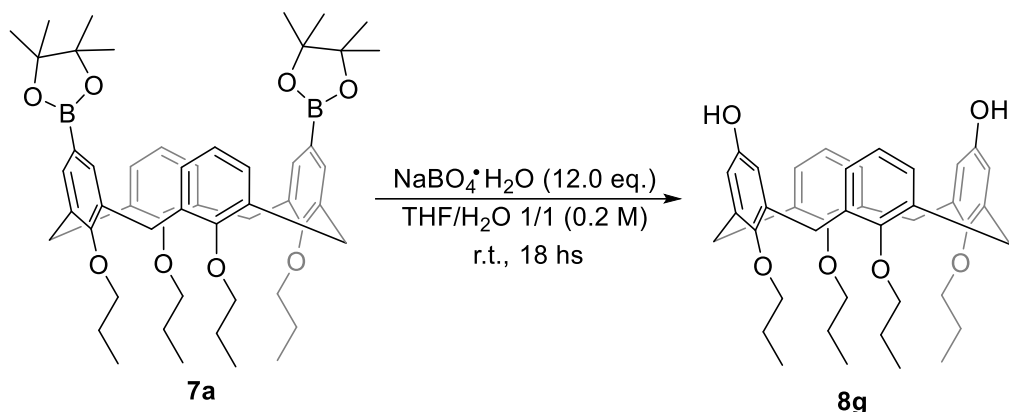
^{13}C NMR (101 MHz, CDCl_3) δ = 157.5 (C_q), 155.8 (C_q), 137.3 (C_q), 134.9 (CH), 133.7 (C_q), 133.5 (C_q), 130.9 (CH), 129.1 (CH), 128.0 (CH), 126.2 (CH), 122.3 (CH), 121.4 (C_q), 76.9 (CH_2), 76.8 (CH_2), 30.8 (CH_2), 23.3 (CH_2), 23.2 (CH_2), 10.5 (CH_3), 10.1 (CH_3).

LC-MS: m/z [$\text{M} + \text{Na}$] $^+$ calculated for $\text{C}_{52}\text{H}_{56}\text{NaO}_4\text{Se}_2$: 927.24; found: 927.43.

HR-MS (ESI): m/z [$\text{M} + \text{NH}_4$] $^+$ calculated for $\text{C}_{52}\text{H}_{60}\text{NO}_4\text{Se}_2$: 922.2847; found: 922.2860.

Chapter 4

Product 8g



Into a Schlenk tube, $\text{NaBO}_4 \cdot \text{H}_2\text{O}$ (180 mg, 12.0 eq.) was added to a solution of **7a** (127 mg, 0.15 mmol) in THF/ H_2O 1/1 (0.2 M). The mixture was left under magnetic stirring at r.t. overnight. The reaction was monitored by TLC (*n*-Hexane:EtOAc 95:5) and complete consumption of **7a** was observed after 18 hs. The mixture was diluted with water (10 mL) and EtOAc (10 mL) was added. The organic layers were extracted, washed with water (10 mL) and brine (10 mL), dried over Na_2SO_4 , filtered and the solvent removed under reduced pressure. Product **8g** was isolated by column chromatography on silica gel (*n*-Hexane:EtOAc 95:5) as a white solid (90 mg, 96%). **M.p.**: 259 – 261 °C.

$^1\text{H NMR}$ (400 MHz, CDCl_3) δ = 7.05 (d, J = 7.4 Hz, 4H), 6.86 (t, J = 7.4 Hz, 2H), 5.75 – 5.61 (bs, 2H), 5.59 (s, 4H), 4.43 (d, J = 13.5 Hz, 4H), 4.03 – 3.94 (m, 4H), 3.65 (t, J = 6.7 Hz, 4H), 3.10 (d, J = 13.5 Hz, 4H), 1.99 – 1.81 (m, 8H), 1.11 (t, J = 7.4 Hz, 6H), 0.88 (t, J = 7.5 Hz, 6H).

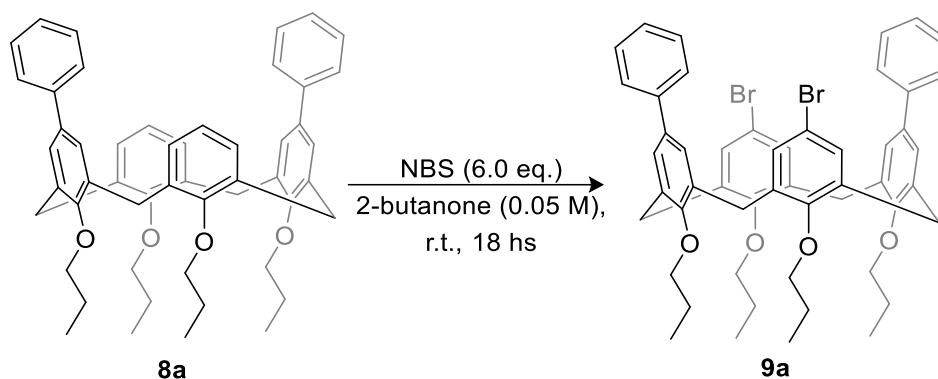
$^{13}\text{C NMR}$ (101 MHz, CDCl_3) δ = 158.0 (C_q), 149.9 (C_q), 149.3 (C_q), 136.7 (C_q), 134.7 (C_q), 129.0 (CH), 121.9 (CH), 114.4 (CH), 76.9 (CH_2), 76.5 (CH_2), 31.1 (CH_2), 23.5 (CH_2), 23.0 (CH_2), 10.9 (CH_3), 9.8 (CH_3).

LC-MS: m/z $[\text{M} + \text{Na}]^+$ calculated for $\text{C}_{40}\text{H}_{48}\text{NaO}_6$: 647.35; found: 647.56.

HR-MS (ESI): m/z $[\text{M} + \text{Na}]^+$ calculated for $\text{C}_{40}\text{H}_{48}\text{NaO}_6$: 647.3451; found: 647.3456.

Chapter 4

Product 9a:



Into a round-bottom flask, *N*-bromo succinimide (373 mg, 6.0 eq.) was added to a solution of **8a** (260 mg, 0.35 mmol) in 2-butanone (0.05 M). The mixture was left under magnetic stirring at r.t. overnight. The mixture was then quenched with water and the precipitate filtered under reduced pressure. The solid residue was dissolved in CH_2Cl_2 (15 mL), washed with water (15 mL) and brine (15 mL), dried over Na_2SO_4 , filtered and the solvent removed under reduced pressure. Product **9a** was isolated by column chromatography on silica gel (*n*-Hexane:EtOAc 95:5) as a white solid (263 mg, 83%). **M.p.:** (Decomp.).

$^1\text{H NMR}$ (400 MHz, CDCl_3) δ = 7.47 – 7.43 (m, 4H), 7.40 – 7.30 (m, 4H), 7.26 (d, J = 7.3 Hz, 2H), 7.16 (s, 4H), 6.64 (s, 4H), 4.49 (d, J = 13.3 Hz, 4H), 4.04 – 3.96 (m, 4H), 3.80 (t, J = 7.2 Hz, 4H), 3.22 (d, J = 13.3 Hz, 4H), 2.04 – 1.92 (m, 8H), 1.09 (t, J = 7.4 Hz, 6H), 0.97 (t, J = 7.5 Hz, 6H).

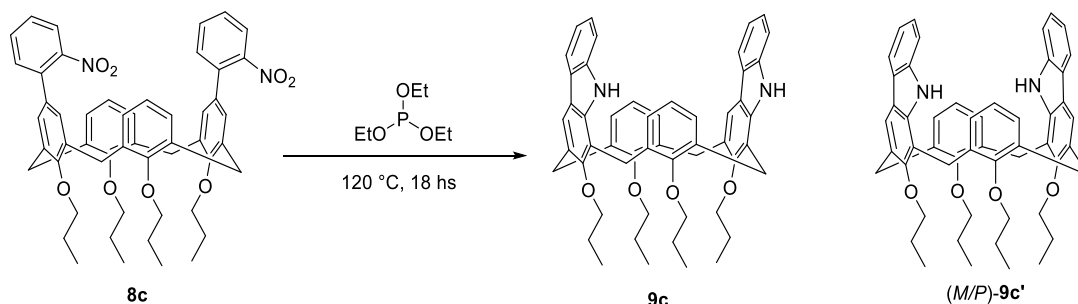
$^{13}\text{C NMR}$ (101 MHz, CDCl_3) δ = 156.7 (C_q), 155.0 (C_q), 140.7 (C_q), 136.1 (C_q), 135.5 (C_q), 135.3 (C_q), 130.6 (CH), 128.6 (CH), 127.3 (CH), 126.8 (CH), 126.6 (CH), 115.1 (C_q), 77.1 (CH_2), 76.9 (CH_2), 31.1 (CH_2), 23.3 (CH_2), 23.1 (CH_2), 10.6 (CH_3), 10.0 (CH_3).

LC-MS: m/z [$\text{M} + \text{Na}$] $^+$ calculated for $\text{C}_{52}\text{H}_{54}\text{Br}_2\text{NaO}_4$: 923.24; found: 923.31.

HR-MS (ESI): m/z [$\text{M} + \text{Na}$] $^+$ calculated for $\text{C}_{52}\text{H}_{54}\text{Br}_2\text{NaO}_4$: 923.2368; found: 923.2374.

Chapter 4

Product **9c** and **9c'**:



Into a Schlenk tube, **8c** (96.0 mg, 0.115 mmol) was dissolved with triethyl phosphite (2.0 mL, 0.05 M). The solution was placed into an oil bath and left under magnetic stirring at $120\text{ }^\circ\text{C}$ overnight. After 18 hs, analysis by TLC (*n*-Hexane:EtOAc 95:5) showed complete consumption of **8c**. The mixture was quenched with water (10 mL) and extracted with EtOAc. The organic layer was washed with water (15 mL) and brine (15 mL), dried over Na_2SO_4 , filtered and the solvent removed under reduced pressure. Products **9c** and **(M/P)-9c'** were isolated by column chromatography on silica gel (*n*-Hexane:EtOAc 95:5) as yellowish solids (**9c**: 35 mg, 39%; **(M/P)-9c'**: 34 mg, 38%).

9c. M.p.: (Decomp.). **$^1\text{H NMR}$** (400 MHz, CDCl_3) δ = 8.08 – 8.00 (m, 4H), 7.83 (s, 2H), 7.43 (d, J = 8.0 Hz, 2H), 7.41 – 7.35 (m, 2H), 7.25 (ddd, J = 8.0, 7.0, 1.2 Hz, 2H), 6.20 – 6.07 (m, 6H), 4.66 (d, J = 13.7 Hz, 2H), 4.65 (d, J = 13.7 Hz, 2H), 4.23 (dt, J = 10.5, 5.9 Hz, 2H), 4.12 (dt, J = 10.5, 6.0 Hz, 2H), 3.90 (t, J = 6.8 Hz, 2H), 3.83 (t, J = 6.8 Hz, 2H), 3.62 (d, J = 14.0 Hz, 2H), 3.41 (d, J = 13.5 Hz, 2H), 2.21 – 1.96 (m, 8H), 1.25 (t, J = 7.3 Hz, 3H), 1.22 (t, J = 7.3 Hz, 3H), 1.00 (t, J = 7.5 Hz, 6H).

$^{13}\text{C NMR}$ (101 MHz, CDCl_3) δ = 156.8 (C_q), 155.3 (C_q), 155.2 (C_q), 139.8 (C_q), 139.0 (C_q), 133.7 (C_q), 133.2 (C_q), 129.7 (C_q), 127.5 (CH), 127.2 (CH), 124.5 (CH), 124.3 (C_q), 122.7 (CH), 122.0 (CH), 119.7 (CH), 119.5 (CH), 119.4 (CH), 119.3 (C_q), 118.1 (C_q), 110.5 (CH), 77.2 (CH_2), 77.2 (CH_2), 77.0 (CH_2), 31.5 (CH_2), 25.3 (CH_2), 23.7 (CH_2), 23.6 (CH_2), 23.1 (CH_2), 11.0 (2 x CH_3), 10.0 (CH_3). **LC-MS:** m/z [$\text{M} + \text{Na}$] $^+$ calculated for $\text{C}_{52}\text{H}_{54}\text{N}_2\text{NaO}_4$: 793.41; found: 793.52. **HR-MS (ESI):** m/z [$\text{M} + \text{Na}$] $^+$ calculated for $\text{C}_{52}\text{H}_{54}\text{N}_2\text{NaO}_4$: 793.4084; found: 793.4090.

(M/P)-9c'. M.p.: (Decomp.). **$^1\text{H NMR}$** (400 MHz, CDCl_3) δ = 8.01 (s, 2H), 7.94 (d, J = 7.8 Hz, 2H), 7.73 (s, 2H), 7.43 (d, J = 8.0 Hz, 2H), 7.37 (ddd, J = 8.1, 7.0, 1.2 Hz, 2H), 7.24 – 7.18 (m, 2H), 6.28 (t, J = 4.7 Hz, 2H), 6.16 (d, J = 4.9 Hz, 4H), 4.65 (d, J = 13.7 Hz, 2H), 4.64 (d, J = 13.7

Chapter 4

Hz, 2H), 4.20 (dt, $J = 10.5, 5.9$ Hz, 2H), 4.08 (dt, $J = 10.4, 5.9$ Hz, 2H), 3.88 (t, $J = 6.9$ Hz, 4H), 3.60 (d, $J = 14.1$ Hz, 2H), 3.40 (d, $J = 13.5$ Hz, 2H), 2.19 – 1.97 (m, 8H), 1.21 (t, $J = 7.4$ Hz, 6H), 1.00 (t, $J = 7.5$ Hz, 6H).

^{13}C NMR (101 MHz, CDCl_3) $\delta = 156.6$ (C_q), 155.5 (C_q), 139.7 (2 x C_q), 139.1 (C_q), 134.3 (C_q), 132.9 (C_q), 129.4 (C_q), 128.2 (CH), 126.7 (CH), 124.4 (CH), 124.2 (C_q), 122.3 (CH), 119.6 (CH), 119.4 (CH), 119.2 (CH), 118.1 (C_q), 110.4 (CH), 77.2 (CH_2), 77.1 (CH_2), 31.6 (CH_2), 25.4 (CH_2), 23.6 (CH_2), 23.1 (CH_2), 10.9 (CH_3), 10.0 (CH_3).

LC-MS: m/z $[\text{M} + \text{Na}]^+$ calculated for $\text{C}_{52}\text{H}_{54}\text{N}_2\text{NaO}_4$: 793.40; found: 793.54.

HR-MS (ESI): m/z $[\text{M} + \text{Na}]^+$ calculated for $\text{C}_{52}\text{H}_{54}\text{N}_2\text{NaO}_4$: 793.4084; found: 793.4088.

Chapter 4

4.5 Bibliography

- [1] a) P. Neri, J. L. Sessler, M. -X. Wang, Calixarenes and Beyond. In *Calixarenes: An Introduction*, 2nd ed.; b) C. D. Gutsche, Ed.; Royal Society of Chemistry: Cambridge, U.K, 2016.
- [2] (a) Q. He, G. I. Vargas-Zúñiga, S. H. Kim, S. K. Kim, J. L. Sessler, *Chem. Rev.*, **2019**, 119, 9753–9835; b) M. Xue, M. Yang, X. Chi, X. Yan, F. Huang, *Chem. Rev.*, **2015**, 115, 7398–7501; c) O. Santoro, C. Redshaw, *Coord. Chem. Rev.*, **2021**, 448, No. 214173.
- [3] a) F. Elaieb, S. Sameni, M. Awada, C. Jeunesse, D. Matt, L. Toupet, J. Harrowfield, D. Takeuchi, S. Takano, *Eur. J. Inorg. Chem.*, **2019**, 4690-4694; b) Z. Xu, N. Fang, Y. Zhao, *J. Am. Chem. Soc.*, **2021**, 143, 3162–3168; c) J. Emerson-King, S. Pan, M. R. Gyton, J. Tonner-Zech, A. B. Chaplin, *Chem. Commun.*, **2023**, 59, 2150–2152.
- [4] A. Arduini, A. Casnati, L. Dodi, A. Pochini, R. Ungaro, *J. Chem. Soc., Chem. Commun.*, **1990**, 1597-1598.
- [5] J. D. van Loon, A. Arduini, L. Coppi, W. Verboom, R. Ungaro, A. Pochini, S. Harkema, D. N. Reinhoudt, *J. Org. Chem.*, **1990**, 55, 5639-5646.
- [6] a) A. Dondoni, C. Ghiglione, A. Marra, M. Scoponi, *J. Org. Chem.*, **1998**, 63, 9535-9539; b) O. Struck, L. A. J. Chrisstoffels, R. J. W. Lugtenberg, W. Verboom, G. J. van Hummel, S. Harkema, D. N. Reinhoudt, *J. Org. Chem.*, **1997**, 62, 2487-2493.
- [7] a) A. Surina, V. Eigner, M. Krupička, P. Lhoták, *J. Org. Chem.*, **2022**, 87, 10080-10089; b) M. Larsen, M. Jorgensen, *J. Org. Chem.*, **1996**, 61, 6651-6655.
- [8] (a) V. Stastny, P. Lhoták, V. Michlova, I. Stibor, J. Sykora, *Tetrahedron*, **2002**, 58, 7207-7211; (b) Arduini, A.; Manfredi, G.; Pochini, A.; Sicuri, A. R.; Ungaro, R., *J. Chem. Soc., Chem. Commun.*, **1991**, 14, 936-937.
- [9] G. Giovanardi, S. Cattani, D. Balestri, A. Secchi, G. Cera, *J. Org. Chem.*, **2024**, 89, 8486-8499.
- [10] a) I. F. Yu, J. W. Wilson, J. F. Hartwig, *Chem. Rev.*, **2023**, 123, 11619-11663; b) R. Bisht, C. Haldar, M. M. Hassan, E. Hoque, J. Chaturvedi, B. Chattopadhyay, *Chem. Soc. Rev.*, **2022**, 51, 5042-5100; c) J. S. Wright, P. J. H. Scott, P. G. Steel, *Angew. Chem. Int. Ed.*, **2021**, 60, 2796-2821.

Chapter 4

- [11] R. Frydrych, T. Lis, W. Bury, J. Cybińska, Marcin Stępień, *J. Am. Chem. Soc.*, **2020**, 142, 15604-15613.
- [12] E. M. Simmons, J. F. Hartwig, *Angew. Chem. Int. Ed.*, **2012**, 51, 3066-3072.
- [13] a) X. Zou, H. Zhao, Y. Li, Q. Gao, Z. Ke, S. Xu, *J. Am. Chem. Soc.*, **2019**, 141, 5334-5342; b) M. A. Larsen, M. A. Hartwig, *J. Am. Chem. Soc.*, **2014**, 136, 4287-4299; c) J.-I. Ito, T. Kaneda, H. Nishiyama, *Organometallics*, **2012**, 31, 4442-4449.
- [14] For mechanism of iridium-catalyzed C–H borylations, see: a) A. G. Green, P. Liu, C. A. Merlic, K. N. Houk, *J. Am. Chem. Soc.*, **2014**, 136, 4575-4583; b) B. A. Vanchura II, S. M. Preshlock, P. C. Roosen, V. A. Kallepalli, R. J. Staples, R. E. Maleczka, D. A. Singleton, M. R. Smith, *Chem. Commun.*, **2010**, 46, 7724-7726; c) T. M. Boller, J. M. Murphy, M. Hapke, T. Ishiyama, N. Miyaura, J. F. Hartwig, *J. Am. Chem. Soc.*, **2005**, 127, 14263-14278; d) H. Tamura, H. Yamazaki, S. Sato, S. Sakaki, *J. Am. Chem. Soc.*, **2003**, 125, 16114-16126.
- [15] M. Kaur, R. Kumar, *Asian J. Org. Chem.*, **2022**, 11, No. e202200092.
- [16] V. Rawat, A. Baheti, O. S. Tiwari, A. Vigalok, *Chem. Commun.*, **2023**, 59, 5543-5546.
- [17] J.-Q. Chen, J.-H. Li, Z.-B. Dong, *Adv. Synth. Catal.*, **2020**, 362, 3311-3331.
- [18] J. Mendez-Arroyo, J. Barroso-Flores, A. M. Lifschitz, A. A. Sarjeant, C. L. Stern, C. A. Mirkin, *J. Am. Chem. Soc.*, **2014**, 136, 10340-10348.
- [19] K. Yoshida, S. Fujii, R. Takahashi, S. Matsumoto, K. Sakurai, *Langmuir*, **2017**, 33, 9122-9128.
- [20] G. V. Zyryanov, Y. Kang, D. M. Rudkevich, *J. Am. Chem. Soc.*, **2003**, 125, 2997-3007.
- [21] M. Strobel, K. Kita-Tokarczyk, A. Taubert, C. Vebert, P. A. Heiney, M. Chami, W. Meier *Adv. Funct. Mater.*, **2006**, 16, 252-259.
- [22] A. R. N. S. Royappa, M. Ayer, A. Fracassi, M.-O. Ebert, S. Aroua, Y. Yamakoshi, *Helv. Chim. Acta*, **2017**, 100, e1600391.
- [23] S. Kim, J. S. Kim, S. K. Kim, I. Suh, S. O. Kang, J. Ko, *Inorg. Chem.*, **2005**, 44, 1846-1851.
- [24] P. Slavík, V. Eigner, P. Lhotak, *Tetrahedron*, **2016**, 72, 6348-6355.
- [25] G. Giovanardi, G. Scarica, V. Pirovano, A. Secchi, G. Cera, *Org. Biomol. Chem.*, **2023**, 21, 4072-4083.
- [26] Z. Li, Y. Chen, C. Zheng, Y. Yin, L. Wang, X. Sun, *Tetrahedron*, **2017**, 73, 78-85.

Chapter 4

- [27] Y. Zhang, M. Xu, X.Si, J. Hou, Q. Cai, *J. Am. Chem. Soc.*, **2022**, 144, 22858-22864.
- [28] Malcolm J. Applewhite, Delia A. Haynes & Gareth E. Arnott, *Supramolecular Chem.*, **2016**, 28, 475-484.
- [29] B. Wrackmeyer, *Progress in NMR Spectroscopy*, **1979**, 12, 227-259.

Chapter 5. New enantioselective approach for the total synthesis of Indidene natural products empowered by gold-catalysis

5.1 Introduction

In the last century, the development of synthetic strategies for the production of plant and marine natural products has gathered a lot of interest due to their potential medical applications. In fact, these secondary metabolites are produced by the plant in order to fight infections caused by various pathogens, such as bacteria, fungi, etc.^[1] For these reasons, chemists have explored among these products, searching for new drugs that could heal or alleviate symptoms.^[2] It's possible to identify some common structures within these molecules, which are defined as core structures. Among these core structures, indane and its derivatives have been noticed to provide useful scaffolds for the rational designing of pharmaceuticals.^[3]

Their structure is characterized by a bicyclic ring where a benzene ring is fused with a 5-membered cyclopentane ring (Figure 5.1, a). A particular class of these natural products are indidenes^[4] and reinfoilins^[5] (Figure 5.1, b), prenylated polyketides that were isolated from *Streblus indicus* and *Desmodium renifolium*, plants native from South-Eastern Asia. This class of indane-based molecules proved to exhibit mild in-vitro cytotoxicity towards cancerous cells, in addition to anti-inflammatory properties recently discovered for involucrasin C, possessing a structure strictly related to indidene A.^[6]

Many different strategies for the construction of the indane-core have already been reported and fully discussed, employing both catalytic and non-catalytic processes.^[7] Thanks to the increase in popularity of transition-metal-catalyzed transformation applied in the synthesis of natural compounds, some examples have reported methodologies that exploit C-H functionalizations catalyzed by said metal nuclei.^[8]

Chapter 5

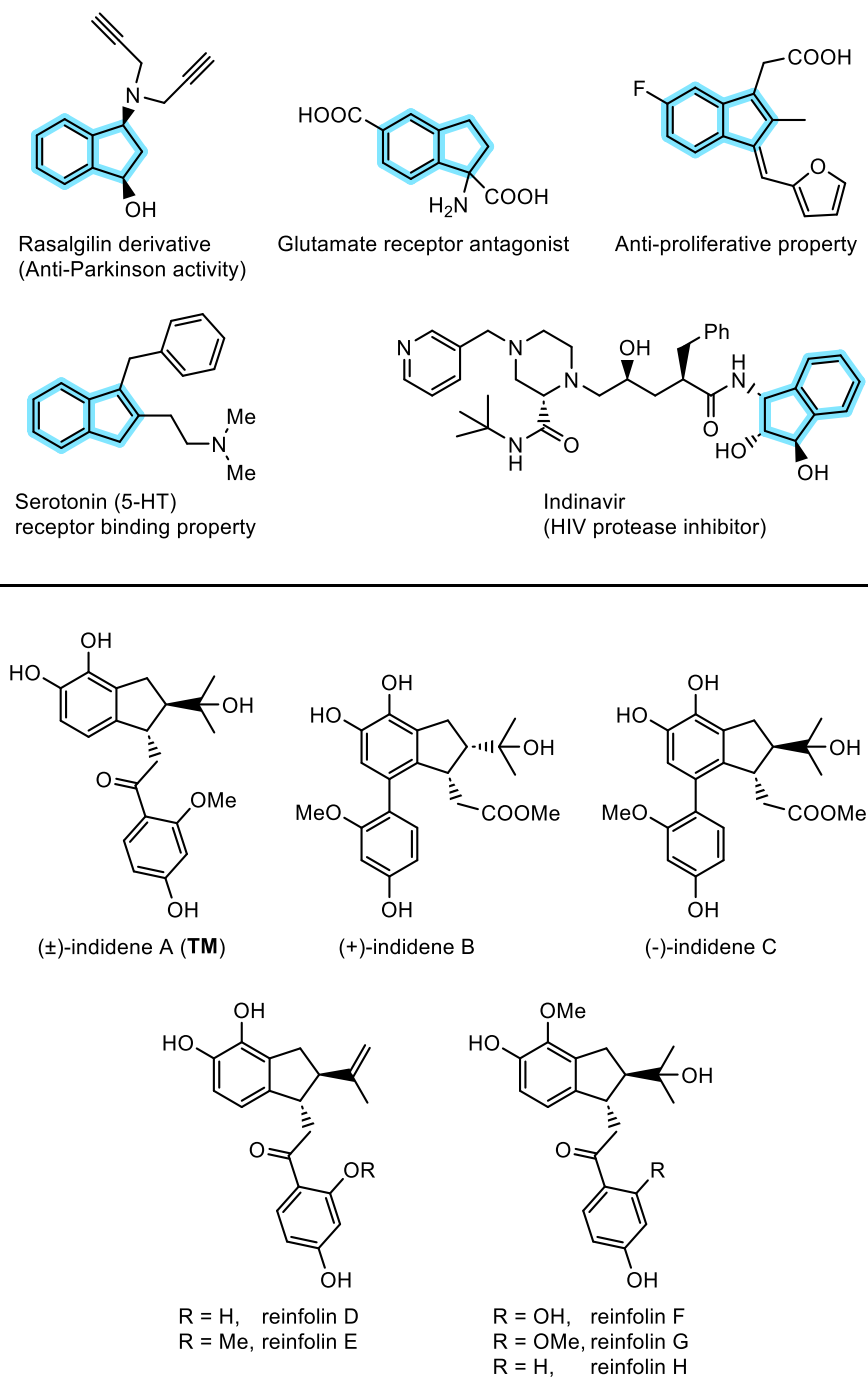
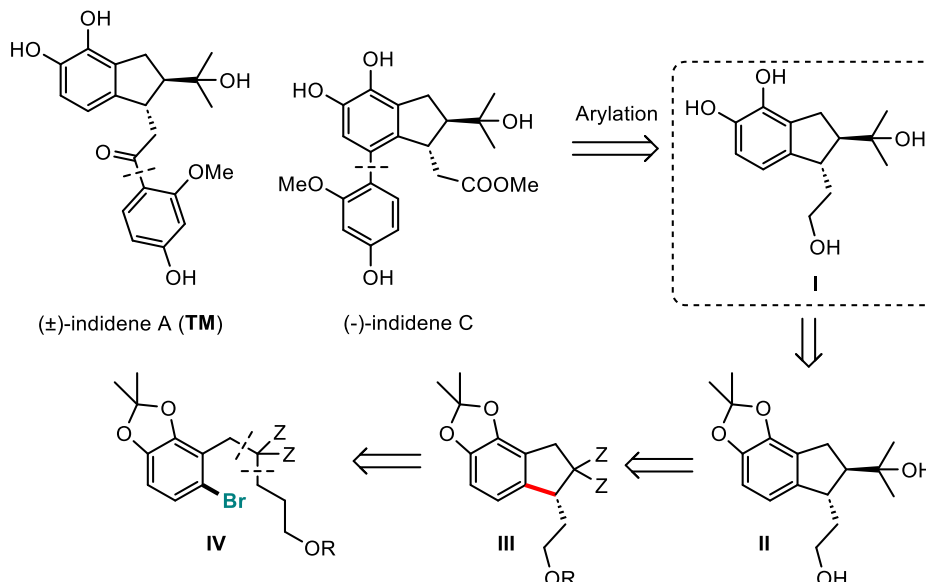


Figure 5.1. a) Selected examples of indane-core (highlighted in blue) natural products; b) Structures of indidenes and reifolins natural products.

Recently, Kudashev tackled the challenge of synthesizing two indidene-based natural products, precisely (±)-indidene A and (-)-indidene C (Figure 5.1, b), exploiting a palladium-catalyzed C(sp³)-H functionalization for the formation of the indane bicyclic core.^[9]

Chapter 5

First, they performed a retrosynthetic analysis of the target molecules, finding that both could be prepared starting from the same key intermediate **I** via arylation of the same aryl fragment in different sites (Scheme 5.1).



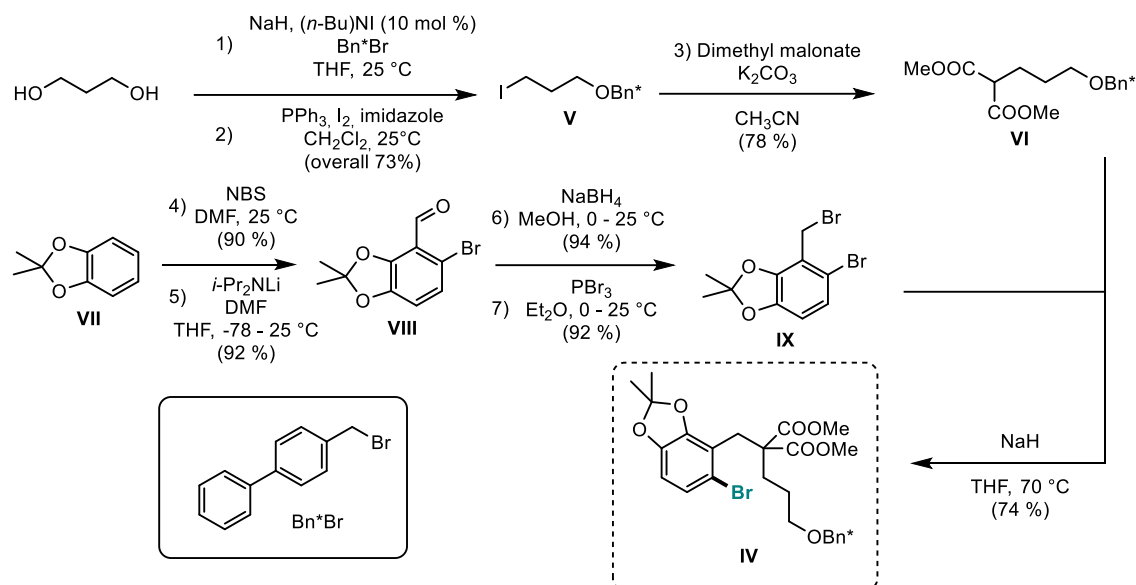
Scheme 5.1. Retrosynthetic analysis for the two indidene natural products converging in the same intermediate **I**.

Then, they determined that the common intermediate **I** could be obtained from the bromo compound **IV** through methylene C(sp³)-H arylation reaction.^[10]

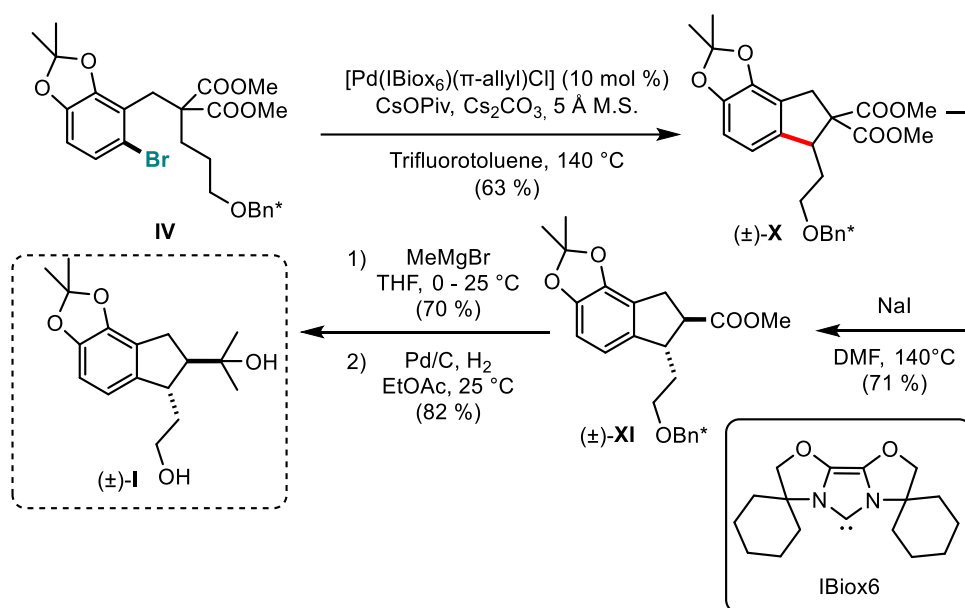
Scheme 5.2 illustrates the convergent synthetic pathway they presented for the synthesis of intermediate **IV**, where they prepared, in parallel, the alkyl chain **VI** and the dibromo aryl derivative **IX** that were then reacted together to obtain the desired product.

Next, intermediate **IV** was further transformed in order to obtain the desired common intermediate **II** to complete the synthesis of both target molecules (Scheme 3.3). The first step was the Pd(0)-catalyzed methylene C(sp³)-H arylation reaction to form the first stereogenic center. Unfortunately, this step was performed without stereometric control, leading to the formation of the racemic mixture of (±)-**X**. The Krapcho decarboxylation of compound (±)-**X** proceeded smoothly to form the thermodynamically favorable *trans*-monoester derivative (±)-**XI**. Finally, double Grignard addition to the ester moiety with MeMgBr and deprotection of the p-phenylbenzyl (Bn*) protecting group by hydrogenolysis lead to compound (±)-**I**.

Chapter 5



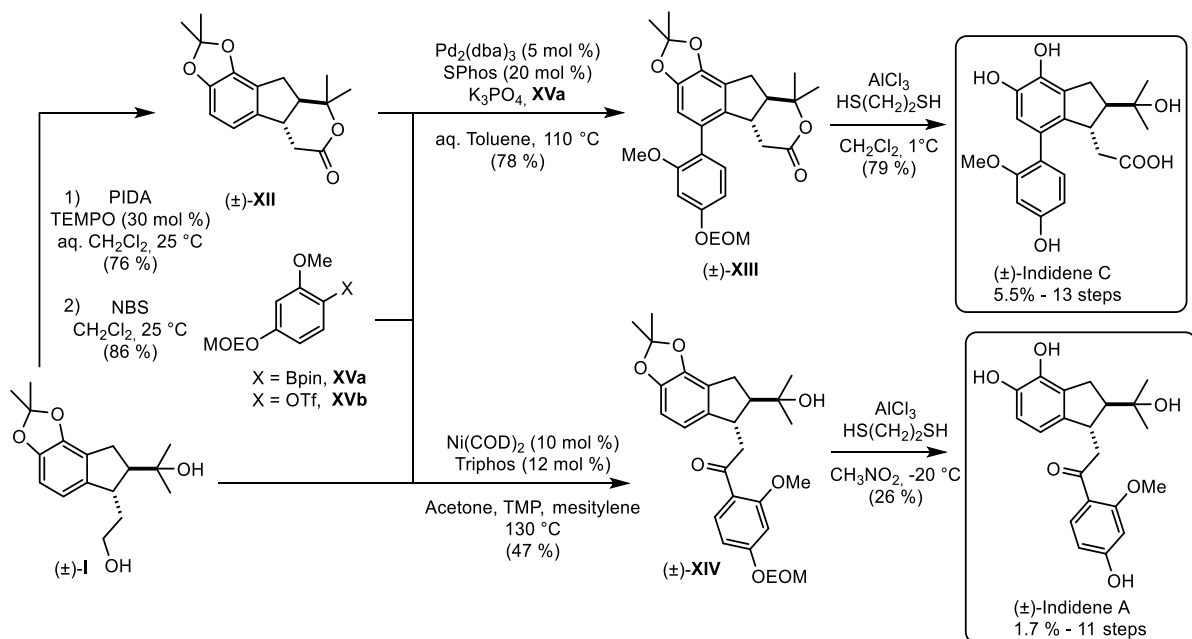
Scheme 5.2. Convergent synthetic pathway for the preparation of intermediate **IV**.



Scheme 5.3. Transformation of compound **IV** into intermediate (±)-**I**.

Once intermediate (±)-**I** was obtained, they proceeded to complete the synthesis for both (±)-indidene **A** and (±)-indidene **C** (Scheme 5.4). These remarkable synthetic strategies still present some limitations due to the lack of enantiomeric control and the overall low yields for the final natural compounds.

Chapter 5

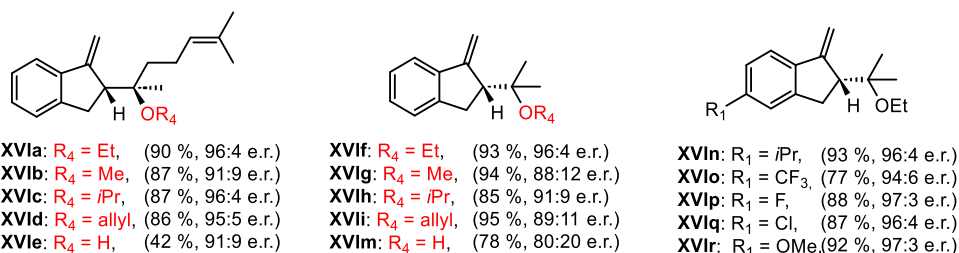
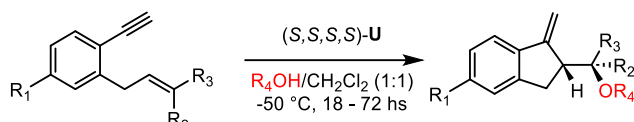
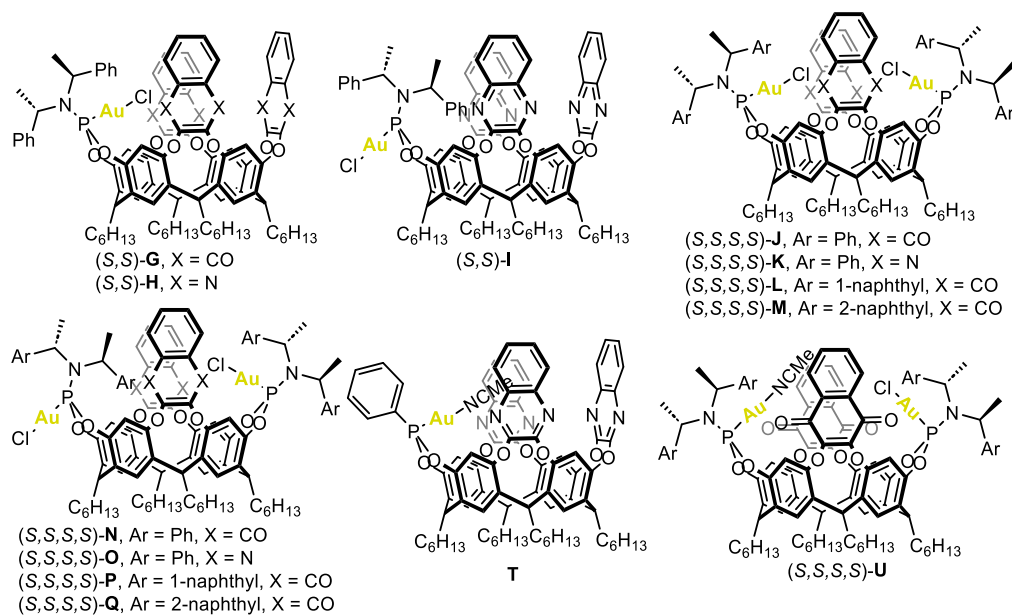


Scheme 5.4. Final functionalizations of (±)-I to (±)-indidene A and (±)-indidene C.

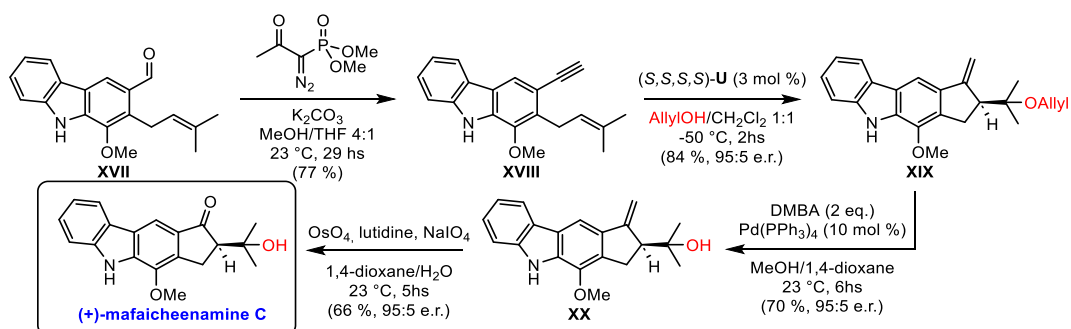
The project discussed in this chapter, which has taken place at the Institut Català d'Investigació Química (ICIQ) under the supervision of Prof. A. M. Echavarren, tackle the challenge of developing a new methodology for the preparation of (-)-indidene A exploiting an enantioselective gold(I)-catalyzed alkoxy cyclization reaction of 1,6-enynes for the formation of the indane-core.^[11] This type of transformation has already been covered by Echavarren's research group in a recent work, where they presented the synthesis of a large number of chiral and achiral resorcin[4]arene-based gold(I)-complexes and studied their application in catalyzing said reaction (Scheme 5.5).^[12]

In this work, they not only showed the tolerance of the catalytic process, testing 1,6-enynes with different substituents in aryl moiety and the alkene and employing different nucleophiles for the alkoxy cyclization (Scheme 3.5, bottom), but they also showed the application of this methodology for the total synthesis of (+)-mafaicheenamine C (Scheme 3.6).

Chapter 5



Scheme 5.5. Selected examples of resorcin[4]arene-based gold(I)-complexes (top), schematic representation of the alkoxy cyclization reaction (middle), and scope of the reaction (bottom).

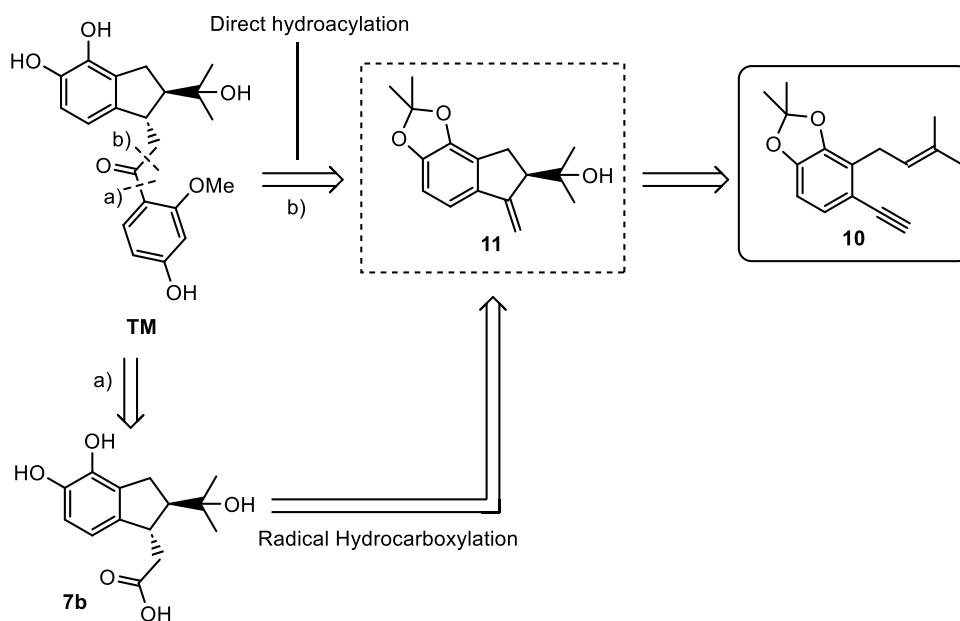


Scheme 5.6. Total synthesis of (+)-mafaicheenamine C employing resorcin[4]arene-based gold(I)-catalytic reaction starting from the reported aldehyde XVII.^[13]

Chapter 5

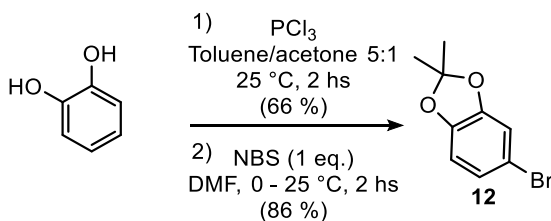
5.2 Results and discussion

The retrosynthetic analysis of (±)-indidene A (**TM**) evidenced that two possible disconnection routes can be pursued. One was characterized by the direct functionalization of the alkoxy cyclization product **11** with the aryl moiety via hydroacylation reaction,^[14] while the other would require the formation of the carboxylic acid intermediate **7b** via radical hydrocarboxylation reaction.^[15] In any case, in order to obtain the common intermediate **11**, it's necessary to develop a synthetic strategy for substrate **10** (Scheme 5.7)



Scheme 5.7. Retrosynthetic analysis for the design of **10**.

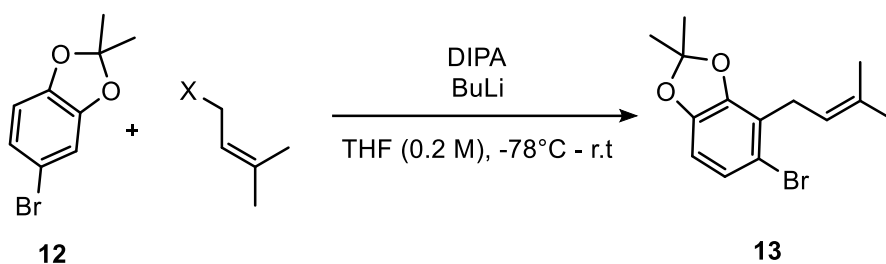
To synthesize **10**, the first step was the protection of the commercially available pyrocatechol to form the corresponding acetal, immediately followed by direct bromination with NBS, obtaining the intermediate **12** (Scheme 3.8).



Scheme 5.8. Synthesis of intermediate **12**.

Chapter 5

Taking inspiration from the previously reported total synthesis of **TM**,^[9] a regioselective functionalization of the *ortho*-position of **12**, by initial lithiation with freshly prepared LDA, followed by the addition of a prenyl bromide (Table 5.1, entry 1), was accomplished to afford **13**. GC-MS analysis of the crude confirmed the formation of the desired compound **13**, even if in traces. Optimization of the conditions allowed to increase the yield of the reaction up to 84 %.



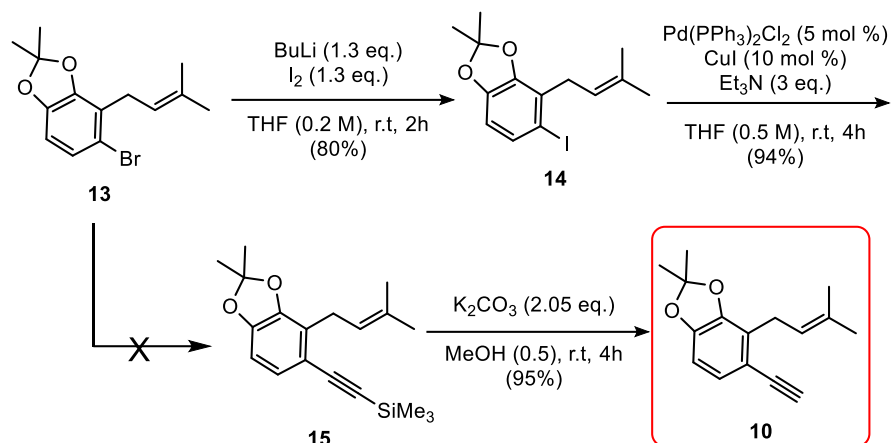
Entry	X	12 (mmol)	BuLi (eq)	DIPA (eq)	X(eq)	Time	Yield ^(a)
1	Br	0.22	1.25	1.25	1.25	18 hs	traces
2	OTs	0.22	1.25	1.25	1.25	18 hs	--
3	OMe	0.22	1.25	1.25	1.25	18 hs	--
4	Cl	0.22	1.25	1.25	1.25	18 hs	--
5	Br	0.22	1.25	1.25	3.00	18 hs	60
6	Br	0.22	1.50	1.50	4.00	18 hs	65
7	Br	0.87	1.50	1.50	4.00	18 hs	71
8	Br	4.37	1.50	1.50	4.00	4 hs	84

(a) Isolated yield via Silica gel column chromatography (Cyclohexane:CH₂Cl₂ 95:5)

Table 5.1. Optimization table for the alkylation of **12** to **13**.

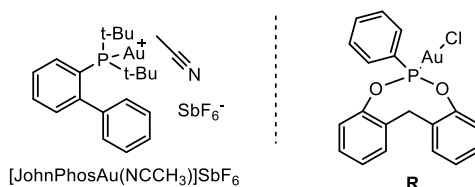
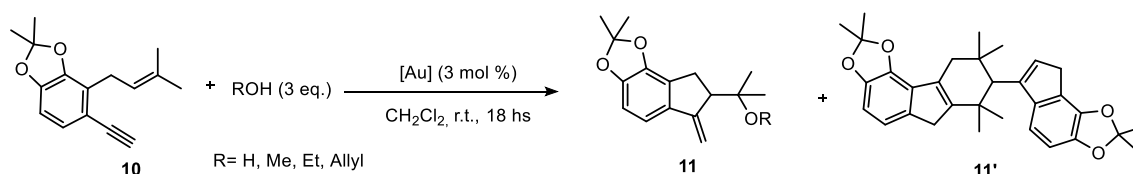
In order to introduce the alkyne moiety, it was necessary to perform a halogen exchange from bromine to iodine to increase the reactivity since the Sonogashira reaction performed directly on **13** unfortunately showed no conversion for intermediate **15** (Scheme 5.9).

Chapter 5



Scheme 5.9. transformation of **13** into substrate **10**.

Once the alkyne has been installed, simple deprotection of the silane unit with K_2CO_3 led to **10** with excellent yields.



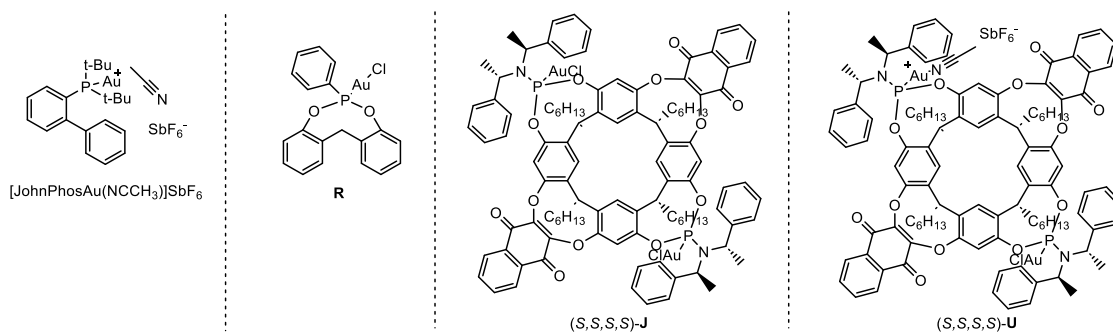
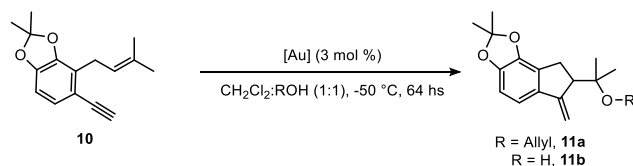
Entry	[Au]	Scavenger (eq)	R	11 (%)	11' (%)
1	[JohnPhosAu(NCCH ₃)]SbF ₆	--	H ^(a)	--	--
2	[JohnPhosAu(NCCH ₃)]SbF ₆	--	Me	--	traces
3	[JohnPhosAu(NCCH ₃)]SbF ₆	--	Et	--	traces
4	[JohnPhosAu(NCCH ₃)]SbF ₆	--	Allyl	--	65
5	R	AgSbF ₆	Allyl	--	61

(a) Acetone was used instead of CH_2Cl_2 as the solvent of the reaction

Table 5.2: Alkoxy-cycloisomerization experiments with 3 equivalents of ROH.

Chapter 5

Once a synthetic procedure for **10** was established, it was decided to investigate the alkoxy-cycloisomerization. First, achiral monomeric catalysts [JohnPhosAu(NCCH₃)]SbF₆ and **R** have been tested under standard reaction conditions,^[16] but instead of the desired product **11**, the formation of the dimer **11'** was observed (Table 5.2).^[17] The experiments were repeated in a 1:1 mixture of solvent and the desired ROH, and the alkoxy-cyclization products were obtained when allyl alcohol and water were used (Table 5.3, entries 1, 2 and 4). Preliminary experiments employing the best resorcin[4]arene-based gold(I)-complexes reported in Echavarren's work, (S,S,S,S)-**J** and (S,S,S,S)-**U**, allowed to achieve very promising enantiomeric ratio in favor of the desired conformation (Table 5.3, entries 3 and 5). These complexes were prepared following reported procedures (Scheme 5.10).^[12]

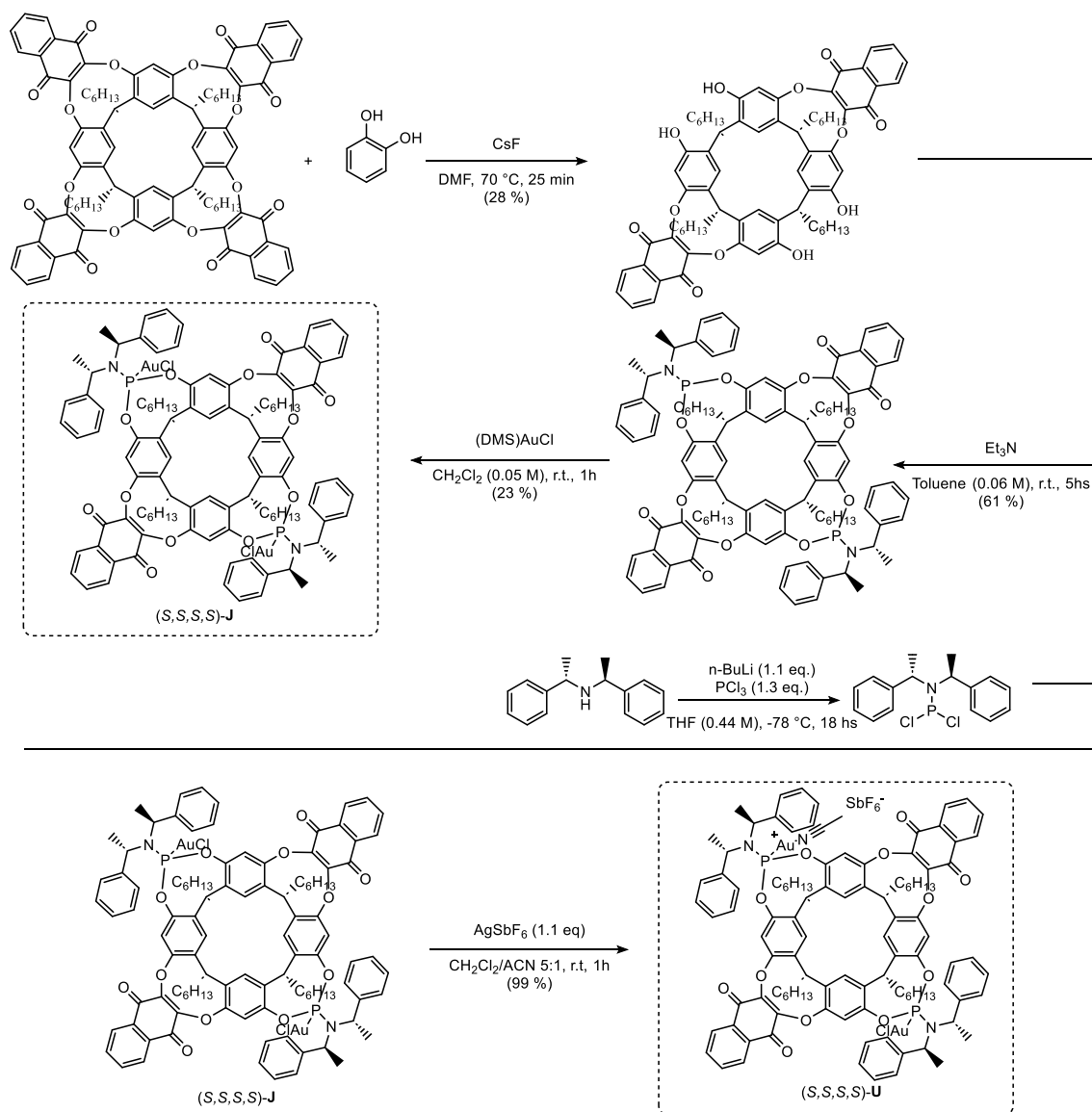


Entry	[Au]	R	Scavenger	11 (%)	e.r.
1	[JohnPhosAu(NCCH ₃)]SbF ₆	Allyl	--	54	--
2	R	Allyl	AgSbF ₆ (3 mol %)	10	--
3	(S,S,S,S)- J	Allyl	AgSbF ₆ (6 mol %)	57	27:73
4 ^a	[JohnPhosAu(NCCH ₃)]SbF ₆	H	--	59	--
5 ^a	(S,S,S,S)- U	H	--	61	11:89

[a]The experiment was performed with Acetone instead of CH₂Cl₂ and at 0 °C

Table 5.3. Catalytic experiment for the conversion of **10** into the indane derivatives **11a-b**.

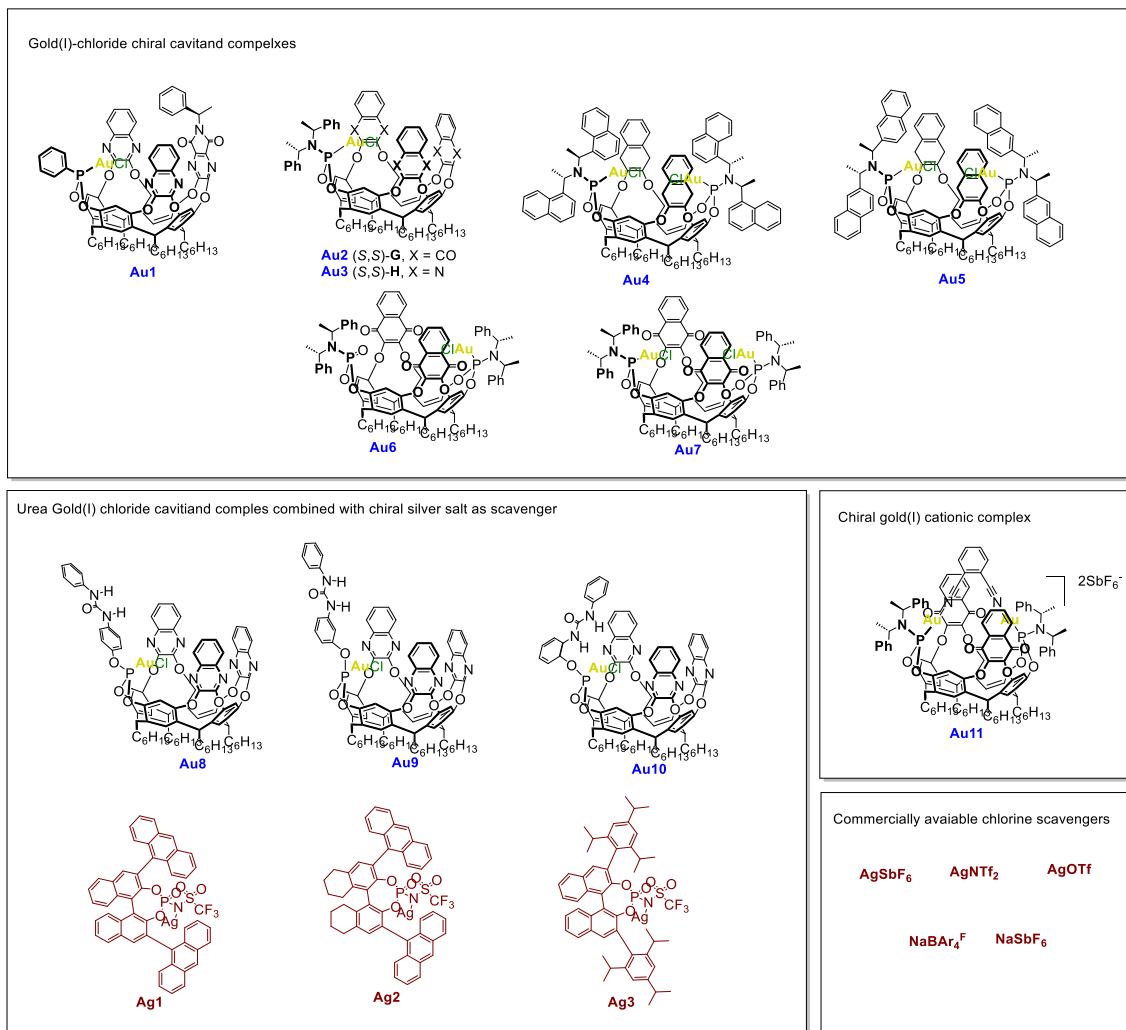
Chapter 5



Scheme 5.10. Synthesis of **(S,S,S,S)-J** and **(S,S,S,S)-U**.

To verify if the selected chiral catalysts were the best-performing ones, High Throughput Experiments (HTE) were performed by testing up to eleven different cavitand-base gold(I)-catalysts and eight different silver salts (Scheme 5.11).

Chapter 5



Scheme 5.11. Structure of cavitiands **Au1-11** and silver salts **Ag1-3** and commercially available ones tested by HTE.

Chapter 5

	AgSbF ₆	AgNTf ₂	NaBAR ₄ ^F	NaSbF ₆	AgOTf	Ag1	Ag2	Ag3	None
Au1	16 % e.r.: 51:49	18 % e.r.: 51:49	30 % e.r.: 51:49	3 % e.r.: 53:47	9 % e.r.: 50:50	--	--	--	--
Au2	72 % e.r.: 52:48	31 % e.r.: 52:48	62 % e.r.: 51:49	107 % e.r.: 51:49	105 % e.r.: 51:49	--	--	--	--
Au3	63 % e.r.: 83:17	26 % e.r.: 84:16	74 % e.r.: 81:19	13 % e.r.: 81:19	32 % e.r.: 84:16	--	--	--	--
Au4	61 % e.r.: 36:64	32 % e.r.: 36:64	59 % e.r.: 36:64	16 % e.r.: 39:61	42 % e.r.: 37:63	--	--	--	--
Au5	72 % e.r.: 80:20	76 % e.r.: 80:20	41 % e.r.: 78:22	72 % e.r.: 79:21	86 % e.r.: 79:21	--	--	--	--
Au6	77 % e.r.: 45:55	26 % e.r.: 47:53	60 % e.r.: 45:55	12 % e.r.: 44:56	66 % e.r.: 46:54	--	--	--	--
Au7	83 % e.r.: 80:20	34 % e.r.: 77:23	26 % e.r.: 77:23	66 % e.r.: 80:20	81 % e.r.: 77:23	--	--	--	--
Au8	--	--	--	--	--	18 % e.r.: 54:46	6 % e.r.: 44:56	16 % e.r.: 53:47	--

Chapter 5

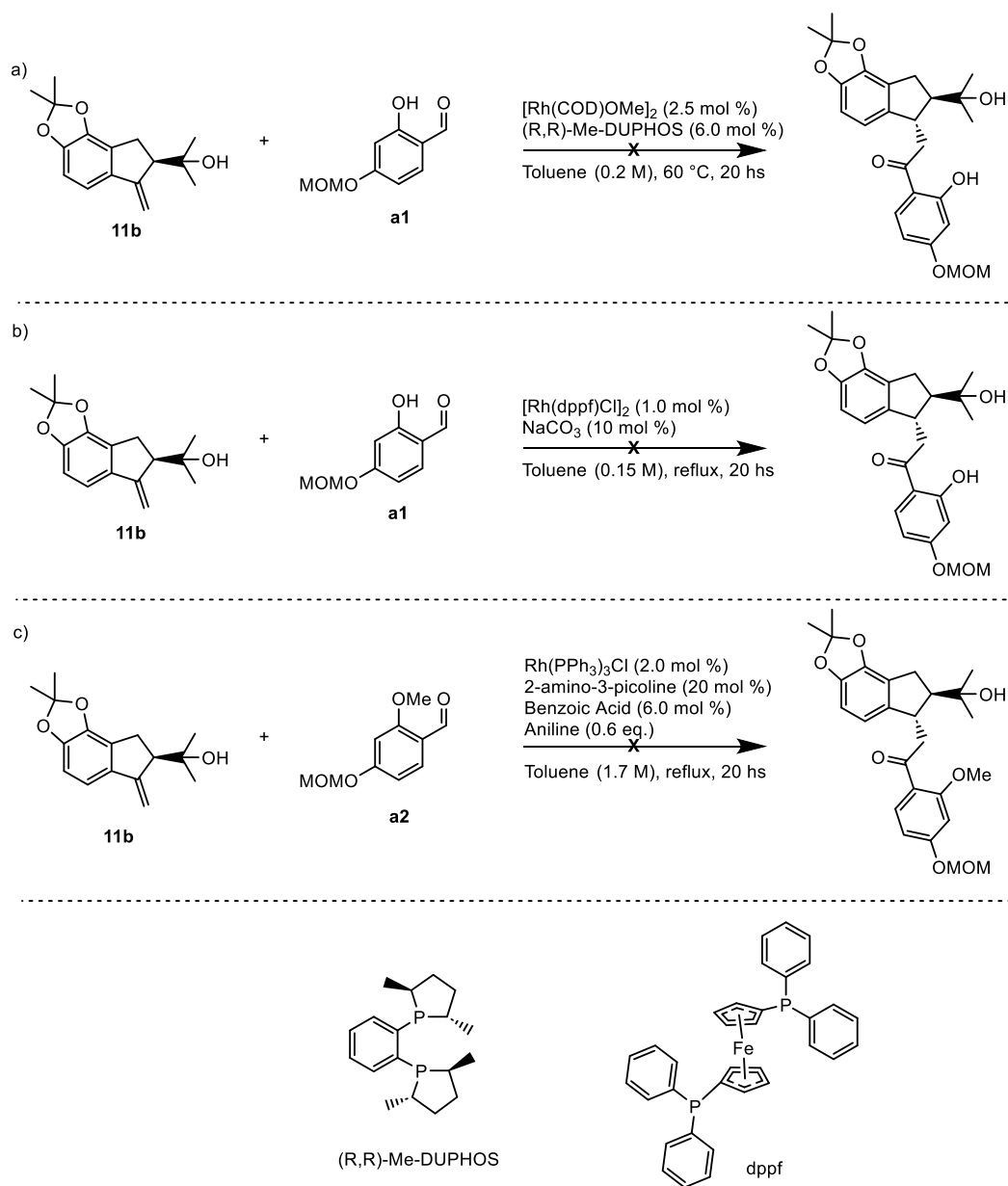
Au9	--	--	--	--	--	51 % e.r.: 47:53	25 % e.r.: 47:53	7 % e.r.: 45:55	--
Au10	--	--	--	--	--	30 % e.r.: 50:50	17 % e.r.: 48:52	1 % e.r.: 50:50	--
Au11	--	--	--	--	--	--	--	--	20 % e.r.: 51:49
None	n.d. e.r.: n.d.	n.d. e.r.: n.d.	n.d. e.r.: n.d.	n.d. e.r.: n.d.	n.d. e.r.: n.d.	--	--	--	--

Table 5.4. Yields and enantiomeric excess of the individual HTE experiments. Procedure: 20 μ L of a solution of each gold complex in DCE (a total of 2.5 mol % of **10**) was added to 20 μ L of the corresponding scavenger solution (a total of 3.75 mol % of **10**) as described in the table. The mixture was left under magnetic stirring for 1 h and then the solvent was removed. 20 μ L of distilled water was added to the resulting cationic complex, followed by 20 μ L of a solution of **10** in 2-butanone (0.4 M). The resulting mixture was left stirring overnight at r.t. The reaction mixture was diluted with 500 μ L of a solution of I.S. (biphenyl, 0.005 M) and directly analyzed by UPLC for determination of the yield and chiral HPLC (column IB).

Among all the possible combinations, only three results presented an improved enantiomeric ratio compared to the control reaction (Table 5.4, yellow box); among these three, only one reached valuable yields (Table 5.4, green box).

Finally, in order to complete the total synthesis of **TM** (Scheme 5.12), we performed some preliminary experiments to functionalize the alkene moiety in **11b** by hydroacylation reaction.

Chapter 5



Scheme 5.12. Hydroacylation attempts for the synthesis of **TM**.

Unfortunately, none of these attempts led to the desired results; therefore, it wasn't possible to conclude the total synthesis of **TM** because of time restrictions.

Chapter 5

5.3 Conclusions

In conclusion, a novel approach to synthesize indane-based natural products empowered by enantioselective gold(I)-catalyzed alkoxy cyclization reaction of 1,6-enynes has been presented, showing promising results in terms of both yields and enantioselectivity towards the total synthesis of (±)-indidene A (**TM**). A large number of chiral resorcin[4]arene-based gold(I)-complexes have been tested in order to optimize the catalytic conditions. Finally, late-stage functionalization of derivative **11b** by direct hydroacylation reaction has been tested but didn't lead to the formation of **TM**.

Chapter 5

5.4 Experimental section

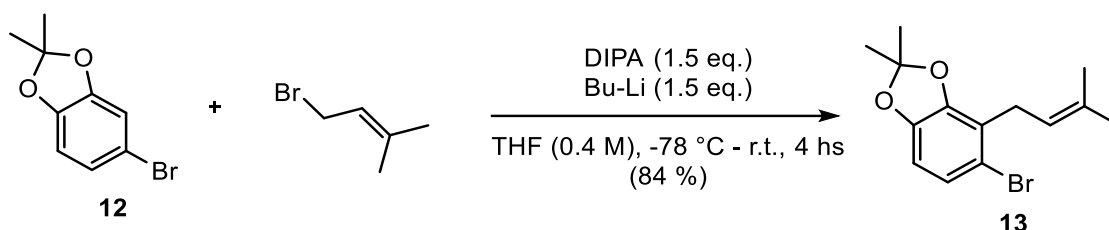
- **General remarks**

The synthesis of the ligands and gold(I) complexes was carried out under argon in solvents dried by passing through an activated alumina column on a PureSolv™ Solvent Purification System (SPS, Innovative Technologies, Inc., MA). Yields refer to chromatographically and spectroscopically pure (¹H NMR) homogeneous material, unless otherwise stated. Thin layer chromatography was carried out using TLC aluminum sheets coated with 0.2 mm of silica gel (Merck Gf234) using short-wave UV light as a visualizing agent and KMnO₄ or acidic vanillin followed by heat as developing agents. Chromatographic purifications were carried out using flash grade silica gel (SDS Chromatogel 60 ACC, 40-60 μm) as the stationary phase manually or using a CombiFlash®Rf instrument with normal phase disposable columns of different sizes (Teledyne Isco). Reactions were monitored by TLC and UHPLC (Agilent Technologies 1290 Infinity II, LC/MS with single-quad detector InfinityLab (APCI ionization source). Melting points were determined using a MP70 Melting Point System (Mettler Toledo). NMR spectra were recorded at 298 K on Bruker Avance Ultrashield NMR spectrometers (300 MHz, 400 MHz, 500 MHz and 500 MHz with CryoProbe). Chemical shifts (δ) are reported in parts per million (ppm) and referenced to residual solvent (For ¹H NMR: CDCl₃ at 7.26 ppm, CD₂Cl₂ at 5.31 ppm, for ¹³C NMR: CDCl₃ at 77.16 ppm, CD₂Cl₂ at 54.00 ppm). The following abbreviations explain multiplicities: s = singlet, d = doublet, t = triplet, q = quartet, p = pentet, m = multiplet, br s = broad singlet. Coupling constants (J) are reported in Hertz (Hz). Mass spectra were recorded on a Waters LCT Premier Spectrometer (ESI and APCI) or on an Autoflex Broker Daltonics (MALDI and LDI). Elemental analyses were performed on a LECO CHNS 932 micro-analyzer at the Universidad Complutense de Madrid. Specific optical rotation measurements were carried out on a Jasco P-1030 model polarimeter equipped with a PMT detector using the sodium line at 589 nm. Chiral HPLC analyses were performed on an Agilent Technologies 1200 series. SFC analyses were performed on an Agilent Technologies 1260 Infinity II, a Waters ACQUITY UPC2 System equipped with a diode array detector and by Chiral Technologies Europe analytical service. X-ray diffraction data were collected at 100 K on a Rigaku MicroMax-007HF, Mo Kα rotating anode, equipped with a Pilatus 200 K detector or on a Bruker APEX DUO, Mo Kα Microfocus source E025 IuS anode, equipped with an APEX DUO detector using omega scans. Unless

Chapter 5

otherwise stated, all reagents were purchased from commercial sources and used without further purification.

The preparation of these compounds has been previously described: (S,S,S,S)-**J**,^[12] (S,S,S,S)-**U**,^[12] **12**.^[9]



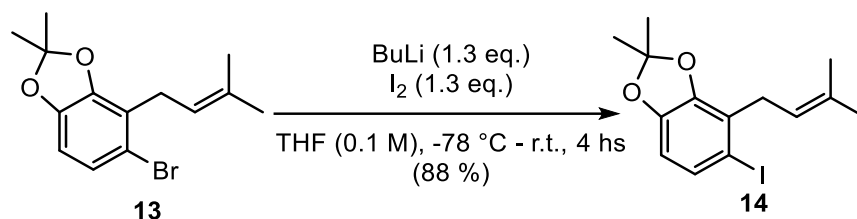
Into a microwave vial, under an inert Ar atmosphere, DIPA (0.924 mL, 1.5 eq.) was dissolved in 8.6 mL of THF and cooled to -78 °C. Freshly titled *n*-Butyl lithium (3.056 mL, 2.14 M in hexane, 1.5 eq.) was added and the solution was stirred at -78 °C for 1 h. A solution of **12** (1.00 g, 4.36 mmol) in 2 mL of THF was slowly added at -78 °C. The mixture was left under magnetic stirring at -78 °C for an additional 30 minutes. Finally, prenyl bromide (2.05 mL, 4.0 eq.) was slowly added dropwise. After approximately 15 minutes, the cooling bath was removed, and the mixture was allowed to slowly warm up to r.t. After 4 hrs, the reaction was monitored by GC-MS and complete consumption of **12** was observed. The reaction was quenched by the addition of sat. NH₄Cl solution, the resulting mixture was recovered with EtOAc and the organic phase was separated, washed with water and brine, dried over Na₂SO₄ and filtered. The crude was purified by silica gel column chromatography (Cyclohexane:EtOAc 95:5) affording **13** as a colorless oil (1.092 g, 84%).

¹H NMR (500 MHz, CDCl₃) δ = 6.97 (d, J = 8.2 Hz, 1H), 6.48 (d, J = 8.3 Hz, 1H), 5.25 (ddq, J = 8.6, 5.8, 1.4 Hz, 1H), 3.38 (ddt, J = 7.3, 2.1, 1.0 Hz, 2H), 1.81 – 1.76 (m, 3H), 1.72 (q, J = 1.3 Hz, 3H), 1.69 (s, 6H).

¹³C NMR (126 MHz, CDCl₃) δ = 146.5 (C_q), 146.4 (C_q), 132.9 (C_q), 124.4 (CH), 123.1 (C_q), 120.4 (CH), 118.4 (C_q), 115.0 (C_q), 107.2 (CH), 28.7 (CH₂), 25.8 (CH₃), 25.8 (CH₃), 18.1 (CH₃).

HR-MS (ESI) *m/z* [M+H]⁺ calculated for C₁₄H₁₈BrO₂: 296.0412; found: 296.0418.

Chapter 5



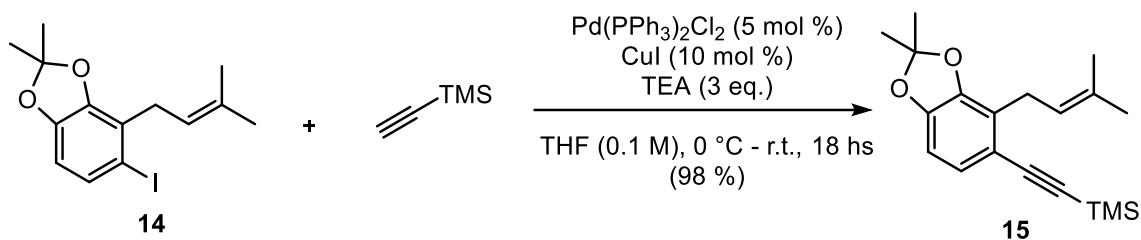
Into a microwave vial, under an inert Ar atmosphere, **13** (1.01 g, 3.71 mmol) was dissolved in 18.5 mL of THF (0.1 M) and cooled to -78°C . Freshly titled *n*-Butyl lithium (2.04 mL, 2.36 M in hexane, 1.3 eq.) was added and the solution was stirred at -78°C for 1 h. Iodine (1.22 g, 1.3 eq.) was dissolved in THF and added at -78°C . The cooling bath was removed, and the colored solution was stirred at room temperature for 4 hrs. The reaction was monitored by GC-MS and a complete consumption of **13** was observed. The reaction was quenched by the addition of sat. Na_2SO_3 solution, the resulting mixture was recovered with EtOAc and the organic phase was separated, washed with water and brine, dried over Na_2SO_4 and filtered. The crude was purified by silica gel column chromatography (Cyclohexane:EtOAc 97:3) affording **14** as a colorless oil (1.124 g, 88%).

$^1\text{H NMR}$ (500 MHz, CDCl_3) δ = 7.22 (d, J = 8.2 Hz, 1H), 6.36 (d, J = 8.1 Hz, 1H), 5.20 (thept, J = 7.1, 1.4 Hz, 1H), 3.35 (dp, J = 7.2, 1.1 Hz, 2H), 1.78 (d, J = 1.4 Hz, 3H), 1.70 (q, J = 1.4 Hz, 3H), 1.66 (s, 6H).

$^{13}\text{C NMR}$ (126 MHz, CDCl_3) δ = 147.4 (C_q), 141.9 (C_q), 132.9 (C_q), 131.2 (CH), 126.0 (C_q), 120.4 (CH), 118.3 (C_q), 108.3 (CH), 88.7 (C_q), 32.9 (CH_2), 25.9 (CH_3), 25.8 (CH_3), 18.4 (CH_3).

HRMS (ESI) m/z $[\text{M}+\text{H}]^+$ calculated for $\text{C}_{14}\text{H}_{18}\text{IO}_2$: 345.0346; found: 345.0340.

Chapter 5



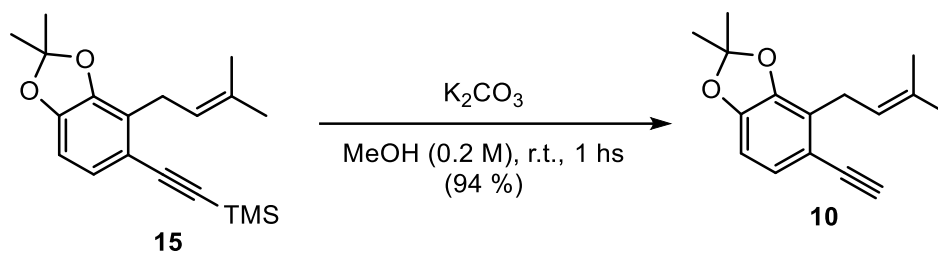
Into a microwave vial, under an inert Ar atmosphere, a solution of Pd(PPh₃)₂Cl₂ (114.7 mg, 0.05 eq.), CuI (62.2 mg, 0.1 eq.) and **14** (79.20 mg, 1.0000 Eq, 230.1 μmol) in THF (6.5 mL, 0.1 M) was degassed with Ar for 10 minutes. Then, TEA (1.37 mL, 3 eq.) was added, and the mixture was cooled to 0 °C (ice bath). Finally, trimethylsilylacetylene (0.51 mL, 1.1 eq.) was added dropwise. The mixture was allowed to slowly warm-up to r.t. and left under magnetic stirring overnight. The reaction was monitored by TLC (Cyclohexane: EtOAc 95:5) and a complete consumption of **14** was observed. The reaction was quenched by the addition of water. Then, the organic layer was recovered, washed with water and brine, dried over Na₂SO₄ and filtered. The crude was purified by silica gel column chromatography (Cyclohexane: EtOAc 95:5) affording **15** as a colorless oil (1.00g, 98 %).

¹H NMR (500 MHz, CDCl₃) δ = 6.98 (d, *J* = 8.1 Hz, 1H), 6.53 (d, *J* = 8.0 Hz, 1H), 5.35 (dddd, *J* = 8.7, 5.8, 2.9, 1.4 Hz, 1H), 3.43 (dt, *J* = 7.2, 1.1 Hz, 2H), 1.78 (d, *J* = 1.3 Hz, 3H), 1.71 (q, *J* = 1.3 Hz, 3H), 1.68 (s, 6H), 0.25 (s, 9H).

¹³C NMR (126 MHz, CDCl₃) δ = 147.5 (C_q), 145.1 (C_q), 132.2 (C_q), 126.6 (CH), 125.3 (C_q), 121.3 (CH), 118.0 (C_q), 115.6 (C_q), 106.0 (CH), 104.2 (C_q), 95.2 (C_q), 27.2 (CH₂), 25.8 (CH₃), 25.7 (CH₃), 18.1 (CH₃), 0.1 (CH₃).

HRMS (ESI) *m/z* [M+H]⁺ calculated for C₁₉H₂₇O₂Si: 315.1775; found: 345.1769.

Chapter 5



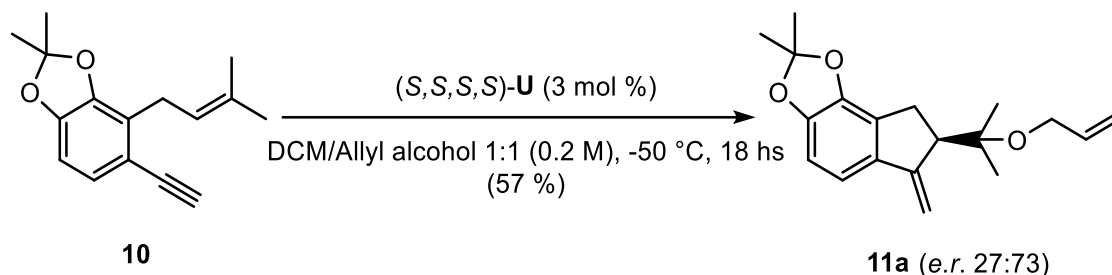
Into a glass vial, potassium carbonate (0.90 g, 2.05 eq.) was added to a solution of **6b** (1.00 g, 3.19 mmol) in MeOH (16.0 mL, 0.2 M) and was left under magnetic stirring at r.t. for 1h. The reaction was monitored by TLC (Cyclohexane: EtOAc 95:5) and a complete consumption of **6b** was observed. The reaction was quenched by the addition of water and the mixture was recovered with EtOAc. The organic phase was separated, washed with water and brine, dried over Na_2SO_4 and filtered. The crude was purified by silica gel column chromatography (Cyclohexane: EtOAc 95:5) affording **1b** as a yellowish oil (727.3 mg, 94 %).

1H NMR (500 MHz, $CDCl_3$) δ = 7.01 (d, J = 8.1 Hz, 1H), 6.55 (d, J = 8.0 Hz, 1H), 5.32 (ddq, J = 8.7, 5.9, 1.4 Hz, 1H), 3.44 (dt, J = 7.2, 1.1 Hz, 2H), 3.13 (s, 1H), 1.78 (dd, J = 1.3, 0.4 Hz, 3H), 1.71 (q, J = 1.4 Hz, 3H), 1.69 (s, 6H).

^{13}C NMR (126 MHz, $CDCl_3$) δ = 147.7 (C_q), 145.5 (C_q), 132.4 (C_q), 126.8 (CH), 125.6 (C_q), 121.1 (CH), 118.2 (C_q), 114.5 (C_q), 106.1 (CH), 78.4 (C_q + CH), 27.1 (CH_2), 25.9 (CH_3), 25.7 (CH_3), 18.0 (CH_3).

HRMS (ESI) m/z $[M+H]^+$ calculated for $C_{19}H_{27}O_2Si$: 315.1775; found: 345.1769.

Chapter 5



Into a microwave vial, under an inert Ar atmosphere, a solution of **10** (15.00 mg, 0.062 mmol) in CH_2Cl_2 (0.31 mL, 0.2 M) was added to a solution of (S,S,S,S) -**U** (4.36 mg, 3 mol %) in allyl alcohol (0.31 mL, 0.2 M) cooled to -50 °C. The mixture was left under magnetic stirring at -50 °C for 18 hs. The reaction was monitored by TLC (Cyclohexane: CH_2Cl_2 8:2) and a complete consumption of **10** was observed. The reaction was quenched with 3 drops of TEA, the solvent was removed under reduced pressure and the crude purified by preparative TLC (Cyclohexane: CH_2Cl_2 8:2) yielding **11a** as a colorless oil (10.6 mg, 57 %).

$^1\text{H NMR}$ (500 MHz, CDCl_3) δ = 6.97 (d, J = 8.0 Hz, 1H), 6.63 (dt, J = 8.0, 0.8 Hz, 1H), 5.97 (ddt, J = 17.2, 10.5, 5.4 Hz, 1H), 5.48 (dd, J = 2.0, 0.6 Hz, 1H), 5.36 – 5.27 (dq, J = 10.5, 1.6 Hz, 1H), 5.15 (dq, J = 10.4, 1.5 Hz, 1H), 5.11 (d, J = 1.7 Hz, 1H), 3.99 (ddt, J = 5.4, 4.6, 1.6 Hz, 2H), 3.28 (ddt, J = 8.0, 4.1, 1.9 Hz, 1H), 2.98 – 2.94 (m, 2H), 1.71 (s, 3H), 1.69 (s, 3H), 1.29 (s, 3H), 1.03 (s, 3H).

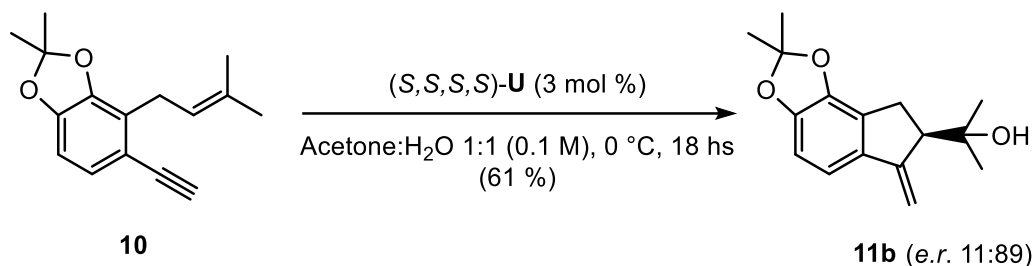
$^{13}\text{C NMR}$ (126 MHz, CDCl_3) δ = 150.0 (C_q), 147.3 (C_q), 137.4 (C_q), 135.8 (CH), 125.4 (C_q), 118.0 (C_q), 115.8 (CH₂), 112.7 (CH), 107.2 (CH), 104.6 (CH₂), 62.5 (CH₂), 51.3 (CH), 28.9 (CH₂), 25.9 (CH₃), 25.9 (CH₃), 22.7 (CH₃), 22.7 (CH₃).

α_D^{589} = -41.6 deg·cm²·g⁻¹ (CH_2Cl_2 , 299 °K).

HPLC Chiralcel OD-H (250 mm x 4.6 mm, 5 μm) at 25 °C, flow 1.0 ml/min, isocratic Hexane/*i*-PrOH 100:0, 254 nm, t_R (minor) 12.8; t_R (major) 13.6.

HRMS (ESI) m/z [$\text{M}+\text{H}$]⁺ calculated for $\text{C}_{20}\text{H}_{24}\text{O}_3$: 300.1725; found: 300.1731.

Chapter 5



Into a microwave vial, under an inert Ar atmosphere, (S,S,S,S)-**U** (14.5 mg, 3 mol %) was added to a suspension of **10** (50.00 mg, 0.206 mmol) in Acetone/water 1:1 (1.04 mL, 0.2 M) cooled to 0°C, under vigorous magnetic stirring. The mixture was left under magnetic stirring at 0 °C for 18 hs. The reaction was monitored by TLC (Cyclohexane: EtOAc 85:15) and a complete consumption of **10** was observed. The reaction was quenched with 3 drops of TEA, the solvent was removed under reduced pressure and the crude purified by preparative TLC (Cyclohexane: EtOAc 85:15) isolating **11b** as a dark-orange oil (32.8 mg, 61 %).

¹H NMR (500 MHz, CDCl₃) δ = 6.98 (d, *J* = 8.0 Hz, 1H), 6.65 (dt, *J* = 8.0, 0.7 Hz, 1H), 5.51 (d, *J* = 1.5 Hz, 1H), 5.11 (d, *J* = 1.3 Hz, 1H), 3.08 – 2.99 (m, 2H), 2.84 – 2.75 (m, 1H), 1.96 (s, 1H), 1.71 (d, *J* = 0.7 Hz, 3H), 1.69 (d, *J* = 0.7 Hz, 3H), 1.24 (s, 3H), 1.05 (s, 3H).

¹³C NMR (126 MHz, CDCl₃) δ = 150.3 (C_q), 147.6 (C_q), 143.0 (C_q), 136.8 (C_q), 125.4 (C_q), 118.2 (C_q), 112.9 (CH), 107.4 (CH), 104.7 (CH₂), 72.7 (C_q), 55.0 (CH), 29.7 (CH₂), 27.4 (CH₃), 25.9 (CH₃), 25.9 (CH₃), 25.3 (CH₃).

α_D⁵⁸⁹ = -48.7 deg·cm²·g⁻¹ (CH₂Cl₂, 299 °K).

HPLC Chiralcel OD-H (250 mm x 4.6 mm, 5 μm) at 25 °C, flow 1.0 ml/min, isocratic Hexane/*i*-PrOH 98:2, 254 nm, *t_R* (minor) 8.6; *t_R* (major) 11.3.

HRMS (ESI) *m/z* [M+H]⁺ calculated for C₂₀H₂₄O₃: 283.1302; found: 283.1300.

Chapter 5

5.5 Bibliography

- [1] a) S. Ito, T. Matsuya, S. Omura, M. Otani, A. Nakagawa, *J. Antibiot.*, **1970**, 23, 61-65 & 315-317; b) S.J. Gould, J. Chen, M.C. Cone, M.P. Gore, C.R. Melville, N. Tamayo, *J. Org. Chem.*, **1996**, 61, 5720-5721; c) S.J. Gould, J. Chen, M.C. Cone, M.P. Gore, C.R. Melville, N. Tamayo, *J. Am. Chem. Soc.*, **1994**, 116, 2207-2208.
- [2] L.F. Silva Jr., M.V. Craveiro, I.R.M. Tebeka, *Tetrahedron*, **2010**, 66, 3875-3895.
- [3] M. Vilums, J. Heuberger, L. H. Heitman, A. P. Ijzerman, *Med. Res. Rev.*, **2015**, 35, 1097-1126.
- [4] R. He, X. Huang, Y. Zhang, L. Wu, H. Nie, D. Zhou, B. Liu, S. Deng, R. Yang, S. Huang, Z. Nong, J. Li, Y. Huang, *J. Nat. Prod.*, **2016**, 79, 2472-2478.
- [5] Y. P. Li, Y. C. Yang, Y. K. Li, Z. Y. Jiang, X. Z. Huang, W. G. Wang, X. M. Gao, Q. F. Hu, *Fitoterapia*, **2014**, 95, 214-219.
- [6] X. Li, F. Huang, B. Zhang, W. Tan, A. Khan, Z. Zhi-Hong, L. Liu, Z. Yang, *Chem. Biodiversity*, **2022**, 19, e202200188.
- [7] a) B. Gabriele, R. Mancuso, L. Veltri, *Chem. Eur. J.*, **2016**, 22, 5056-5094; b) C. Borie, L. Ackermann, M. Nechab, *Chem. Soc. Rev.*, **2016**, 45, 1368-1386; c) A. Rinaldi, D. Scarpi, E. G. Occhiato, *Eur. J. Org. Chem.*, **2019**, 7401-7419.
- [8] Selected examples for transition-metal-catalyzed C-H functionalization for the formation of the indane-core: a) R. Melot, M. V. Craveiro, T. Burgi, O. Baudoin, *Org. Lett.*, **2019**, 21, 812-815; b) R. Melot, M. V. Craveiro, O. Baudoin, *J. Org. Chem.*, **2019**, 84, 12933-2945; c) S. Gao, G. Qian, H. Tang, Z. Yang, Q. Zhou, *ChemCatChem*, **2019**, 11, 5762-5765; d) Z. Zhuang, A. N. Herron, S. Liu, J.-Q. Yu, *J. Am. Chem. Soc.*, **2021**, 143, 687-692; e) M. Tomanik, J.-Q. Yu, *J. Am. Chem. Soc.*, **2023**, 145, 17919-17925; f) B. Hong, C. Li, Z. Wang, J. Chen, H. Li, X. Lei, *J. Am. Chem. Soc.*, **2015**, 137, 11946-11949; g) J. Chen, Z. Shi, P. Lu, *Org. Lett.*, **2021**, 23, 7359-7363.
- [9] A. Kudashev, S. Vergura, M. Zuccarello, T. Bürgi, O. Baudoin, *Angew. Chem. Int. Ed.*, **2023**, e202316103.

Chapter 5

- [10] a) R. Melot, M. Zuccarello, D. Cavalli, N. Niggli, M. Devereux, T. Burgi, O. Baudoin, *Angew. Chem. Int. Ed.*, **2021**, 60, 7245-7250; b) S. Wurtz, F. Glorius, *Acc. Chem. Res.*, **2008**, 41, 1523-1533; c) T. Gaich, P. S. Baran, *J. Org. Chem.*, **2010**, 75, 4657-4673; d) J. Schwan, M. Christmann, *Chem. Soc. Rev.*, **2018**, 47, 7985-7995.
- [11] M. P. Muñoz, J. Adrio, J. C. Carretero, A. M. Echavarren, *Organometallics*, **2005**, 24, 6, 1293-1300.
- [12] I. Martín-Torres, G. Ogalla, J. M. Yang, A. Rinaldi, A. M. Echavarren, *Angew. Chem. Int. Ed.*, **2021**, 60, 9339-9344.
- [13] Y. Liu, Y. Guo, F. Ji, D. Gao, C. Song, J. Chang, *J. Org. Chem.*, **2016**, 81, 4310-4315
- [14] a) J. D. Osborne, H. E. Randell-Sly, G. S. Currie, A. R. Cowley, M. C. Willis, *J. Am. Chem. Soc.*, **2008**, 130, 17232-17233; b) K. Kokobu, K. Matsumasa, Y. Nishinaka, M. Miura, M. Nomura, *Bull. Chem. Soc. Jpn.*, **1999**, 72, 303; c) C.-H. Jun, D.-Y. Lee, H. Lee, J.-B. Hong, *Angew. Chem., Int. Ed.*, **2000**, 39, 3070-3072.
- [15] a) S. N. Alektiar, J. Han, Y. Dang, C. Z. Rubel, Z. K. Wickens, *J. Am. Chem. Soc.*, **2023**, 145, 10991-10997; b) B.-L. Wu, J.-N. Yao, X.-X. Long, Z.-Q. Tan, X. Liang, L. Feng, K. Wei, Y.-R. Yang, *J. Am. Chem. Soc.*, **2024**, 146, 1262-1268.
- [16] C. Nieto-Oberhuber, M. P. MuÇoz, S. L_pez, E. Jim_nez-NfflÇez, C. Nevado, E. Herrero-G_mez, M. Raducan, A. M. Echavarren, *Chem. Eur. J.*, **2006**, 12, 1677-1693.
- [17] M. Álvarez-Pérez, M. Frutos, A. Viso, R. F. de la Pradilla, M. C. de la Torre, M. A. Sierra, H. Gornitzka, C. Hemmer, *J. Org. Chem.*, **2017**, 82, 7546-7554.

Publications

G. Cera, **G. Giovanardi**, A. Secchi, A. Arduini, Merging Molecular Recognition and Gold(I) Catalysis with Triphoscalix[6]arene Ligands, *Chem. Eur. J.*, **2021**, 27, 10261-10266.

G. Giovanardi, A. Secchi, A. Arduini, G. Cera, Diametric calix[6]arene-based phosphine gold(I) cavitands, *Beilstein J. Org. Chem.*, **2022**, 18, 190-196.

G. Giovanardi, D. Balestri, A. Secchi, G. Cera, Diametric calix[6]arene gold(I) catalysts for intramolecular cyclopropanations of 1,6-dienynes, *Org. Biomol. Chem.*, **2022**, 20, 6464-6472.

L. Andreoni, G. Mariano Beneventi, **G. Giovanardi**, G. Cera, A. Credi, A. Arduini, A. Secchi, S. Silvi, A Multiresponsive Calix[6]arene Pseudorotaxane Empowered by Fluorophoric Dansyl Groups, *Chem. Eur. J.*, **2023**, e202203472.

G. Giovanardi, G. Scarica, V. Pirovano, A. Secchi, G. Cera, Gold(I)-catalysed hydroarylations of alkynes for the synthesis of inherently chiral calix[4]arenes, *Org. Biomol. Chem.*, **2023**, 21, 4072-4083.

G. Giovanardi, S. Cattani, D. Balestri, A. Secchi, G. Cera, Iridium-Catalyzed C–H Borylations: Regioselective Functionalizations of Calix[4]arene Macrocycles, *J. Org. Chem.*, **2024**, 89, 8486-8499.